

**Investigations into the mechanism of the coenzyme B<sub>12</sub>  
dependent reaction catalyzed by glutamate mutase from  
*Clostridium cochlearium***



**Dissertation**

zur

Erlangung des Doktorgrades

der Naturwissenschaften

(Dr. rer. nat.)

dem

Fachbereich Biologie

der Philipps-Universität Marburg

vorgelegt von

**Fredrick Edwin Lyatuu**

aus Kilimanjaro, Tansania

Marburg/Lahn 2012

Die Untersuchungen zur vorliegenden Arbeit wurden von Dezember 2007 bis März 2008 an der School of Chemistry at Newcastle University unter der Leitung von Herrn Prof. Dr. B. T. Golding und von Oktober 2008 bis Dezember 2012 am Fachbereich Biologie der Philipps-Universität Marburg unter der Leitung von Herrn Prof. Dr. W. Buckel durchgeführt.

Vom  
Fachbereich Biologie der Philipps-Universität Marburg als  
Dissertation am 28.01.2013 angenommen.

Erstgutachter: Prof. Dr. W. Buckel  
Zweitgutachter: Prof. Dr. B.T. Golding

Tag der mündlichen Prüfung: 11.02.2013

To my wife Catherine Ngirwa and our five months old son Edwin Lyatuu

Ein Teil der im Rahmen dieser Dissertation erzielten Ergebnisse wurden in folgenden Publikationen veröffentlicht:

Friedrich, P., Baisch, U., Harrington, R. W., **Lyatuu, F.**, Zhou, K., Zelder, F., McFarlane, W., Buckel, W. and Golding, B. T. (2012), Experimental Study of Hydrogen Bonding Potentially Stabilizing the 5'-Deoxyadenosyl Radical from Coenzyme B<sub>12</sub>. *Chem. Eur. J.*, **18**: 16114-16122. doi: 10.1002/chem.201201840

Zhou, K., Oetterli, R. M., Brandl, H., **Lyatuu, F. E.**, Buckel, W. and Zelder, F. (2012), Chemistry and Bioactivity of an Artificial Adenosylpeptide B<sub>12</sub> Cofactor. *ChemBioChem*, **13**: 2052–2055. doi: 10.1002/cbic.201200429

**Lyatuu, F.E.**, Parthasarathy, A., Zhoi, K., Zelenka, K., Zelder, F.H., Buckel, W. (2012). Probing the Cob(II)alamin Conductor Hypothesis with Glutamate Mutase from *Clostridium cochlearium*. Proceedings of the 2<sup>nd</sup> Tanzania Chemical Society International Conference. 5<sup>th</sup> -7<sup>th</sup> October, 2011. Dar Es Salaam, Tanzania. *Tanz. J. Sci.* <http://www.ajol.info/index.php/tjs>, In press

<b>Contents</b> .....	i
<b>Abbreviations</b> .....	vii
<b>Zusammenfassung</b> .....	viii
<b>Summary</b> .....	xi
<b>1. Introduction</b> .....	<b>1</b>
1.1 The anti-pernicious anemia discovery of vitamin B <sub>12</sub> .....	1
1.2 Vitamin B <sub>12</sub> structure .....	2
1.3 Vitamin B <sub>12</sub> transport and delivery .....	4
1.3.1 The gastrointestinal pathway for vitamin B <sub>12</sub> .....	4
1.3.2 Application of B <sub>12</sub> uptake for delivery of therapeutic agents .....	6
1.4 B <sub>12</sub> dependent enzymatic reactions .....	9
1.4.1 The cob(D)alamin dehalogenations .....	9
1.4.2 Methylcobalamin dependent enzymatic reactions .....	11
1.4.3 Coenzyme B <sub>12</sub> dependent enzymatic reactions .....	18
1.5 The diversity of B <sub>12</sub> in metabolism .....	21
1.5.1 Medical aspects of B <sub>12</sub> in metabolism .....	22
1.5.2 Energy conservations in anaerobic food chains .....	26
1.5.2.1 Amino acids fermentations .....	26
1.5.2.2 Nicotinate fermentation .....	30
1.5.2.3 Anaerobic n-hexane oxidation .....	31
1.5.3 Metabolic pathways for carbon assimilation and biosynthesis .....	32
1.6 Mechanisms for rearrangements by coenzyme B <sub>12</sub> dependent enzymes .....	34
1.6.1 Coenzyme B <sub>12</sub> dependent carbon skeleton mutases .....	35
1.6.1.1 2-Methyleneglutarate mutase .....	35
1.6.1.2 Methylmalonyl CoA mutase .....	40
1.6.1.3 Glutamate mutase .....	46
1.6.2 Coenzyme B <sub>12</sub> dependent eliminases .....	49
1.6.2.1 Ethanolamine ammonia lyase (EAL) .....	51
1.6.2.2 Ribonucleotide reductases (RNRs) .....	53

1.7	Objectives of the studies .....	56
<b>2.</b>	<b>Experimental .....</b>	<b>58</b>
2.1	Materials .....	58
2.1.1	Chemicals, biochemicals and reagents.....	58
2.1.2	Equipments .....	58
2.2	Experiments and methods .....	59
2.2.1	Cultivation of bacteria .....	59
2.2.1.1	Cultivation of <i>Clostridium tetanomorphum</i> .....	59
2.2.1.2	Cultivation of <i>E.coli</i> DH5 $\alpha$ with pOZ3 and pOZ5 construct plasmids .....	60
2.2.1.3	Cultivation of MutL expressing <i>E.coli</i> ROSETTA .....	61
2.2.1.4	Cultivation of <i>E.coli</i> MG 1655 .....	62
2.2.1.5	Cultivation of 2-hydroxyglutarate dehydrogenase expressing <i>E.coli</i> BL21 .....	63
2.2.2	General methods for protein biochemistry .....	64
2.2.2.1	Methods for cells disruptions .....	64
2.2.2.2	Identification of proteins .....	64
2.2.2.3	Protein dialysis and determination of concentration .....	65
2.2.3	Purification of proteins .....	66
2.2.3.1	Purification of methylaspartase .....	66
2.2.3.2	Purification of component S of glutamate mutase .....	67
2.2.3.3	Purification of component E of glutamate mutase .....	67
2.2.3.4	Purification of 2-hydroxyglutarate dehydrogenase .....	68
2.2.4	General methods for molecular biology .....	69
2.2.4.1	Identification of DNAs .....	69
2.2.4.2	DNA purification .....	69
2.2.4.3	Determination of DNA purity and concentration .....	70
2.2.5	Preparations of pASG-IBA3 and pASG-IBA5 clones of <i>mutL</i> .....	70
2.2.5.1	Extraction of <i>Clostridium tetanomorphum</i> total genome .....	70

2.2.5.2 PCR amplification of <i>mutL</i> from the genome of <i>C. tetanomorphum</i> .....	70
2.2.5.3 Cloning of <i>mutL</i> into pASG-IBA3 and pASG-IBA5 vector plasmids .....	71
2.2.6 Synthesis of chemicals .....	72
2.2.6.1 Synthesis of <i>cis</i> -glutaconic acid .....	72
2.2.6.2 Synthesis of 3-[ <sup>13</sup> C- <i>methyl</i> ]methylitaconic acid .....	76
2.2.6.3 Synthesis of coenzyme B <sub>12</sub> structural derivatives cofactors .....	78
2.2.7 Assays for invitro enzymatic reactions .....	78
2.2.7.1 Assays for methylaspartase .....	78
2.2.7.2 Assays for glutamate mutase catalyzed conversion of ( <i>S</i> )-glutamate to (2 <i>S</i> , 3 <i>S</i> )-3-methylaspartate .....	79
2.2.7.3 Assays for determining the effects of the proposed glutamate mutase inhibitors on methylaspartase .....	80
2.2.7.4 Assays for determining effects of the proposed inactivators on glutamate mutase .....	81
2.2.7.5 Assay for conversion of (2 <i>S</i> , 3 <i>S</i> )-3-methylaspartate to ( <i>S</i> )-glutamate catalyzed by glutamate mutase .....	81
2.2.7.6 Assaying effect of inhibitors on auxiliary transaminase and dehydrogenase system .....	83
2.2.7.7 Characterizations on the interactions of glutamate mutase with its proposed inhibitors by the developed glutamic-pyruvic transaminase and 2-hydroxyglutarate dehydrogenase coupled assay .....	83
2.2.7.8 Assays for measurements of kinetic constants of cofactors in the reaction of glutamate mutase .....	84
2.2.7.9 Spectroscopic characterizations on the interactions of holo-glutamate mutase with its proposed inhibitors .....	85
2.2.8.0 Assays for the evaluations on the interactions of glutamate mutase with 2-haloglutarates .....	85

<b>3. Results</b> .....	<b>87</b>
3.1 Growth of bacteria and proteins purifications .....	87
3.1.1 Purification of methylaspartase from <i>Clostridium tetanomorphum</i> .....	87
3.1.2 Purifications of glutamate mutase protein components S and E from <i>E. coli</i> DH5 $\alpha$ .....	90
3.1.3 Characterization of the partial purified glutamate mutase .....	92
3.1.4 Purification of 2-hydroxyglutarate dehydrogenase from <i>E.coli</i> BL21 .....	97
3.2 Synthesis of chemicals used in probing the reaction of glutamate mutase by the mechanism based inactivation approach .....	97
3.2.1 Synthesis of <i>cis</i> -glutaconic acid .....	97
3.2.2 Synthesis of 3-[ <sup>13</sup> C- <i>methyl</i> ]itaconic acid .....	101
3.3 Mechanism based inactivation of glutamate mutase by inhibitors mimic of the 4-glutamyl and (2 <i>S</i> , 3 <i>S</i> ) 3-methyleneaspartate radicals in the enzyme active site .....	102
3.3.1 The interactions of the proposed inhibitors of glutamate mutase with methylaspartase .....	105
3.3.2 Evaluations on the interactions of glutamate mutase with its proposed inhibitors by the modified methylaspartase coupled assay .....	107
3.3.3 Development of a novel assay for glutamate mutase catalyzed conversion of (2 <i>S</i> , 3 <i>S</i> )-3-methylaspartate to ( <i>S</i> )-glutamate .....	109
3.3.4 Determination of the kinetic constants of (2 <i>S</i> , 3 <i>S</i> )-3-methylaspartate in the reaction of glutamate mutase .....	112
3.3.5 Summary of the kinetic constants for the reaction catalyzed by the partial purified glutamate mutase and determination of the reaction equilibrium constant by Briggs-Haldane equation .....	113



3.3.6	Evaluations on the interactions of glutamate mutase with its proposed inhibitors by the glutamic-pyruvic transaminase and 2-hydroxyglutarate dehydrogenase coupled assay .....	114
3.3.7	The reaction of glutamate mutase with 2-fluoroglutaric acid .....	115
3.4	Kinetic probing of the glutamate mutase reaction by the structural derivatives of coenzyme B <sub>12</sub> cofactors .....	118
3.4.1	Investigations into the role of the 5, 6 -dimethylbenzimidazole D-ribonucleotide tail of coenzyme B <sub>12</sub> in the “base off, his on” catalysis by glutamate mutase .....	118
3.4.1.1	Reconstitution of holo-glutamate mutase with an adenosylpeptide B <sub>12</sub> as a cofactor .....	120
3.4.1.2	Kinetic constants of an adenosylpeptide B <sub>12</sub> in the reaction of glutamate mutase .....	122
3.4.1.3	B <sub>12</sub> dependent bacteria growth on three carbon substrates .....	124
3.4.2	Probing the formation of the primary organic radical: 5'-deoxyadenosyl and the participation of cob(II)alamin in the stabilization of substrate activation during the glutamate mutase reaction .....	125
3.4.2.1	Assembling of apoglutamate mutase with β-ligand modified coenzyme B <sub>12</sub> derivatives .....	128
3.4.2.2	Determination of kinetic constants of 3',5'-dideoxyadenosylcobalamin in the reaction of glutamate mutase .....	130
3.5	Investigations into the role of MutL chaperone in glutamate mutase catalysis .....	132
3.5.1	Cloning of <i>Clostridium tetanomorphum mutL</i> gene in pASG-IBA3 and pASG-IBA5 expression vectors .....	133
3.5.2	Expression of <i>mutL</i> in <i>E.coli</i> .....	135

<b>4. Discussion .....</b>	<b>136</b>
4.1 Reconstitution of holo-glutamate mutase from protein components S and E with cofactors .....	136
4.2 Mechanism based inactivations of glutamate mutase .....	137
4.2.1 Evaluations on the interactions of glutamate mutase with its proposed inhibitors by the coupled assay with methylaspartase .....	137
4.2.2 Evaluations on the interactions of glutamate mutase with its inhibitors by a coupled assay with glutamic-pyruvic transaminase and 2-hydroxylglutarate dehydrogenase .....	139
4.2.3 The reaction of glutamate mutase with 2-fluoroglutarate .....	142
4.3 Kinetic probing of glutamate mutase reaction by coenzyme B <sub>12</sub> derivatives cofactors .....	144
4.3.1 Investigations on the role of the 5,6-dimethylbenzimidazole ribonucleotide tail of coenzyme B <sub>12</sub> in the reaction of glutamate mutase .....	144
4.3.2 Probing the stabilization of hydrogen abstraction from the substrate by 5'-deoxyadenosyl radical in the reaction of glutamate mutase.....	147
<b>5. References .....</b>	<b>153</b>
<b>Acknowledgements .....</b>	<b>171</b>
<b>Curriculum Vitae .....</b>	<b>172</b>
<b>Erklärung .....</b>	<b>174</b>

## Abbreviations

AHT	Anhydrotetracycline
DCM	Dichloromethane
DFT	Density Functional Theory
DTT	Dithiothreitol
EPR	Electron Paramagnetic Resonance
FPLC	Fast Protein Liquid Chromatography
HPLC	High Performance Liquid Chromatography
$\beta$ - IPTG	beta-Isopropyl thiogalactoside
LC-MS	Liquid Chromatography Mass Spectrometry
Mops	4-Morpholinepropanesulfonic acid
MS	Mass Spectrometry
NAD <sup>+</sup>	Nicotineamide Adenine Dinucleotide
NMR	Nuclear Magnetic Resonance
OD	Optical Density
PA	Pernicious Anaemia
RNR	Ribonucleotide reductase
SDS	Sodium dodecylsulfate
TEMED	N, N, N', N'-Tetraethylethylenediamine
THF	Tetrahydrofuran
TLC	Thin Layer Chromatography
Tris	2-Amino-2-(hydroxymethyl)-1,3-propanediol
UV-vis	Ultraviolet visible

## Zusammenfassung

Ziele dieser Untersuchungen waren zum einen die Suche nach neuen Inhibitoren der Coenzym-B<sub>12</sub> abhängigen Glutamat-Mutase und zum anderen der Mechanismus des ersten Schritts der Katalyse, die Homolyse der Kobalt-Kohlenstoff-Bindung. Das Enzym Glutamat-Mutase aus dem Glutamat-fermentierenden *Clostridium cochlearium* ist aus zwei getrennt isolierbaren Untereinheiten, S und E<sub>2</sub> aufgebaut, die in sich in Gegenwart Coenzym-B<sub>12</sub> zu dem enzymatisch aktiven Holoenzym E<sub>2</sub>S<sub>2</sub>-B<sub>12</sub> vereinigen, das die reversible Isomerisierung von (*S*)-Glutamat zu (2*S*,3*S*)-3-Methylaspartat katalysiert. Diese Reaktion wurde mit der Deaminierung von Methylaspartat zu dem bei 240 nm absorbierenden Mesaconat gekoppelt, um einen UV-spektrophotometrischen Test für die Glutamat-Mutase zu erhalten. Als potentielle Inhibitoren wurden Verbindungen ausgewählt, die *sp*<sup>2</sup>-Zentren und strukturelle Ähnlichkeiten zu den im Mechanismus postulierten Radikalen aufwiesen. Als Analoga zum 4-Glutamylradikal wurden (*E*)- und (*Z*)-Glutaconat verwandt, während als Analoga zum 3-Methylenaspartat-Radikal Itaconat, Buta-1,3-dien-2,3-dicarboxylat, Mesaconat, Fumarat und Maleat eingesetzt wurden. Da alle diese ungesättigten Dicarbonsäuren das Hilfsenzym Methylaspartase inhibierten, wurde Glutamat-Mutase mit je einem der potentiellen Inaktivatoren inkubiert und nach Abtrennung der niedermolekularen Verbindungen mittels Gelfiltration, die Restaktivität bestimmt. Dabei zeigte sich, dass unerwarteter Weise nur Mesaconat, Fumarat und Maleat das Enzym inaktivierten. Um zu prüfen, ob die anderen Verbindungen das Enzym reversibel inhibierten, wurde ein neuer Test mit (2*S*,3*S*)-3-Methylaspartat, Pyruvat und NAD<sup>+</sup> als Substrate ausgearbeitet. Mit Hilfe der Enzyme Glutamat-Pyruvat-Aminotransferase und (*R*)-2-Hydroxyglutarat-Dehydrogenase konnte die Bildung von Glutamat bei 340 nm gemessen werden. Dabei zeigte es sich, dass 2.5 mM Itaconat oder 8 mM (*E*)-Glutaconat die Glutamat-Mutase in Gegenwart von 200 mM (2*S*,3*S*)-3-Methylaspartat zu 50% inhibierten. Zur Überprüfung der Zuverlässigkeit des neuen Tests wurden die kinetischen Konstanten für (2*S*,3*S*)-3-Methylaspartat bestimmt:  $K_m = 7 \pm 0.07$  mM,  $k_{cat} = 0.54 \pm 0.6$  s<sup>-1</sup> und  $k_{cat}K_m^{-1} = 77$  s<sup>-1</sup>M<sup>-1</sup>. Daraus berechnet sich mit den bekannten Konstanten für Glutamat und der Briggs-Haldane Gleichung die Gleichgewichtskonstante  $K_{eq} = [\text{Glutamat}] \times [\text{Methylaspartat}]^{-1} = 16$ , die mit dem Literaturwert von 12 gut übereinstimmt.

Ob 2-Fluoroglutarat, das Marta Drozdowska und Bernard T. Golding (Newcastle) synthetisiert worden war, als Substrat oder Inhibitor agiert, wurde sowohl mit dem Methylaspartase Test als auch mittels  $^{19}\text{F}$ -NMR und LC-MS bestimmt. Die Ergebnisse zeigten, dass 2-Fluoroglutarat zwar das Enzym inhibierte aber auch langsam zu einer anderen Verbindung mit gleicher Masse, sehr wahrscheinlich 3-Fluormethylaspartat, umgesetzt wurde. Die weitere Deaminierung zu Fluormethylfumarat konnte nicht beobachtet werden.

Die Bildung, Stabilisierung und Wanderung des primären organischen 5'-Desoxyadenosylradikals zum Substrat wurde kinetisch mit Hilfe folgender Coenzym  $\text{B}_{12}$  Derivative untersucht: 2',5'-Didesoxyadenosylcobalamin, 3',5'-Didesoxyadenosylcobalamin und Peptidoadenosylcobalamin, die von Felix Zelder (Zürich) synthetisiert worden waren; in letzterer Verbindung ist die Ribose des 5'-Desoxyadenosylliganden durch Peptid mit der gleichen Länge ersetzt. Mit diesen modifizierten Kofaktoren konnte zwar der  $\text{E}_2\text{S}_2\text{-B}_{12}$  Komplex rekonstituiert werden, aber nur das 3',5'-Derivat zeigte Aktivität:  $K_m = 0.56 \pm 0.02 \mu\text{M}$ ,  $k_{\text{cat}} = 0.089 \pm 0.01 \text{ s}^{-1}$ . Beim Vergleich mit den Werten für Coenzym  $\text{B}_{12}$ ,  $K_m = 0.52 \pm 0.06 \mu\text{M}$ ,  $k_{\text{cat}} = 1.24 \pm 0.36 \text{ s}^{-1}$ , fällt auf, dass die Bindungseigenschaften fast gleich sind, während der Verlust des 3'-O  $k_{\text{cat}}/K_m$  15-fach erniedrigte. Diese Ergebnisse unterstützen Daten der Röntgenkristallographie und quantenmechanische Rechnungen. Beide Methoden zeigten, dass 2'-OH und 3'-OH Wasserstoffbrücken mit Glutamat E330 und  $\text{C}_{19}\text{-H}$  des Corrinrings bilden. Während eine konstante Brücke zwischen 3'-OH und Glutamat E330 besteht, erleichtern Brückenbildungen zwischen 2'-OH mit Glu330 und 3'-O mit  $\text{C}_{19}\text{-H}$  die Homolyse der Kobalt-Kohlenstoff-Bindung. Diese neuen Interaktionen geleiten das 5'-Desoxyadenosylradikal zum Substrat, dass in einer Entfernung von 6 Å in der sogenannten "arginine claw" gebunden ist. Die kinetischen Daten ergaben mit weniger als 7 kJ, eine wesentlich niedrigere Interaktion als der berechnete Wert von 30 kJ/mol. Sie passen daher viel besser zu der von Peter Friedrich in unserem Labor bestimmten äußerst niedrigen  $\text{C}_{19}\text{-H}$  Azidität.

Kinetische Messungen mit einem Coenzym  $\text{B}_{12}$  Derivat, in dem die untere Ribonukleotidschleife durch ein gleichlanges Peptid ersetzt ist, ergab wieder einen ähnlichen  $K_m = 0.35 \pm 0.05 \mu\text{M}$  aber einen 10-fach niedrigeren  $k_{\text{cat}} = 0.12 \pm 0.01 \text{ s}^{-1}$  im Vergleich zu den Werten von Coenzym  $\text{B}_{12}$ . Offensichtlich bindet das Derivat wie das natürliche Coenzym ähnlich fest ans Enzym, aber in einer leicht veränderten Konformation, die die Homolyse erschwert.

Das *mutL* Gen von *Clostridium tetanomorphum* liegt zwischen den strukturellen Genen der Glutamat-Mutase, *mutE* and *mutS*. Wir spekulieren, dass MutL als ATP-abhängiges Chaperon Co(II)alamin aus inaktiven Glutamat-Mutase-Komplexen entfernt. Die dabei freigesetzten Komponenten MutE und MutS vereinigen sich mit Coenzym B<sub>12</sub> wieder zum aktiven Enzym. Um diese Hypothese zu überprüfen, wurde *mutL* in pASG-IBA3 und pASG-IBA5 Expressionsvektoren über den pre-entry vector IBA-20 kloniert. Die Expression in *E. coli* Rossetta führte zu guten Ausbeuten.

## Summary

Aims of this study were the search for inhibitors of the coenzyme B<sub>12</sub>-dependent glutamate mutase and for insight into the first step of its catalytic mechanism, the homolytic cleavage of the cobalt-carbon bond. Glutamate mutase is composed of two separately isolated protein components S and E<sub>2</sub>, which in the presence of coenzyme B<sub>12</sub> assemble to the active holo-glutamate mutase E<sub>2</sub>S<sub>2</sub>-B<sub>12</sub> that catalyzes the reversible conversion of (*S*)-glutamate to (2*S*,3*S*)-3-methylaspartate. This reaction has been coupled with methylaspartase, which deaminates (2*S*,3*S*)-3-methylaspartate to mesaconate absorbing at 240 nm, to allow activity assays for glutamate mutase by UV-spectrophotometry. As potential inhibitors, compounds with *sp*<sup>2</sup>-centers and structural analogies to the intermediate radicals in the proposed mechanism were selected. Analogues to the 4-glutamyl radical were (*E*)- and (*Z*)-glutaconates, whereas analogues to the (2*S*,3*S*)-3-methyleneaspartate radical included itaconate, buta-1,3-diene-2,3-dicarboxylate, fumarate, maleate and mesaconate. Because all these compounds inhibited the auxiliary enzyme methylaspartase, glutamate mutase was incubated with these compounds for a certain time, followed by gel filtration on Sephadex G25. The residual activity of the inactivator-free enzyme was then determined by the coupled assay described above, whereby unexpectedly fumarate, maleate and mesaconate caused inactivation of the mutase. To check whether the other compounds acted as reversible inhibitors, a new assay with (2*S*,3*S*)-3-methylaspartate and pyruvate as substrates involving glutamate-pyruvate aminotransferase and the NADH-dependent (*R*)-2-hydroxyglutarate dehydrogenase was developed. Application of this assay showed that 2.5 mM itaconate and 8 mM (*E*)-glutaconate inhibited glutamate mutase in the presence of 200 mM (2*S*,3*S*)-3-methylaspartate by 50%. Furthermore, the kinetic constants of (2*S*,3*S*)-3-methylaspartate in the reaction of glutamate mutase were determined as  $K_m = 7 \pm 0.07$  mM,  $k_{cat} = 0.54 \pm 0.06$  s<sup>-1</sup> and  $k_{cat}K_m^{-1} = 77$  s<sup>-1</sup>M<sup>-1</sup>. Together with the kinetic constants of (*S*)-glutamate determined with the methylaspartase assay ( $K_m = 2.25 \pm 0.03$  mM,  $k_{cat} = 2.85 \pm 0.5$  s<sup>-1</sup> and  $k_{cat}K_m^{-1} = 1.3 \times 10^{-3}$  s<sup>-1</sup>M<sup>-1</sup>), an equilibrium constant of  $K_{eq} = [\text{glutamate}] \times [\text{methylaspartate}]^{-1} = 16$  was calculated by the Briggs-Haldane equation close to that described in the literature ( $K_{eq} = 12$ ).

Whether 2-fluoroglutarate acted as substrate or inhibitor was analyzed by the coupled assay as well as by  $^{19}\text{F}$  NMR and LC-MS. The results showed that 2-fluoroglutarate inhibited the enzyme but was slowly converted to most likely 3-fluoromethylaspartate, which was not deaminated by methylaspartase.

The formation, stabilization and movement of the primary organic 5'-deoxyadenosylradical to the substrate was kinetically investigated by the coenzyme  $\text{B}_{12}$  derivatives 2',5'-dideoxyadenosylcobalamin, 3',5'-dideoxyadenosylcobalamin and peptidoadenosylcobalamin. In the latter compound the ribose of the 5'-deoxyadenosyl ligand was replaced by a peptide of the same length. These modified cofactors accomplished the reconstitution of holo-glutamate mutase but only the 3',5'-dideoxy derivative gave measurable activity:  $K_m = 0.56 \pm 0.02 \mu\text{M}$ ,  $k_{\text{cat}} = 0.089 \pm 0.01 \text{ s}^{-1}$ . When compared with the values for coenzyme  $\text{B}_{12}$ ,  $K_m = 0.52 \pm 0.06 \mu\text{M}$ ,  $k_{\text{cat}} = 1.24 \pm 0.36 \text{ s}^{-1}$ , the almost equal  $K_m$  suggested similar binding properties to the enzyme, whereas the loss of the 3'-oxygen caused a 15-times reduced  $k_{\text{cat}}/K_m$ . These results support data from X-ray crystallography as well as from quantum mechanical calculations, which revealed hydrogen-bond interactions of the 2'- and 3'-oxygens with the conserved glutamate residue 330 of component E of glutamate mutase and  $\text{C}_{19}\text{-H}$  of the corrin ring of the coenzyme. The calculations established a constant interaction of 3'-OH with Glu330, whereas the homolytic cleavage of the cobalt-carbon bond was promoted by the emerging hydrogen bonds of 2'-OH with Glu330 and 3'-O with  $\text{C}_{19}\text{-H}$  of the corrin ring. This new interactions guide the 5'-deoxyadenosylradical to the substrate bound in the "arginine claw" 6.6 Å apart from the cobalt. The kinetic data, however, revealed an interaction between  $\text{C}_{19}\text{-H}$  and 3'-O of less than  $7 \text{ kJmol}^{-1}$ , much lower than the calculated value of  $30 \text{ kJ/mol}$ , which is in complete agreement with measurements of the low  $\text{C}_{19}\text{-H}$  acidity.

Kinetic investigations with a derivative of coenzyme  $\text{B}_{12}$ , in which the ribonucleotide loop connecting the lower ligand of the cobalt atom, 5,6-dimethylbenzimidazole, to the corrin ring was replaced by a peptide, again revealed a similar  $K_m = 0.35 \pm 0.05 \mu\text{M}$  but a 10-fold lower  $k_{\text{cat}} = 0.12 \pm 0.01 \text{ s}^{-1}$ . Apparently, this derivative binds to the enzyme in a similar tight manner as coenzyme  $\text{B}_{12}$ , but in a slightly different conformation that impedes homolytic cleavage of Co-C bond.



The *mutL* gene from *Clostridium tetanomorphum* is located between the structural genes of glutamate mutase. We speculate that MutL acts as chaperone, which removes cob(II)alamin from inactive glutamate mutase complexes in an ATP dependent manner. The liberated components E<sub>2</sub> and S recombine with coenzyme B<sub>12</sub> to form a new active enzyme. To check this hypothesis, *mutL* was successfully cloned on pASG-IBA3 and pASG-IBA 5 expression vectors via the pre-entry vector IBA-20. The MutL chaperone was produced in *E. coli* Rossetta in good yields

# 1. Introduction

## 1.1 The anti-pernicious anemia discovery of vitamin B<sub>12</sub>

The corrinoid cobalt complex vitamin B<sub>12</sub> was discovered from diet in relation to the treatment of pernicious anemia (PA) after almost a century of the search for the cause and cure of pernicious anemia (PA) from the mid of the 19<sup>th</sup> century. An earliest literature on the PA as authored by a Scottish physician J S Combe appears in the 1824 Transactions of Medico-Chirurgical Society in Edinburgh.<sup>1</sup> Twenty five years later the foremost clinical descriptions for the disease were presented by an English physician, Thomas Addison at the meeting of the South London Medical Society in 1849.<sup>2</sup> Addison's accounts defined the pallor, weakness and a progressive decline in health which culminated to death as the diagnostic symptoms for the idiopathic anemic syndrome which was later named after him.<sup>2,3</sup>

However, the cause for the disease remained uncertain throughout during the 19<sup>th</sup> century with emerged cases which were clinically diagnosed concurrent with neurological symptoms as first reported in the late 1860s by a German physician Anton Biermer.<sup>4</sup> Despite with insufficient details, further descriptions for associating PA with spinal cord lesions followed in 1887 and 1900 by Lichtheim and Russell respectively.<sup>5</sup> A breakthrough for understanding PA association with the neurological disorders came in 1922 when Arthur Hurst at Guy's Hospital in London revealed the same underlying pathological cause for the two diseases.<sup>6</sup> Hurst's finding also established the relation between the two diseases with the loss of hydrochloric acid in gastric juice as earlier demonstrated by Cahn and Mering in 1886.<sup>7</sup>

Despite the recognitions on the influence of diet in the recovery of PA patients by the disease earlier investigators; Habershon (1863), Biermer (1872) and Pepper (1875),<sup>8,9</sup> greater emphasis on investigations for the identification of nutritional components related to anti-PA began five decades later. It was from the early 1920s studies of food efficacy in restoring haemoglobin level of experimental anemic dogs: George Whipple reported liver was the most effective.<sup>10</sup> Expanding the work of Whipple and other medical records, George Minot and William Murphy successfully treated 45 PA patients with enormous liver diet in 1926.<sup>11</sup>

The publication of the therapy by Minot and Murphy prompted investigations for searching the liver component which is responsible for the recovery of the PA patients. Further studies on factors contributing to the therapy by William Castle in 1926 revealed the recovery of only PA patients fed with both liver and gastric juices taken from stomachs of health individuals. Non-response of patients fed with only one factor, either liver or gastric juice as control experiments, led to Castle's descriptions on the requirement of the interactions between the liver and stomach respectively extrinsic and intrinsic factors for the health status.<sup>12</sup> Endeavors to identify the liver factor by various laboratories was accomplished in 1948 when Folkers at Merck research laboratories in New Jersey successfully isolated small quantities of red crystalline compound from relative large amount of liver.<sup>13</sup> Microgram quantities of the crystalline compound which was branded as vitamin B<sub>12</sub> elicited rapid haematological restorations in PA patients.

## 1.2 Vitamin B<sub>12</sub> structure

Preliminary chemical analysis for the determination of the isolated liver crystalline vitamin composition disclosed its cyano and cobalt contents. In the same year of isolation, E.L. Smith at Glaxo research laboratories in Greenford reported about 11.7 to 13.9% of nitrogen content in the crystalline.<sup>14</sup> Despite the several efforts for structure elucidation by various laboratories, it was not until 1954 when Dorothy Hodgkin and her group in Oxford solved the complete structure of the liver isolated vitamin B<sub>12</sub> by using x-ray crystallography.<sup>15, 16</sup>

The x-ray crystal structure revealed an octahedral complex of nearly planar porphyrin resembling a macro corrinoid core constructed from 3,4-dihydro-2H-pyrrole subunits which provide nitrogen atoms for the completion of complex four equatorial coordinates to the central cobalt atom. The complex  $\alpha$ -coordinate (lower face) is completed by a dimethylbenzyl imidazole which is covalently bonded to D-ribonucleotide. The latter structure is linked back to the corrinoid system by a phosphodiester bond and has been useful in defining the vitamin B<sub>12</sub> derivatives cobalamins as those corrinoid complexes of cobalt with  $\alpha$ -dimethylbenzyl imidazole-D-ribonucleotide coordinate that distinguishes them from pseudocobalamins. The structure of the  $\beta$ -coordinate (upper face) specifies the cobalamin among the existing four forms.

As revealed in the preliminary chemical analysis and later x-ray crystallography, the liver crystalline vitamin was isolated with a cyano-group completing the upper coordinate for which it has also being known as cyanocobalamin (**1**). Generally referred as vitamin B<sub>12</sub>, cyanocobalamin (**1**) is widely used as a food additive through which consumers of processed food are supplied with the vitamin. However, cynocobalamin (**1**) does not exist in any biological system and the original liver isolate was an artifact due to the used purification protocol which involved treatment with potassium cyanide.<sup>17</sup>

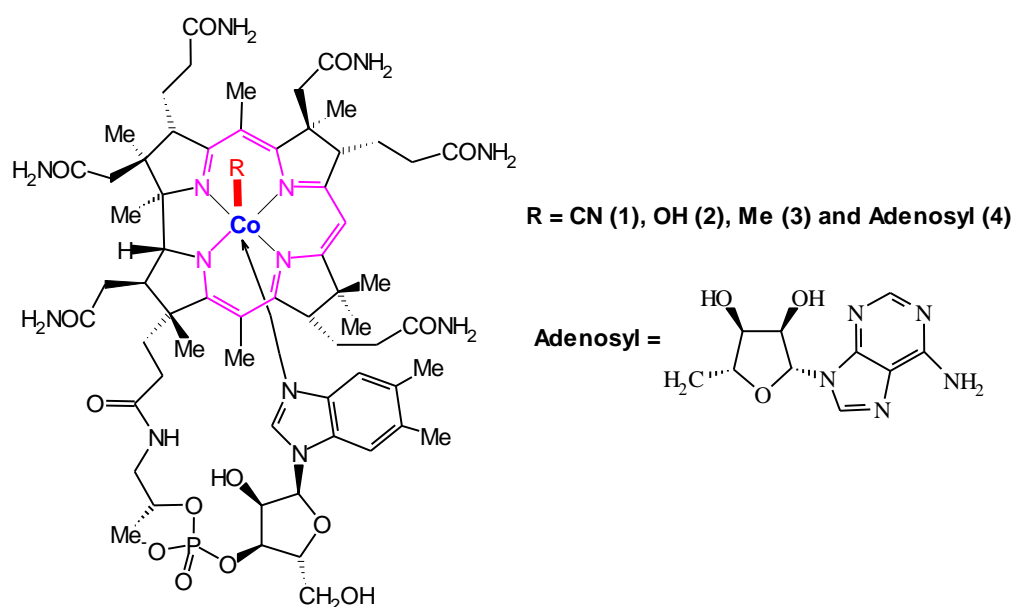


Figure 1: Structures of vitamin B<sub>12</sub> derivatives

Other cobalamins are; hydroxocobalamin (**2**), known as from the β-hydroxyl ligand and the biological active forms; methylcobalamin (**3**) and adenosylcobalamin (**4**) with respective methyl and adenosyl groups completing the β-coordinate. Adenosylcobalamin (**4**), which is also known as the coenzyme B<sub>12</sub>, as well as the methylcobalamin (**3**), are cofactors for several known reactions of archaea, bacteria and higher animals. Most of the industrial used bacteria for commercial production of vitamin B<sub>12</sub> biosynthesize hydroxycobalamin (**2**), which is converted to cyanocobalamin (**1**) during the purification stage that employs an activated charcoal.

Also industrial important are mixed culture fermentation that give a mixture of hydroxycobalamin (2), methylcobalamin (3), and adenosylcobalamin (4) which are converted to cyanocobalamin (1) by heating with potassium cyanide and sodium nitrite.

Determinations on the magnetic properties of cobalamins revealed the octahedrals diamagnetisms in all four forms of cobalamins. These diamagnetisms have been demonstrated by the existence of Co(III) state with ( $d^6$ ) configuration. The alterations between the 2 electrons filled  $d_z$  orbital Co(III) with the Co(II) which is filled with 1 electron in the  $d_z$  orbital, as well as the Co(I) which contains 2 electrons in the  $d_z$  orbital during the respective coenzyme B<sub>12</sub> and methylcobalamin co-enzymatic catalysis cause changes in both the UV/Vis absorptions and the magnetic properties of cobalamin. These redox states changes have been followed spectrophotometrically in both the coenzyme B<sub>12</sub> and methylcobalamin dependent reactions.<sup>18, 19</sup> The Co(II) state cause paramagnetisms and absorption peak at 470 nm, whereas Co(I) retains diamagnetism with maximum absorption peak close to 400 nm, hence provided insights on the two cofactors mode of actions.

### **1.3 Vitamin B<sub>12</sub> transport and delivery**

#### **1.3.1 The gastrointestinal pathway for vitamin B<sub>12</sub>**

In contrast to those archaea and bacteria species, which are able to synthesize cobalamins, higher animals depend on vitamin B<sub>12</sub> supplied with diet. Although the amount of the vitamin B<sub>12</sub> differs with food type, most contain enough quantity to meet the minimum requirement for the health status. An individual is required to ingest 1-2  $\mu\text{g}$  of the vitamin per day.<sup>20</sup> The main vitamin B<sub>12</sub> source for humans include liver, meat, fish, eggs and milk. In access to balance diet, an adult ingests between 5 to 30  $\mu\text{g}$  of vitamin B<sub>12</sub> daily, from which about 2 to 3 mg is retained by the body store of cobalamin with permanent reserve of about 1 mg in the liver.<sup>21</sup>

Three soluble carrier proteins; haptocorrin (HP), intrinsic factor (IF) and transcobalamin (TC) are involved in the uptake of vitamin B<sub>12</sub> along the gastrointestinal track and circulation to its two intracellular destinations; cytosolic methionine synthase and mitochondrial methylmalonyl -CoA mutase, where it plays a role as coenzyme.<sup>22-25</sup> Cobalamins bound to diet proteins are usually

released during food preparation or due to acidic conditions of gastrointestinal tract and actions of peptic enzymes after which they bind to haptocorrins (HP) present in saliva during ingestion. Secreted by saliva glands and gastric mucosa, haptocorrins (HP) bind cobalamins with high affinity in low pH and therefore protect them from the acidic environment as well as intestinal bacteria while transported along the track. The decreased cobalamins affinities to haptocorrins due to the increased pH in duodenum together with the digestion of carrier proteins by the action of pancreatic enzymes liberate cobalamins which are then taken by intrinsic factors in intestines.<sup>26</sup> Intrinsic factors are secreted with gastric juices in stomach but bind cobalamins at the alkaline pH in intestines where they assist their transportation across intestinal enterocyte to circulation by cubilin mediated IF-B<sub>12</sub> endocytosis.<sup>27,28</sup> It takes up to 4 hours after ingestion for cobalamins to enter the circulation where they bind transcobalamins (TC) present in blood plasma. Up to 1.4 µg per day of vitamin B<sub>12</sub> from enterohepatic circulation is excreted via bile salts through which it lost from being taken intracellular.<sup>21</sup> With such a discharge amount, the several years of optimal B<sub>12</sub> level after an individual absorption has been impaired is accounted by the fact that the enterohepatic circulation is coupled with total body reserve of B<sub>12</sub>. The plasma TC-B<sub>12</sub> complexes are subsequently taken intracellular by membrane receptors mediated endocytosis where cobalamins are freed from TC and exposed for enzymatic transformations to coenzyme forms after the carrier protein digestion by lysozymes.<sup>28</sup>

The delivery of vitamin B<sub>12</sub> from diet to cells consequently requires an intact and functioning gastro-intestinal track. Impairment of any organ involved during its uptake pathway will eventually lead to the vitamin B<sub>12</sub> deficiency diseases due to the decrease of intracellular level of cobalamins as it has been mostly attributed by failure of the vitamin absorption. The current comprehended mechanism for the vitamin uptake along the tract explains the clinical association of PA and neurological symptoms which have been diagnosed concurrent since the mid-19th century era of controversial relation between these two diseases. Mysterious during those times, the cobalamin carrier protein intrinsic factor (IF) was the focus of those earlier landmark descriptions for the relation between the two diseases. Among several, the foremost were; the same underlying pathological cause for PA and its associated neurological lesions which also relates the diseases with the gastric juice by Arthur Hurst in 1920<sup>6</sup> and the existence of intrinsic factor in the stomach that both with the liver factor are necessary for the health status of PA patients by William Castle in 1926.<sup>12</sup>

### 1.3.2 Application of B<sub>12</sub> uptake for delivery of therapeutic agents

The mechanism by which B<sub>12</sub> is shielded from various unfavorable conditions as well as intestinal fauna while transported to cells along the gastrointestinal track promises the provision of a reliable mean for delivery of molecules into cells. Potentials for protection against enzymatic degradation and efficiencies in absorption from intestines while coupled with B<sub>12</sub> have brought particular interest to parenteral administered peptides and protein drugs. Developments to exploit the B<sub>12</sub> diet uptake pathway for oral delivery of therapeutic agents have therefore gained extraordinary attention over the last five decades. However, the effective delivery through the pathway is relying on the ability of those therapeutic agents to travel with the vitamin without interfering with its uptake mechanism while remain unaltered. Vital to success has therefore been the coupling of B<sub>12</sub> with an agent in a manner such that neither is impeded by the other.<sup>21</sup> Restoration of carrier proteins specificities and affinities to the modified vitamin (i.e drug linked B<sub>12</sub>) with achieved agents desired effects at the target require conjugation on functional groups which are not involved in either molecule mechanism.

Several endeavors by various laboratories to combine these acquaintances toward delivery of drugs and radiopharmaceuticals have been reported. Attempted exploitation of the uptake mechanism to deliver peptide and protein drugs employed various length of spacer linkers which achieved tuning to ideal recognition and affinity of modified B<sub>12</sub> to carrier proteins as well as absorption from intestines. B<sub>12</sub> offers three sites for conjugation with this class of drugs;  $\epsilon$ -propionamide,  $\alpha$ -5'-hydroxy and  $\alpha$ -phosphate (Figure 2a).<sup>21, 29</sup> Among the described successful deliveries since 1990s include that of a 34 kDa erythropoietin (EPO), which stimulate erythroid progenitors maturation to erythrocytes for increasing erythrocytes count in patients receiving kidney treatment by dialysis. The oral delivery of granulocyte-colony-stimulating factor (G-CSF) (19.6 kDa) by B<sub>12</sub> for increasing the production of leucocytes during chemotherapy treatment of cancer was also reported.<sup>30,31</sup> Other published results from this area include the delivery of 1.2 kDa luteinizing-hormone-releasing hormone (LHRH) and 1.6 kDa LHRH antagonists (ANTIDE).<sup>32</sup> LHRH and LHRH ANTIDE proteins have been used for management of disorders which arises in due to the impairment of gonadotropin level. The coupling of insulin (5.7 kDa) with B<sub>12</sub> and its subsequent delivery to circulation via the oral route has also been reported (Figure 2b).<sup>33</sup> Delivering insulin into the circulation is necessary for maintaining optimal level of

sugar in blood of diabetic patients. Synthesis for delivery of EPO, G-CSF and ANTIDE employed linkers which conjugated the proteins from  $\epsilon$ -propionamide on the B<sub>12</sub> while insulin was linked from either  $\epsilon$ -propionamide or  $\alpha$ -5'-hydroxy with maximal affinities to IF as well as absorption to circulation from intestines.

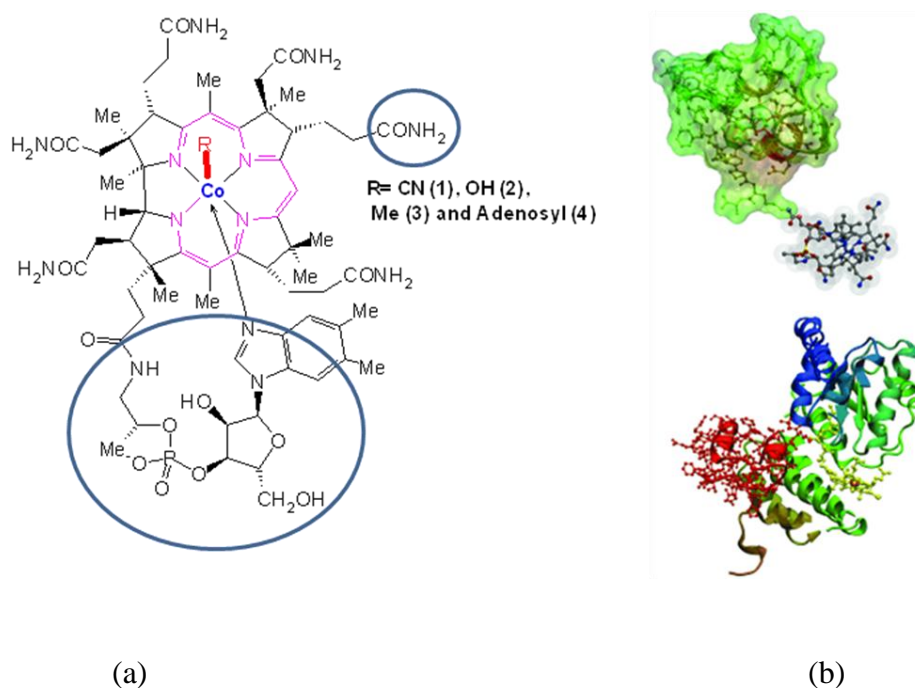


Figure 2 (a) Cobalamins functional groups (in circle) for conjugations to peptides/protein drugs with optimal affinities of the modified vitamin to the transporting proteins HP, IF and TC. (b) Top: vitamin B<sub>12</sub> conjugated to insulin by linker which connects the vitamin ribose hydroxyl group with lysine 29 residue of insulin B strand. Bottom: The modified vitamin B<sub>12</sub> i.e B<sub>12</sub>-insulin conjugate bound to transcobalamin<sup>21</sup>

Other studies for exploring the applications of B<sub>12</sub> uptake have been those aimed to deliver metal agents for both diseases diagnosis and treatment. There have been many reports from this line of research including the synthesis and hypoglycemic properties of vanadium-B<sub>12</sub> bioconjugates<sup>34</sup> (figure 3) and those for developing B<sub>12</sub>-conjugated radiolabelled agents for tissue imaging and cytotoxicity.<sup>35, 36</sup> Among several reported successful delivery of imaging agents has been the results of the studies based on the fact that rapid proliferating cells up-regulate transcobalamin II receptors during DNA replication in preparations for cells division. This hypothesis led to the work which achieved the delivery of radiolabelled diethylenetriaminepentaacetate (DTPA) cobalamin derivatives for imaging malignant and non-malignant transcobalamin II expressing



tissues.<sup>37</sup> Pilot experiments with animals have led to recommendations for further development towards the in vivo application of DTPA cobalamin derivative in imaging transcobalamin II expressing tissues. Hypothetical relation to the transcobalamin II target of DTPA is that for studies which aimed towards the development of B<sub>12</sub> mediated endocytosis of therapeutic agents in choriocarcinoma placental BeWo cell lines. These cells express cubilin receptors for anchoring IF-B<sub>12</sub> complex. Cubilins were targeted for selectively delivery of B<sub>12</sub> conjugated rhenium complex bioprobe in experiments which reported uptake and cytotoxicity effects of the complex as well as its interaction with nuclear DNA.<sup>38</sup> This study has demonstrated the potential of cubilin mediated endocytosis in delivering B<sub>12</sub> conjugated agents which can be used in both diagnosis and treatment of cancer.

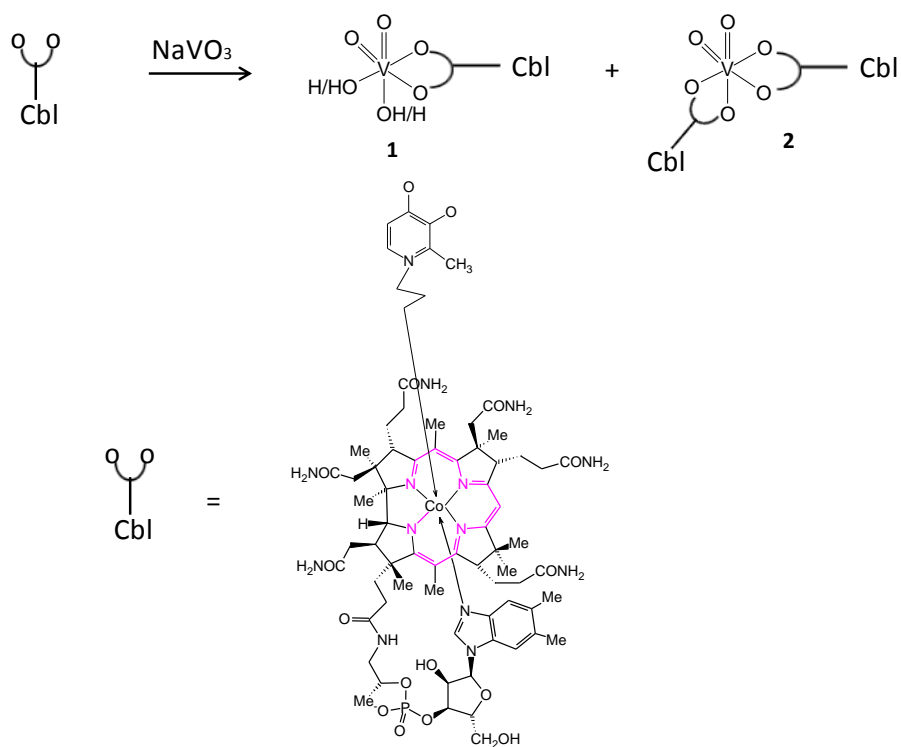


Figure 3: Structures of hypoglycemic mono- (**1**) and bis- (**2**) ligated vanadium-B<sub>12</sub> conjugates<sup>34</sup>

## 1.4 B<sub>12</sub> dependent enzymatic reactions

The B<sub>12</sub> dependent enzymes are found in archaea, bacteria and higher animal domains where they are involved in the catalysis of various reactions for several biosynthesis and energy conservation metabolisms. The classification of these enzymes into three major groups; 1) methylcobalamin, 2) coenzyme B<sub>12</sub> and 3) cob(I)alamin dependent enzymes has based on the participating cobalamin cofactor during their respective reactions.<sup>39</sup> While the methylcobalamin dependent enzymes catalyze the addition of methyl group to substrate and therefore conversion to the methylated product, the coenzyme B<sub>12</sub> dependent group comprises enzymes which catalyze the skeletal rearrangement of substrates to their structure isomers products. The described environmental useful cob(I)alamin mediated abiotic and enzymatic dehalogenations have form a third type of B<sub>12</sub> dependent reactions.

### 1.4.1 The cob(I)alamin dehalogenations

The cob(I)alamin mediated dehalogenations have been generally postulated to proceed via the S<sub>N</sub>2 substitution reaction of cob(I)alamin with alkyl halides which form an alkylcobalamin as an intermediate of the catalytic cycle. Conversely, the well studied abiotic reductive dehalogenation of polychlorinated ethenes revealed cob(I)alamin initiates the reaction by releasing an electron which is transferred to the halogenated ethene. This one electron reduction lead to a free polychlorinated ethene radical that proceed by disintegration to halogenide ion and dehalogenated product related radical which is further reduced to dehalogenated product.<sup>40, 41</sup> Reduction rates for these cob(I)alamin mediated dehalogenations highly depend on the number of halogen substituents on the organohalide as verified by the 82,000-times lower rate of vinylchloride dehalogenation in comparison to that of CCl<sub>4</sub>.<sup>40, 42</sup>

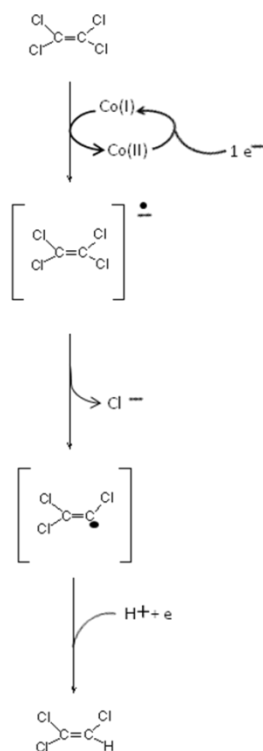


Figure 4: The proposed mechanism for the abiotic cob(I)alamin mediated reductive dechlorination of tetrachloroethene<sup>40</sup>

The mechanism for dehalogenation of polychlorinated ethenes by reductive dehalogenases from *Dehalobacter restrictus*, *Dehalospirillum multivorans* and *Desulfitobacterium* strain PCE-S has also been proposed to be initiated by cob(I)alamin. In these enzymatic dehalogenations, which are believed to be in compliance with the largely accepted tentative mechanism, the cob(I)alamin is alkylated by chlorinated ethene in the S<sub>N</sub>2 substitution which is followed by heterolytic cleavage of the alkylated cobalamin Co-C bond into cob(III)alamin and chlorinated ethene with the loss of chloride ion.<sup>43, 44</sup> Electrons generated from oxidations of Fe-S clusters reduce the former to cob(I)alamin via cob(II)alamin to complete the redox cobalamin reductive dehalogenation cycle.

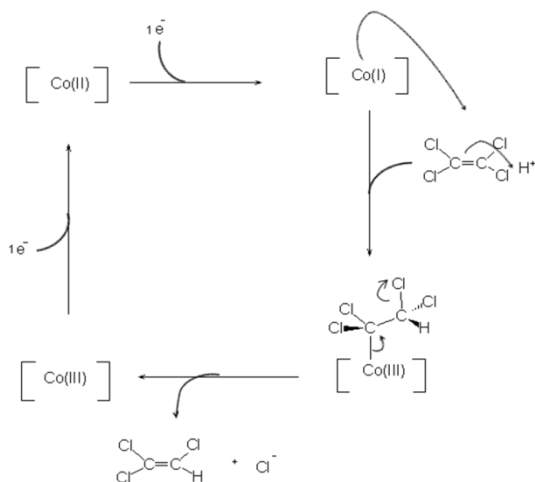


Figure 5: Proposed mechanism for the dehalogenases catalyzed reductive dechlorination of tetrachloroethene via the addition of cob(I)alamin at C1 which is followed by the loss of  $\text{Cl}^-$  at C2 <sup>40</sup>

Since chlorinated hydrocarbons also occur naturally,<sup>45</sup> this redox cobalamin mechanism for their reductive dehalogenations has been considered to evolve specifically for the bacterial adaptation on these xenobiotics well before their industrial use. Recent era of industrial pollutions by these organochlorines have led to the exploration of the mechanism for possible application in bioremediations of polychloroethenes polluted environments.

#### 1.4.2 Methylcobalamin dependent enzymatic reactions

The three types of methylcobalamin dependent enzymes; methionine synthase, CoM methyltransferase and corrinoid Fe/S proteins are known to catalyze the transfer of a methyl group from pterin compounds to nucleophilic substrates, usually thiolated compounds with potential to accept methyl carbocation (Table 1).<sup>46</sup> The mechanism for methylations by these enzymes proceeds via the heterolytic cleavage of the methylcobalamin Co-C  $\beta$ -coordinate resulting into the super nucleophile cob(I)alamin and methyl carbocation. The latter is subsequently accepted by a thiol group of the substrate to give the methylated product. The catalytic cycle achieves the regeneration of methylcobalamin through the donation of the methyl

group by activated pterins,  $N^5$ -methyltetrahydrofolate or  $N^5$ -methyltetrahydromethanopterin to cob(I)alamin.

<b>Methyltransferases</b>	<b>Cobalamin dependent methyltransferases reactions</b>	<b>Methyl donors</b>
Methionine synthase	$\text{Homocysteine} + \text{CH}_3\text{-H}_4\text{folate} \rightarrow \text{Methionine} + \text{H}_4\text{folate}$	$N^5$ -methyltetrahydrofolate
CoM methyltransferase	$\text{CH}_3\text{-H}_4\text{MPT} + \text{HSCoM} \rightarrow \text{H}_4\text{MPT} + \text{CH}_3\text{-SCoM}$  $\text{CH}_3\text{-OH} + \text{HSCoM} \rightarrow \text{CH}_3\text{-SCoM} + \text{H}_2\text{O}$	$N^5$ -methyltetrahydromethanopterin  Methanol
Corrinoid Fe/S proteins	(i) $\text{CH}_3\text{-H}_4\text{folate} + \text{Corrinoid/FeS protein} \rightarrow \text{H}_4\text{folate} + \text{CH}_3\text{-corrinoid Fe/S protein}$  (ii) $\text{CH}_3\text{-corrinoid Fe/S protein} + \text{CO dehydrogenase} \rightarrow \text{Corrinoid Fe/S protein} + \text{CH}_3\text{-CO dehydrogenase}$	$N^5$ -methyltetrahydrofolate

Table 1: Cobalamin dependent methyltransferases catalysed transfer of methyl group from pterins or methanol (methyl donors) to nucleophilic substrates (usually thiolated compounds) which are transformed to methylated products

The de novo biosynthesis of pterins is restricted to certain plants and bacteria. Similar to cobalamins, in mammals pterins are supplied via diet and recycled by various folate dependent metabolic pathways like those for thymidylate biosynthesis (figure 12). Main diet source of folate include leaf vegetables, egg yolks, sunflower seeds, legumes e.g beans and peas, as well as baker's yeast. Liver provides a secondary source of folate to human since it contains derivatives of folate metabolites. In some countries fortifications of grains with vitamin B9 have been useful in supplementing diet with folate.

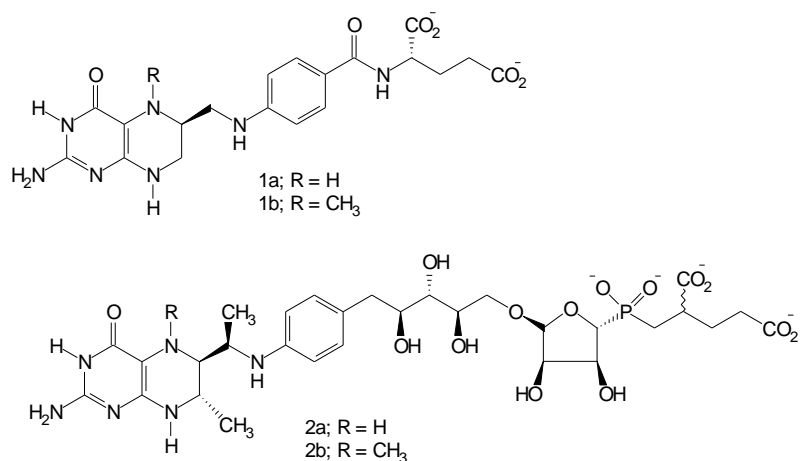


Figure 6: Structures of pterins methyl donors in methylcobalamin dependent methyltransferase reactions: tetrahydrofolate (1a),  $N^5$ -methyltetrahydrofolate (1b), tetrahydromethanopterin (2a) and  $N^5$ -methyltetrahydromethanopterin (2b)

The well-studied bacterial (136 kDa) and mammalian (141-155 kDa) methionine synthase systems catalyse the addition of a methyl group donated by  $N^5$ -methyltetrahydrofolate (5) to homocysteine (6) which is converted to methionine (7).<sup>46, 47, 48</sup> While in bacteria this methylation forms the last step of the de novo bio-synthesis of methionine, in mammals it is also significant in recycling of homocysteine via methionine. Being a proteinoic amino acid, the methionine is either incorporated in protein during the translation of the mRNA codons to peptide amino acid sequence, or converted to S-adenosylmethionine (SAM) (8) during its ATP dependent reaction with an adenosine which is catalyzed by S-adenosylmethionine synthase. The positive charged sulfur atom in SAM promotes the leaving of methyl group as carbocation, hence makes SAM to be a potent methylating agent for various biological nucleophiles. During these SAM dependent specific methyltransferase catalyzed reactions, SAM is converted to adenosylhomocysteine (9) along with the formation of the methylated products. The hydrolysis of adenosylhomocysteine (9) achieves an adenine and homocysteine (6) which keeps recycling by accepting methyl carbocation donated by  $N^5$ -methyltetrahydrofolate (5) via cob(I)alamin. The deficiency of cobalamin leads to decline of tetrahydrofolate level in cells with increased concentrations of  $N^5$ -methyltetrahydrofolate and homocysteine. The medical consequences resulted from this decrease of the cellular level of tetrahydrofolate is discussed in the section for the medical aspects of B<sub>12</sub> in metabolisms (1.5.1).

The deviations from the primary catalytic cycle resulted from the cob(I)alamin oxidative deactivation or the photolysis of methylcobalamin which form cob(II)alamin are enzymatically re-directed to the catalytic active cob(I)alamin in a single electron reduction process. The electron used in this reductive activation is derived from NADPH and transferred to cobalamin via flavodoxin.<sup>49</sup> Regeneration of methylcobalamin cofactor is subsequent achieved from the irreversible methylation of cob(I)alamin by SAM.<sup>50</sup> Since the cob(I)alamin inactivating oxidant is molecular oxygen, the methionine synthase system for reductive activation has not been required during the enzyme anaerobic turnover.<sup>49, 51, 52</sup>

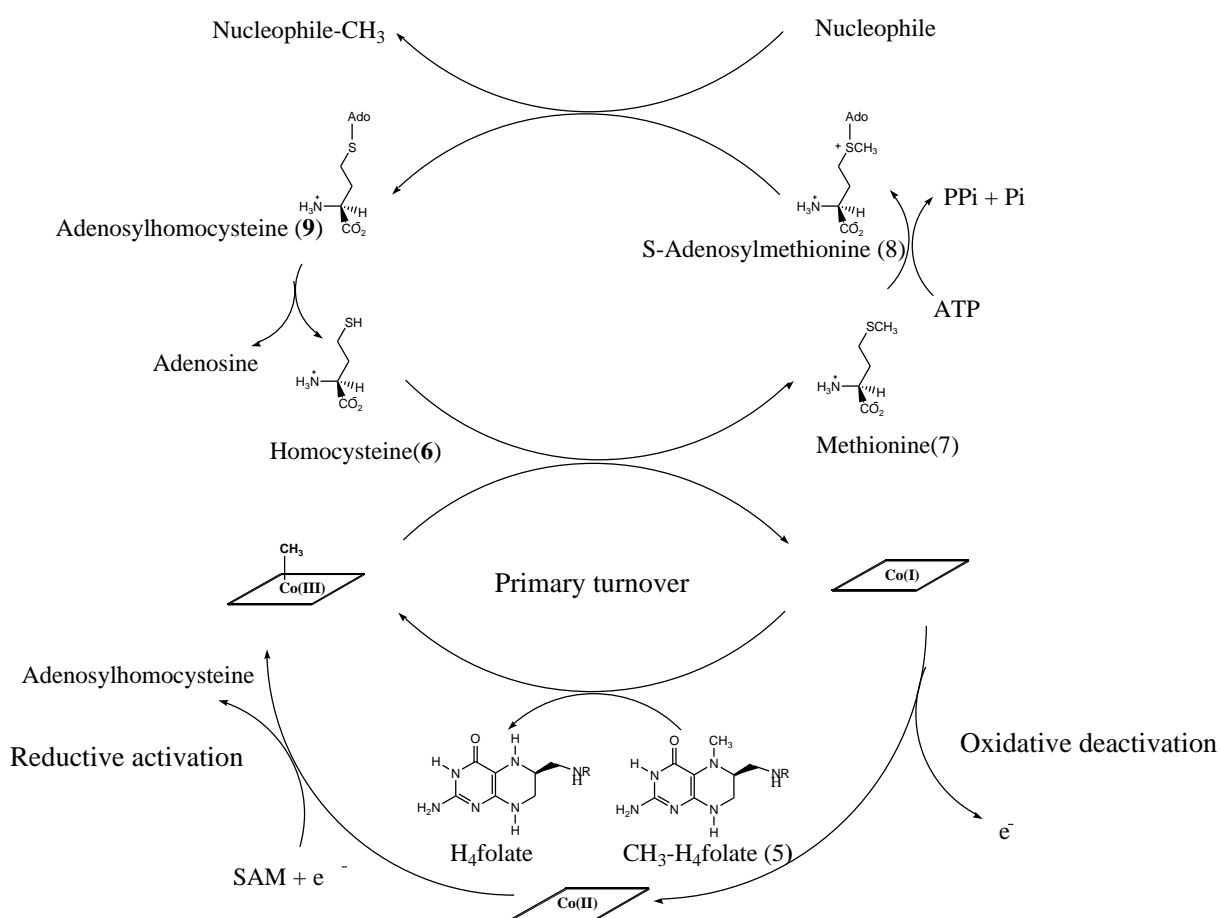


Figure 7: The catalytic cycle of the folate and cobalamin dependent methylation reaction which is catalyzed by methionine synthase. The deviation from the primary turnover due to the oxidative deactivation to cob(II)alamin is enzymatically re-directed to the primary cycle in the one electron reduction to cob(I)alamin by flavin which is followed by the irreversible methylation to methylcobalamin by SAM.

The methionine synthase system efficiently enhances the heterolytic cleavage of the methylcobalamin  $\beta$  coordinate by  $10^5$  folds.<sup>46,53</sup> During the catalytic cycle, the formation of cob(I)alamin from the cofactor bond cleavage as well as cob(II)alamin which resulted from the oxidative deactivation of cob(I)alamin have been demonstrated by UV/Vis spectroscopy.<sup>18,19</sup> Further characterization on the methionine synthase catalytic cycle by EPR spectroscopy also established the formation of cob(II)alamin which disappears following the reductive methylation in consistency with the results of the UV/Vis spectroscopy.<sup>18,47</sup> While in action the holomethionine synthase has been composed of two alternating methylating coenzymes; the  $N^5$ -methyltetrahydrofolate and methylcobalamin which are constantly recycled after their demethylations. Other catalytically significant prosthetic groups are also existing in the methionine synthase as well as the coenzyme M and corrinoid Fe/S methyltransferases. Studies for methionine synthase by proteolytic approach established the four domains modular constitution of the apo-enzyme with defined catalytic functions of its residues.<sup>54, 55, 56</sup> Tryptic digestion of the bacterial methionine synthase led to the enzyme domains fragmentation which allowed experimental verifications of the different catalytic roles by various enzyme regions.<sup>57, 58</sup> The 61 kDa amino terminal fragment was revealed to contain cysteines bound  $Zn^{2+}$ . Purified recombinant protein comprising residue 2-353 of methionine synthase was able to catalyze the transfer of methyl group from free methylcobalamin to homocysteine but not from  $N^5$ -methyltetrahydrofolate to free cob(I)alamin. In another study, a portion containing residue 2-649 of the truncated enzyme was demonstrated with ability to catalyze the transfer of methyl group from  $N^5$ -methyltetrahydrofolate to free cob(I)alamin and further methylation of homocysteine by free methylcobalamin. The Cys310Ala and Cys311Ala mutations of residue 2-649 portion retained only the ability of this fragment to transfer the methyl group from the  $N^5$ -methyltetrahydrofolate to the free cob(I)alamin. The fragment's ability to catalyze the transfer of the methyl group from the free methylcobalamin to homocysteine was completely lost due to these mutations. These results indicate that homocysteine is bound within the residue 2-353 portion of the enzyme whereas the residues 354-649 bind the  $N^5$ -methyltetrahydrofolate.<sup>55</sup> The cysteines bound  $Zn^{2+}$  in the region 2-353 are postulated to act as a Lewis acid by which the homocysteine is activated to accept the methyl carbocation in the course of  $Zn^{2+}$  coordination to the thiol group from the homocysteine.<sup>59</sup> Moreover, the methionine synthase mechanism is fascinating because the supernucleophile cob(I)alamin is unreactive toward  $N^5$ -methyltetrahydrofolate in the absence



of an enzyme because of the unactivated  $N^5$  methyl group on the folate which is in contrast to the non-enzymatic  $S_N2$  methylation of cob(I)alamin by SAM. This folate inertness demonstrates the uniqueness of methionine synthase catalysis that involves the enzymatic activation of  $N^5$ -methyltetrahydrofolate which is necessary for methyl donation in the mechanism with no similarity in conventional chemistry. The activation is predicted to be accomplished within the proximity of the identified folate binding region. Based on the structure of the methyl donor tertiary amine on the  $N^5$ -methyltetrahydrofolate, four mechanisms have been proposed for the activations of the  $N^5$ -methyltetrahydrofolate.<sup>18, 19</sup> Proposed two electrons oxidation on either of the two carbons  $\alpha$  to the methyl donor tertiary amine lead to the formation of the quinoid 5-methyldihydrofolate (8a) and 5-methyl-7, 8-dihydrofolate (8b) intermediates with activated  $N^5$  methyl group due to the quaternization of the folate  $N^5$ . The amine one electron oxidation will form the hypothetical potential methyl donor amine radical (8c). Also proposed mechanism for the  $N^5$ -methyltetrahydrofolate activation is the quaternization of the folate tertiary amine nitrogen by protonation (8d).<sup>18</sup> These proposed activations by oxidations and protonation have exhausted the theoretical mechanistic possibilities for the activation of the methyl donor tertiary amine group on the  $N^5$ -methyltetrahydrofolate.

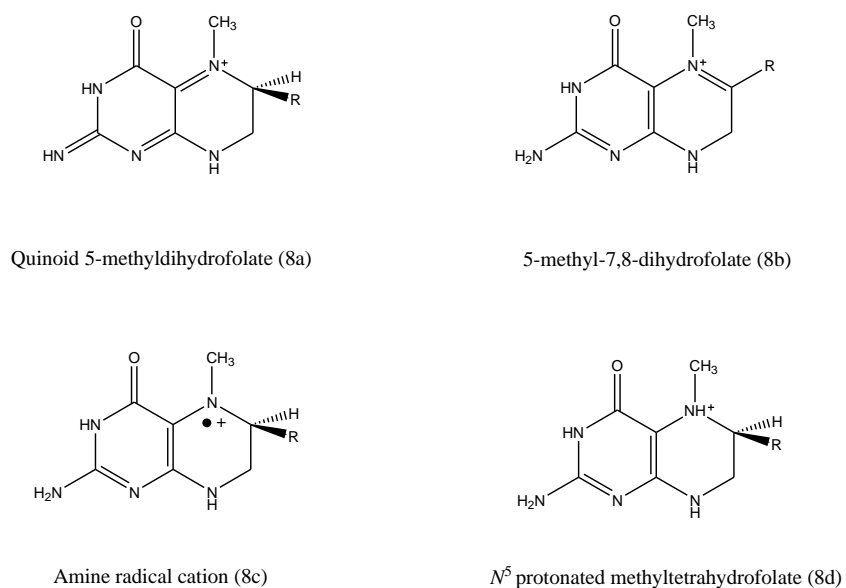


Figure 8: Structures of the proposed activated states of  $N^5$ -methyltetrahydrofolate.<sup>18</sup> The structure of the R group is shown in figure 6

However, the non-existence of any group which can be reduced by the hydride within the holomethionine synthase system has waived the possibilities for the activations by the two electrons oxidations of either of the two carbons  $\alpha$  to the tertiary amine of the  $N^5$ -methyltetrahydrofolate. Furthermore, neither the successful characterization of amine radical cation nor the loss of tritium from the C-6 tritium labeled  $N^5$ -methyltetrahydrofolate when in the solution has been established.<sup>60</sup> The  $N^5$ -methyltetrahydrofolate susceptibility for protonation<sup>61</sup> has suggested the activation by protonation via the intermediate (8d). However, the activation by protonation of  $N^5$  cannot be concluded since atoms which accept protons on the  $N^5$ -methyltetrahydrofolate are yet to be identified.

The cobalamin binding motif, His759-Asp-Ser triad is located within residues 650 to 896 which form a 27 kDa fragment following the partial proteolysis.<sup>58</sup> This 650-896 region was established to be responsible for binding the cobalamin by the x-ray crystallography.<sup>62</sup> The methionine synthase without this cobalamin binding domain catalyses the transfer of methyl group from the  $N^5$ -methyltetrahydrofolate to homocysteine via the free cob(I)alamin.<sup>55</sup> Crystal structure of this cobalamin binding region revealed that methylcobalamin is bound to methionine synthase through cobalt coordination to imidazole from the enzyme his-759 which replaces the dimethylbenzimidazole. This B<sub>12</sub> “base off, his on” binding mode has also been reported in other B<sub>12</sub> partner proteins with conserved triad motif (His-Asp-Ser) for cobalamin binding. Replaced dimethylbenzimidazole in the “base off, his on” binding mode is usually found deposited in protein hydrophobic patches. Residues 897-1227 forms the 38 kDa c-terminal fragment of the methionine synthase which binds SAM.<sup>55</sup> This fragment interacts with the methionine synthase reductase (MSR) which depends on NADPH and diflavin oxidoreductase to accomplish the reductive activation of the cob(II)alamin that arises following the deviation from the catalysis primary turnover resulted from oxidative deactivation of cob(I)alamin or the photolysis of methylcobalamin.<sup>56</sup> Muting of this fragment was characterized with a comparable rate of methyl group transfer from the  $N^5$ -methyltetrahydrofolate to homocysteine with that of complete enzyme, but with decreasing activity after about 2000 turnovers which could not be rescued by SAM.<sup>58</sup> The decreasing of the holoenzyme activity due to the absence of this domain has also been associated with the build up of the cob(II)alamin which provided further evidence for the reductive activation of methionine synthase by this domain.

### 1.4.3 Coenzyme B<sub>12</sub> dependent enzymatic reactions

Coenzyme B<sub>12</sub> dependent enzymes accomplish the catalysis of an unusual vicinal exchange between a hydrogen atom and a functional group on the substrate molecule resulting into skeletal rearrangement to a product which is a structure isomer of the reaction substrate. There are more than ten so far described coenzyme B<sub>12</sub> dependent enzymes, which are classified into two major groups; mutases and eliminases. The rearrangement reactions catalyzed by these enzymes are represented by the below general equation (figure 9), where the migrating group X is usually an electron withdrawing functional group.

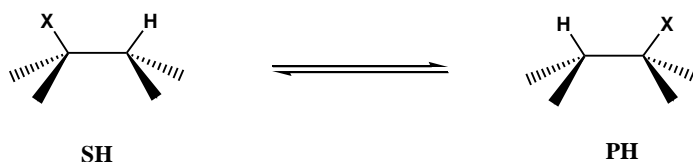


Figure 9: Schematic presentation for the coenzyme B<sub>12</sub> dependent vicinal groups exchange resulting into the rearrangement of substrate (SH) to form product (PH)

Based on their substrate migrating groups; mutases have been further classified into carbon skeleton and amino mutases with respective migrating skeletal carbon structures and amino group of substrates (table 2). While all mutases have the conserved His-Asp-Ser triad motif for “base off, his on” binding of the coenzyme B<sub>12</sub> like in methylcobalamin dependent methyltransferases, in eliminases the coenzyme is bound to a partner enzyme by hydrogen bonding between its various functional groups and active sites protein residues.<sup>63</sup> Since in the latter mode of binding the cobalamin  $\alpha$  Co-N coordinate remain intact when the cofactor is bound to protein as shown only in the described eliminases, hence it has been known as “his-off, base on”. It is therefore important to note that; the “his-off base on” binding of coenzyme B<sub>12</sub> to eliminases represent a third type of mode for cobalamins binding to their partner proteins after “base off his-on” as well as that for binding HP, IF and TC carrier proteins.

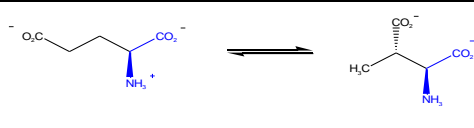
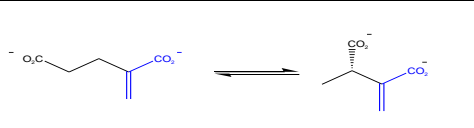
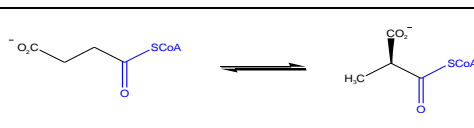
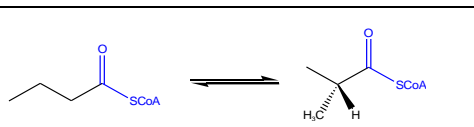
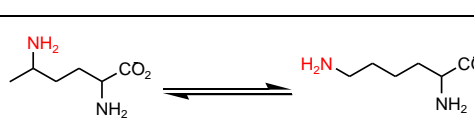
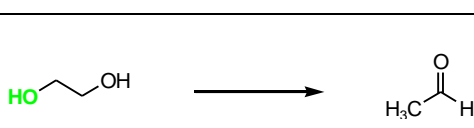
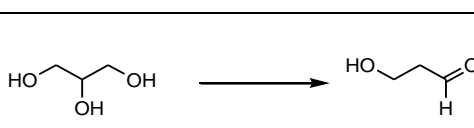
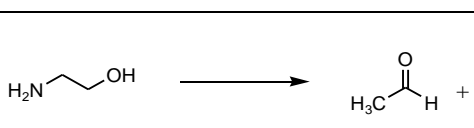
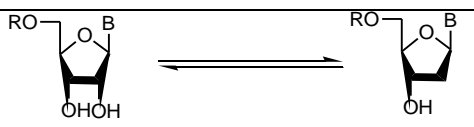
Enzyme	Rearrangment reaction	Group X
Glutamate mutase		-CH(NH <sub>2</sub> )CO <sub>2</sub> H
2-Methyleneglutarate mutase		-C(=CH <sub>2</sub> )CO <sub>2</sub> H
Methylmalonyl-CoA mutase		-COSCoA
Isobutyryl-CoA mutase		-COSCoA
D-α-Lysine-5,6-aminomutase		-NH <sub>2</sub>
1,2-Diol dehydratase		-OH
Glycerol dehydratase		-OH
Ethanolamine amino lyase		-NH <sub>2</sub>
Ribonucleotide reductase		None

Table 2: Selected rearrangement reactions catalyzed by coenzyme B<sub>12</sub> dependent enzymes. The migrating carbon skeleton groups in carbon skeleton mutases are shown in blue and in amino mutase the migrating amine is in red. In the eliminases the migrating groups which are irreversible eliminated are shown in green.

Unlike the methylcobalamin dependent methylations by methyltransferases, the coenzyme B<sub>12</sub> dependent reactions involve the homolytic cleavage of the cofactor Co-C bond that switches to the radical mechanism which accomplishes the rearrangement of substrates to products. The reported 130 kJmol<sup>-1</sup> bond strength of the coenzyme B<sub>12</sub> β coordinate<sup>64</sup> has been predicted to be not exceedingly weak to an extent which will allow the facile homolysis to occur. The addition of extra energy towards the homolysis of Co-C bond during the catalysis by the coenzyme B<sub>12</sub> dependent enzymes has consequently been considered compulsory. This extra energy has long been suggested to be derived from the conformational changes by both the coenzyme B<sub>12</sub> and partner protein which are induced by binding of the substrate to holoenzyme. Although the mechanism by which these enzymes accomplish the bond homolysis is yet to be uncovered, the extent of assistance derived from the conformational changes is estimated to 1 x 10<sup>11</sup>.<sup>65, 66</sup> Coenzyme B<sub>12</sub> dependent reactions are therefore initiated by substrates binding to holoenzymes which triggers the homolysis of the cofactor Co-C β coordinate resulting into the primary organic radical; 5'-deoxyadenosyl and the paramagnetic species; cob(II)alamin (figure 10).

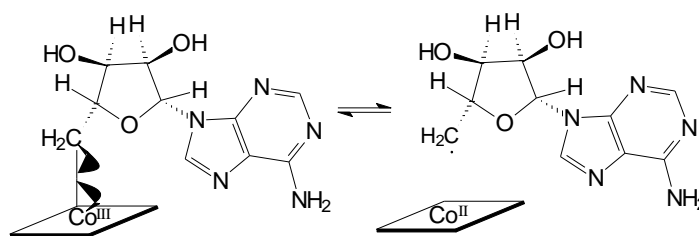


Figure 10: Homolytic cleavage of the coenzyme B<sub>12</sub> Co-C β coordinate resulting into 5'-deoxyadenosyl radical and the paramagnetic species; cob(II)alamin.

The 5'-deoxyadenosyl radical stereo-selectively abstracts hydrogen atoms vinyl to the migrating electron withdrawing functional groups on substrates molecules to give an adenosine and the substrates derived radicals which rearrange to products related radicals. Hydrogen from the methyl group of the 5'-deoxyadenosine is finally claimed back by the product related radical to form the reaction product with regeneration of the coenzyme. The minimal mechanistic scheme for coenzyme B<sub>12</sub> dependent rearrangements shows the hydrogen atom and its vicinal electron withdrawing functional group migrations and subsequent exchange of positions which lead to

products of these reactions. The hydrogen atom migrates inter-molecularly via 5'-deoxyadenosyl radical while that of an electron withdrawing group is happening intra-molecularly.<sup>67, 68</sup>

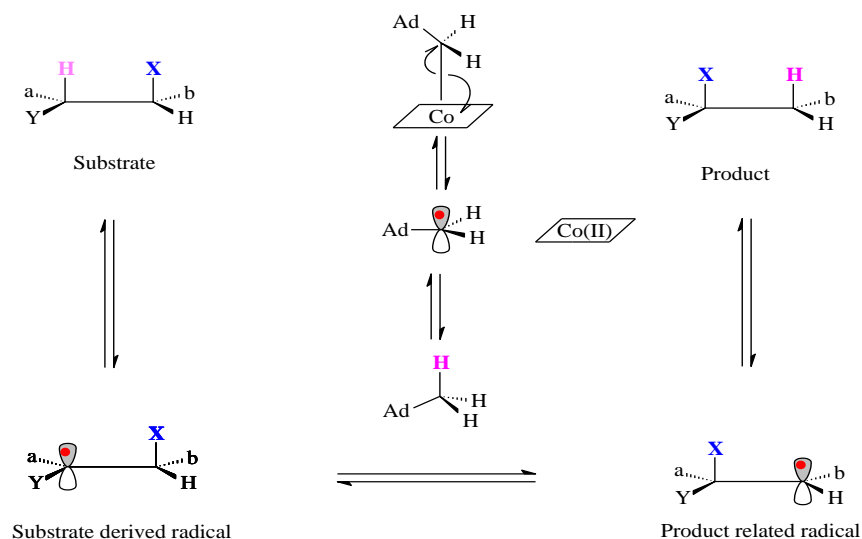


Figure 11: The minimal mechanistic scheme for coenzyme B<sub>12</sub> dependent reactions showing the rearrangement of the substrate to form the reaction product via the intermediates substrate derived and product related radicals<sup>68</sup>

As shown in the minimal mechanistic scheme, the vicinal interchange is reversible in all coenzyme B<sub>12</sub> dependent reactions. In eliminases catalyzed reactions the irreversible loss of the migrating groups occur after the vicinal exchange which leads to their elimination as water or ammonia as implied by the class name.

## 1.5 The diversity of B<sub>12</sub> in metabolism

Exceptions to the methylation of homocysteine (6) to methionine (7) by the methylcobalamin dependent methionine synthase and the coenzyme B<sub>12</sub> dependent rearrangement of methylmalonyl -CoA to succinyl -CoA by methylmalonyl -CoA mutase which are also found in mammals,<sup>69</sup> all other discovered B<sub>12</sub> dependent reactions are confined to archaea and bacteria.

Nature solution to the protection of the highly reactive intermediate radicals from reacting with dioxygen in coenzyme B<sub>12</sub> dependent reactions is restriction of most of these enzymes to strictly

anaerobic organisms where they catalyze intermediate rearrangement reactions for various energy conservation and biosynthesis metabolisms. Besides the fermentations and biosynthesis pathways with intermediate coenzyme B<sub>12</sub> dependent rearrangements, other described metabolisms with intermediate B<sub>12</sub> dependent reactions are those in human beings through which the deficiency of the vitamin consequent lead to PA and neurological disorders. Methylmalonyl-CoA mutase in mitochondria protects the radicals from oxygen by a protein-sealed active site.

Recent reports on coenzyme B<sub>12</sub> dependent rearrangements in bacteria new discovered pathway for acetyl CoA assimilation<sup>70, 71</sup> and the speculation on the intermediate mutase reaction in the tentative pathway for the anaerobic respiration of n-hexane<sup>72</sup> have expanded the diversity of B<sub>12</sub> in metabolism. The highlight of co-enzymatic role by B<sub>12</sub> has therefore spans in wide variety of metabolic pathways from those of medical usefulness with which the vitamin was discovered in relation to human diseases to pathways for biosynthesis, carbon assimilation and anaerobic energy conservations in archaea and bacteria.

### 1.5.1 Medical aspects of B<sub>12</sub> in metabolism

The methionine synthase catalyzed transfer of methyl group from *N*<sup>5</sup>-methyltetrahydrofolate (**5**) to homocysteine (**6**) via cob(I)alamin lead to the formation of methionine (**7**) along with demethylated product; the tetrahydrofolate (**10**). By the action of serine-hydroxymethyl transferase, the latter is converted to 5,10-methylenetetrahydrofolate (**11**) which serves to donate the methyl group during the thymidylate synthase catalyzed methylation of dUMP (**12**) to form dTMP (**13**) for use as a precursor in DNA synthesis. In this methylation, 5,10-methylenetetrahydrofolate(**11**) is converted to 7,8-dihydrofolate(**14**) which together with non demethylated molecules of 5,10-methylenetetrahydrofolate(**11**) are respective reduced to tetrahydrofolate(**10**) and *N*<sup>5</sup>-methyltetrahydrofolate(**5**), hence completing the metabolic cycle. This human metabolic pathway is fundamental to DNA replication as it maintains a constant supply of dTMP which is achieved via the folate-B<sub>12</sub> dependent methyl transfer reaction of methionine synthase.<sup>20</sup> Since the pterin donor of methyl group is *N*<sup>5</sup>-methyltetrahydrofolate, the mammalian methionine synthase has also been known as *N*<sup>5</sup>-methyltetrahydrofolate homocysteine methyltransferase.

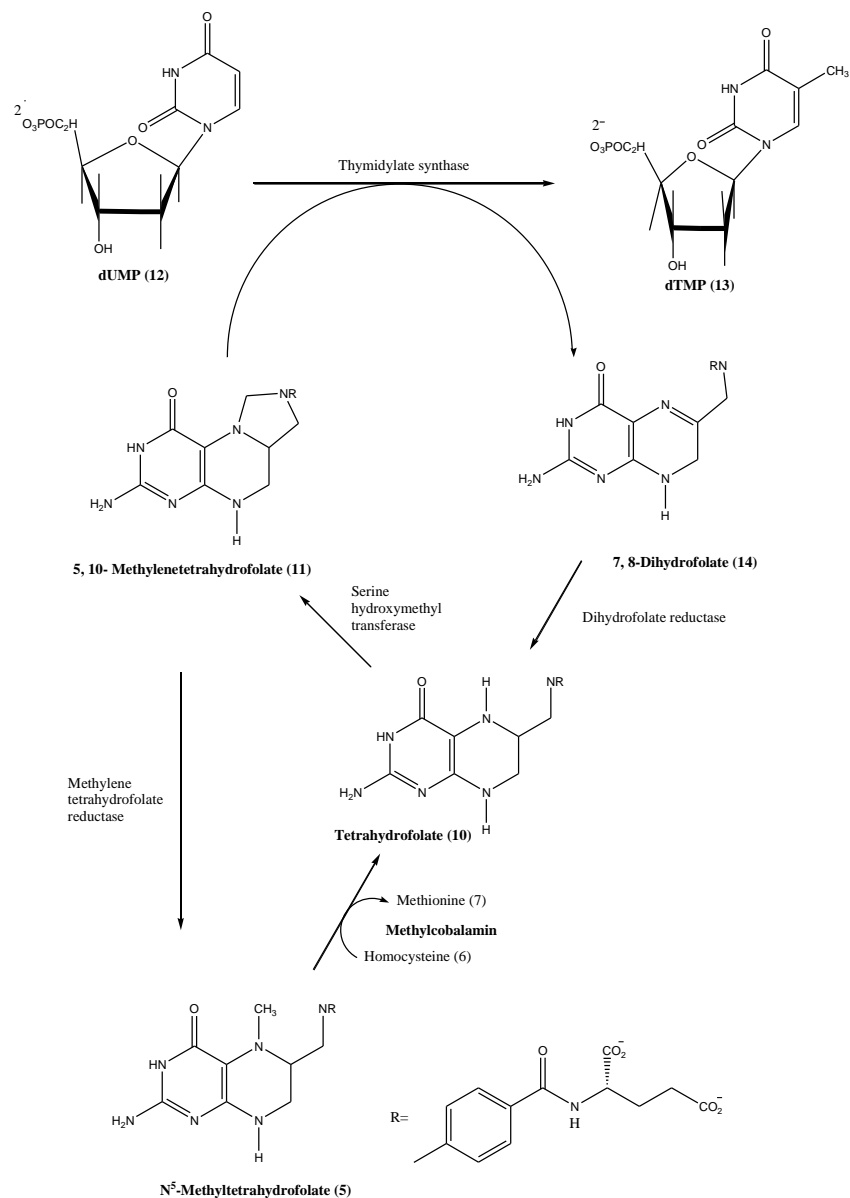


Figure 12: Interacting B<sub>12</sub>-folate metabolic pathway which provides precursor for synthesis of DNA

Deficiencies of vitamin B<sub>12</sub> or folate conspicuously lead to the accumulation of N<sup>5</sup>-methyltetrahydrofolate resulted from the failure of its cobalamin and folate dependent conversion to tetrahydrofolate. These deficiencies, so as any other impairment of the interacting B<sub>12</sub>-folate metabolism lead to the unavailability of the methyl donor; 5, 10 – methylenetetrahydrofolate (**11**) during the thymidylate synthase catalyzed methylation for synthesis of DNA precursors. Because the mitotic division of a cell relies on the doubling of



DNA content in the nucleus of the cell, the end result of the deficiencies of these vitamins is the inability of cells to multiply. Rapid proliferating cells like erythrocytes in the bone marrow and cells of organs like tongue and small intestines are severely affected, hence the development to PA as well as other clinical symptoms for B<sub>12</sub> deficiency in association to these organs.

However, the remarkable development to PA and other clinical symptoms of B<sub>12</sub> deficiency without extended to the neurological disorders resulted from the lack of folate alone<sup>73</sup> indicates the PA associated neurological diseases are not related to the B<sub>12</sub>-folate shared metabolic pathway. Metabolism with another coenzyme form of B<sub>12</sub> was then sensible implicated to the PA associated neurological diseases. The mammalian conventional oxidation of branched chain amino acids to pyruvate via a metabolic pathway which exploits coenzyme B<sub>12</sub> for the intermediate reaction catalyzed by methylmalonyl -CoA mutase converts B<sub>12</sub> in the course of development to neurological diseases. Odd chain fatty acids and cholestols share the same oxidation pathway with branched chain amino acids with which B<sub>12</sub> deficiency leads to failure in methylmalonyl -CoA mutase catalyzed rearrangement of methylmalonyl -CoA to succinyl -CoA resulting into the medical condition known as methylmalonic aciduria.<sup>74</sup> Although, yet the mechanism to the neurological disorder is controversial, the accumulated methylmalonate resulted from the B<sub>12</sub> deficiency has been linked with the formation of the alkyl chains with methyl groups which cause nerve damage.

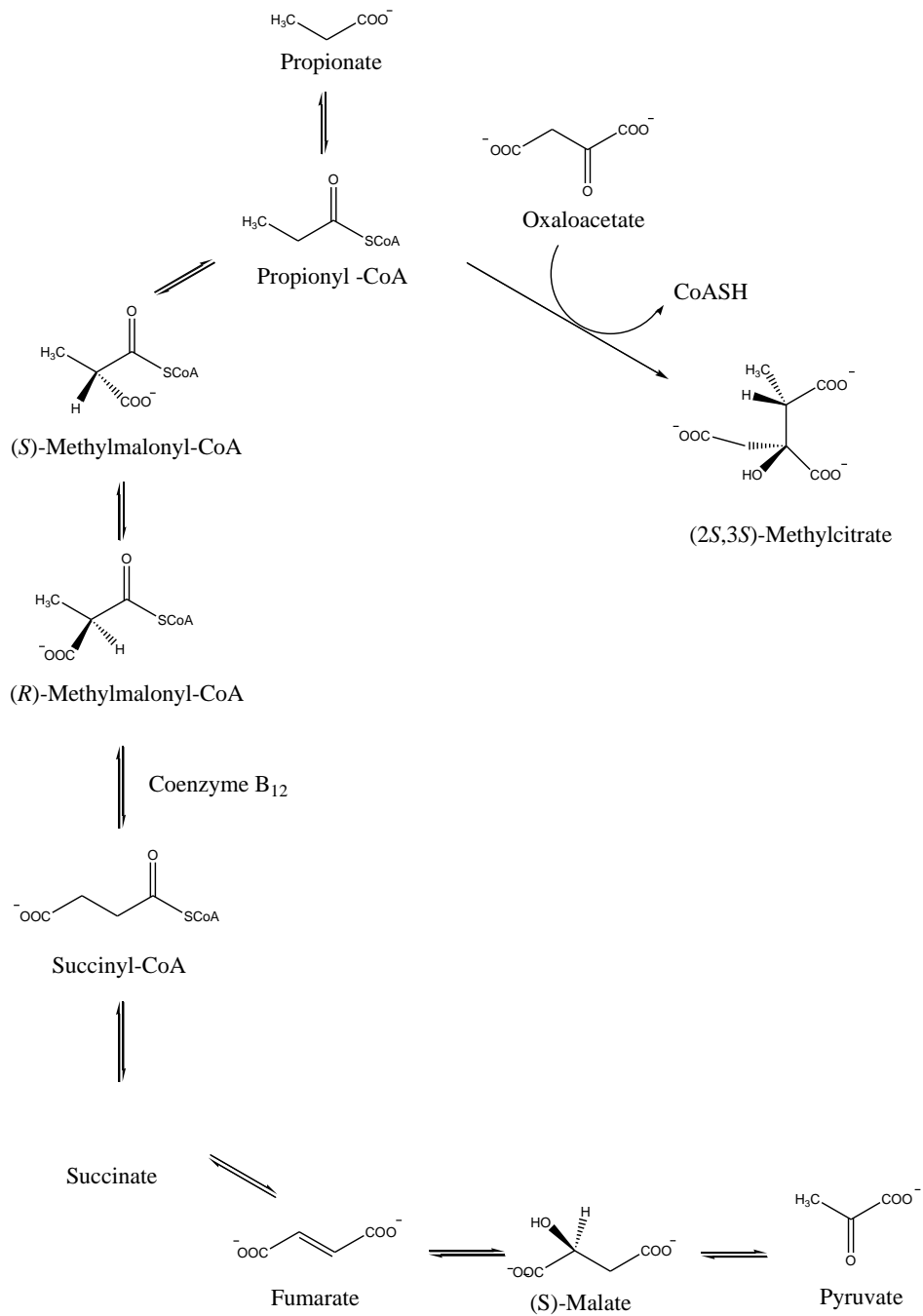


Figure 13: The mammalian oxidation of propionate to pyruvate with intermediate coenzyme B<sub>12</sub> dependent rearrangement of (*R*)-3-methylmalonyl -CoA to succinyl -CoA by methylmalonyl -CoA mutase

The present time medical triumph from the discovery of B<sub>12</sub> in relation to PA together with the comprehension of the B<sub>12</sub>-folate shared pathway for DNA synthesis is the prescriptions of cyanocobalamin or hydroxocobalamin for the treatment of pernicious anaemia. These cobalamins are also prescribed for the treatment of the demyelinating diseases of the spinal cord which are caused by methylmalonic aciduria. The two B<sub>12</sub> metabolic pathways in human have therefore mark a clear cut between PA and its associated nerve diseases which have become apparent as a result of these conceptions on the medical aspects of B<sub>12</sub> in metabolism.

### **1.5.2 Energy conservations in anaerobic food chains**

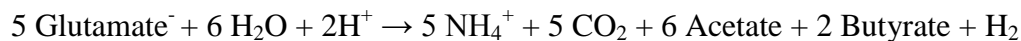
Owing to the putrefactive processes by aerobic organisms, niches of oxygen deficiency have been created to inhabit life<sup>75</sup> with metabolisms which have successful lead the food chain to ecological consequent transformations into a simplest hydrocarbon; the methane and CO<sub>2</sub>.<sup>76, 77</sup> In these anoxic habitats the hydrolysis of carbohydrates and proteins to energy rich sugar monomers and amino acids by the actions of exogenous enzymes is succeeded by non-oxygenic respirations. Chemotrophic anaerobes treasure metabolisms which have purposely evolved with potential to achieve oxidations of varieties of compounds in devoid of oxygen. Among described anaerobic respirations are the fermentations of several compounds including proteinogenic amino acids,<sup>78-81</sup> as well as various oxidation pathways with terminal inorganic electron acceptors.<sup>82,83</sup> These metabolisms derive entire energy from the products of exogenous hydrolysis and other energy rich compounds for sustaining the life of anaerobes in their anoxic habitats like soil, sewage sludge, marine and fresh water sediments as well as in the gastrointestinal tract of animals. The significant role by B<sub>12</sub> in the anaerobic life is revealed from the described coenzyme B<sub>12</sub> dependent enzymatic reactions which serve as intermediate steps to several energy conservations pathways. The major role of these pathways has been to provide energy for sustaining the anaerobic life.

#### **1.5.2.1 Amino acids fermentations**

Proteinogenic amino acids form a major source of energy to anaerobic life that is conserved in various archaeal and bacterial fermentation pathways. The fermentative degradations of amino acids are accomplished in redox reactions<sup>75, 84, 85</sup> which involve either a pair of amino acids as

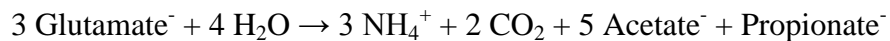
described in Stickland metabolism or between an amino acid with non-nitrogenous compounds formed as intermediates during fermentation. Unlike the aerobic respirations, oxygenations are not found in fermentations. However, other non-oxygen requiring oxidation reactions of fermentations such as oxidative deaminations, transaminations and keto acid oxidations are similar to those found in aerobic respiration. Fermentation processes differ from aerobic respiration by their reduction reactions which have to depend on electron acceptors generated during the organism metabolisms.<sup>79</sup> Anaerobes metabolic reactions usually lead to substrates conversions into both electrons acceptors oxidants as well as reductant metabolites which accomplish the electron transferring processes for fermentations energy productions. Used electron acceptors in amino acid fermentations include amino acids themselves, unsaturated  $\alpha$ - and  $\beta$ -acids and their coenzyme A thioesters as well as protons.<sup>79</sup>

Fermentative bacteria are the metabolic most diversified in the anaerobic food chain in view of the fact that; each amino acid among the twenty proteinogenic amino acids can be fermented with others being fermented in more than one pathway.<sup>78, 79, 81, 86</sup> Also several other pathways for fermentations of non-amino acids compounds have been reported. An exceptional substrate for fermentation has been glutamate which can be fermented via five different pathways.<sup>86</sup> Nature's solution to the metabolic chemical challenging removal of  $-\text{NH}_2$  group from glutamate in the two methylaspartate pathways for this amino acid fermentation by clostridia is the rearrangement to (2*S*,3*S*)-3-methylaspartate by coenzyme B<sub>12</sub> dependent glutamate mutase. The enzyme base abstraction of a proton on carbon 3 of (2*S*,3*S*)-3-methylaspartate during the pathway's subsequent reaction of methylaspartase readily eliminates the  $-\text{NH}_2$  group as ammonia leaving mesaconate as an intermediate of the pathway (figure 14). Further transformations by the hydration and cleavage reactions lead to the formation of acetate and pyruvate.<sup>87</sup> The latter is either converted to acetyl-CoA with subsequent catabolic transformations to butyrate or carboxylated to oxaloacetate before further conversions to propionate.<sup>86</sup> In the metabolic route via acetyl-CoA, 0.6 ATP (63.5 kJmol<sup>-1</sup>) per glutamate is conserved via substrate level phosphorylation<sup>84, 88</sup> while the conservation of the additional 42.5 kJmol<sup>-1</sup> is achieved via electrochemical H<sup>+</sup> or Na<sup>+</sup> gradients generated via electron bifurcation and the membrane-bound ferredoxin-NAD<sup>+</sup> reductase.<sup>89</sup>



$$\Delta G^{\circ'} = -63.5 \text{ kJmol}^{-1} \text{ Glutamate} : 106 \text{ kJmol}^{-1} \text{ ATP}$$

In the alternate metabolic branch, 3 glutamates give rise to 3 acetates and 3 pyruvates. Two pyruvates are oxidized to 2 acetyl-CoA from which 2 acetates and 2 ATPs are formed. The third pyruvate is reduced via oxaloacetate, succinate and methylmalonyl-CoA to propionate. The coenzyme B<sub>12</sub> dependent rearrangement by methylmalonyl CoA mutase is an intermediate in the pathway. 2 ATPs are conserved via acetyl-CoA and further energy is conserved via proton/Na<sup>+</sup> translocating ferredoxin oxidation and fumarate respiration.<sup>86,90</sup>



$$\Delta G^{\circ'} = -69.0 \text{ kJmol}^{-1} \text{ glutamate}; \geq 62 \text{ kJmol}^{-1} \text{ ATP}$$

Other described routes for the fermentation of glutamate are the (*R*)- 2-hydroxyglutaryl -CoA and 4-hydroxybutyrate-CoA pathways (figure 14) as well as the glutamate fermentation via 5-aminovelarate which has form the 5<sup>th</sup> route for this amino acid fermentation. However, the coenzyme B<sub>12</sub> cofactor participates only in the two methylaspartate routes.

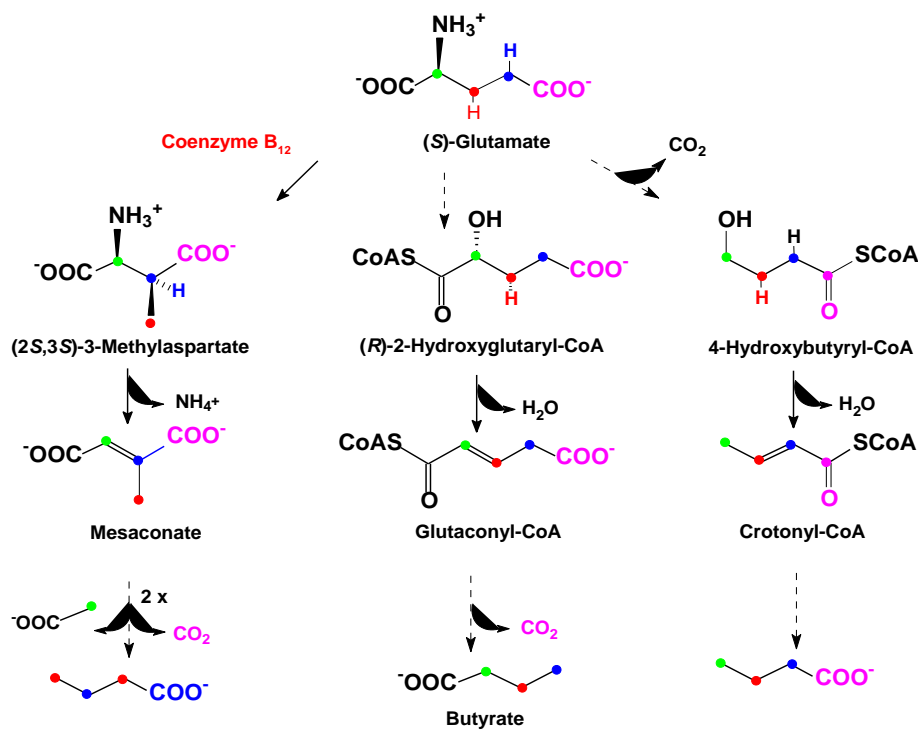


Figure 14; Isotopically traced intermediates of the three clostridia fermentation pathways leading from (S)-glutamate to butyrate. The coenzyme B<sub>12</sub> dependent methylaspartate pathway (left), (R)- 2-hydroxyglutaryl -CoA pathway (middle) and the inter-organismic route via the 4-hydroxybutyrate-CoA (right).

Besides the methylaspartate routes for glutamate fermentation; the participation of B<sub>12</sub> in amino acids fermentation has also been described in a fermentation pathway which leads from L-lysine to acetate and butyrate in several clostridia, fusobacteria and Porphyromonas. The first reaction for this pathway is catalyzed by L-lysine-2,3-aminomutase which converts L-lysine to (3S)-3,6-diaminohexanoate or β-lysine, that rearranges to (3S, 5S)-3,5-diaminohexanoate during the coenzyme-B<sub>12</sub> dependent reaction of L-β-lysine-5,6-aminomutase. Pyridoxal-5'-phosphate is also a cofactor for the L-β-lysine-5,6-aminomutase catalyzed rearrangement. Removal of the two amine groups present in L-lysine is accomplished during the reactions of L-erythro-3,5-diaminohexanoate dehydrogenase and L-3-aminobutyryl coenzyme A deaminase in the pathway.<sup>91,92</sup>

### 1.5.2.2 Nicotinate fermentation

Being a constituent of nicotinamide adenine dinucleotide (NAD) cofactor; nicotinate is abundant in environments where it offers energy for supporting anaerobic life by a fermentation pathway which B<sub>12</sub> participate. The enzymatic transformations leading from nicotinate to NH<sub>3</sub>, CO<sub>2</sub>, acetate and propionate have been described in *Eubacteria barkerei*<sup>93</sup> with which the organism has been able to grow anaerobically on nicotine as the only carbon source. The formed 2-methyleneglutarate intermediate of the pathway is converted to (R)-3-methylitaconate in the coenzyme B<sub>12</sub> dependent rearrangement reaction by 2-methyleneglutarate mutase.<sup>93</sup>

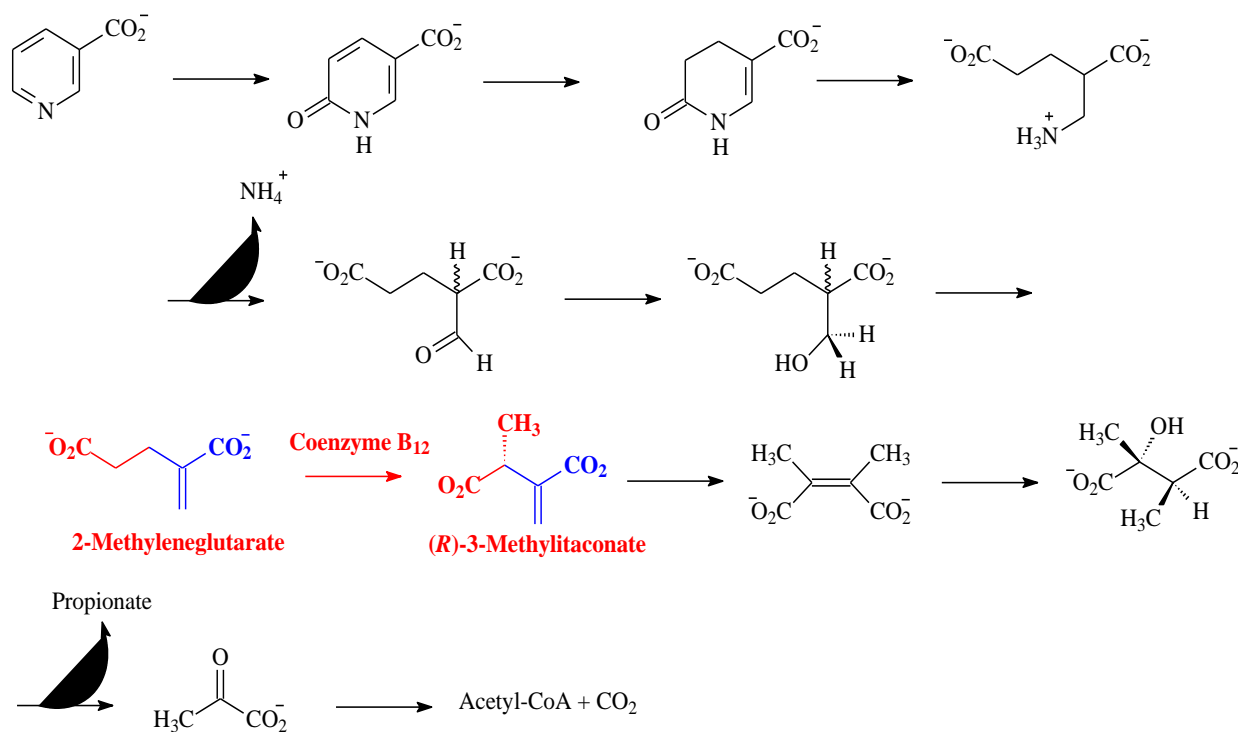


Figure15: Fermentation pathway leading from nicotinate to NH<sub>3</sub>, CO<sub>2</sub>, acetate and propionate in *Eubacteria barkerei*

Genes encoding nine enzymes for this fermentation have been spotted in recent released genomes of environmental isolates *Natranaerobius thermophilus*, *Bacteroides capillosus*, and *Anaerotruncus colihominis*.<sup>94</sup> Medical relevant has been *B. capillosus* is a known resident of human intestines where it can cause neonatal sepsis as well as both cysts and wounds. Also a

medical implication is the recent isolation of *A. colihominis* in human stool specimens although the clinical significance in relation to this organism is yet to be established.<sup>95,96</sup>

### 1.5.2.3 Anaerobic n-hexane oxidation

Potentials of n-alkanes to be used as substrates for growth of organisms was first recognized with aerobic bacteria in the beginning of the last century. The terminal electron acceptor role by the dioxygen in the respiration during the aerobic growth of bacterial on n-alkanes is as important as other known aerobic respirations. However, the metabolic challenge to n-alkanes degradation for which growth on these hydrocarbons has been considered unique are the inert C-H bonds which make them resistant to enzymatic transformations. During the aerobic growth on n-alkanes the dioxygen has been established with an extra role of being co-substrate of the oxidation that is necessary for the activation of n-alkane by transformations into oxygen containing metabolites which are suitable for enzymatic degradation.<sup>97</sup> The anaerobic growth on such inert hydrocarbons was therefore considered impossible over years. However, the n-alkanes dependent anaerobic growths were later described in various denitrifying, iron (III) and sulfate reducing bacteria.<sup>72</sup> The activation of apolar C-H bonds of n-alkanes for oxidation during the growth in such strict anoxic environment is achieved through novel chemical steps which exclusively rely on metallocofactors as well as radical mechanisms.<sup>98</sup> Among several examples is a recent report from the studies on the oxidation of n-hexane by the anaerobic denitrifying betaproteobacterium “*Aromatoleum*” strain HxN1 that describes the hydrocarbon tentative degradation pathway which coenzyme B<sub>12</sub> participates in rearrangement of metabolites.<sup>72</sup> EPR spectroscopy identified glycy radical enzyme; (1- methylalkyl)succinate synthase which has been convicted with the condensation of n-hexane with fumarate. The carboxylate of the metabolic active condensation product (1-methylpentyl)succinate is believed to be transformed to CoA ester by (1-methylalkyl)succinate -CoA ligase before the epimerization which is followed by the postulated rearrangement reaction by a tentative coenzyme B<sub>12</sub> dependent mutase.<sup>72</sup> Further work for comprehending this mutase is current carried jointly in the laboratories of Wolfgang Buckel in the University of Marburg and Bernard Golding in Newcastle University. The mutase rearranged product is believed to be decarboxylated and subsequently oxidized before enters the oxidation  $\beta$ -pathway.



### 1.5.3 Metabolic pathways for carbon assimilation and biosynthesis

Growth of organisms on two and three carbon compounds like acetate and ethanol which have to enter the central carbon metabolism in acetyl -CoA level has become possible because of evolutions to pathways which can assimilate acetyl -CoA. The isocitrate lyase metabolic switches to glyoxylate shunt in some bacteria have been the only known route for assimilating acetyl -CoA over the last 50 years.<sup>99-101</sup> This metabolic switches to glyoxylate shunt has enables bacteria with isocitrate lyase to grow on two and three carbon sugars. The medical relevance to the glyoxylate cycle has been the *Mycobacterium tuberculosis* periods of latency survival with three carbon sugars diet in leucocytes which lead to their unique penetrance to human population via chronic tuberculosis.<sup>102</sup> Bacteria of the genus *Pseudomonous* and several strains of *E. coli* as well as many moulds were among early known organisms to demonstrate the growth on two carbon compounds with which they meet all their carbon requirements through conversions to any cell constituents via the glyoxylate shunt.<sup>101</sup>

Recently, a pathway for acetyl -CoA assimilation with intermediate coenzyme B<sub>12</sub> dependent rearrangements reactions by a new described ethylmalonyl-CoA mutase as well as methylmalonyl-CoA mutase has been discovered in *Rhodobacter sphaeroides*.<sup>99, 100</sup> The new pathway achieves the formation of the malate and succinyl -CoA from metabolic condensation of three molecules of acetyl -CoA, one molecule of CO<sub>2</sub>, and one molecule of HCO<sub>3</sub><sup>-</sup> (figure 16). Early steps of the pathway are reactions common to the synthesis of polyhydroxybutyrate which achieve the condensation of two molecules of acetyl-CoA and subsequent transformations to crotonyl -CoA that is carboxylated to (2*S*)-ethylmalonyl -CoA. Epimerization by methylmalonyl-CoA/ethylmalonyl -CoA epimerases forms (2*R*)-ethylmalonyl -CoA which is rearranged to (2*S*)-methylsuccinyl-CoA during the coenzyme B<sub>12</sub> dependent reaction of ethylmalonyl -CoA mutase before further enzymatic conversions to glyoxylate and propionyl -CoA.<sup>100</sup>

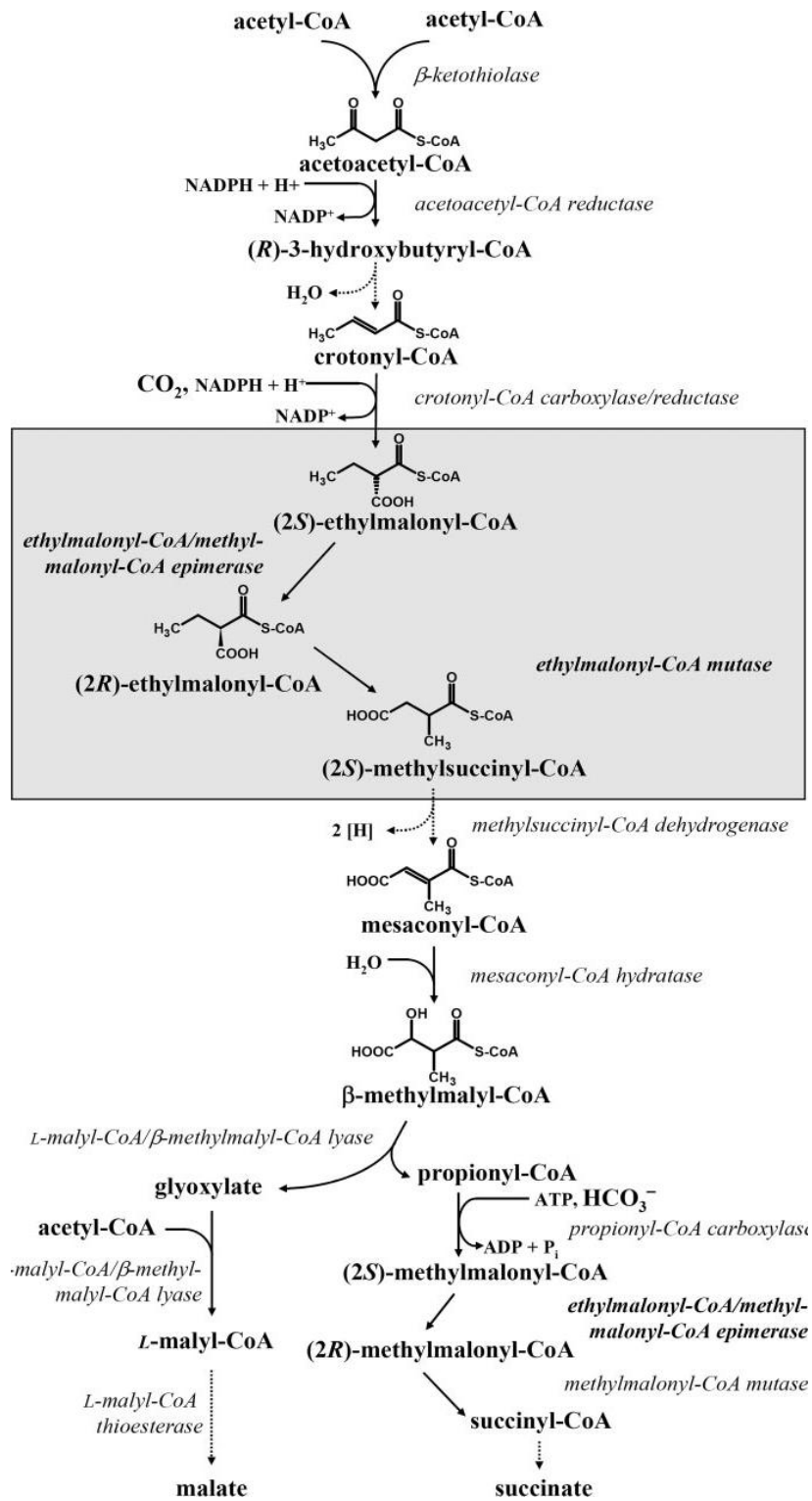


Figure 16: Proposed ethylmalonyl -CoA pathway for acetyl-CoA assimilation in phototrophic bacterium *R. sphaeroides*. Adapted from reference 100

While glyoxylate is converted to malate via L-malyl CoA, propionyl CoA is carboxylated to (2*S*)-methylmalonyl -CoA and subsequent epimerized by methylmalonyl -CoA epimerase to (2*R*)-methylmalonyl -CoA before rearranged to succinyl -CoA by the coenzyme B<sub>12</sub> dependent methylmalonyl -CoA mutase. Hydrolysis of CoA ester achieves succinate which enters citric acid cycle like malate or succinyl -CoA. This novel acetyl -CoA assimilation pathway is believed to be in other bacteria like *Methylobacterium extorquens* and *Streptomyces coelicolor* as they have been known to lack isocitrate lyase which is in contrary to their demonstrated growth on two and three carbon substrates.<sup>99, 100, 103, 104</sup>

Cofactor roles by B<sub>12</sub> are also revealed in lipids and glycerolipids metabolisms with which coenzyme B<sub>12</sub> dependent propanediol dehydratase and ethanol amine ammonia lyase participate in intermediate steps by catalyzing rearrangements with irreversible elimination of water and NH<sub>3</sub>. These coenzyme B<sub>12</sub> dependent conversions lead to metabolites which are fed into various pathways including those for propionate and pyruvate metabolisms. Also significant cofactor role by coenzyme B<sub>12</sub> is that for DNA synthesis by class II ribonucleotide reductases (RNRs) in some bacteria.

## **1.6 Mechanisms for rearrangements by coenzyme B<sub>12</sub> dependent enzymes**

Various experimental authentications of the minimal mechanistic scheme for coenzyme B<sub>12</sub> dependent reactions have describe successful characterizations of substrate derived and product related radicals. For example the 4-glutamyl radical derived from glutamate during the reaction of glutamate mutase was identified by successions of EPR measurements in experiments involved the incubations of holoenzyme with glutamate and series of <sup>13</sup>C labeled glutamates.<sup>105</sup> During these experiments, freeze quenching of the reactions after few seconds of holoenzyme incubations with glutamates gave EPR signals which were interpreted to the substrate derived radical. Studies on the reaction of 2-methyleneglutarate mutase by mechanism based inactivation approach demonstrated the formation of radical adducts of 5'-deoxyadenosyl and enzyme inhibitors mimic of substrate derived and product related radicals.<sup>106</sup>

The used analogues of 2-methyleneglutarate derived and itaconate related radicals; *cis*-glutaconate and but-1,3-diene-2,3-dicarboxylate inactivate the enzyme by the mechanism which involve the addition of 5'-deoxyadenosyl radical to SP<sup>2</sup> carbon centers on inhibitors resulting into adduct radicals. The EPR characterization of these adduct radicals verified the proposed minimal mechanistic scheme for coenzyme B<sub>12</sub> dependent rearrangements. A similar approach was used to investigate propane-1,2-diol dehydratase by but-3-ene-1,2-diol which established the enzyme mechanism for regioselectivity towards the formation of the substrate derived radical.<sup>107</sup>

Present time endeavors to comprehend coenzyme B<sub>12</sub> dependent reactions by many laboratories focus on the mechanisms by which substrates derived radicals rearrange reversibly to products related radicals. Theoretical chemistry based predictions on the reactivity of intermediate substrate derived and product related radicals in most of these reactions have put forward several mechanistic proposals for their inter-conversions rearrangements. Most on-going studies on this theme are aiming at experimental verifications on those proposed rearrangement mechanisms. For the purpose of introducing the work reported in this thesis; various published findings on the experimental verifications of different mechanistic proposals for rearrangement reactions by selected carbon skeleton mutases; 2-methyleneglutarate mutase, methylmalonyl-CoA mutase, glutamate mutase as well as eliminases; ethanolamineammonia lyase and ribonucleotide reductases are highlighted in briefly. The successful productions of recombinant apo-proteins for these enzymes have allowed extensive invitro studies for the mechanisms of the reaction they catalyse.<sup>108, 109, 110, 111</sup>

## **1.6.1 Coenzyme B<sub>12</sub> dependent carbon skeleton mutases**

### **1.6.1.1 2-Methyleneglutarate mutase**

2-Methyleneglutarate mutase was discovered from *Clostridium barkeri* in early 1970s.<sup>112</sup> This species which was later re-classified as *Eubacterium barkeri* ferments nicotinate to NH<sub>3</sub>, CO<sub>2</sub>, acetate and propionate. Recent, the *mgm* gene which encodes for the 2-methyleneglutarate mutase together with other genes encoding for enzymes of the established pathway for nicotinate fermentation have also been found in the environmental isolates; *Natranaerobius thermophilus*, *Bacteroides capillosus*, and *Anaerotruncus colihominis*.<sup>94</sup> 2-Methyleneglutarate mutase catalyzes

the coenzyme B<sub>12</sub> dependent reversible conversion of 2-methyleneglutarate (**15**) to (*R*)-3-methylitaconate (**16**) which forms an intermediate step of the pathway for nicotinate fermentation by these bacteria (figure 15).

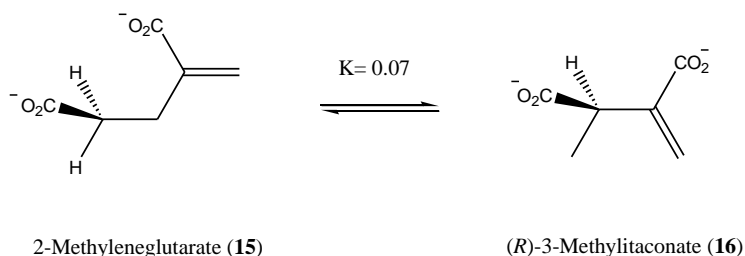


Figure 17: The coenzyme B<sub>12</sub> dependent 2-methyleneglutarate mutase catalyzed reversible rearrangement between 2-methyleneglutarate (**15**) and (*R*)-3-methylitaconate (**16**)

Hitherto, the crystal structure of 2-methyleneglutarate mutase has not been solved, hence the mechanistic insights from the 3D structure of the holoenzyme complex is unavailable. The current understandings on the mechanism of 2-methyleneglutarate mutase catalysis have been provided from its mutation, kinetic and spectroscopic studies. Successful cloning of *mgm* gene from *Eubacterium barkeri* has allowed the over-production of the recombinant single  $\alpha$  protein (70 kDa) of 2-methyleneglutarate mutase in *E.coli* and the invitro reconstitution of the active holoenzyme by assembling of the  $\alpha$ -protein with the coenzyme B<sub>12</sub>.<sup>108</sup> The holoenzyme complex of 2-methyleneglutarate mutase is postulated to be heterotetramer of the  $\alpha$ -protein ( $\alpha_4$ , 4 x 70 kDa) with the two bound coenzyme B<sub>12</sub>. The *mii* gene which encode for the 3-methylitaconate- $\Delta$  isomerase has also been cloned from *Eubacterium barkeri* and over-produced in *E.coli*. This isomerase catalyzes the elimination of the methine hydrogen from the product of the 2-methyleneglutarate mutase reaction, the (*R*)-3-methylitaconate, which is converted to 2, 3-dimethylmaleate during the nicotinate fermentation. The recombinant production of 3-methylitaconate- $\Delta$  isomerase has allowed its application as an auxiliary enzyme for assaying 2-methyleneglutarate mutase by converting the (*R*)-3-methylitaconate which is produced by 2-methyleneglutarate mutase to 2,3-dimethylmaleate. The activity of 2-methyleneglutarate mutase has therefore been measured spectrophotometrically as the rate of 2, 3-dimethylmaleate formation at 256 nm in the coupled assay with 3-methylitaconate- $\Delta$  isomerase.<sup>113</sup> In the studies approach by mutation of the *mgm* gene, the demonstrated decrease of the substrate turnover due

to the site directed mutation of the conserved cobalamin binding motif of the 2-methyleneglutarate mutase  $\alpha$  protein has implied the coenzyme B<sub>12</sub> is bound to the apoenzyme by “base off, his on”.<sup>114</sup> Additional support for the “base off, his on” binding of cofactor to the 2-methyleneglutarate mutase protein comes from the study which the (Co $\beta$ -5'-deoxyadenosin-5'-yl)-(p-cresyl)cobamide base off analogue of the coenzyme B<sub>12</sub> was demonstrated to be an excellent cofactor of 2-methyleneglutarate mutase reaction with 5 times increased affinity to the apoenzyme in comparison to coenzyme B<sub>12</sub>.<sup>115</sup>

The interpretation of cob(II)alamin and an organic radical from the results of an EPR study of 2-methyleneglutarate mutase has implied the radical mechanism by this enzyme is initiated by the homolytic cleavage of coenzyme B<sub>12</sub> Co-C bond. The cob(II)alamin formed from the homolysis of the cofactor Co-C bond has been identified by its anaerobic UV/Vis absorption peak at 470 nm in several studies of 2-methyleneglutarate mutase. An organic radical, the 5'-deoxyadenosyl which is formed along with cob(II)alamin from the bond cleavage, stereoselective abstracts the pro-*R* hydrogen on the C-4 of 2-methyleneglutarate to form the substrate derived radical and a molecule of adenosine.<sup>116</sup> The 2-methyleneglutarate radical rearranges reversibly to (*R*)-3-methylitaconate radical which abstracts hydrogen from the methyl group of the adenosine to form (*R*)-3-methylitaconate with the regeneration of the coenzyme B<sub>12</sub>. The formation of the intermediate substrate derived and product related radicals have been demonstrated by EPR spectroscopy from the reactions of their structural analogues compounds, *cis*-glutaconate and buta-1,3-diene-2,3-dicarboxylate with 2-methyleneglutarate mutase.<sup>106</sup> Two mechanistic possibilities for reversible inter-conversions between 2-methyleneglutarate and (*R*)-3-methylitaconate radicals have been; 1) either via the fragmentation of the 2-methyleneglutarate radical into acrylate and acrylate radical which recombine to form (*R*)-3-methylitaconate radical (fragmentation-recombination) or, 2) because of the  $\pi$  electrons  $\beta$  to C4 radical on 2-methyleneglutarate radical, the C4 radical is intra-molecularly added to the  $\beta$   $\pi$ -electrons. The addition resulting into the formation of the cyclopropylcarbinyl radical intermediate which opens at C2-C3 bond to give the product related radical (addition –elimination) (figure 18).<sup>114, 117</sup>

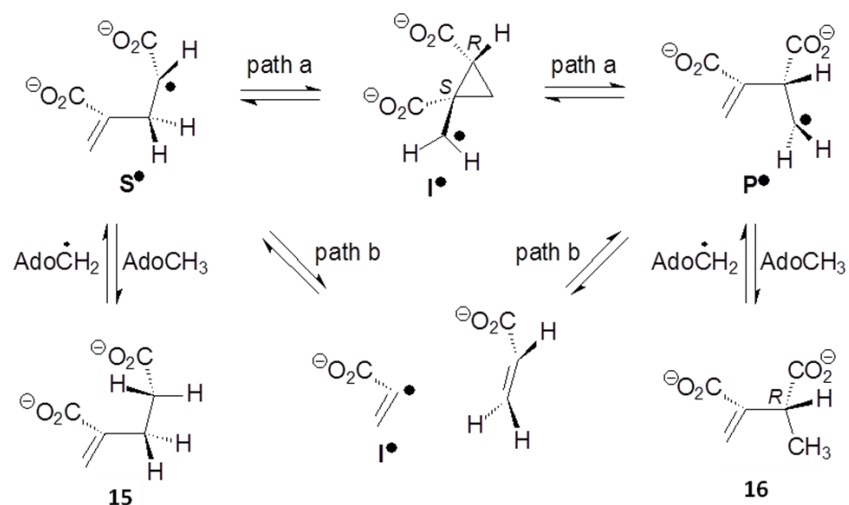


Figure 18: Proposed mechanisms for the coenzyme B<sub>12</sub> dependent 2-methyleneglutarate mutase catalyzed reversible rearrangement between 2-methyleneglutarate derived and (*R*)-3-methylitaconate related radicals. Path a; is rearrangement by the addition elimination mechanism via the intermediate cyclopropylcarbinyl radical and path b; is the rearrangement via fragmentation into acrylate radical and acrylate which recombine to give the product related radical

Performed experiments for identifying the mechanism of rearrangement by 2-methyleneglutarate mutase from the two proposals demonstrated the enzyme inhibition by the square concentration of acrylate. The inhibition was characterized by an EPR signal of an organic radical in interaction with cob(II)alamin similar to the reaction of the enzyme with 2-methyleneglutarate.<sup>114, 117</sup> This observation suggests the presence of two acrylate molecules provides structure which is analogue to the intermediate of the rearrangement mechanism which is catalyzed by this enzyme. However, these results were not sufficient to define which of the three steps intermediates; 2-methyleneglutarate radical, acrylate and acrylate radical fragments or (*R*) 3-methylitaconate radical has been mimicked by the two molecules of acrylate in case of the rearrangement by fragmentation- recombination. Since it is not possible to establish that the square concentration of acrylate mimics only the acrylate and acrylate radical fragments, these results could not be adequate to conclude the rearrangement is by fragmentation-recombination. The possibility for the formation of the cyclopropylcarbinyl radical as an intermediate of the rearrangement by intra-molecular addition of radical carbon to  $\pi$ -electrons on the molecule of the substrate derived radical was investigated by evaluating the interaction of 2-methyleneglutarate

mutase with cyclopropane stereoisomers **17-20**. These stereoisomers were designated to mimic the cyclopropylcarbinyl radical in the enzyme active site. Study which explored the potentials for inhibiting 2-methyleneglutarate mutase by these compounds, could not establish an enzyme inhibition by any of the stereoisomer.<sup>117</sup> The results obtained from this study had therefore implied the cyclopropylcarbinyl radical does not exist as an intermediate in the reaction of 2-methyleneglutarate mutase, hence the mechanism for rearrangement by this enzyme is not by addition-elimination. However, since the competition of the reaction intermediate with an enzyme inhibitor requires the formation of the intermediate to be a reaction rate determining step, the possibility for the addition-elimination mechanism cannot be excluded because the rate determined step during the rearrangement by this mechanism is the abstraction of hydrogen atom from the substrate.

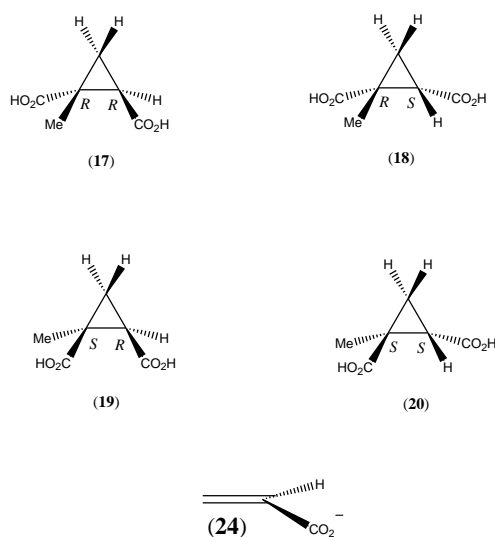


Figure 19: Compounds used to investigate the reaction of 2-methyleneglutarate mutase. The compounds **17-20** are stereoisomers of 1-methylcyclopropane-1,2-dicarboxylic acids which are analogue to the intermediate cyclopropylcarbinyl radical in the proposed rearrangement by the addition-elimination mechanism. The acrylate (**24**) was used to mimic the intermediate steps of the proposed rearrangement by fragmentation-recombination.

The computational study by *ab initio* calculations reported ca 100 kJ mol<sup>-1</sup> more energy requirement for the rearrangement by fragmentation-recombination as compared to that by addition-elimination.<sup>118</sup> These computational studies also investigated the impact of protonating



the 2-*exo* methylene group on the substrate i.e, 2-methyleneglutarate or (*R*)-3-methylitaconate which was reported to be important in facilitating the migration of acrylate moiety by lowering the activation energy of the reaction. In the enzyme system, the protonation can be accomplished by amino acid residues within the proximity of the enzyme active site. However, the effect of protonating 2-*exo* methylene group on the activation energy of the reaction stands relative to both proposed mechanistic routes and therefore left them undistinguished.

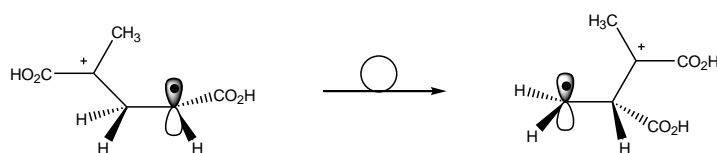


Figure 20: Schematic presentation on the proposed facilitation of 2-methyleneglutarate mutase catalyzed rearrangement by protonation of substrate 2-*exo* methylene group.

### 1.6.1.2 Methylmalonyl -CoA mutase

The coenzyme B<sub>12</sub> dependent methylmalonyl -CoA mutase is metabolically important for the catalysis of the reversible stereospecific rearrangement between succinyl -CoA (**21**) and (*R*)-methylmalonyl -CoA (**22**) (figure 21). This catalysis achieves the exchange between the substrate carbonyl-CoA group and its vinyl hydrogen atom which results in the formation of the rearranged product. The verification on the migration of carbonyl -CoA group during the catalysis by the methylmalonyl-CoA mutase was established from the experiments which 2-[<sup>14</sup>C]-methylmalonyl-CoA was used as the substrate.<sup>119</sup>

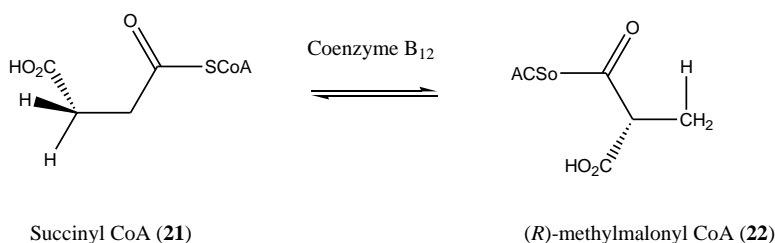


Figure 21: The coenzyme B<sub>12</sub> dependent interconversions between succinyl-CoA (**21**) and (*R*)-methylmalonyl-CoA (**22**) which is catalyzed by methylmalonyl-CoA mutase

The methylmalonyl -CoA mutase system is one of the well studied among the discovered coenzyme B<sub>12</sub> dependent enzymes. This enzyme has been isolated from both bacteria and mitochondria of eucaryotes. The mammalian methylmalonyl -CoA mutase is homodimeric of  $\alpha$  units ( $\alpha_2$ : 160 kDa), whereas the bacterial enzyme is an  $\alpha\beta$  heterodimer (150 kDa;  $\alpha$ -subunit 80 kDa and  $\beta$ -subunit 70 kDa).<sup>120, 121</sup> The sequence as well as the structure of the bacteria  $\alpha$  subunit show high similarity with that of the mammalian enzyme. Since the cobalamin binding His-asp-ser trid is in the  $\alpha$  subunit, hence the bacterial  $\alpha\beta$  holoenzyme is reconstituted with one cofactor whereas the mammalian homodimeric assembly is ideal for two active sites.

In mammals the rearrangement by the coenzyme B<sub>12</sub> dependent methylmalonyl -CoA mutase is an intermediate step in the oxidation of several branched chain amino acids e.g isoleucine as well as odd chain fatty acids and cholesterol. This mammalian oxidation pathway leads to pyruvate via propionate (figure 13).<sup>122</sup> The medical relevance of this pathway is the progression to nerve damage which is caused by the methylmalonic aciduria resulted from the failure of the catalysis by the methylmalonyl-CoA mutase.<sup>123</sup> Two types of aciduria;  $mut^-$  and  $mut^0$  which arise from the accumulation of methylmalonyl-CoA have been described. In the  $mut^-$  aciduria the gene encoding the methylmalonyl -CoA mutase is present but the accumulation of methylmalonic acid is caused by the deficiency of cobalamin due to the defect in the genes encoding for the cobalamin carrier proteins. The  $mut^0$  type of aciduria arises due to the defect of the gene encoding the methylmalonyl -CoA mutase and has been reported with even severe neurological complication.<sup>124</sup> Also the physiological relevant in due to this oxidation has been the detoxification of propionate which accumulates from the oxidation of branched chain amino acids and cholesterol. In bacteria like *Propionibacterium shermanii*, *Streptomyces cinnamonensis* the rearrangement by this enzyme is an intermediate of the pathway leading from pyruvate to propionate.<sup>125,126</sup> This bacteria metabolism forms a pathway which is reverse of the mammalian oxidation of propionate to pyruvate. In addition to succinyl -CoA which enters the central carbon metabolism at the level of the citric acid cycle in both mammalian and bacterial pathways, other intermediates provide precursors for the biosynthesis of polyketide anti-biotics in bacteria.<sup>127</sup>

The methylmalonyl -CoA mutase catalyzed rearrangement has been extensively studied by both kinetic and spectroscopic methods. Several developed continuous spectrophotometric as well as radiolabelled assays for methylmalonyl -CoA mutase<sup>128</sup> have allowed the determinations of the kinetic constants of both methylmalonyl -CoA and succinyl -CoA in their respective reactions with this enzyme. The reaction *Keq* has been established to range between 20 and 30 in favor of the less branched succinyl -CoA.<sup>125,129,130</sup> In addition to methylmalonyl -CoA and succinyl -CoA, the substrate spectrum of methylmalonyl -CoA mutase has been extended to succinyl(carba)dethia-CoA, succinyl(dicarba)dethia -CoA and 4-carboxy-2-oxy-butyl-CoA. The kinetic constants for all these substrates in their reactions with methylmalonyl -CoA mutase have also been reported.<sup>128</sup>

Significant mechanistic insights on the methylmalonyl -CoA mutase catalyzed reaction have been obtained from the enzyme 3D structures. The crystal structures of methylmalonyl -CoA mutase have been solved without substrate as well as with substrate and varieties of the enzyme inhibitors.<sup>131, 132</sup> The substrate free holo-enzyme has been revealed to be in an open conformation with an accessible active site where the coenzyme B<sub>12</sub> can be seen bound by “base off, his on” mode. Binding of the substrate causes holoenzyme to adopt a closed conformation with which the active site becomes inaccessible. The substrate as well as the bound cob(II)alamin stay enclosed whereas the adenosine moiety derived from the cofactor during the Co-C bond homolysis locates outside the active site. This conformational change in due to substrate binding is speculated to provide energy for assisting the homolysis of coenzyme Co-C bond.

Similar to other coenzyme B<sub>12</sub> dependent reactions, the 5'-deoxyadenosyl radical generated from Co-C bond homolysis is postulated to abstracts hydrogen from (*R*)-methylmalonyl-CoA to form (*R*)-methylmalonyl-CoA radical which rearranges reversibly to succinyl-CoA radical. The homolytic cleavage of the Co-C bond and reversible hydrogen abstraction during the catalysis by methylmalonyl -CoA mutase were demonstrated by EPR spectroscopy and tritium transfer experiments which the tritium labelled 3-carboxypropyl -CoA was used to inhibit the enzyme.<sup>125</sup> Furthermore, evidence on the existence of the intermediate radicals in the methylmalonyl -CoA mutase catalysis has been provided by EPR signal which was measured from the freeze quenching of the enzyme reaction under the steady state conditions.<sup>125, 133</sup> The steric course of catalysis by

this enzyme has been well established. In the conversion of (*R*)-methylmalonyl-CoA to succinyl-CoA, the migrating groups (hydrogen and carbonyl-CoA) retain the original configuration of the group they displace.<sup>128</sup> The displaced group is either the hydrogen when the migrating group is carbonyl-CoA or the carbonyl-CoA group which is displaced by the migrating hydrogen to accomplish the enzyme catalyzed vicinal groups exchange. In contrast to other mutases like glutamate mutase as well as the 2-methyleneglutarate mutase, the methylmalonyl-CoA mutase either poorly distinguishes the 3-pro-*R* and 3-pro-*S* hydrogen atoms on the succinyl-CoA, or the migrating groups fail to retain the original configuration of the displaced group due to inversion during the mechanism for the conversion to (*R*)-methylmalonyl-CoA.<sup>134</sup> This stereospecificity incapability is probably caused by the conformational flexibility at C2 or C3 (or both positions) of succinyl-CoA which have accounts for the poor selectivity in the movement of hydrogen during the catalysis by methylmalonyl-CoA mutase. The enzyme stereospecificity towards the (*R*)-methylmalonyl-CoA is predicted to be controlled by the interaction of the substrate with the active site residues His244, Arg207, and Tyr89.<sup>128</sup>

Earlier mechanistic proposals for methylmalonyl-CoA mutase catalyzed reversible inter-conversions between the postulated (*R*)-methylmalonyl -CoA and succinyl-CoA radicals included the rearrangements either via substrate carbocation or carboanion. Rearrangements via organocobalt intermediates was also considered (figure 22). Since the cob(I)alamin has never been detected in the methylmalonyl -CoA mutase catalytic cycle,<sup>65</sup> the possibility for the rearrangement via substrate carbocation which has to be formed along with the reduction of Co(II) to Co(I) was dropped. The rearrangement via substrate anion was investigated in the studies which the application of the model compounds [EtSC(=O)C(CH<sub>3</sub>)(CH<sub>2</sub><sup>•</sup>)COOEt] and [EtSC(=O)C(CH<sub>3</sub>)(CH<sub>2</sub><sup>-</sup>)COOEt] demonstrated its mechanism to be less rapid and selective.<sup>128,135</sup> Furthermore, the reduction to the substrate anion has to be accomplished along with the oxidation of Co(II) to Co(III) which is against the potential gradient. This unfavourable redox gradient has also implied the rearrangement via the carboanion will be hard to precede.<sup>128</sup> The possibility for rearrangement via organocobalt intermediates was investigated by model compounds which contain cobalt-bonded adducts. Although the used organocobalt compounds revealed the 1, 2 -migration of the groups by the enzyme, the results of these experiments were likely to have errors from the used organo-cobalt compounds because of their ability to form free

organic radicals. Furthermore, the methylmalonyl-CoA mutase crystal structures opposed the rearrangement via the organocobalt on the basis of the distance between the substrate and cob(II)alamin which seem not to allow the organocobalt intermediate to participate in the rearrangement.<sup>128, 136</sup>

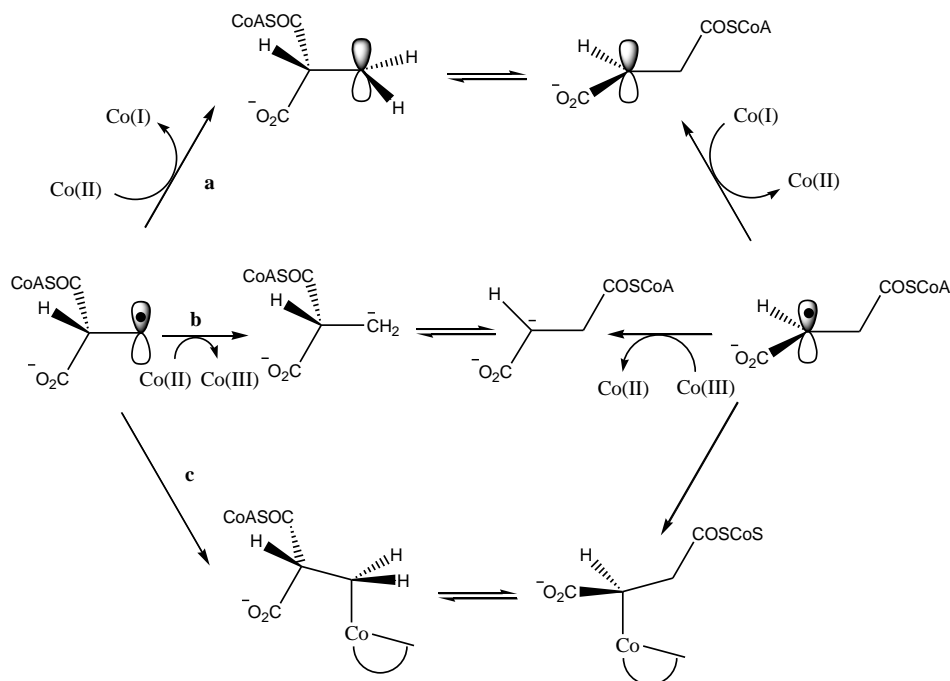


Figure 22: Proposed mechanisms for the rearrangement of (*R*)-methylmalonyl -CoA (**22**) to succinyl -CoA (**21**) via carbocation (route a), carboanion (route b) and organocobalt (route c) intermediates.

Also proposed were rearrangement mechanisms via fragmentation of succinyl -CoA radical (**23**) into acrylate (**24**) and formyl-CoA radical (**25**) which recombine to (*R*)-methylmalonyl -CoA radical (**26**), as well as the possibility for rearrangement by addition-elimination via a cyclopropoxy radical (**27**) due to the  $\pi$ -electron system  $\beta$  to radical carbon like in the 2-methylglutarate mutase.

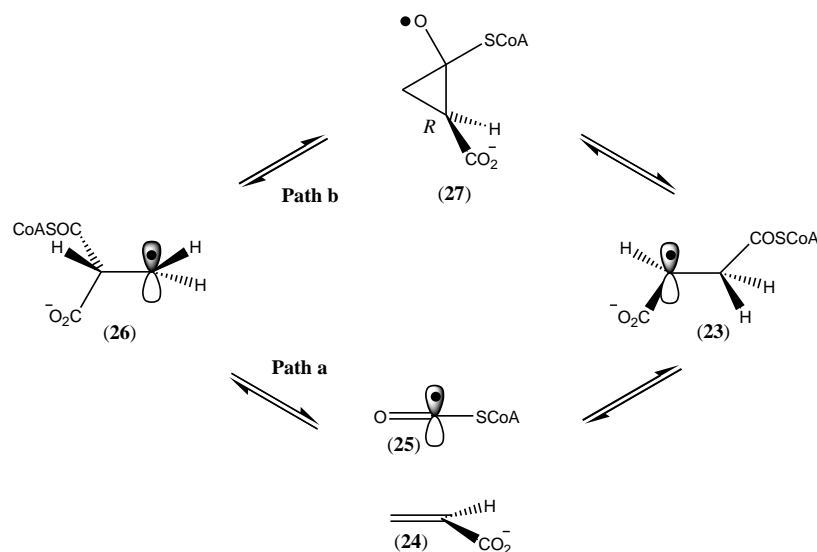


Figure 23: The proposed fragmentation-recombination (path a) and addition-elimination (path b) mechanisms for reversible rearrangement of (*R*)-methylmalonyl -CoA radical to succinyl -CoA radical in the reaction catalyzed by methylmalonyl -CoA mutase

Although the methylmalonyl-CoA mutase was inhibited by the mixture of the acrylate and formyl -CoA, the conclusion on whether the mechanism of this enzyme is by the fragmentation-recombination was still far from reach since the inhibition was EPR silent. Furthermore, from the inhibition results it could not be established which among the three steps intermediates; the methylmalonyl -CoA related radical (26), the acrylate (24) and formyl -CoA radical (25) fragments or succinyl -CoA radical (23) were mimicked by the mixture of acrylate and formyl-CoA. Also considered for distinguishing these two possibilities has been the result obtained from theoretical studies by the *Ab initio* molecular orbital calculations which reported less energy requirement in due to the rearrangement by the addition -elimination in comparison to that by fragmentation -recombination.<sup>118</sup>

Recent reports from the studies of the methylmalonyl -CoA mutase by the group of Banerjee in the University of Michigan have described the role of the cobalamin binding his610 in facilitating the coenzyme B<sub>12</sub> high affinity to apoenzyme.<sup>137</sup> The same group has also described the mechanisms for preventing the apomethylmalonyl -CoA mutase partnership with the cob(II)alamin as well as reviving of the cob(II)alamin inactivated enzyme after several catalytic

turnovers.<sup>138</sup> These preventions of the enzyme from being inactivated by cob(II)alamin were demonstrated to be accomplished by the methylmalonyl-CoA mutase associated MeaB molecular chaperon in the mechanisms which derive energy from GTP and ATP. Similar phenomena has also been described in diol and glycerol dehydratases where the reactivase protein has been demonstrated to accomplish the revive of the cob(II)alamin bound enzyme by removing the cob(II)alamin from the inactivated enzyme.<sup>139</sup>

### 1.6.1.3 Glutamate mutase

The coenzyme B<sub>12</sub> dependent glutamate mutase catalyses the reversible inter-conversion between (S)-glutamate (**28**) and (2S, 3S)-3-methylaspartate (**29**). This reaction forms the first step of the methylaspartate route for glutamate fermentation in *Clostridia* (figure 14).<sup>5, 140</sup>

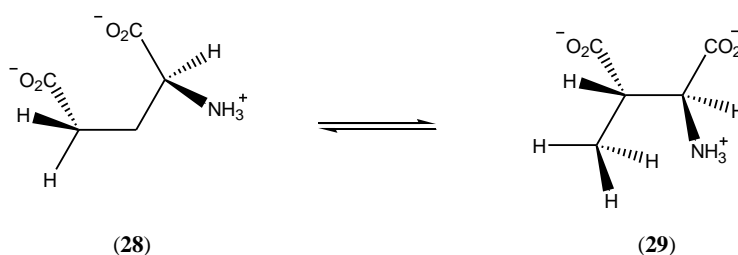


Figure 24: Rearrangement reaction catalyzed by the coenzyme B<sub>12</sub> dependent glutamate mutase

The apo-glutamate mutase is composed of protein subunits; S, a monomer ( $\sigma$ , 14.8 kDa) and E, a homodimer ( $\epsilon_2$ ,  $2 \times 53.5$  kDa). An open reading frame encoding a molecular chaperon L ( $\lambda$ , 50.2 kDa) has also been detected between the genes encoding components S and E in *C. tetanomorphum* and *C. cochlearium*. However, functioning holo-glutamate mutase has been reconstituted in vitro from the incubation of components S and E with coenzyme B<sub>12</sub>. Because the component L is not compulsory for functional reconstitution of the enzyme, glutamate mutase has been studied extensively by only recombinant components S and E overproduced in *E.coli*.<sup>117, 141-145</sup> An active heterotetramer holo-glutamate mutase ( $\epsilon_2\sigma_2$ ) possible bound by two molecules of coenzyme B<sub>12</sub> is formed by assembling of protein components S and E with coenzyme B<sub>12</sub>. In other studies the holoenzyme has been prepared from assembling of the fused components S and E with coenzyme B<sub>12</sub>. The crystal structures of holo-glutamate mutase have

been solved with both an enzyme inhibitor (2*S*, 3*S*)-tartate and the substrate (2*S*, 3*S*)-3-methylaspartate which revealed the “base off, his on” binding of coenzyme B<sub>12</sub> to apoenzyme. The substrate is bound to the enzyme active site by hydrogen bonding of its carboxylate groups with arginines 149, 66 and 100 residues of the active site.<sup>145, 146</sup> Glutamate mutase catalytic cycle start with the binding of substrate to holo-enzyme which triggers the homolysis of the coenzyme Co-C bond resulting into the formation of primary organic radical; 5'-deoxyadenosyl and cob(II)alamin. The former radical is directed by the holoenzyme system to C4 position of (*S*)-glutamate where it stereo-specific abstracts pro *S*- *H*<sub>si</sub> to form the substrate derived 4-glutamyl radical. In contrast to mechanisms of 2-methyleneglutarate mutase as well as methylmalonyl - CoA mutase and other carbon skeleton mutases with  $\pi$ -electrons  $\beta$  to the radical carbons of their substrate derived radicals, the 4-glutamyl radical does not possess  $\pi$ -system  $\beta$  to radical carbon. The rearrangement of 4-glutamyl radical to (2*S*, 3*S*)-3-methylaspartate related radical is therefore possible only by fragmentation –recombination mechanism. In this proposed mechanism; the 4-glutamyl radical fragments into glycine radical (**30**) and acrylate (**24b**) which recombine to form (2*S*, 3*S*)-3- methylenespartate radical (figure 25).



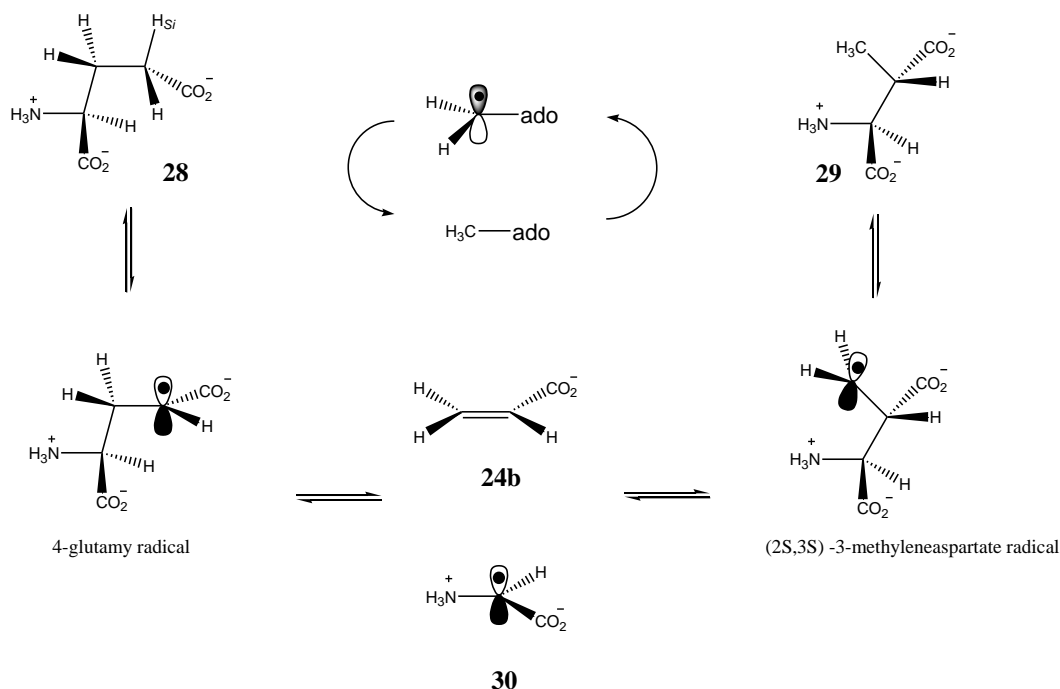


Figure 25: Proposed mechanism for the rearrangement reaction catalyzed by glutamate mutase. The 4-glutamyl radical derived from (*S*)-glutamate fragments into glycine radical (**30**) and acrylate (**24b**) which recombines to form (2*S*, 3*S*)-3-methyleneaspartate radical.

Experimental verifications on the rearrangement of 4-glutamyl radical to (2*S*, 3*S*)-3-methyleneaspartate radical by fragmentation-recombination has been provided from the work of Neil Marsh and his co-workers in the University of Michigan which reported the characterization of acrylate by HPLC during the enzyme reaction with (*S*)-glutamate.<sup>147</sup> The same group also reported the EPR characterization of thioglycolyl radical from the reaction of glutamate mutase with 2-thioglutarate.<sup>148</sup> During the reaction of glutamate mutase with 2-thioglutarate, the intermediate formed thioglycolyl radical mimics the glycine radical intermediate of the proposed fragmentation-recombination mechanism of glutamate mutase. Current studies on glutamate mutase by many laboratories are concentrating on gaining insights into the mechanism of homolytic cleavage of the cofactor Co-C bond and stabilizations of intermediate methylene radicals during the catalysis by this enzyme. The contribution of this thesis towards understanding the mechanism of Co-C bond cleavage and stabilization of intermediate radicals in glutamate mutase catalysis is given in the result and discussion chapters. The experimental designs with well defined aims of studies reported in this thesis are provided in the section for the objective of the studies (section 1.7) as well as in the result chapter.

## 1.6.2 Coenzyme B<sub>12</sub> dependent eliminases

The eliminase class of the coenzyme B<sub>12</sub> dependent enzymes comprises glycerol dehydratase, propanediol dehydratase, ethyleneglycol dehydratase, ethanolamine ammonia lyase (EAL) as well as the ribonucleotide reductases (RNRs). Enzymes of this class are distinguished from mutases by their extended irreversible catalytic elimination of the migrating group X as water or NH<sub>3</sub> after the vicinal exchange rearrangement they catalyze (figure 26).

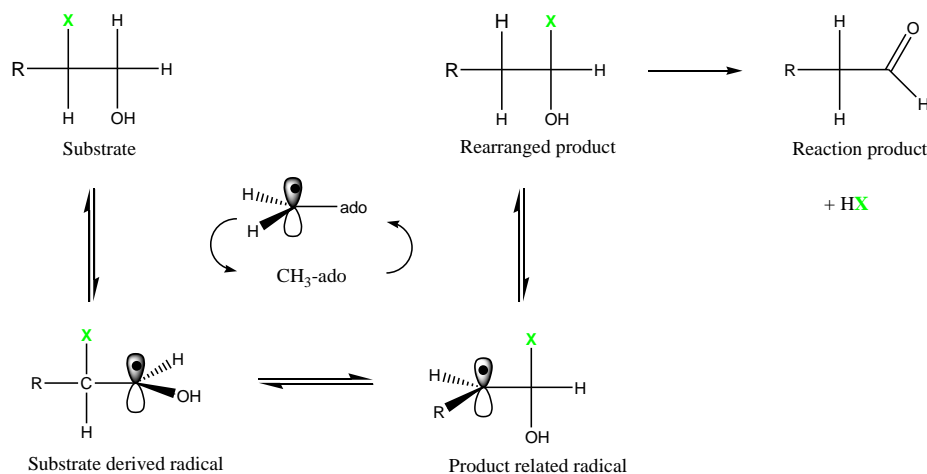


Figure 26. Schematic presentation on the reactions of the coenzyme B<sub>12</sub> dependent eliminases. The vicinal exchange between hydrogen and group X is followed by the elimination of X (X= NH<sub>2</sub> or OH and R = H or CH<sub>3</sub>-)

The minimal mechanistic scheme for the eliminases catalyzed rearrangements has mostly been predicted to resemble that of mutases. However, the mechanistic differences between the mutases and eliminases catalysis were at largely being revealed from the 3D structures of the so far structure solved coenzyme B<sub>12</sub> dependent enzymes. The “base off, his on” partnerships between coenzyme B<sub>12</sub> and mutases proteins so as the “base on, his off” for eliminases have been clearly confirmed by crystal structures of these enzymes. Since the axial ligands in the coenzyme B<sub>12</sub> dependent holoenzymes have been postulated to labilise the cofactor β coordinate which promotes its homolytic cleavage following binding of the substrate to holoenzymes,<sup>137</sup> the difference in the cofactor binding suggests the mechanistic difference in the β coordinate labilisations between mutases and eliminases. Solution of structures of these enzymes by x-ray

crystallography have also revealed difference on the location of the cob(II)alamin between mutases and eliminases catalyzed reactions after the homolysis of the Co-C bond. While in the eliminases the cob(II)alamin has been revealed to locate at a distance from the intermediates of the rearrangements from which it has been considered not involved with the rearrangement mechanisms (spectator), in mutases the cob(II)alamin locates reasonable close to the intermediates of the rearrangements. This observations have lead to the suggestion on the stabilizations of the rearrangement intermediates by cob(II)alamin in mutases (conductor).<sup>149</sup> However, although the cob(II)alamin which is formed along with the 5'-deoxyadenosylradical from the Co-C bond homolysis has been postulated to be insensitive to the intermediates of the rearrangements in the eliminases catalyzed reactions, the course of the 5'-deoxyadenosylradical reactivity has largely resemble that of mutases. In the glycerol, propanediol and ethyleneglycol dehydratases as well as the ethanolamine ammonia lyase (EAL), the substrates derived radicals are usually direct formed by the 5'-deoxyadenosylradical and rearrange to products related radicals before the products are formed along with the regeneration of the coenzyme B<sub>12</sub> and proceed to the elimination of the migrating group x. The intermediate radical species useful stabilization feature in the catalysis by eliminases which also distinguishes them from mutases is the presence of the hydroxyl group bonded to the same carbon which bonds the abstracted hydrogen when the substrate derived radical is formed. This structure feature suggests the stabilization of the substrate derived radical by negative inductive effect from the hydroxyl group as well as promotion of the immigrant group elimination via deprotonation of the hydroxyl group by enzyme base. The migrating group in eliminases reactions is either hydroxyl or amine vinyl to the radical stabilizing hydroxyl group on the substrate.

It is therefore important to highlight on the stabilizations of the intermediates of the coenzyme B<sub>12</sub> dependent reactions as being postulated to be provided by the cob(II)alamin in the mutases and the negative inductive effect by the substrates hydroxyl group in the eliminases. These stabilization mechanisms have been among notable mechanistic differences between the rearrangements by mutases and eliminases which in recent years have become an active theme of investigations.

### 1.6.2.1 Ethanolamine ammonia lyase (EAL)

The coenzyme B<sub>12</sub> dependent ethanolamine ammonia lyase (EAL) is a substrate promiscuous enzyme which catalyses the irreversible conversion of protonated 2-aminoethanol to ethanal as well as both protonated *R* and *S* 2-aminopropanol to propanaldehyde. Ammonia is also formed as a product in all EAL catalyzed reactions. This enzyme was first described in *Clostridium sp.* with relation to choline fermentation before it was also found in several other organisms including *Salmonella typhimurium* and *E. coli*.<sup>150, 151</sup>

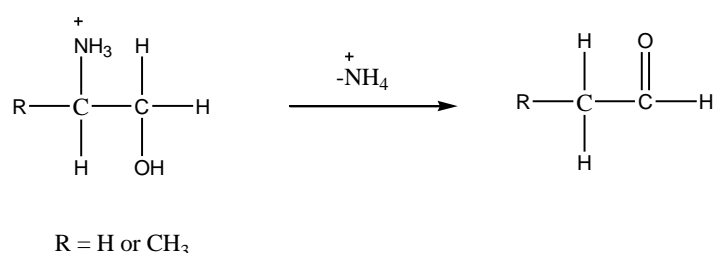


Figure 27: Conversions of the substrates with vicinal amine and -OH groups to their corresponding aldehydes with elimination of NH<sub>3</sub> by the coenzyme B<sub>12</sub> dependent ethanolamine ammonia lyase (EAL)

The EAL has been considered as a key enzyme during the growth of bacteria like *Salmonella enterica* when the phospholipids derived ethanolamine forms the only source of carbon and nitrogen.<sup>152,153</sup> The purification of EAL to homogeneity from *Clostridium sp.* and *E. coli* has allowed several extensive studies on this coenzyme B<sub>12</sub> enzyme which has been revealed to be composed of two subunits, α (51 kDa) and β (36 kDa). These subunits are alleged to oligomerise with coenzyme B<sub>12</sub> to form functioning holoenzyme which is composed of heterohexamer α<sub>6</sub>β<sub>6</sub> apo-protein complex.<sup>111</sup> The number of coenzyme B<sub>12</sub> per oligomeric assembling of holo-EAL has been uncertain. Results from the different experiments for the determination of the number of active sites per the EAL oligomer were not consistent.<sup>151</sup> While the kinetic studies on the EAL suggested the existence of six active sites per oligomer, the titration of EAL with analogues of coenzyme B<sub>12</sub> compounds indicated the existence of two active sites per oligomeric assembly.<sup>111, 154</sup> Extensive kinetics and spectroscopic studies on the EAL catalyzed reaction with different substrates and enzyme inactivators which are analogues to the substrates have been reported to support the formation of the substrate derived 2-amino-1-hydroxyethyl radical. Among theoretical and experimental investigated prediction on the reactivity of the protonated 2-

amino-1-hydroxyethyl radical has been its proposed rearrangement to 1-amino-1-hydroxyethyl radical by the intramolecular 1,2 –shift of the  $\text{NH}_3^+$  group. The latter radical proceed to 1-amino-1-hydroxyethane by claiming hydrogen from the adenosine before being converted to ethanal by the heterolytic elimination of  $\text{NH}_4^+$ . The proposed direct elimination of  $\text{NH}_4^+$  from the 2-amino-1-hydroxyethyl radical to form an allyloxy radical which proceed to ethanal by abstracting hydrogen from the adenosine was similarly investigated <sup>155</sup> (figure 28).

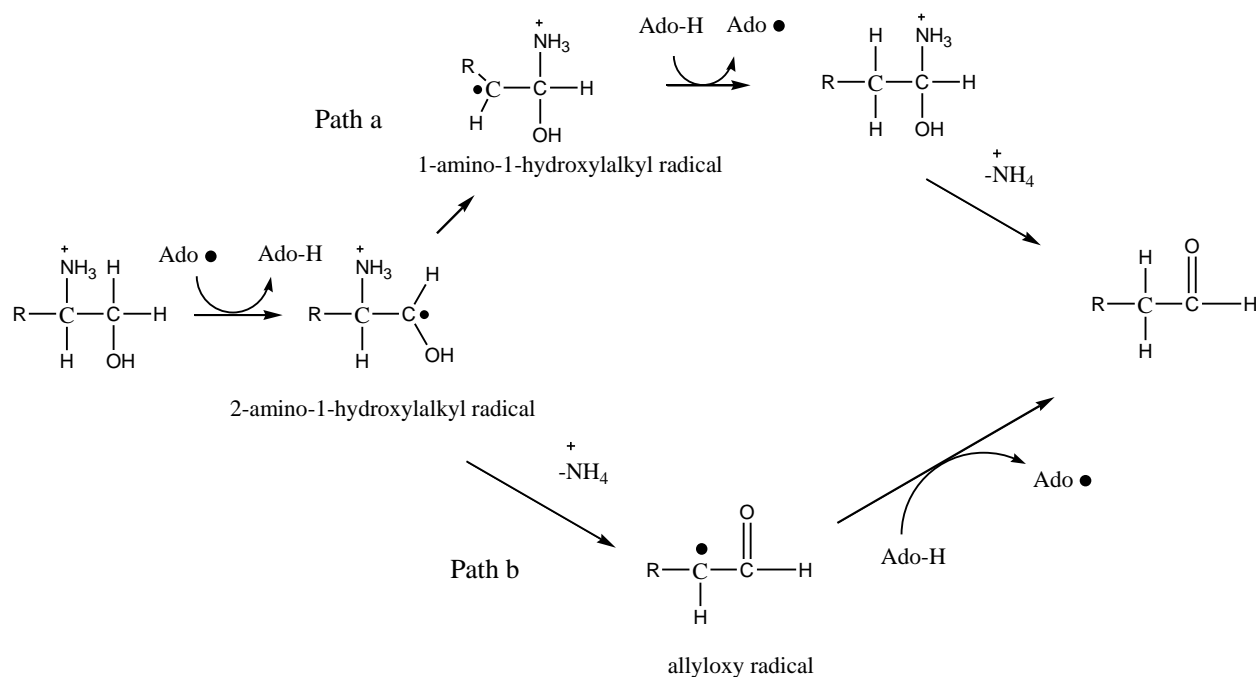


Figure 28: Proposed mechanisms for the respective EAL catalyzed rearrangements of the ethanolamine and enantiomers of the aminopropanol to ethanal and propanaldehydes. Path a is the rearrangement by 1,2-shift of the amine group to form 1-amino-1-hydroxyethyl radicals which proceed to the aldehydes products and path b is the rearrangement to the aldehydes via an allyloxy radicals by the direct elimination of  $\text{NH}_4^+$ . <sup>155</sup>

Although the application of EPR spectroscopy in the studies for the EAL catalyzed reaction identified the radical which was related to the product of the rearrangement, clear characterizations on whether this radical was 1-amino-1-hydroxyethyl (path a) or an allyloxy (path b) could not be achieved. However, the rearrangement by 1,2- shift of the  $\text{NH}_3^+$  group has

been predicted to be assisted by the groups in the EAL active site which are speculated to promote the recombination of  $\text{NH}_3^+$  with the two carbon residue intermediate resulted from the fragmentation to form 1-amino-1-hydroxyethyl radical.<sup>156</sup> Substantial theoretical support for the rearrangement by the migration of the  $\text{NH}_3^+$  group to form 1-amino-1-hydroxyethyl radical comes from the evaluation on the relative reactivity of 1-amino-1-hydroxyethyl and allyloxy radicals. Ab initial calculations by Wetmore, S.D., et al revealed 1-amino-1-hydroxyethyl radical is much more reactive than the allyloxy radical of path b.<sup>155</sup> This results suggest the migration of  $\text{NH}_3^+$  group (path a) is the likely mechanisms for rearrangement by EAL because the formed 1-amino-1-hydroxyethyl radical is more capable of abstracting hydrogen from an adenosine than the allyloxy radical which seem to be stabilized by conjugation.

Numerous putative mechanisms for the rearrangement of the protonated 2-amino-1-hydroxyethyl radical to 1-amino-1-hydroxyethyl radical by the 1,2 migration of  $\text{NH}_3^+$  group have been proposed from the theoretical predictions on the reactivity of these radicals. Their reversible interconversions via a ketyl radical which is predicted to allow the migration of the  $\text{NH}_2$  group to the carbon which bonds OH- where it finally eliminated as  $\text{NH}_3$  as well as the intra-molecular migration of  $-\text{NH}_2$  to the rearranged product before it is eliminated have been among considered mechanisms. Also proposed has been the possibility of the deamination of the protonated 2-amino-1-hydroxyethyl radical to form the resonance stabilized radical cation that allows re-addition of ammonia at the hydroxyl bearing carbon.<sup>151</sup>

### **1.6.2.2 Ribonucleotide reductases (RNRs)**

Ribonucleotide reductases (RNRs) catalyze the conversions of ribonucleoside diphosphate or triphosphate to 2'-deoxyribonucleoside diphosphate or triphosphate (figure 29) during the reactions which the hydride is supplied from the oxidation of NADPH or formate. These unique transformations are accomplished by the radical mechanism that achieves the reductions of ribonucleotides to deoxyribonucleotides for incorporation in DNA in all organisms.

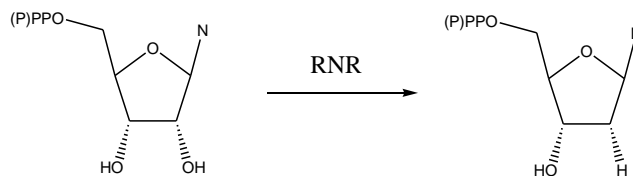


Figure 29: The ribonucleotide reductases (RNRs) catalyzed reduction of ribonucleoside diphosphate or triphosphate to 2'-deoxyribonucleoside diphosphate or triphosphate

Hitherto, all known RNRs have been described to depend on three types of metallocofactors in generating their primary radicals. A chain of reaction is initiated by those primary radicals which create a transient thiyl radical that induces the nucleotide reduction by the radical mechanism in the enzyme active site.<sup>157</sup> This cysteine radical formed by the primary radical is a common species in the mechanism of all RNRs. The radical mechanism of nucleotide reduction induced by the thiyl radical which efficiently achieves the transformations to deoxyribonucleotide is also similar to all RNRs. However, despite all RNRs shares the common role for providing deoxynucleotide monomeric precursors for DNA synthesis with similarities in radical mechanism, their only difference in metallocofactor generators of primary radicals has provided the basis for their classification. The three classes of RNRs have therefore been formed on the basis of their metallocofactors and mechanisms for the formation of primary radicals. While in the *E. coli* and mammalian class-I RNRs chain radical is initiated by the diiron(III)-tyrosine radical, *Lactobacillus leichmannii* class-II RNRs uses coenzyme B<sub>12</sub> to generate the 5'-deoxyadenosyl radical which initiates the chain radical for nucleotide reduction. The chain radical in the class III RNRs which are found in anaerobic *E. coli* is also initiated by 5'-deoxyadenosyl radical. However, in contrast to class II RNRs, the 5' deoxyadenosyl radical in class III RNRs is derived from S-adenosylmethionine (SAM) when it is coordinated with Fe from [4Fe-4S] cluster in the enzyme active site. RNRs which use dimanganese-tyrosine cofactor to generate primary radical have recently been described by the groups of JoAnne Stubbe (Massachusetts Institute of Technology) and Wolfgang Lubitz (Max Planck Institute for Bioorganic Chemistry, Hannover), hence form the subclass Ib of RNRs.<sup>158, 159</sup>

Although the class II RNRs initiate the radical mechanism by the homolytic cleavage of the coenzyme B<sub>12</sub> Co-C bond which forms the 5'-deoxyadenosyl radical, the mechanism of these RNRs have slightly deviated from the established minimal mechanistic scheme for the coenzyme

B<sub>12</sub> dependent enzymes. The formation of substrate derived radical in class II RNRs is achieved via the thiyl radical while in other coenzyme B<sub>12</sub> dependent enzymes, the substrate derived radicals are formed direct by 5'-deoxyadenosyl radical. Established mechanism for class II RNRs revealed the regioselective abstraction of hydrogen from the 3'-position of the ribonucleotide by the thiyl radical to form the substrate derived radical. Deprotonation of the hydroxyl bonded to the 3'-radical carbon by Glu 441 achieves the formation of a carbonyl group with radical migration to 2'-position which eliminates the 2'-hydroxyl group that forms water with a proton from a cysteine residue.<sup>160</sup> The intermediate carbonyl conjugated radical abstracts a hydrogen atom from a cysteine which gives disulfide radical anion. One electron reduction by disulfide radical anion forms an intermediate anion radical that abstracts hydrogen from thiol group with protonation by Glu 441 residue to form the deoxyribonucleotide product. The protein disulfide is reduced by NADPH dependant thioredoxin reductase which recycles them for another turnover.

161, 162

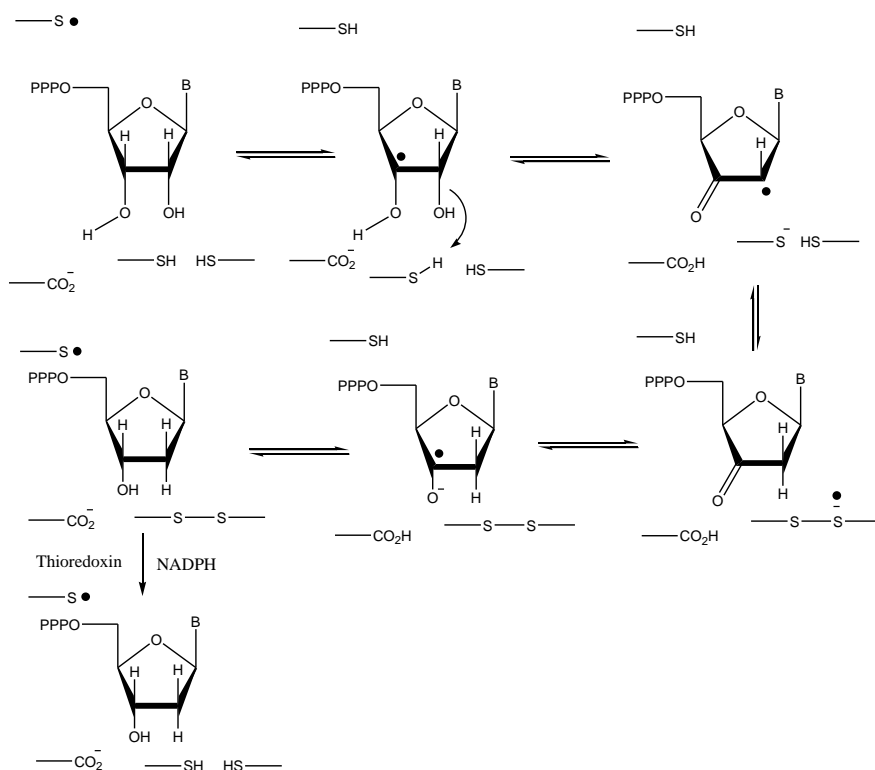


Figure 30: Mechanism of RNRs catalyzed reduction of ribonucleoside diphosphate or triphosphate to deoxyribonucleoside diphosphate or triphosphate



## 1.7 Objectives of the studies

Studies reported in this thesis were aimed toward deriving mechanistic insights into the coenzyme B<sub>12</sub> dependent glutamate mutase catalyzed reversible rearrangement between (*S*)-glutamate and (2*S*,3*S*)-3-methylaspartate from the mechanism based inactivation of the holoenzyme as well as kinetic investigations on the reaction by using coenzyme B<sub>12</sub> structural derivatives.

The mechanism-based inactivation studies were specifically designed to demonstrate the formation of the postulated substrate-derived 4-glutamyl as well as the product-related (2*S*, 3*S*)-3-methyleneaspartate radicals as the intermediates during the reaction of glutamate mutase. Used inhibitors, which are analogues to the 4-glutamyl radical, were *trans*- and *cis*-glutaconates, while structural analogues to (2*S*,3*S*)-3-methyleneaspartate radical included buta-1,3-diene-2,3-dicarboxylate, itaconate, fumarate, maleate, and mesaconate. The mechanism for the hypothetical glutamate mutase inactivations by these inhibitors were theoretically predicted to end up with the formation of an adduct of the 5'-deoxyadenosyl radical at the inhibitor. Experiments in this thesis were focusing on the kinetic characterization of the enzyme inactivation by these inhibitors as well as spectroscopic identification of the postulated radical adducts. The halogenated glutaric acids, 2-fluoroglutaric acid and 2-chloroglutaric acid have been deliberately used to explore as substrates for glutamate mutase as well as deriving mechanistic insights from spectroscopic characterizations of their reactions with holo-glutamate mutase.

Investigations with the structural derivatives of coenzyme B<sub>12</sub>, 2',5'-dideoxyadenosylcobalamin (**32**), 3',5'-dideoxyadenosylcobalamin (**33**), and peptidoadenylcobalamin (**34**) were intended to uncover the mechanisms for assisting the homolytic cleavage of Co-C bond and guiding the 5'-deoxyadenosyl radical towards the substrate by hydrogen bonding interactions. The calculated stabilization of the 5'-deoxyadenosyl radical by hydrogen-bonding of its 3'-O with C<sub>19</sub>-H of cob(II)alamin and its 2'-OH with a conserved glutamate residue of the protein were evaluated kinetically by applying **32**, **33** and **34**.

Furthermore, the structural role for the reaction rate enhancement at the level of homolytic cleavage of the Co-C bond by the 5,6-dimethylbenzimidazole ribonucleotide tail of coenzyme B<sub>12</sub> was also investigated kinetically by using the adenosylpeptide B<sub>12</sub> (**31**) as cofactor for the glutamate mutase reaction during these studies.

An open reading frame encoding a putative chaperon (GlmL, 50.2 kDa) was detected between the genes coding for glutamate mutase components E and S. While GlmL is not necessary for functional expression of *glmE* and *glmS* in *E. coli*, recently it has been speculated that this protein helps to revive the cob(II)alamin containing glutamate mutase by exchange of the inactive cofactor with coenzyme B<sub>12</sub>. Also aimed during the period of this thesis was over expression of the homologous *mutL* gene from *C. tetanomorphum* in *E. coli* to investigate the postulated function of MutL, which is closely related to GlmL.

## **2. Experimental**

### **2.1 Materials**

#### **2.1.1 Chemicals, biochemicals and reagents**

Chemicals and biochemicals were purchased for direct use without any further purification from Sigma Aldrich (Steinheim), Fluka (Neu-Ulm), Merck (Darmstadt), Roth (Karlsruhe) and Bio-Rad-Laboratories (München), except where sources have been mentioned separate in texts. When necessary, organic solvents were distilled from calcium hydride before used. Petrol refers to the petrol fraction with boiling point range 40-60 °C. Protein molecular mass markers, DNA size markers, enzymes for DNA manipulations, oligonucleotides and vector plasmids were from Fermentas GmbH (St. Leon-Rot, Germany). Primers were prepared by MWG-Biotech AG (Ebersberg, Germany) and oligonucleotides sequencing were by Seqlab (Göttingen, Germany).

#### **2.1.2 Equipments**

Large cultures of 10 L and 100 L were grown in a fermenter (Braun, Melsungen, Germany) and anaerobic experiments were performed in a glove box supplied by Coy Laboratories (Ann Arbor, MI, USA). Bacterial cells were opened by a French press (American Instruments, Maryland, USA) or a sonifier (Branson 250, Heinemann, Germany) and the used ultra-centrifuge was supplied by Beckman (München, Germany). DEAE-Sephacel, Superdex 200 and phenyl-Sephacel columns from Merck (Darmstadt) were used for protein purifications with FPLC systems supplied by Pharmacia (Sweden). The Ultimate 300 nano LC/MS system (Dionex, Idstein, Germany) was used for analysis of peptides. UV/visible spectrophotometric measurements of activities and absorption characteristics of enzymes were performed with Ultrospec 1100 pro (Amersham Biosciences) and Uvikon 943 (Kontron Instruments, Switzerland) photometers. T Gradient thermal cycler (Biometra GmbH, Göttingen, Germany) was used for PCR and the purifications of DNA were performed by following appropriate procedures as described in standard protocols supplied with the purification kits (Fermentas GmbH, St. Leon-Rot, Germany and Qiagen Düsseldorf, Germany).

Electrophoresis power supplier (Knürr-Heinzinger, Rosenheim, Germany) was used for providing voltage during DNA gel electrophoreses and visualizations were under high intensity UV light after staining in ethidium bromide. PAC 200 Bio-rad power supplier (Ontario, Canada) was used to provide voltage for proteins SDS-PAGEs.

TLCs were carried out on silica gel (Kieselgel 60 F<sub>254</sub>, 0.2 mm, Merck, Darmstadt) pre-coated aluminium plates. Separated compounds were visualized by both UV light and spraying with 0.1% aqueous KMnO<sub>4</sub>. Silica gel ('flash', Kieselgel 40-63 U 60A) was used in medium pressure chromatography. Deuterated solvents with internal standard proton residual were used in NMR spectroscopy measured at stated frequencies in Bruker Advance spectrometers. Data were reported as follows: chemical shifts  $\delta$  scale in ppm, multiplicity (s = singlet, d = doublet, t = triplet, m = multiplet) and coupling constant (Hz).

## 2.2 Experiments and methods

### 2.2.1 Cultivations of bacteria

#### 2.2.1.1 Cultivation of *Clostridium tetanomorphum*

*Clostridium tetanomorphum* (DSM 576) was anaerobically cultivated at 37°C in overnight cultures from 70 ml followed by 1.5 L which was inoculated to 10 L pre-culture used in the preparation of 100 L main fermenter culture.<sup>163, 164</sup> Wet cells of *C. tetanomorphum* were harvested from the 100 L main culture and stored at -80° C.

Medium composition

	Per liter
▪ Sodium glutamate	18.0 g
▪ Yeast extract	5.0 g
▪ Sodium thioglycolate	1.0 g
▪ 1 M Phosphate buffer (pH 7.4)	20.0 ml
▪ Trace elements (SL10)	10.0 ml

## Trace elements solution (SL10) composition

	Per liter
▪ Hydrochloric acid (25%, 7.7 M)	10.0 ml
▪ FeCl <sub>2</sub> •4H <sub>2</sub> O	1.5 g
▪ ZnCl <sub>2</sub>	70.0 mg
▪ MnCl <sub>2</sub> •4H <sub>2</sub> O	100.0 mg
▪ H <sub>3</sub> BO <sub>3</sub>	6.0 mg
▪ CoCl <sub>2</sub> •6H <sub>2</sub> O	190.0 mg
▪ CuCl <sub>2</sub> •2H <sub>2</sub> O	2.0 mg
▪ NiCl <sub>2</sub> •6H <sub>2</sub> O	24.0 mg
▪ Na <sub>2</sub> MoO <sub>4</sub> •2H <sub>2</sub> O	36.0 mg

The media (70 ml and 1.5 L) in tight closed bottles were boiled, degassed and filled with nitrogen gas which replaced the removed air. During degassing, the anoxic were indicated by resazurin color change to reddish blue. Finally the media were autoclaved (121°C, 30 min) and stored at room temperature in the dark. Preparations of 10 L and 100 L media in fermenters were by the same procedure.<sup>163, 164</sup>

### 2.2.1.2 Cultivation of *E.coli* DH5α with pOZ3 and pOZ5 construct plasmids

Construct plasmids pOZ3 and pOZ5 with respective *glmS* and *glmE* inserts for production of glutamate mutase protein components S and E were prepared and transformed separately in *E.coli* DH5α.<sup>109,110</sup> Cells of *E.coli* DH5α carrying the construct plasmids were aerobically cultivated overnight at 37° C on standard I medium in 5 ml cultures before 250 ml pre-cultures. The 2 L main cultures were prepared by inoculations to 0.1 OD<sub>578</sub> from pre-cultures and incubations at 37 °C for 3 hours to 0.5 OD<sub>578</sub> before inductions by 1 mM IPTG. The induced main cultures producing components S and E were further incubated at 37 °C for 3 hours and overnight respectively before cells were harvested (6000 × g, 20 min) and kept at -80 °C.

## Composition of standard I broth – KOH pH 7.4

	Per Liter
▪ Standard I	25.0 g
▪ Mops	14.0 g
▪ Carbenicillin	50.0 mg
▪ Water	1.0 L

The solution of KOH (aq) was titrated to the mixture of Standard I, Mops and water to pH 7.4 before the mixture was sterilized (121° C, 30 min). Carbenicillin was added aseptically after sterilization.

### 2.2.1.3 Cultivation of MutL expressing *E.coli* ROSETTA

Constructed pASG-IBA3 vectors with component L of glutamate mutase encoding *mutL* insert were chemically transformed into *E. coli* ROSETTA cells which were overnight aerobic cultivated on LB medium at 37 °C from agar to 5 ml cultures. The 500 ml cultures of *mutL* expressing cells were finally prepared from the 5 ml cultures by inoculation to 0.1 OD<sub>578</sub> and incubation for 4 hours at 37 °C to 0.5 OD<sub>578</sub> before the cultures were induced by AHT (200µg/L) and further incubated for overnight. After overnight growth, cells were harvested (6000 × g, 20 min) and kept at -80 °C.

A similar cultivation procedure was used to prepare *E.coli* ROSETTA cells during the production of component L protein of glutamate mutase by 1 mM IPTG induction of cells transformed with pASG-IBA5 clone of *mutL*.

## Composition of the LB medium -HCl pH 7.4

	Per Liter
▪ Tryptone	10.0 g
▪ Yeast extracts	5.0 g
▪ NaCl	10.0 g
▪ Water	1.0 L
▪ Carbenicillin	50.0 mg

HCl (aq.) was titrated to the mixture of tryptone, yeast extracts, NaCl, and water to pH 7.4 before the mixture was sterilized (121 °C, 30 min). During the preparation of LB agar plates, the bacteriological agar (15 g/L) was also added to the above medium composition before sterilization. Carbenicillin was added aseptically after sterilization.

### 2.2.1.4 Cultivation of *E.coli* MG 1655

*E. coli* MG1655 (CGSC 6300) was aerobically cultivated at 37 °C on minimum basic media with various carbon sources and vitamin B<sub>12</sub> supplement.<sup>165</sup> The bacterial growth on the carbon sources and vitamin B<sub>12</sub> media were measured at regular intervals for 7 days.

#### Media composition

Minimum basic medium: - 60 mM K<sub>2</sub>HPO<sub>4</sub>, 33 mM KH<sub>2</sub>PO<sub>4</sub>, 76 mM (NH<sub>4</sub>)<sub>2</sub>SO<sub>4</sub>,  
2 mM tri-sodiumcitrate, 0.1 % (v/v) SL 10<sup>R</sup>, 1 mM MgSO<sub>4</sub>

Carbon sources and B<sub>12</sub> supplement: -

- 20 mM Glucose
- 20 mM Methylmalonate
- 20 mM Methylmalonate and 10 µM cyanocobalamin
- 20 mM Propionate
- 20 mM Propionate and 10 µM cyanocobalamin

Media were sterilized by autoclaving (121° C, 30 min) before glucose, propionic acid, methylmalonic acid and cyanocobalamin were aseptically added. Media with cyanocobalamin supplement were covered by aluminium foils in order to protect the vitamin from light.

#### **2.2.1.5. Cultivation of 2-hydroxyglutarate dehydrogenase expressing *E.coli* BL21**

The pACYCDuet<sup>TM</sup>-1 vector with 2-hydroxyglutarate dehydrogenase encoding hgdH insert was obtained from Ivana Djurdjevic and transformed into *E. coli* BL21.<sup>166</sup> The transformed cells were cultivated overnight at 37 °C on LB medium from an agar via 5 ml and 500 ml pre-cultures to 2 L main cultures which grew from 0.1 OD<sub>578</sub> to 0.5 OD<sub>578</sub> before they were induced by AHT (200µg/L) and further overnight incubated. After the overnight growth, the 2-hydroxyglutarate dehydrogenase expressing cells were finally harvested (6000 × g, 20 min) and kept at -80 °C.

Composition of the LB medium pH 7.4

	Per Liter
▪ Tryptone	10.0 g
▪ Yeast extracts	5.0 g
▪ NaCl	10.0 g
▪ Water	1.0 L
▪ Carbenicillin	50.0 mg

HCl (1 M) was titrated to the mixture of tryptone, yeast extracts, NaCl, and water to pH 7.4 before the mixture was sterilized by autoclaving (121 °C, 30 min). During the preparation of LB agar plates, the bacteriological agar (15 g/L) was also added in the above medium composition before sterilization. Carbenicillin was added aseptically after sterilization.



## **2.2.2 General methods for protein biochemistry**

### **2.2.2.1 Methods for cells disruptions**

Cells were suspended in appropriate buffers and disrupted by pressure (up to 1.4 MPa) applied by pre-cooled French press or ultrasonication under ice- cooling. Cells lyses were monitored by centrifugations ( $6000 \times g$ , 1 min) or microscope and cells free extracts were separated from cells debris and unbroken cells by ultra-centrifugations ( $100,000 \times g$ ,  $4^{\circ}\text{C}$ , 30 min).

### **2.2.2.2 Identification of proteins**

SDS-PAGE was used for qualitative identifications of proteins by comparing their masses with those from the standard protein molecular mass markers. Protein samples for analysis were mixed with 1-2 parts of SDS-buffer (125 mM Tris/HCl, pH 6.8, 10% glycerol, 10% mercaptoethanol, 4% SDS and 0.2% bromophenol blue) and boiled ( $98^{\circ}\text{C}$ , 5- 10 min) to denature proteins. Standard proteins markers were loaded on the gel parallel to the prepared samples and run across stacking and separating gels in electrolyte buffer (25 mM Tris, pH 8.8, 190 mM glycine, 0.1% SDS) by a constant applied voltage (up to 200 mV). The protein migration speed from cathode (-) to anode (+) increases with decreasing size, hence small proteins move faster across the gel than large proteins. The mass dependent migration speed achieves the separation of denatured proteins when running across the gel and therefore allowed their identification by comparing with the standard masses from the marker. Protein bands were visualized by staining (Coomassie brilliant blue R-250 in methanol: water: glacial acetic acid ratio 4:5:1) and destaining (ethanol: water: glacial acetic acid ration 4:5:1).

Components	Separating gel	Stacking gel
1 M Tris/HCl pH 8.8	3000 $\mu$ l	-
1 M Tris/HCl pH 6.8	-	470 $\mu$ l
H <sub>2</sub> O	1370 $\mu$ l	2900 $\mu$ l
10% SDS	85 $\mu$ l	40 $\mu$ l
Acrylamide/Bisacrylamide (40%/1.6%)	2750 $\mu$ l	585 $\mu$ l
5% TEMED	85 $\mu$ l	40 $\mu$ l
10% Ammonium peroxodisulfate	115 $\mu$ l	80 $\mu$ l

Table 3: Composition of SDS-PAGE. The migration speed of polypeptides from cathode(-) to anode (+) across stacking and separating gels due to the applied voltage increases with decreasing protein mass .

When necessary, protein gel bands were accurately identified by peptide sequencing and LC-MS characterisations. Methylaspartase, 2-hydroxylglutarate dehydrogenase and components S and E of glutamate mutase were throughout confirmed by activity assays.

### 2.2.2.3 Protein dialysis and determination of concentration

Protein dialysis for removal of salt after saturation with (NH<sub>4</sub>)<sub>2</sub>SO<sub>4</sub> or NaCl separation gradients during purification was achieved by salts diffusion across membranes of protein dialyzing tubes to KPP buffers. Concentrating protein solutions were accomplished by spinning in appropriate Centricons among the available cutting sizes of 3, 10, 30 and 50 kDa. Proteins concentrations were determined by the Bradford method which uses the principle of the Coomassie brilliant blue maximum absorption shift from 465 to 595 nm after its reaction with the protein.<sup>167</sup> In this method the protein concentration is obtained by fitting the sample absorption at 595 nm to a standard curve obtained with serum albumin.

## 2.2.3 Purification of proteins

### 2.2.3.1 Purification of methylaspartase

#### Purification buffers

Buffer A: 50 mM KPP, pH 7.4, 1 mM MgCl<sub>2</sub>, 1 mg DNase

Buffer B: 5 mM KPP, pH 7.4

Buffer C: 20 mM KPP, pH 7.4, 1 mM EDTA

Buffer D: 20 mM KPP, pH 7.4, 1 mM EDTA, 3 mM DTT

Buffer E: 20 mM KPP, pH 7.4, 1 mM EDTA, 3 mM DTT, 1 M NaCl

Buffer F: 5 mM KPP, pH 7.4, 1 mM EDTA, 3 mM DTT

Buffer G: 50 mM KPP, pH 7.4, 1 mM EDTA, 3 mM DTT, 100 mM KCl

Frozen cells of *Clostridium tetanomorphum* (30 g) were suspended in buffer A (70 ml) before opened by sonication at 50% duty time under ice cooling for 4 × 5 minutes, with 5 minutes of cooling in between, which achieved approximately 70% of broken cells. The sonicated suspension was ultra-centrifuged (100,000 × g, 4 °C, 45 min) and (NH<sub>4</sub>)<sub>2</sub>SO<sub>4</sub> (17 g) was added to the supernatant (74 ml) to attain 40% saturation. The protein solution was then ultra-centrifuged (25,000 × g, 4 °C, 30 min) and the obtained supernatant (72 ml) was further saturated to 70% (NH<sub>4</sub>)<sub>2</sub>SO<sub>4</sub> (14g) with subsequently ultra-centrifugation (25,000 × g, 4 °C, 30 min). Pellets obtained at this step were dissolved in buffer B (25ml) and the formed protein solution was dialyzed for 6 hours (buffer C). DTT (18 mg, 5 mM) was added to the dialyzed protein solution (23 ml) before the solution was loaded to DEAE-Sephacel column pre-equilibrated with buffer D on the FPLC system. Proteins were eluted from the column by an increasing NaCl gradient from 0 to 1 M (buffer E) through which methylaspartase was collected from 20% to 33% and identified by both SDS-PAGE and activity assays. Combined fractions of methylaspartase (68 ml) was saturated to 80% (NH<sub>4</sub>)<sub>2</sub>SO<sub>4</sub> (36 g), ultra-centrifuged (25,000 × g, 4 °C, 30 min) and pellets were dissolved in buffer F (25 ml). The formed protein solution was dialyzed for 4 hours (buffer F) before loaded on gel filtration column (Superdex 200) which was pre-equilibrated by buffer G and eluted by the same buffer.

Fractions containing methylaspartase were again identified by activity assays and SDS-PAGE, combined and concentrated to 2.8 ml (18 mg/ml) by Centricon (30 K). The partial purified enzyme was stored at  $-80\text{ }^{\circ}\text{C}$ .<sup>168, 169</sup>

### **2.2.3.2 Purification of component S of glutamate mutase**

#### **Purification buffers**

Buffer A: 20 mM KPP, pH 7.4, 1 mM EDTA, 2 mM DTT

Buffer B: 20 mM KPP, pH 7.4, 1 mM EDTA, 2 mM DTT, 1 M  $(\text{NH}_4)_2\text{SO}_4$

The GlnS expressing *E. coli* DH5 $\alpha$  cells (10 g) were suspended in buffer A (25 ml) and opened by sonication at 5% duty time under ice cooling for  $3 \times 5$  min, with 5 min cooling intervals in between. The sonicated suspension was ultra-centrifuged ( $100,000 \times g$ ,  $4\text{ }^{\circ}\text{C}$ , 1 hour) and  $(\text{NH}_4)_2\text{SO}_4$  (4 g) was added to the obtained supernatant (30 ml) which brought it to 1M  $(\text{NH}_4)_2\text{SO}_4$ . DTT (20 mg) was also added to the supernatant (30 ml) to bring to 5 mM DTT, before it was loaded on phenyl-Sepharose column on FPLC system which was pre-equilibrated with buffer B. Column bound proteins were eluted by a decreasing  $(\text{NH}_4)_2\text{SO}_4$  gradient from 1 M to 0 during which component S of glutamate mutase was eluted approximately after 20% of buffer B and identified by activity assays. Column fractions containing the component S of glutamate mutase were combined, dialyzed for 6 hours (buffer A), concentrated (20 ml) and loaded on gel filtration column (Superdex 200) pre-equilibrated with buffer A. Proteins were eluted on Superdex 200 column by buffer A and fractions containing GlnS were identified by activity assays, combined and finally concentrated to 3 ml (10 mg/ml) by centricom (3 kDa). The partial purified component S protein was kept at  $-80\text{ }^{\circ}\text{C}$ .<sup>168, 169</sup>

### **2.2.3.3 Purification of component E of glutamate mutase**

#### **Purification buffers**

Buffer A: 20 mM KPP, pH 7.4, 1 mM EDTA

Buffer B: 20 mM KPP, pH 7.4, 1 mM EDTA, 1 M  $(\text{NH}_4)_2\text{SO}_4$

*E. coli* DH5 $\alpha$  cells (6 g) producing component E of glutamate mutase were suspended in buffer A (17 ml) before cells were opened by sonication at 5% duty time under ice cooling for 3  $\times$  5 min, with 5 min cooling intervals in between. The sonicated suspension was ultra-centrifuged (100,000  $\times$  g, 4  $^{\circ}$ C, 1 hour) in order to separate cell debris and unbroken cells (pellets) from the cell free extracts (29 ml supernatant) which was brought to 1 M (NH $_4$ ) $_2$ SO $_4$  (4 g) before loaded on a phenyl-Sepharose column pre-equilibrated with buffer B attached to a FPLC system. Column bound proteins were eluted by decreasing (NH $_4$ ) $_2$ SO $_4$  gradient from 1 M to 0 through which component E of glutamate mutase was eluted after about 60% of buffer B before being identified by activity assays. Column fractions with mutase component E were combined, dialysed for 6 hours (buffer A) and concentrated to 20 ml before loaded on a gel filtration column (Superdex 200) which was pre-equilibrated with buffer A. Proteins were eluted on the gel filtration column by buffer A before column fractions containing glutamate mutase component E were identified by activity assays, combined and finally concentrated to 2.4 ml (5.2 mg/ml) by centricom (30 kDa). The partial purified component E of glutamate mutase was stored at -80  $^{\circ}$ C.<sup>168, 169</sup>

#### **2.2.3.4 Purification of 2-hydroxyglutarate dehydrogenase**

##### **Purification buffers**

Buffer A: 100 mM Tris, pH 8, 150 mM NaCl

Buffer B: 100 mM Tris, pH 8, 150 mM NaCl, 2.5 mM Desthiobiotine

The 2-hydroxyglutarate dehydrogenase producing *E. coli* BL21 cells (5 g) were suspended in buffer A (15 ml) and opened by a pre-cooled French press with an applied pressure of 1.4 MPa. The suspension of opened cells was ultra-centrifuged (100,000  $\times$  g, 4  $^{\circ}$ C, 1 hour) and the obtained supernatant of cell free extract (17 ml) was loaded on the Strep-Tactin affinity column (5 ml) pre-equilibrated with buffer A at 4  $^{\circ}$ C. The recombinant 2-hydroxyglutarate dehydrogenase protein was washed on the column by buffer A (20ml) before being eluted by buffer B (15 ml), concentrated (10 kDa Centricon) and finally kept at -20  $^{\circ}$ C.

## **2.2.4 General methods for molecular biology**

### **2.2.4.1 Identification of DNAs**

DNAs were identified on the basis of their sizes by agarose gel electrophoresis. Depending on the gel concentration, agarose was mixed with TAE buffer (50× diluted, 2 M Tris, 1ml acetic acid, 50 mM EDTA) in appropriate concentrations followed by microwave heating that dissolved the agarose in buffer. The hot agarose solution was cooled to 60 °C before poured into the casting tray fixed with wells shaping comb where it was allowed to solidify by cooling to room temperature. DNA samples were mixed with the loading buffer (0.21% bromophenol blue, 0.21% xylene cyanol FF, 0.2 M EDTA, 50% glycerol, pH 8.0) and loaded on the gel parallel to the DNA ladder. Voltage potential which leads to the migration of double stranded DNA fragments (300 to 4000 base pairs) from cathode (-) to anode (+) was then applied across the gel in TAE buffer. As the DNA migration speed in due to the applied voltage increases with decreasing fragment size, DNAs were separated and identified by comparing their sizes with those of standard DNA fragments from the ladder. The visualization of DNA fragments was by UV light after staining in ethidium bromide. Purified DNA and plasmid clones were further precisely characterized by sequencing.

### **2.2.4.2 DNA purification**

After extracted from *C. tetanomorphum*, the total genomic DNA was further purified by ethanol precipitation during the following procedure:-

The mixture of DNA sample (2 ml), sodium acetate (3 M, pH 4.5, 200 µl) and 96% cold ethanol (4 ml, -20°C) was kept at -80 °C for 30 minutes during which DNAs precipitated. The solution with DNA precipitates was thereafter transferred to Eppendorf cups (1 ml each), centrifuged (15,000 × g, 30 min). Obtained pellets (DNAs) were further washed by suspending in 70% cold ethanol (200 µl, -20 °C), centrifuged (15,000 × g, 30 min) and dried (37 °C, 20 min). Finally the DNAs pellets were dissolved in sterile water (500 µl) and kept at 4 °C.

PCR products and cloned plasmids were purified by established procedures from standard protocols which were provided with Gene JET™ purification kits.

### 2.2.4.3 Determination of DNA purity and concentration

The index of DNA sample absorptions ratio at 260 nm to 280 nm ( $A_{260}/A_{280}$ ) was useful in determining the purity of extracted total genome. The index 1.8  $A_{260}/A_{280}$  indicated more than 90% DNA purity. Concentrations of purified DNAs and vector plasmids were measured by UV/Visible spectrophotometer.

## 2.2.5 Preparations of pASG-IBA3 and pASG-IBA5 clones of mutL

### 2.2.5.1 Extraction of *Clostridium tetanomorphum* total genome

#### Extraction buffers

Buffer A: - 50 mM Tris-HCl pH 8, 25% Saccharose

Buffer B: - 50 mM Tris-HCl, pH 8, 25 mM EDTA

Buffer C: - 50 mM Tris-HCl, Ph 8, 50 mM EDTA, 1% SDS

Buffer D: - 10 mM Tris, pH 7.4, 1 mM EDTA

Cells of *C. tetanomorphum* (2 g) were suspended in buffer A (4 ml) before lysozyme (50 mg) was added to the cells suspension and gently shaken at 37 °C for 90 minutes. After the shaking incubation, buffer B (4 ml) was added to the solution of suspended cells and further incubated in ice for 15 minutes. The suspended cells were thereafter lysed by the addition of buffer C, RNase (100 µg), proteinase K (10 mg) and shaking at 37 °C for 3 hours. Proteins were extracted from the solution of lysed cells (10 ml) by phenol (3 x 10 ml) and phenol-chloroform (2 x 10 ml) before the DNA solution was dialyzed for 24 hours (buffer D) and further purified to 1.8  $A_{260}/A_{280}$  by ethanol precipitation. The extracted genome was finally stored at 4 °C.

### 2.2.5.2 PCR amplification of mutL from the genome of *C. tetanomorphum*

The mutL gene from the genome of *C. tetanomorphum* was multiplied in a 50 µl PCR with the below sequence of primers and composition:-

Forward primer: - **aagctcttcagtgatgcttattacttttag**

Reverse primer: - **aagctcttcaccaacttaaccaataacttttc**

PCR composition: - dNTP 200  $\mu$ M  
Forward primer 500 nM  
Reverse primer 500 nM  
Template DNA 2 to 50 ng/ $\mu$ L  
Polymerase 1 U

Temperature cycling: - 98 ° C 30 sec  
98 ° C 10 sec  
72 ° C 45 sec  
72 ° C 10 sec  
4 ° C 4 sec

### **2.2.5.3 Cloning of mutL into pASG-IBA3 and pASG-IBA5 vector plasmids**

The PCR amplified mutL gene was inserted on IBA-20 pre-entry vectors by L<sub>g</sub>ul and T4 ligase respective restriction and ligation reactions before the vectors were chemically transformed into *E. coli* DH5 $\alpha$  cells which grew overnight at 37 °C on X-gal supplemented LB ager. White colonies from the ager culture were inoculated on LB medium (3 ml) and grew overnight at 37 °C. IBA-20 vector plasmids with the mutL insert were purified (min-prep) from the 3 ml broth cultures and the mutL genes from these pre-entry vectors were thereafter inserted on pASG-IBA3 and pASG-IBA5 expression vectors during the separate restriction and ligation reactions by  $\epsilon$ sp3I and T4 ligase respectively. Constructed expression pASG-IBA3 and pASG-IBA5 vectors with mutL inserts were chemically transformed into *E. coli* DH5 $\alpha$  cells which grew at 37 °C on LB medium in overnights ager and broth cultures (3 ml) before were purified (min-prep) and finally kept at -20 °C.

The standard LB medium pH 7.4 composition was supplemented with x-gal (25  $\mu$ gml<sup>-1</sup>), kanamycin (50  $\mu$ gml<sup>-1</sup>) and carbenicillin (100  $\mu$ gml<sup>-1</sup>) which were added aseptically after sterilization of the medium by autoclaving (121 °C, 30 min).



## 2.2.6 Synthesis of chemicals

### 2.2.6.1 Synthesis of *cis*-glutaconic acid

#### 2.2.6.1.1 Dibromolaevulinic acid

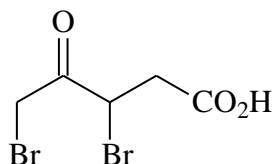


Figure 31: Dibromolaevulinic acid

Bromine (8.28 g, 51.8 mmol, 2.66 mL) was added drop wise to laevulinic acid (3.06 g, 25.86 mmol) in 48 % HBr (2.81 mL, 51.7 mmol) at 0 °C over 30 min. The reaction mixture was stirred at 0 °C for 4 h. Excess of bromine was removed by a nitrogen flow. The resulting solution was kept overnight at 0 °C to give a solid which was taken up in ethyl acetate (70 mL), washed with saturated aqueous sodium metabisulfate (3 x 15 mL). After drying (MgSO<sub>4</sub>) the solvent was removed to afford a pale yellow crude solid (6.02 g).

Recrystallisation from ethyl acetate/petrol afforded the title compound as a white solid (4.30 g, 61 % yield). m.p. 109-112 °C.<sup>106, 170</sup>

<sup>1</sup>H NMR (300 MHz, CDCl<sub>3</sub>): δ= 2.97 (dd, *J* = 5.6 and 17.6 Hz, 1 H, CHHCO<sub>2</sub>H), 3.29 (dd, *J* = 8.1 and 17.4 Hz, 1 H, CHHCO<sub>2</sub>H), 4.07 (d, *J* = 13.2 Hz, 1H, CHHBr), 4.28 (d, *J* = 12.9 Hz, 1 H, CHHBr), 4.94 (br. t, *J* = 6 Hz, 1 H, CHBr) ppm.

<sup>13</sup>C NMR (75 MHz, CDCl<sub>3</sub>): δ = 30.9 (C-2), 38.4 (C-5), 41.1 (C-3), 174.5 (C-1), 194.4 (C-4) ppm.

### 2.2.6.1.2 Tert-butyltrichloroacetinidate

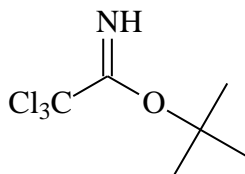


Figure 32: t-Butyltrichloroacetinidate

A solution of trichloroacetonitrile (5.0 g, 34.6 mmol) in dry diethyl ether (12 mL) was added dropwise to a solution of potassium t-butoxide (0.38 g, 3.46 mmol) in t-butanol (7 mL) and dry diethyl ether (8 mL) at 0 °C under nitrogen. The reaction mixture was allowed to warm up at room temperature for 1 h before being heated at reflux under nitrogen for 1 h. After cooling to room temperature, the solvent was removed to give a residual oil, which was taken in n-pentane, filtered and evaporated to give a crude oil (6.26 g). Distillation at water pump pressure gave the title compound (4.58g, 61%).<sup>170</sup>

<sup>1</sup>H NMR (300 MHz, CDCl<sub>3</sub>): δ = 1.5 (9H, s, O-C (CH<sub>3</sub>)<sub>3</sub>), 8.15 (1H, s, =NH)

### 2.2.6.1.3 3, 5-Dibromolaevulinic t-butylester

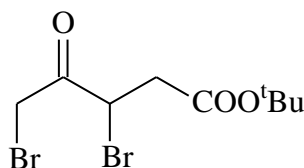


Figure 33: 3, 5-Dibromolaevulinic t-butylester

A solution of t-butyltrichloroacetinidate (0.81 g, 3.71 mmol, 2 equivalents) in dichloromethane (5 mL) was added dropwise to a solution of dibromolaevulinic acid (0.52 g, 1.90 mmol) in dichloromethane (5 mL). After the overnight room temperature stirring, the reaction mixture was quickly treated with ice cold 5% NaHCO<sub>3</sub> (2 x 10 mL), washed with water (2 x 10 mL) and dried (Na<sub>2</sub>SO<sub>4</sub>).

Solvent removal gave the crude solid (0.93 g) which was purified by flash chromatography (ether: petrol 10%) to give oil of the title compound (0.52 g, 83%).

$^1\text{H}$  NMR (300 MHz,  $\text{CDCl}_3$ ):  $\delta = 1.37$  (9H, s,  $-\text{C}(\text{CH}_3)_3$ ), 2.80 (dd,  $J = 5.6$  and 17.6 Hz, 1 H,  $\text{CHHCO}_2\text{H}$ ), 3.15 (dd,  $J = 8.1$  and 17.4 Hz, 1 H,  $\text{CHHCO}_2\text{H}$ ), 4.14 (d,  $J = 13.2$  Hz, 1H,  $\text{CHHBr}$ ), 4.31 (d,  $J = 12.9$  Hz, 1 H,  $\text{CHHBr}$ ), 4.90 (br. t,  $J = 6.0$  Hz, 1 H,  $\text{CHBr}$ ) ppm.

#### 2.2.6.1.4 *Cis*-glutaconic acid

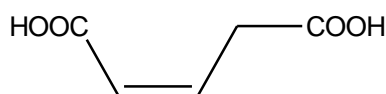


Figure 34: *Cis*-glutaconic acid

$\text{KHCO}_3$  (17.0 g, 169 mmol) in water (210 mL) was added to 3, 5-dibromolaevulinic acid (5.5 g, 21 mmol). The mixture was vigorously stirred for 19 h before the reaction was quenched by acidification (aq. HCl) to pH 2-3 and extracted by diethyl ether ( $10 \times 30$  mL). After drying the combined organic extracts ( $\text{Na}_2\text{SO}_4$ ) the solvent was removed. The obtained yellow solid was decolourised by charcoal and recrystallised from acetonitrile to give the titled compound (0.22 g, 8%). m. p. 132- 133 ° C.<sup>106, 170, 171</sup>

$^1\text{H}$  NMR (300 MHz,  $\text{CD}_3\text{OD}$ ):  $\delta = 3.71$  (dd,  $J = 3.0$  and 7.0 Hz, 2H,  $\text{CH}_2\text{CO}_2\text{H}$ ), 5.93 (dt,  $J = 2.0$  and 11.5 Hz, 1 H, CH), 6.52 (dt,  $J = 7.0$  and 11.6 Hz, 1 H, CH) ppm.

$^{13}\text{C}$  NMR [ $\delta_{\text{C}}$  (75 MHz,  $\text{CD}_3\text{OD}$ ):  $\delta = 35.2$  (C-4), 123.5 (C-3), 142.2 (C-2), 169.5 (C-1), 174.7 (C-5) ppm.

### 2.2.6.1.5 *Cis*-glutaconic t-butylester

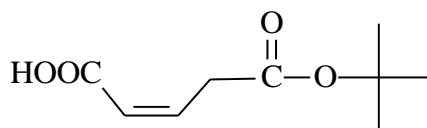


Figure 35: *Cis*-glutaconic t-butylester

During the different experiments performed in the below chemical equivalence with reaction time varied from 3 to 72 h and different workup attempts:-

Solutions of dibromolaevulinic t-butylester (0.25 g, 0.76 mmol) in THF (1 mL) were added dropwise over 5 min to solutions of  $\text{KHCO}_3$  (0.40 g, 3.8 mmol) in water (3 mL) at room temperature. Reaction mixtures were kept stirred and monitored by TLC. In each experiment, the product (*cis*-glutaconic t-butylester) spot was formed after 2 h and the starting material spot was not decreasing even to those reaction mixtures which were left for 72 h. In the work up procedure which the reaction mixture was first diluted with water (10 mL), washed with ether (3 x 10 mL) and acidified to pH 2 (aq. HCl) before extracted by diethyl ether (10 x 10 mL), dried ( $\text{MgSO}_4$ ) and evaporated, the mixture of *cis* and *trans*- glutaconic t-butylester (0.01 g, 10%) was obtained. 56% of starting material (dibromolaevulinic t-butylester) was recovered from diethyl ether washings.

In another work up procedure; the reaction mixture was washed with ether (2 x 10 mL), acidified to pH 2-3 (aq. HCl) and quickly saturated with brine before extracted by dichloromethane (10 x 10 mL) afforded the same yield of the mixture of *cis*- and *trans*- glutaconic t-butylester.

$^1\text{H}$  NMR (300 MHz,  $\text{CDCl}_3$ ):  $\delta$  = 1.40 (9H, s, -C ( $\text{CH}_3$ )<sub>3</sub>), 3.60 (dd,  $J$  = 3.0 and 7.0 Hz, 2H,  $\text{CH}_2\text{CO}_2\text{H}$ ), 5.90 (dt,  $J$  = 2.0 and 11.5 Hz, 1 H, CH), 6.57 and 6.85 (dt,  $J$  = 7.0 and 11.6 Hz, 1 H, CH) ppm.

#### 2.2.6.1.6 4-Bromodihydropyran-2, 5-dione

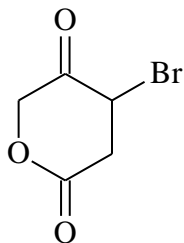


Figure 36: 4-Bromodihydropyran-2, 5-dione

A solution of LiOH (0.153 g, 3.65 mmol) in water (35 mL) was added to dibromolaevulinic acid (0.90 g, 3.29 mmol) and stirred overnight at room temperature. The reaction mixture was then extracted by dichloromethane (5 x 10 mL), dried (MgSO<sub>4</sub>) and evaporated to give crude solid (0.24 g). TLC and NMR analysis showed the product 4-bromodihydropyran-2,5-dione was formed and the starting material dibromolaevulinic acid.

<sup>1</sup>H NMR (300 MHz, CDCl<sub>3</sub>): Dibromolaevulinic acid δ = 3.00 and 3.32 (2H, m, -CH -COOH), 4.11 and 4.31 (2H, m, -CH -Br), 4.94 (1H, q, -CHBr-) and (4-bromodihydropyran-2,5-dione): δ = 2.99 (2H, m, -COCH CHBr-), 4.93 (1H, m, -CHBr-), 5.24 (2H, s, -OCH CO-).

#### 2.2.6.2 Synthesis of 3-[<sup>13</sup>C-*methyl*]methylitaconic Acid

##### 2.2.6.2.1 <sup>13</sup>C- triethylbut-1-ene-2, 3, 3-tricarboxylate

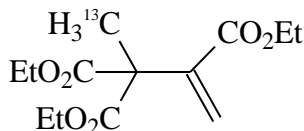


Figure 37: <sup>13</sup>C-triethylbut-1-ene-2,3,3-tricarboxylate

The reaction involved the Malachowski's mixture (Triethylprop-1-ene-2, 3, 3-tricarboxylate and triethyl prop-2-ene-2, 3, 3-tricarboxylate).

Sodium hydride (60 %, 140 mg, 3.5 mmol) was washed with petrol three times, dried, suspended in anhydrous THF (7 mL) and cooled in an ice-bath. Malachowski's mixture (0.645 g, 2.49 mmol) was added dropwise and the reaction mixture was stirred at room temperature for 40 min.  $^{13}\text{C}$ -methyl iodide (0.5 g, 0.22 mL, 3.5 mmol) was added and the reaction was heated (bath temperature 55 °C) for 2.5 h. The solvent was removed and the resulting residue was dissolved in water (30 mL) before extracted with ether (3 x 20 mL). The ethereal solution was washed with water (1 x 10 mL) and standard brine (1 x 10 mL), dried ( $\text{MgSO}_4$ ). Solvent was removed and the yellow oil residue was purified by a silica gel flash column chromatography (10 % ethylacetate: petrol) to afford light yellow oil (0.30 g, 1.1 mmol, 44 %).<sup>172, 173</sup>

$^1\text{H}$  NMR (300 MHz,  $\text{CD}_3\text{CN}$ ),  $\delta$  = 1.23 (t,  $J$  = 7.1, 6H), 1.27 (t,  $J$  = 7.1, 3H), 1.60 (d,  $J$  = 130, 3H), 4.18 (q,  $J$  = 7.1, 6H), 5.79 (s, 1H), 6.30 (s, 1H)

$^{13}\text{C}$  NMR (300 MHz,  $\text{CD}_3\text{CN}$ )  $\delta$  = 15.35 ( $^{13}\text{CH}_3$ )

#### 2.2.6.2.2 3- [ $^{13}\text{C}$ -methyl]methylitaconic acid

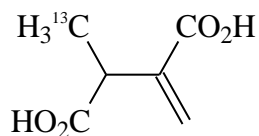


Figure 38: 3- [ $^{13}\text{C}$ -methyl] methylitaconic acid

The mixture of  $^{13}\text{C}$ - triethylbut-1-ene-2, 3, 3-tricarboxylate (0.27 g, 1 mmol) and 20 % HCl (20 mL) was heated (Oil bath temperature of 80 °C) for 72 h. The solvent was removed and the resulting solid (0.12 g) was recrystallized from acetonitrile to give the title compound as a white crystalline solid (0.05 g, 0.34 mmol, 34 %).<sup>172, 173</sup>

$^1\text{H}$ NMR (300 MHz,  $\text{CD}_3\text{CN}$ ),  $\delta$  = 1.30 (dd, 3H  $^{13}\text{CH}_3$ ), 3.53 ( q, 1H CH), 5.79 (s, 1H =CH<sub>2</sub>), 6.30 ( s, 1H =CH<sub>2</sub> )

$^{13}\text{C}$  NMR (300 MHz,  $\text{CD}_3\text{CN}$ ), 15.35 ( $^{13}\text{CH}_3$ )

### **2.2.6.3 Synthesis of coenzyme B<sub>12</sub> structural derivatives cofactors and other probes**

Coenzyme B<sub>12</sub> structural derivatives were synthesized in the laboratory of Dr. Felix H. Zelder, University of Zürich by slightly modified procedures from those described in the literature.<sup>174-178</sup> Buta-1,3-diene-2,3-dicarboxylate and 2-fluoroglutaric acid were synthesized in the laboratory of Prof. B. T. Golding, Newcastle University.

### **2.2.7 Assays for invitro enzymatic reactions**

Hologlutamate mutase was in vitro prepared from glutamate mutase components S and E as well as the coenzyme B<sub>12</sub> or its structural derivatives cofactors. Light sensitive cofactors; coenzyme B<sub>12</sub>, active structural derivatives of coenzyme B<sub>12</sub> and pyridoxal-5'-phosphate were throughout protected from light (aluminum foil shielding) and measurements involved these cofactors were under red light. Quartz cuvettes were used in all absorptions which were measured at any wavelength below 320 nm and 0.5 cm length cuvettes were important in decreasing absorptions to photometer measured range especially in those assays with multi-holoenzyme systems. Appropriate concentrations of all used free cobalamins in “base on” form as well as their reconstitutions to hologlutamate mutase with proteins S and E in Tris-HCl were scanned from 300 nm to 700 nm by using quartz cuvette. Free cobalamins were scanned direct while in the reconstitutions of holoenzymes excess cobalamins were removed by sephadex G25 before scanning.

#### **2.2.7.1 Assays for methylaspartase**

Activity of the in vitro methylaspartase catalyzed irreversible conversion of (2*S*, 3*S*) 3-methylaspartate to mesaconate was generated by the addition of (2*S*, 3*S*) 3-methylaspartate to the enzyme in Tris/HCl buffer (pH 8.3) at 37°C. The enzyme activity were direct assayed by measuring the formation of mesaconate at 240 nm ( $\epsilon_{240} = 3.8 \text{ mM}^{-1} \text{ cm}^{-1}$ ).<sup>179</sup> Assays for identification of column fractions containing the enzyme during purification were composed of Tris/HCl buffer (45 mM, pH 8.3), column fraction and (2*S*, 3*S*) 3-methylaspartate (70 mM)

which was added prior to the spectrophotometric measurement of mesaconate formation. Specific activities of methylaspartase in the form of the rate of mesaconate formation were measured by the same assay during each stage of its purification along with the protein concentrations (Bradford method) and therefore allowed the presentation of the purification report with the specific activities stated in  $\text{Umg}^{-1}$ . During the series of assays for determination of the partial purified enzyme kinetic parameters by the Michaelis-Menten method, initial rates of mesaconate formation by the partial purified methylaspartase ( $0.018 \text{ mgml}^{-1}$ ,  $43.5 \text{ Umg}^{-1}$ ) were measured in due to the variation of (2*S*, 3*S*) 3-methylaspartate concentrations from 5 mM to 250 mM and plotted against the substrate concentrations (Michaelis-Menten curve).

#### **2.2.7.2 Assays for glutamate mutase catalyzed conversion of (*S*)-glutamate to (2*S*, 3*S*)-3-methylaspartate**

Activity due to in vitro glutamate mutase catalysed conversion of (*S*)-glutamate to (2*S*, 3*S*)-3-methylaspartate was measured by the methylaspartase coupled assay which was developed in 1964 by Horace A. Barker.<sup>180</sup> The assay employed an auxiliary enzyme; methylaspartase to convert the (2*S*, 3*S*)-3-methylaspartate generated from (*S*)-glutamate during the coenzyme B<sub>12</sub> dependent reaction of glutamate mutase to mesaconate which is measured at 240 nm ( $\epsilon_{240} = 3.8 \text{ mM}^{-1} \text{ cm}^{-1}$ ). The activity of glutamate mutase was measured as the rate of mesaconate formation by addition of (*S*)-glutamate (40 mM) to the mixture of protein components S and E of glutamate mutase, coenzyme B<sub>12</sub> (0.05 mM) and the partial purified methylaspartase ( $0.072 \text{ mgml}^{-1}$ ,  $43.5 \text{ Umg}^{-1}$ ) dissolved in Tris/HCl (30 mM, pH 8.3) with mercaptoethanol (1 mM) at 37 °C. The concentrations of coenzyme B<sub>12</sub> and methylaspartase were throughout in excess of those of protein components S and E to assure the mutase activity being limiting. During purification of the glutamate mutase protein components S and E, the measurement of the specific activities in each stage of either component purification required excess of the other component. Proteins concentrations were also determined in each purification stage by Bradford method which allowed the presentation of the purification report with specific activities in  $\text{Umg}^{-1}$ .



The kinetics for (*S*)-glutamate was determined with partial purified enzymes by the following 0.5 ml assays:-

▪ Tris-HCl pH 8.3	30 mM
▪ Mercaptoethanol	1 mM
▪ GlmS	5.0 µg
▪ GlmE	2.6 µg
▪ Coenzyme B <sub>12</sub>	0.05 mM
▪ Methylaspartase (43.5 U/mg)	36 µg
▪ ( <i>S</i> )-glutamate	Varied from 5 mM to 300 mM

In each assay a particular concentration of (*S*)-glutamate was added prior to the measurement of initial rate for mesaconate formation in due to the added substrate concentration. Measured data were presented by Michaelis-Menten plotting of initial velocities against (*S*)-glutamate concentrations with stated  $k_{cat}$  and  $K_m$  values which were obtained from the plot.

### **2.2.7.3 Assays for determining the effects of the proposed glutamate mutase inhibitors on methylaspartase**

In the different measurements by the modified methylaspartase assay; glutamate mutase inhibitors (1 mM and 2.5 mM) were incubated for 2 and 6 minutes with the partial purified methylaspartase (9 µgml<sup>-1</sup>, 43.5 Umg<sup>-1</sup>) in 45 mM Tris-HCl (pH 8.3) at 37 °C before methylaspartate (70 mM) were added prior to the measurement of enzyme activities. The activities of methylaspartase measured after the enzyme interactions with particular concentration of an inhibitor in specified duration in minutes were compared to the enzyme specific activity measured by the methylaspartase assay and reported as percent of methylaspartase specific activity.

#### **2.2.7.4 Assays for determining effects of the proposed inactivators on glutamate mutase**

During the measurements by the modified assay for glutamate mutase catalyzed conversion of (*S*)-glutamate to (2*S*, 3*S*)-3-methylaspartate: the holoenzyme generated from the assembly of glutamate mutase components S (0.01 mgml<sup>-1</sup>) and E (0.0052 mgml<sup>-1</sup>) with coenzyme B<sub>12</sub> (0.05 mM) in Tris-HCl (30 mM, pH 8.3) and mercaptoethanol (1 mM) was incubated with glutamate mutase inhibitors (3 mM) at 37 °C for 5 minutes. Excess coenzyme B<sub>12</sub> and inhibitors were filtered (Sephadex G25) before methylaspartase (0.072 mgml<sup>-1</sup>) was added and the mutase catalysis was assessed by measurement of the rate of mesaconate formation after the addition of (*S*)-glutamate (40 mM). The removal of excess inhibitors by filtration prevented the auxiliary enzyme from being inactivated by those inhibitors while allowed measurement of mutase inactivations following its incubation with inhibitors. The measured activities for glutamate mutase after being incubated with these inhibitors were reported as the percentage of mutase specific activity. The reconstituted holo-glutamate mutase was also characterized by UV/visible wave scanning.

#### **2.2.7.5 Assay for conversion of (2*S*, 3*S*)-3-methylaspartate to (*S*)-glutamate catalyzed by glutamate mutase**

During the studies for this thesis an assay for measuring the activity of glutamate mutase in the reverse direction; the conversion of (2*S*, 3*S*)-3-methylaspartate to (*S*)-glutamate was developed. The new assay employed two auxiliary enzymes; the pyridoxal-5'-phosphate dependent glutamic- pyruvic transaminase for respective conversion of (*S*)-glutamate and pyruvate to 2-oxoglutarate and alanine and the NADH dependent 2-hydroxyglutarate dehydrogenase for further conversion of 2-oxoglutarate to 2-hydroxyglutarate. Since the (*S*)-glutamate substrate for glutamic-pyruvic transaminase was generated from (2*S*, 3*S*)-3-methylaspartate by the coenzyme B<sub>12</sub> dependent glutamate mutase rearrangement, hence the mutase reverse reaction was assayed by measuring the depletion of NADH at 340 nm ( $\epsilon_{340} = 6.3 \text{ mM}^{-1} \text{ cm}^{-1}$ ).

(2*S*,3*S*)-3-Methylaspartate = L-Glutamate

L-Glutamate + Pyruvate = 2-Oxoglutarate + L-Alanine

2-Oxoglutarate + NADH + H<sup>+</sup> → (*R*)-2-Hydroxyglutarate + NAD<sup>+</sup>

Sum: (2*S*,3*S*)-3-Methylaspartate + Pyruvate + NADH + H<sup>+</sup> → L-Alanine + (*R*)-2-Hydroxyglutarate + NAD<sup>+</sup>

The 1 ml assay mixture for the determination of kinetic constants of (2*S*, 3*S*)-3-methylaspartate in the reaction of glutamate mutase was with the following composition:-

▪ Test buffer	30.00 mM
▪ Mercaptoethanol	0.05 mM
▪ GlnS	10.00 µg
▪ GlnE	5.20 µg
▪ Coenzyme B <sub>12</sub>	0.025 mM
▪ Pyruvate	20.00 mM
▪ Glutamic pyruvic transaminase (81 U <sub>mg</sub> <sup>-1</sup> )	40.00 µg
▪ Pyridoxal 5- phosphate	0.02 mM
▪ 2-hydroxyglutarate dehydrogenase (1 K <sub>U</sub> <sub>mg</sub> <sup>-1</sup> )	20.00 µg
▪ NADH	0.20 mM
▪ (2 <i>S</i> , 3 <i>S</i> )-3-Methylaspartate	varied from 5 mM to 300 mM

(2*S*, 3*S*)-3-Methylaspartate was added to the solution of glutamate mutase components S and E, coenzyme B<sub>12</sub>, pyruvate, glutamic pyruvic transaminase, pyridoxal 5-phosphate, 2-hydroxyglutarate dehydrogenase and NADH in Tris-HCl pH 8.3 with mercaptoethanol at 37 °C in the above concentrations prior to the measurement of NADH depletion at 340nm. The concentration of (2*S*, 3*S*)-3-methylaspartate was varied during the series of measurements for determination of kinetic constants of (2*S*, 3*S*)-3-methylaspartate by Michaelis-Menten method.

### 2.2.7.6 Assaying effect of inhibitors on auxiliary transaminase and dehydrogenase system

Activities for the pyridoxal-5-phosphate dependent glutamic pyruvic transaminase and NADH dependent 2-hydroxyglutarate dehydrogenase reactions were measured in both without and with proposed glutamate mutase inhibitors at 340 nm ( $\epsilon_{340} = 6.3 \text{ mM}^{-1} \text{ cm}^{-1}$ ) by below 1 ml assays and compared.

#### ‘Transaminase assay’

▪ Tris-HCl pH 8.3	30.00 mM
▪ Mercaptoethanol	0.05 mM
▪ Glutamic-pyruvic transaminase (81 U <sub>mg</sub> -1)	40.00 µg
▪ Pyridoxal 5-phosphate	0.02 mM
▪ 2-Hydroxyglutarate dehydrogenase (1 K <sub>U</sub> mg-1)	20.00 µg
▪ NADH	0.2 mM
▪ INHIBITOR	without, 5 mM, 10 mM, 15 mM and 20 mM
▪ Pyruvate	20.00 mM
▪ Glutamate	20.00 mM

### 2.2.7.7 Characterizations on the interactions of glutamate mutase with its proposed inhibitors by the developed glutamic-pyruvic transaminase and 2-hydroxyglutarate dehydrogenase coupled assay

In the below modified assay for conversion of (2*S*, 3*S*)-3-methylaspartate to (*S*)-glutamate by glutamate mutase; the assay mixture was incubated with proposed inhibitors of glutamate mutase for six minutes before (2*S*, 3*S*)-3-methylaspartate was added prior to the measurement of the rate of NADH depletion at 340 nm ( $\epsilon_{340} = 6.3 \text{ mM}^{-1} \text{ cm}^{-1}$ ). The measured activities of glutamate mutase after incubations with inhibitors were compared with activity measured without incubation with an inhibitor.

The 1 ml assay was with the following composition;-

▪ Test buffer		30.00 mM
▪ Mercaptoethanol		0.05 mM
▪ GlmS		10.00 µg
▪ GlmE		5.20 µg
▪ Coenzyme B <sub>12</sub>		0.025 mM
▪ Inhibitor	Without, 2.5 mM, 5 mM, 7.5 mM, 10 mM, 15 mM	
▪ Pyruvate		20.00 mM
▪ Glutamic pyruvic transaminase (81 U <sub>mg</sub> <sup>-1</sup> )		40.00 µg
▪ Pyridoxal 5- phosphate		0.02 mM
▪ 2-hydroxylglutarate dehydrogenase (1 KU <sub>mg</sub> <sup>-1</sup> )		20.00 µg
▪ NADH		0.20 mM
▪ (2S, 3S)-3-Methylaspartate		200 mM

#### **2.2.7.8 Assays for measurements of kinetic constants of cofactors in the reaction of glutamate mutase**

Kinetic constants of coenzyme B<sub>12</sub> and its active structural derivative cofactors were measured at 37 °C by using standard methylaspartase coupled assay for glutamate mutase with Tris/HCl (50 mM, pH 8.3), mercaptoethanol (0.05 mM) and partially purified enzymes: methylaspartase (43.5 U/mg), GlmS (0.8 U/mg), and GlmE (1.6 U/mg). Hologlutamate mutase was generated from assembly of glutamate mutase components S, E and coenzyme B<sub>12</sub> or its active structural derivative.  $K_m$  and  $V_{max}$  for the natural cofactor were determined in the presence of GlmS (5 µg), GlmE (2.6 µg), methylaspartase (36 µg), glutamic acid (20 mM) and coenzyme B<sub>12</sub> (0.32 – 25 µM) in 1 ml assays.  $K_m$  and  $V_{max}$  for the cobalamin derivatives were determined with 10-times increased amounts of components S and E and concentrations of active coenzyme B<sub>12</sub> derivatives were varied from 0.35µM to 70 µM.  $K_m$  and  $V_{max}$  were obtained from the Michaelis-Menten presentation of activity data. The calculations of  $k_{cat}$  for both coenzyme B<sub>12</sub> and active derivatives were based on component E.

### 2.2.7.9 Spectroscopic characterizations on the interactions of holo-glutamate mutase with its proposed inhibitors

The anaerobic reconstitution of holo-glutamate mutase from GlnS (68  $\mu\text{M}$ ), GlnE (19  $\mu\text{M}$ ) and coenzyme B<sub>12</sub> (250  $\mu\text{M}$ ) in Tris-HCl pH 8.3 (30 mM) and mercaptoethanol (5 mM) was filtered by centricon to remove excess coenzyme B<sub>12</sub> before incubated with fumarate (10 mM) at 37 °C for 1 hour. The UV/visible spectra of the mixture were recorded before fumarate was added as well as after 5 minutes, 30 minutes and 1 hour of incubation with fumarate. In the control experiment, the auxiliary enzyme; methylaspartate (80  $\mu\text{M}$ , 43.5 U mg<sup>-1</sup>) was added to the similar preparation of holo-glutamate mutase without fumarate and the activity of the glutamate mutase was measured at 240 nm ( $\epsilon_{240} = 3.8 \text{ mM}^{-1} \text{ cm}^{-1}$ ) by addition of (*S*)-glutamate.

In another experiment; 2-fluoroglutarate (10 mM) and 2-chloroglutarate (10 mM) were separate aerobic incubated with the holo-glutamate mutase reconstituted from GlnS (6.8  $\mu\text{M}$ ), GlnE (0.5  $\mu\text{M}$ ) and coenzyme B<sub>12</sub> (250  $\mu\text{M}$ ) in dark at room temperature for overnight. The protein components of the mixture (GlnS, GlnE and reconstituted holo-glutamate mutase) were removed by centricon and the obtained mixtures were analyzed by F<sup>19</sup> NMR and LC-MS.

### 2.2.8.0 Assays for the evaluations on the interactions of glutamate mutase with 2-haloglutarates

Since the incubation of 2-fluoroglutarate with methylaspartase (2.2.7.3) demonstrated the complete recovered of methylaspartase activity, the activity of glutamate mutase when 2-fluoroglutarate was used as the substrate was measured by the standard methylaspartase coupled assay in the below composition of 0.5 ml assay mixture:-

▪ Tris-HCl pH 8.3	30 mM
▪ Mercaptoethanol	1 mM
▪ GlnS	5.0 $\mu\text{g}$
▪ GlnE	2.6 $\mu\text{g}$
▪ Coenzyme B <sub>12</sub>	0.05 mM
▪ Methylaspartase (43.5 U/mg)	36 $\mu\text{g}$
▪ 2-fluoroglutarate	10 mM

Glutamate mutase activity was also measured by the standard methylaspartase coupled assay after the incubation of holo-glutamate mutase with 2-fluoroglutarate at 37 °C for 5 minutes and compared with glutamate mutase specific activities by using the below 0.5 ml assays:-

▪ Tris-HCl pH 8.3	30 mM
▪ Mercaptoethanol	1 mM
▪ GlmS	5.0 µg
▪ GlmE	2.6 µg
▪ Coenzyme B <sub>12</sub>	0.05 mM
▪ 2-fluoroglutarate	0, 10 mM
▪ 5 minutes incubation at 37° C	
▪ Methylaspartase (43.5 U/mg)	36 µg
▪ (S)-glutamate	10 mM

## 3. Results

### 3.1 Growth of bacteria and proteins purifications

#### 3.1.1 Purification of methylaspartase from *Clostridium tetanomorphum*

*Clostridium tetanomorphum* (DSM 576) grew anaerobically on the medium with the composition specified in the experimental section 2.2.1.1 during the periods of overnight incubations at 37 °C to the cultivated 50 ml, 1.5 L and 10 L cultures as well as to the final 100 L main fermenter culture. The 340 g of *C. tetanomorphum* wet cells were harvested from the 100 L fermenter culture and used as the source of native methylaspartase as well as for the *mutL* gene during the three years period of these studies. Growth of *C. tetanomorphum* to  $> 1.8 \text{ OD}_{578}$  in all culture volumes as well as to the 340 g which was harvested from the main fermenter culture required up to three days of incubation at 37 °C.

The methylaspartase activity following the addition of (2*S*, 3*S*)-3-methylaspartate to the cell free extract of the harvested *C. tetanomorphum* was up to  $13.7 \text{ U mg}^{-1}$  with the measured  $K_m = 2 \text{ mM}$  for the (2*S*, 3*S*)-3-methylaspartate. The used method for assaying methylaspartase (section 2.2.7.1) was developed in 1958 by Horace A. Barker.<sup>179</sup> This method is based on the methylaspartase catalyzed conversion of (2*S*, 3*S*)-3-methylaspartate to mesaconate which absorbs UV at 240 nm, hence allows the activity assay by measuring the rate of mesaconate formation at 240 nm ( $\epsilon_{240} = 3.8 \text{ mM}^{-1} \text{ cm}^{-1}$ ). Glutamate mutase activity due to the conversion of (*S*)-glutamate to (2*S*, 3*S*)-3-methylaspartate was also detected upon addition of coenzyme B<sub>12</sub> and (*S*)-glutamate to the cell free extract of *C. tetanomorphum*. The used method for assaying glutamate mutase exploits methylaspartase as the helping enzyme (section 2.2.7.2). Also developed by Barker in 1964,<sup>180</sup> this method is based on coupling the glutamate mutase catalyzed conversion of (*S*)-glutamate to (2*S*, 3*S*)-3-methylaspartate with the methylaspartase which converts the (2*S*, 3*S*)-3-methylaspartate produced by glutamate mutase to mesaconate (Figure 39). The methylaspartase has therefore been used as the auxiliary enzyme for assaying glutamate mutase since early 1960's when these enzymes were discovered by H. A. Barker. Most of the glutamate mutase kinetic results reported in literatures were determined by this assay.



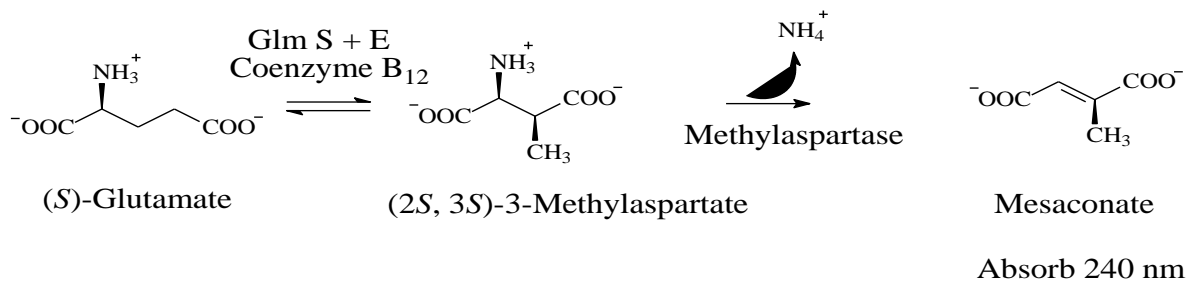


Figure 39: Enzymatic transformations for assaying methylaspartase and glutamate mutase. The conversion of (2*S*, 3*S*)-3-methylaspartate to mesaconate is assayed directly by measuring the rate of mesaconate formation at 240 nm ( $\epsilon_{240} = 3.8 \text{ mM}^{-1} \text{ cm}^{-1}$ ). The conversion of (*S*)-glutamate to (2*S*, 3*S*)-3-methylaspartate by glutamate mutase is assayed by coupling with methylaspartase.

The saturation of *C. tetanomorphum* cell free extracts with  $(\text{NH}_4)_2\text{SO}_4$  up to 70% of the salt during the early steps of the methylaspartase purification was futile in improving the methylaspartase activity and removal of glutamate mutase, although a significant amount of protein was removed. Subsequent purification steps by increased NaCl gradient from 0 to 1 M on a DEAE Sephacel column which was followed by saturation with  $(\text{NH}_4)_2\text{SO}_4$  to 80% of the salt achieved almost twice enrichment of the methylaspartase activity which was elevated to 19.8 U  $\text{mg}^{-1}$ . Further polishing by gel filtration elevated the activity of methylaspartase to 43.5 U  $\text{mg}^{-1}$  with complete separation of methylaspartase from glutamate mutase. Although after the gel filtration column the methylaspartase was still partial purified, the achieved three times enrichment of the activity as well as the separation of glutamate mutase after this step appropriated the methylaspartase for the application to the proposed kinetics and spectroscopic studies on glutamate mutase.

Purification Stage	Activity (U)	Protein (mg)	Spec. Act. (U mg <sup>-1</sup> )	Enr. Factor	Yield (%)
Cell free extract	386.7	2141.2	13.7	1	100
(NH <sub>4</sub> ) <sub>2</sub> SO <sub>4</sub> 40%	204.2	1492.1	10.1	0.7	53
(NH <sub>4</sub> ) <sub>2</sub> SO <sub>4</sub> 70%	262	689.7	9.5	0.7	68
DEAE-Sephacel	138.7	353.9	26.6	2	36
(NH <sub>4</sub> ) <sub>2</sub> SO <sub>4</sub> 80%	239.4	302.1	19.8	1.4	62
Superdex 200	96.7	50.3	43.5	3.2	25

Table 4: Summarized results for the purification of the native methylaspartase from *C. tetanomorphum*

During the course of its purification from *C. tetanomorphum*, methylaspartase demonstrated instability at 4 °C by rapidly decreasing its activity within 3 days of handling at 4 °C. The purification of methylaspartase is therefore strictly entailed to be completed at least within 48 hours in order to allow storage of the enzyme at -80 °C where it significantly retains its activity up to the period of four years as observed during these studies. Portions of methylaspartase which were stored in 50% and 70% (NH<sub>4</sub>)<sub>2</sub>SO<sub>4</sub> at -80 °C also persisted with similar stability as compared to their salt free counterpart which was stored at -80 °C.

Measurement of activities with variations of (2*S*, 3*S*) 3-methylaspartate concentrations from 0 to 250 mM (section 2.2.7.1) lead to the determination of the kinetic constants of (2*S*, 3*S*)-3-methylaspartate;  $V_{\max} = 38 \pm 0.4 \text{ U mg}^{-1}$  and  $K_m = 1.81 \pm 0.05 \text{ mM}$  (literature  $K_m = 2.37 \text{ mM}$ ) in the reaction of the partial purified methylaspartase by the Michaelis–Menten method. The kinetic constants  $k_{\text{cat}} = 29 \text{ s}^{-1}$  and  $k_{\text{cat}}K_m^{-1} = 1.6 \times 10^4 \text{ s}^{-1}\text{M}^{-1}$  were also calculated from the parameters determined by the Michaelis-Menten method.

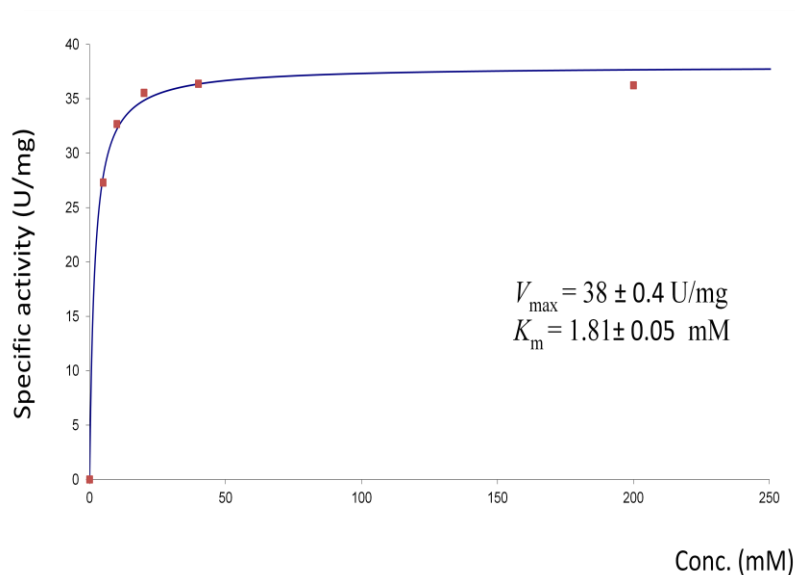


Figure 40: Michaelis-Menten plot for the determination of the kinetic constants of (2*S*, 3*S*)-3-methylaspartate in the reaction catalyzed by the partial purified methylaspartase

### 3.1.2 Purifications of glutamate mutase protein components S and E from *E. coli* DH5 $\alpha$

Cells of *E.coli* DH5 $\alpha$  transformed with pOZ3 and pOZ5 vector plasmids for respective productions of components S and E of glutamate mutase grew aerobically at 37 °C on Standard I medium. The 5 ml culture as well as the 250 ml pre-culture grew from inoculated  $\leq 0.1$  to  $> 2$  OD<sub>578</sub> during the overnight incubations. The 2 L main cultures grew from the inoculated 0.1 to 0.5 OD<sub>578</sub> for about 3 hours before they were induced by 1 mM IPTG to produce components S and E of glutamate mutase. Component S was produced within 3 hours of *E. coli* DH5 $\alpha$  growth to  $\geq 2$  OD<sub>578</sub> after induction while that of component E required an overnight growth to  $> 5$  OD<sub>578</sub>. The production of components S and E were enzymatically confirmed from the glutamate mutase activity which was detected after the addition of (S)-glutamate to the mixture of cell free extracts from both S and E preparations, coenzyme B<sub>12</sub> and methylaspartase in Tris-HCl pH 8.3 buffer as outlined in section 2.2.7.2. The measured glutamate mutase specific activity of expressed components S and E cell free extracts was up to 1.3 Umg<sup>-1</sup>. During the section 2.2.3.2 outlined procedure for the purification of glutamate mutase components S, the decreased gradient of (NH<sub>4</sub>)<sub>2</sub>SO<sub>4</sub> from 1 M to 0 on a phenyl Sepharose column achieved 11 times

enrichment of protein S activity by promoting its specific activity to 15 U $\text{mg}^{-1}$ . Further purification by gel filtration elevated the specific activity of component S to 66 U $\text{mg}^{-1}$  which was an enrichment of the activity by 51.

<b>Pur. stage</b>	<b>Protein (mg)</b>	<b>Spec. activity (U<math>\text{mg}^{-1}</math>)</b>	<b>Enri. factor</b>	<b>Yield (%)</b>
Cell free extract	516	1.3	1	100
Phenyl Sephadex	33	15	11	72
Superdex 200	7	66	51	65

Table 5: Summarized results for the purification of the recombinant component S of glutamate mutase from *E.coli* DH5 $\alpha$

By a procedure similar to that used in the purification of component S, component E was enriched 12 times from 0.5 U  $\text{mg}^{-1}$  in the cell free extract to 5.7 U  $\text{mg}^{-1}$  by the decreased gradient of  $(\text{NH}_4)_2\text{SO}_4$  on a phenyl Sephadex column. The gel filtration by Superdex 200 elevated the activity of component E to 18.1 U $\text{mg}^{-1}$  which is 38-times enrichment. Measurement of the activities of the purification steps of component E were done with the partial purified component S (66 U  $\text{mg}^{-1}$ ).

Although the recombinant glutamate mutase proteins S and E were only partial purified, the achieved specific activity was satisfactory for the proposed kinetic studies on the reaction of glutamate mutase as well as the spectroscopic experiments. Throughout during the studies for this thesis, holo-glutamate mutase was successfully generated from assembly of protein components S and E with the cobalamin cofactors (coenzyme B<sub>12</sub> and its structure derivatives).

<b>Pur. stage</b>	<b>Protein (mg)</b>	<b>Spec. activity (U mg<sup>-1</sup>)</b>	<b>Enr. factor</b>	<b>Yield (%)</b>
Cell free extract	516	0.5	1	100
Phenyl sepharose	28	6	11	66
Superdex 200	7	18	38	58

Table 6: Summarized results for the purification of the recombinant component E of glutamate mutase from *E. coli* DH5 $\alpha$

### 3.1.3 Characterization of the partial purified glutamate mutase

The UV-vis spectrum of the holo-glutamate mutase system generated from the assembling of the partial purified recombinant protein components S and E with coenzyme B<sub>12</sub> closely follow that of coenzyme B<sub>12</sub> in the base on state with characteristic absorption peaks at 490 nm and the maximum at 520 nm (Figure 41). This close resemblance as well as the detection of glutamate mutase activity indicates the presence of the protein bound cob(III)alamin. The spectrum also implies binding of coenzyme B<sub>12</sub> to the apoenzyme in the “base off, his on” mode to form the holoenzyme system with cobalt in the Co (3+) d<sup>6</sup> state. Activities generated due to the conversion of (*S*)-glutamate to (2*S*, 3*S*)-3-methylaspartate by the holo-glutamate mutase reconstituted from the assembling of partial purified proteins S and E with coenzyme B<sub>12</sub> were measured by the described standard methylaspartase coupled assay.<sup>180</sup>

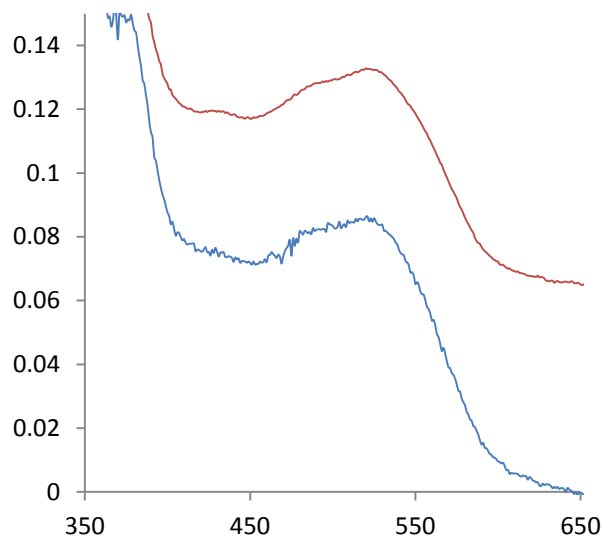


Figure 41: UV-vis spectrum of 0.013 mM coenzyme B<sub>12</sub> (red) and holo-glutamate mutase (blue) reconstituted from the mixture of 0.68 μM component S, 0.05 μM component E and equimolar concentration of coenzyme B<sub>12</sub> which was achieved by Sephadex G25 filtration after mixing with excess coenzyme B<sub>12</sub>. Note the spectrum of coenzyme B<sub>12</sub> is reduced by 2.5

The oligomeric nature of the holo-glutamate mutase system, which brings protein components S and E with the cofactor together for the reconstitution of the holoenzyme has allowed the determinations of the kinetic constants of (*S*)-glutamate as well as that of the coenzyme B<sub>12</sub> in the glutamate mutase reaction from different compositions of apo-proteins S and E. Measurements of glutamate mutase activity for determinations of the kinetic constants were accomplished by the methylaspartase coupled assay (section 2.2.7.2 and 2.2.7.8). The kinetic constants of (*S*)-glutamate in the reaction of the partial purified glutamate mutase reconstituted with 14 excess folds of component S;  $V_{\max} = 3.2 \pm 0.5 \text{ U (mg GlnE)}^{-1}$  and  $K_m = 2.25 \pm 0.03 \text{ mM}$  were obtained from the Michaelis-Menten method. These kinetic constants were used to characterize further the reaction of the partial purified glutamate mutase by calculating  $k_{\text{cat}} = 2.85 \text{ s}^{-1}$  as well as the  $k_{\text{cat}}K_m^{-1} = 1.3 \times 10^{-3} \text{ M s}^{-1}$  for the conversion of (*S*)-glutamate to (2*S*, 3*S*)-3-methylaspartate.

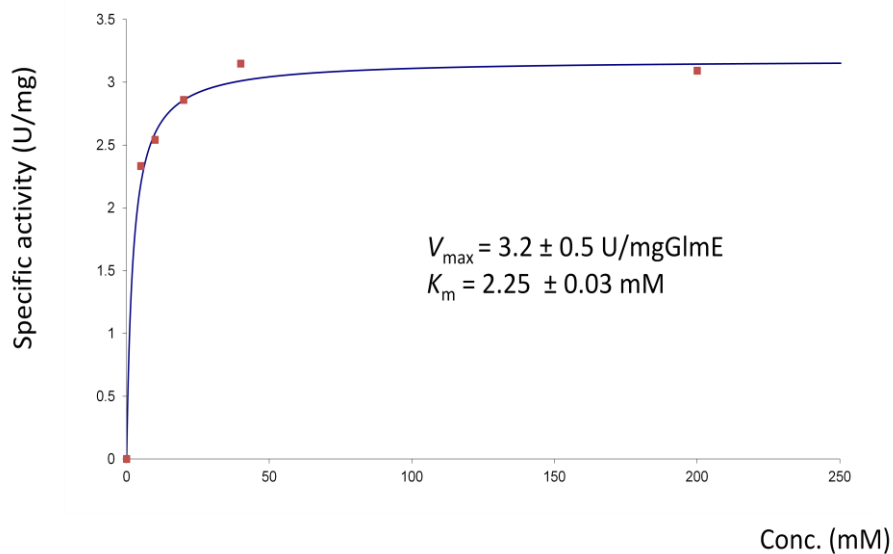


Figure 42: Michaelis- Menten plot for the determination of kinetic constants of (*S*)-glutamate in the reaction catalyzed by the partial purified glutamate mutase reconstituted with 14 excess folds of protein component S

Kinetic constants of coenzyme B<sub>12</sub> during the conversion of (*S*)-glutamate to (2*S*, 3*S*)-3-methylaspartate by the partial purified glutamate mutase reconstituted with 2 folds excess of component S;  $V_{\max} = 1.34 \pm 0.40 \text{ U (mg GlmE)}^{-1}$ ,  $K_m = 1.12 \pm 0.04 \mu\text{M}$  as well as  $k_{\text{cat}} = 1.24 \pm 0.36 \text{ s}^{-1}$  and  $k_{\text{cat}}K_m^{-1} = 1.10 \times 10^6 \text{ s}^{-1}\text{M}^{-1}$  were also determined by Michaelis-Menten method.

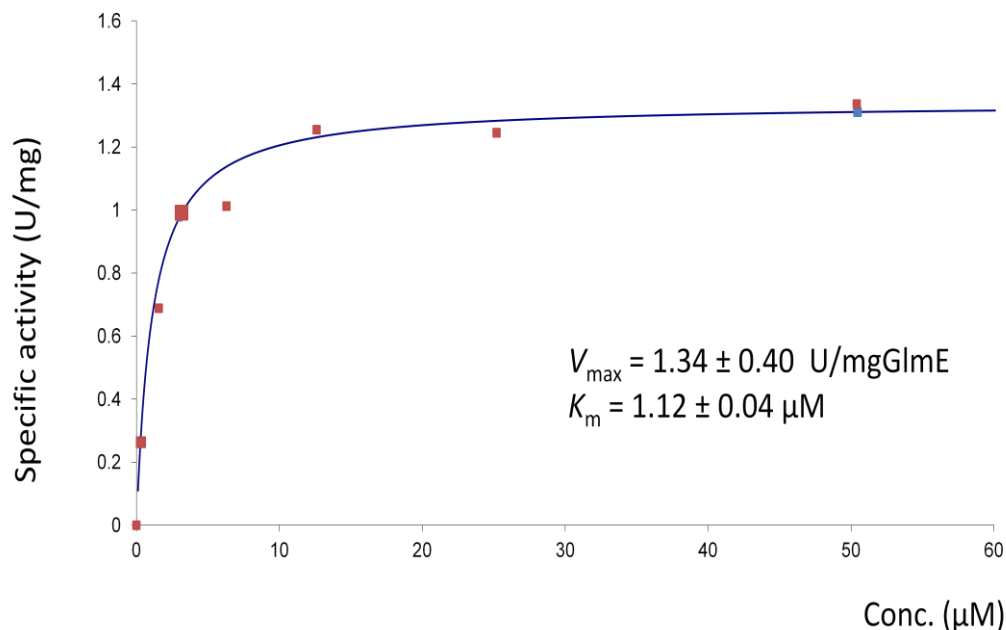


Figure 43: Michaelis-Menten plot for the determination of kinetic constants of coenzyme B<sub>12</sub> during the conversion of (*S*)-glutamate to (2*S*, 3*S*)-3-methylaspartate by the partial purified glutamate mutase reconstituted with a 2-fold excess of component S

Kinetic constants of coenzyme B<sub>12</sub> for the same catalytic conversion of (*S*)-glutamate to (2*S*, 3*S*)-3-methylaspartate were also determined from the reconstitution of the enzyme with 7 as well as 14-fold excess of component S. While the measured specific activities remained almost the same, the  $K_m$  values of the coenzyme B<sub>12</sub> when the enzyme was reconstituted with 7 and 14 folds excess of component S were  $0.70 \pm 0.05 \text{ µM}$  and  $0.52 \pm 0.06 \text{ µM}$  respectively. These kinetics lead to the respective calculated  $k_{cat}K_m^{-1}$  of  $2.4 \times 10^6 \text{ s}^{-1}\text{M}^{-1}$  and  $2.38 \times 10^6 \text{ s}^{-1}\text{M}^{-1}$  from reconstitution of glutamate mutase with 7 and 14 folds excess of component S. It is important to mention on; the specific activity of glutamate mutase decreased from the reported  $18.1 \text{ U(mgGlmE)}^{-1}$  when the enzyme was purified to between  $3.2 \text{ U(mgGlmE)}^{-1}$  and  $1.34 \text{ U(mgGlmE)}^{-1}$  which were measured after 18 months and 2 years of  $-80 \text{ ° C}$  storage of components S and E.



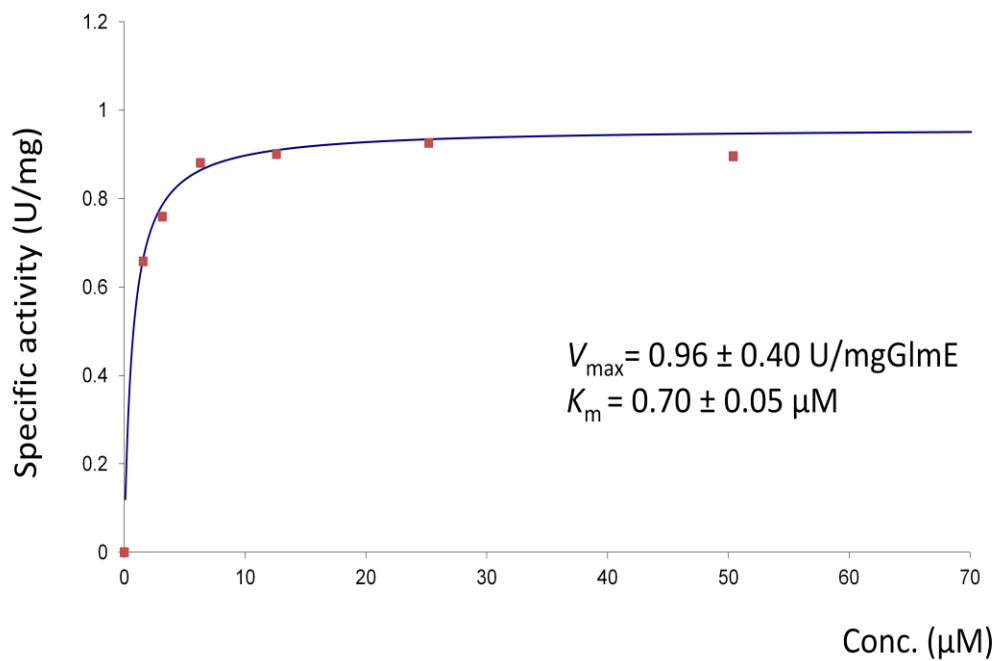


Figure 44; Michaelis-Menten plot for the determination of the kinetic constants of coenzyme B<sub>12</sub> during the conversion of (*S*)-glutamate to (2*S*, 3*S*)-3-methylaspartate by the partial purified glutamate mutase reconstituted with 7-fold excess of component S

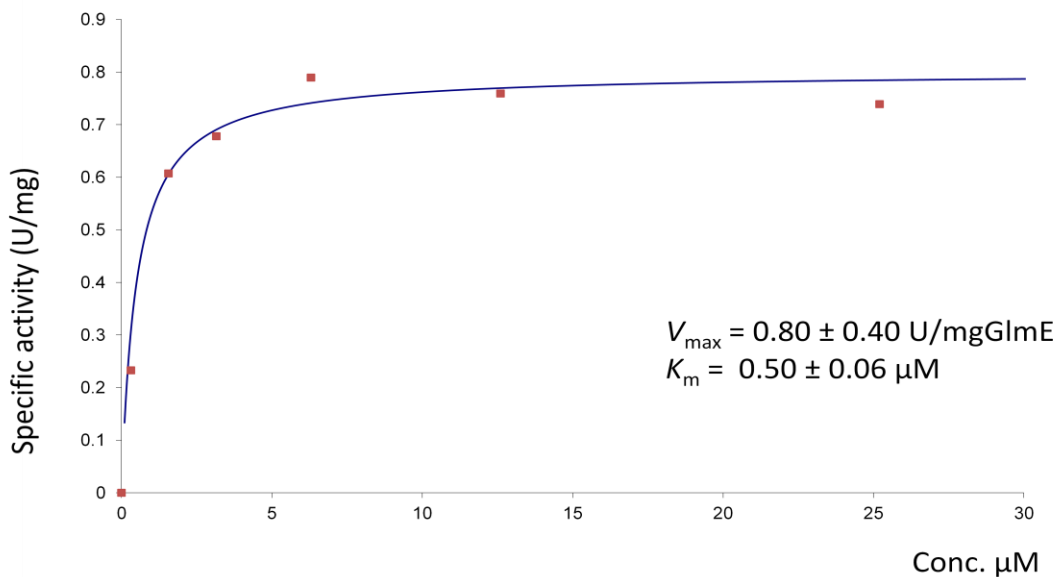


Figure 45; Michaelis-Menten plot for the determination of the kinetic constants of coenzyme B<sub>12</sub> during the partial purified glutamate mutase catalyzed conversion of (*S*)-glutamate to (2*S*, 3*S*)-3-methylaspartate when the enzyme is reconstituted with 14 folds excess of component S

### 3.1.4 Purification of 2-hydroxyglutarate dehydrogenase from *E.coli* BL21

*E. coli* BL21 transformed with pACYCDuet<sup>TM</sup>-1 vector which carries the 2-hydroxyglutarate dehydrogenase encoding *hgdH* gene grew at 37 °C on LB medium from agar colonies to 5 ml and 250 ml broth cultures which grew from  $\leq 0.1$  OD<sub>578</sub> to cultures of  $> 2$  OD<sub>578</sub> in the overnight incubations. The 2 L main culture was first grown for about three hours from 0.1 to 0.5 OD<sub>578</sub> before it was induced by 200  $\mu\text{g L}^{-1}$  anhydrotetracyclin (AHT) to produce 2-hydroxyglutarate dehydrogenase and further incubated for overnight from which it grew to  $> 5$  OD<sub>578</sub>. The activity of 2-hydroxyglutarate dehydrogenase ( $0.13 \text{ kU mg}^{-1}$ ) was determined from the cell free extract of *E.coli* BL21 harvested from the 2 L main culture by addition of excess amount of 2-oxoglutarate to the mixture of the cell free extract ( $105 \mu\text{g ml}^{-1}$ ) and NADH (0.2 mM) dissolved in Tris-HCl (100 mM, pH 8.0). The purification by Streptag (2.2.3.4) enriched the 2-hydroxyglutarate dehydrogenase 8 times by promoting its specific activity to  $1 \text{ kU mg}^{-1}$ .

## 3.2 Synthesis of chemicals used in probing the reaction of glutamate mutase by the mechanism based inactivation approach

### 3.2.1 Synthesis of *cis*-glutaconic acid

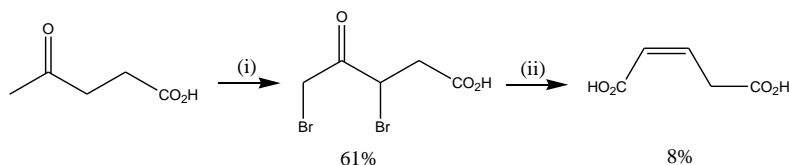


Figure 46: Synthesis of *cis*-glutaconic acid. Reagents (i) Br<sub>2</sub>, aq. 48% HBr; (ii) aq. KHCO<sub>3</sub>

*Cis*-glutaconic acid was prepared in a two-step synthetic scheme from laevulinic acid via dibromolaevulinic acid (figure 46).<sup>106</sup> The first step, aqueous acidic bromination of laevulinic acid, yielded up to 61% of 3,5-dibromolaevulinic acid. This low temperature (0 °C) sensitive regio-specific brominations on the two carbons  $\alpha$  to the carbonyl group of the laevulinic acid starts with a rate determining enolisation catalyzed by 48% HBr before progressing to rapid attack by bromine on the enol  $\pi$ -electrons. Since the ketone is able to form an enol with either of

the two carbons  $\alpha$  to the carbonyl group, further bromination proceeds to form the dibromoketone.

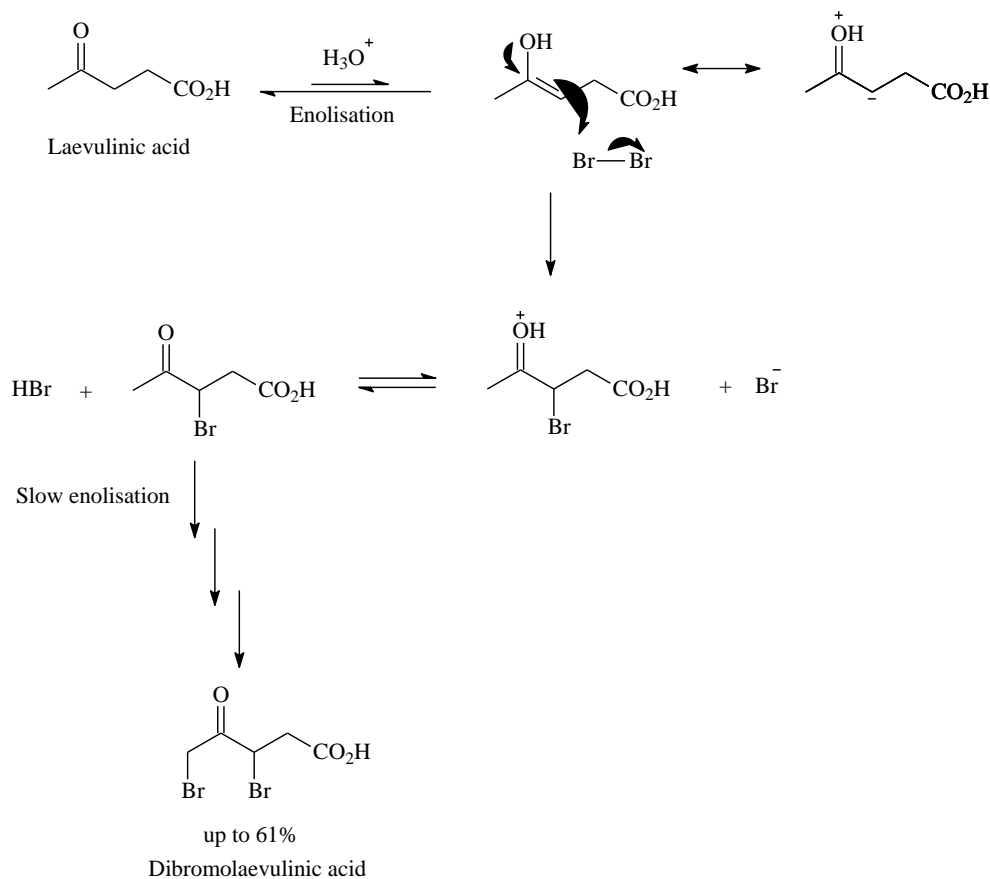


Figure 47: The mechanism for the acidic bromination of laevulinic acid to 3,5-dibromolaevulinic acid

The 2<sup>nd</sup> step for the synthesis of *cis*-glutaconic acid is the rearrangement of the dibromolaevulinic acid by the Favorski mechanism induced by aqueous  $\text{KHCO}_3$  to yield *cis*-glutaconic acid in 8% yield with traces of *trans*-glutaconic acid (less than 2% of the total product)

A revised synthetic scheme aimed at improving the yield of *cis*-glutaconic acid during the Favorski reaction involved the protection of the carboxylic acid group on the dibromolaevulinic acid as a t-butyl ester. The dibromolaevulinic t-butyl ester was therefore synthesized in 83% yield during an overnight room temperature reaction between dibromolaevulinic acid and t-butyltrichloroacetimidate in dichloromethane (DCM). The t-butyltrichloroacetimidate was

prepared in 61% from the reaction between trichloroacetonitrile and potassium tert-butoxide in *t*-BuOH (Figure 48). However, the rearrangement of dibromolaevulinic *t*-butylester by Favorskii mechanism when reacted with aq. potassium bicarbonate yielded *cis*-glutaconic mono-*t*-butyl ester in 8% yield with traces of *trans*-glutaconic mono-*t*-butyl ester. Attempted improvements by increasing the time for the rearrangement by Favorskii mechanism to 72 hours and a significant decrease in the amount of water used during work up after the reaction were futile toward increasing the yield of *cis*-glutaconic acid. The yield of *cis*-glutaconic acid was improved to 10% by saturation of the aqueous reaction mixture with brine after acidification to pH 2 followed by extensive extraction by dichloromethane.

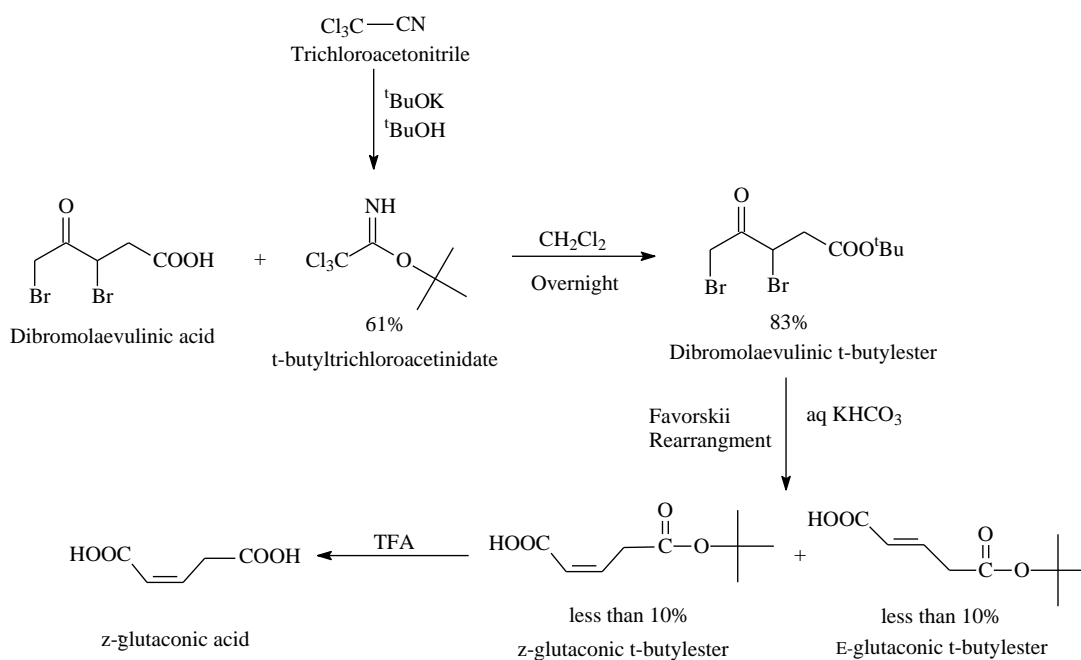


Figure 48: Alternative scheme for the synthesis of *cis*-glutaconic acid.

An also explored synthetic strategy to *cis*-glutaconic acid was via 4-bromodihydropyran-2, 5-dione, which was obtained by a base-induced cyclisation of 3,5-dibromolaevulinic acid (Figure 49). 4-Bromodihydropyran-2, 5-dione is also predicted to rearrange to *cis*-glutaconic acid by the Favorskii reaction with bicarbonate (figure 49).

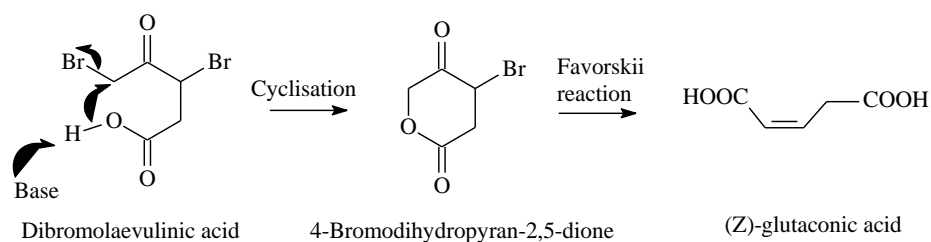


Figure 49: A synthetic strategy to *cis*-glutaconic acid via 4-bromodihydropyran-2, 5-dione.

Attempted cyclisation of 3,5-dibromolaevulinic acid by triethylamine in diethyl ether gave pyran-2, 5-dione, which resulted from base-induced elimination of HBr from the initially formed 4-bromodihydropyran-2, 5-dione (figure 50). An overnight reaction of 3,5-dibromolaevulinic acid with aqueous LiOH demonstrated slow formation of 4-bromodihydropyran-2, 5-dione in an estimated 20% yield from the analysis of TLC and  $^1\text{H-NMR}$ .

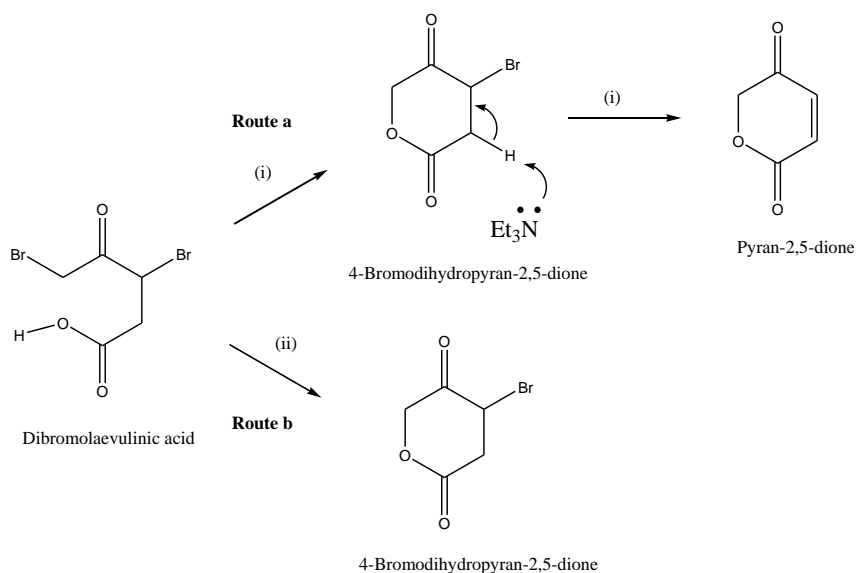


Figure 50: Base induced cyclisation of 3, 5-dibromolaevulinic acid to 4-bromodihydropyran-2, 5-dione. Route a (i) triethylamine, diethyl ether and route b (ii) aq. LiOH.

### 3.2.2 Synthesis of 3-[<sup>13</sup>C-*methyl*]itaconic acid

3-[<sup>13</sup>C-*methyl*]itaconic acid was prepared by a synthetic pathway already developed in the laboratory of Professor Bernard Golding (Newcastle University), which starts with NaH abstraction of protons on the methyl group of triethyl prop-2-ene-2,3,3-tricarboxylate and C-3 of triethyl prop-1-ene-2,3,3-tricarboxylate, which constitutes “Malachowski’s mixture”. The carbanion thus formed Malachowski’s mixture is methylated to <sup>13</sup>C-triethyl but-1-ene-2, 3, 3-tricarboxylate by addition of <sup>13</sup>C-labelled methyl iodide. The methylation was complete in 40 minutes and gave yields of up to 44 % tricarboxylate product. The last step, hydrolysis of two of the diethyl esters and removal of one carboxyethyl group bound to C- 3 of triethyl but-1-ene-2,3,3-tricarboxylate was achieved by heating the tricarboxylate with 20% HCl at 80 °C for 72 hours which afforded racemic 3-[<sup>13</sup>C-*methyl*]itaconate in 34 % yield.

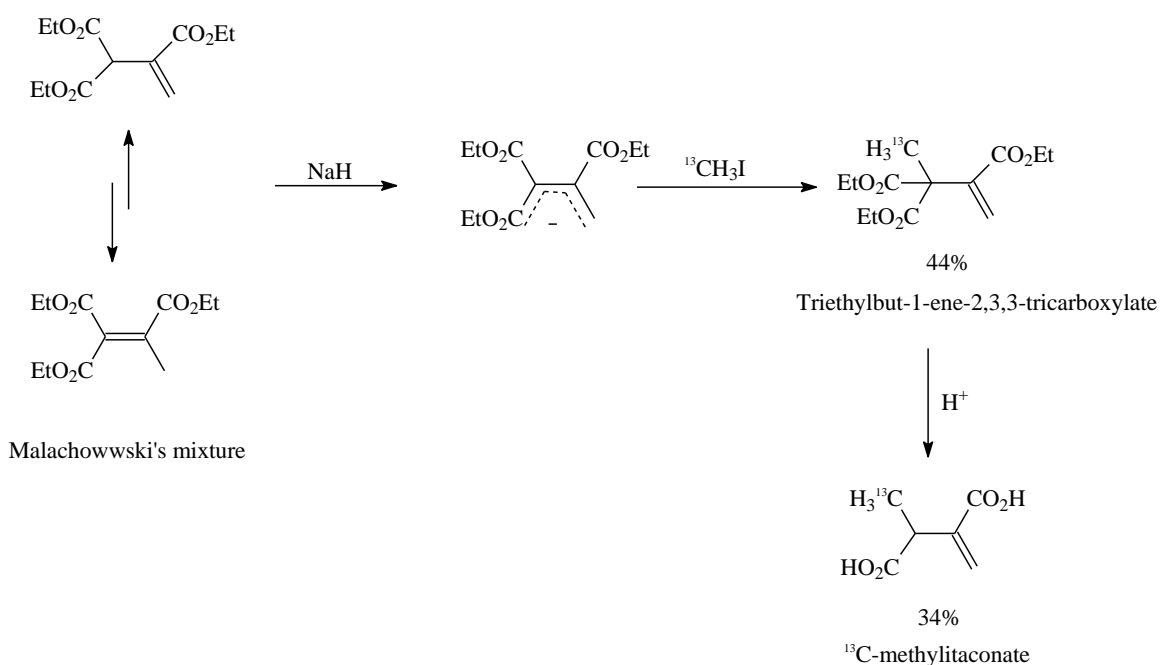


Figure 51: Synthetic route to 3-[<sup>13</sup>C-*methyl*]itaconic acid

### 3.3 Mechanism based inactivation of glutamate mutase by inhibitors mimic of the 4-glutamyl and (2*S*, 3*S*) 3-methyleneaspartate radicals in the enzyme active site

Studies approach by the mechanism based inactivation of glutamate mutase was performed during the period of this thesis in order to provide experimental verifications on the mechanism via the 4-glutamyl as well as the (2*S*, 3*S*)-3-methyleneaspartate radicals as proposed in the minimum mechanistic scheme for the coenzyme B<sub>12</sub> dependent rearrangements. Inhibitors with structures analogue to the 4-glutamyl and (2*S*, 3*S*)-3-methyleneaspartate radicals intermediates in the proposed mechanism of the reaction catalyzed by glutamate mutase were designed. Inhibitors with structures analogue to the 4-glutamyl radical used in experiments reported in this thesis were *trans*- and *cis*-glutaconates whereas those which were designed to mimic (2*S*, 3*S*)-3-methyleneaspartate radicals in the enzyme active site were buta-1,3-diene-2,3-dicarboxylate, itaconate, fumarate, mesaconate and maleate. Fumarate, mesaconate and maleate have been also postulated to mimic the intermediate fragments; glycyl radical (**30**) and acrylate (**24b**) in the proposed rearrangement by fragmentation- recombination (figure 25). Also proposed inhibitors for use in this project included (*Z*, *S*)-aminoglutaconate and (*E*, *S*)-aminoglutaconate which are analogue to the 4-glutamyl radical.

Name	Structure	Mimicked intermediate of the enzyme reaction
<i>cis</i> -glutaconate		4-glutamyl radical
<i>trans</i> -glutaconate		4-glutamyl radical
( <i>Z,S</i> )-aminoglutaconate		4-glutamyl radical
( <i>E,S</i> )-aminoglutaconate		4-glutamyl radical
Fumarate		( <i>2S, 3S</i> )-3-methyleneaspartate radical as well as the intermediate fragments; glycyl radical and acrylate
Maleate		( <i>2S, 3S</i> )-3-methyleneaspartate radical as well as the intermediate fragments; glycyl radical and acrylate
Itaconate		( <i>2S, 3S</i> )-3-methyleneaspartate radical
Buta-1,3-diene-2,3-dicarboxylate		( <i>2S, 3S</i> )-3-methyleneaspartate radical
Mesaconate		( <i>2S, 3S</i> )-3-methyleneaspartate radical and intermediate fragments; glycyl radical and acrylate

Table 7: List of proposed inhibitors of glutamate mutase with structures analogue to 4-glutamyl and (*2S, 3S*)-3-methyleneaspartate radicals. Results reported in this thesis were from the studies on the interactions of glutamate mutase, methylaspartase, glutamic-pyruvic transaminase and 2-hydroxyglutarate dehydrogenase with *cis* and *trans*-glutaconates, fumarate, maleate, Itaconate and buta-1,3-diene-2,3-dicarboxylate



The designing of these inhibitors considered both the size with respect to the number of carbon atoms as well as the skeletal resemblance to the 4-glutamyl and (2*S*, 3*S*)-3-methyleneaspartate radicals in order to arrive into structures which fit on the glutamate mutase active site. The SP<sup>2</sup> carbons of the inhibitors were specifically designated to mimic the radical centers in the 4-glutamyl as well as the (2*S*, 3*S*)-3-methyleneaspartate radicals while in the enzyme active site. The hypothetical potentials for these structures to bind enzyme active site by hydrogen bonding interactions of their terminal carboxylate with active site arginines 66, 100 and 149 like substrates and the intermediate radicals they are mimicking is postulated to be followed by their predicted reactivity on the enzyme active site. Binding of these inhibitors to the active site is expected to trigger the homolytic cleavage of the Co-C bond like the substrate. The 5'-deoxyadenosyl radical resulted from the coenzyme β coordinate homolysis has been predicted to be added on the SP<sup>2</sup> carbons of the inhibitors with hypothetical formation of radical adducts of inhibitors and the 5'-deoxyadenosyl radical.

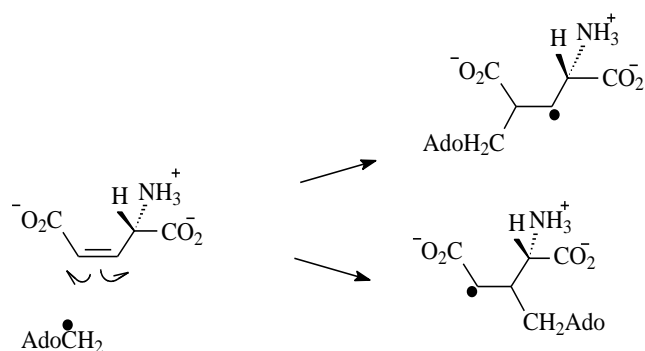
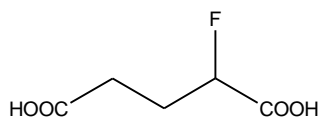
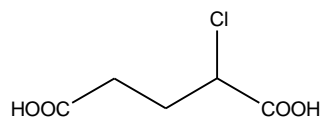


Figure 52: Postulated mechanism for the reaction of holo- glutamate mutase with (Z, S)-aminoglutaconate to form radical adduct

The halogenated glutaric acids; 2-fluoroglutaric acid and 2-chloroglutaric acid have also been hypothesized to bind the glutamate mutase active site and react with the enzyme by rearrangement to the corresponding methylhaloglutarates in the mechanism similar to the rearrangement of (*S*)-glutamate to (2*S*, 3*S*)-3-methylaspartate. This thesis reports on the findings from the kinetic studies as well as the spectroscopic characterizations of the holo-glutamate mutase interactions with the aforementioned proposed compounds and discusses several suggestions on their further exploitations toward experimental verifications on the proposed mechanism for the reaction of glutamate mutase.



2-fluoroglutaric acid



2-chloroglutaric acid

Figure 53: Structures of haloglutaric acids for use in the investigations on the mechanism of glutamate mutase catalyzed reaction

### 3.3.1 The interactions of the proposed inhibitors of glutamate mutase with methylaspartase

Evaluations on the interactions of glutamate mutase with its proposed inhibitors by the standard methylaspartase coupled assay require non inactivation of the auxiliary methylaspartase by those inhibitors with structures analogue of the 4-glutamyl and (2*S*, 3*S*)-3-methyleneaspartate radicals. Determinations on the effects of these proposed inhibitors of glutamate mutase on methylaspartase by their direct incubations with methylaspartase (2.2.7.3) revealed the reduction of methylaspartase specific activity to less than 40% by at least 2 mM of *trans*-glutaconate, *cis*-glutaconate and itaconate within 2 minutes of incubations which were performed separate for each inhibitor. The 2 mM concentrations of these inhibitors which were equivalent to  $K_m$  values of (*S*)-glutamate and (2*S*, 3*S*)-3-methylaspartate in the respective reactions of glutamate mutase and methylaspartase further lowered the specific activity of methylaspartase when incubated longer with the enzyme. Fumarate and maleate exhibited the most effective inhibitions by complete inactivations of methylaspartase within 2 minutes of the enzyme incubation with 1 mM of either fumarate or maleate. The least inhibition effect on methylaspartase was found with the but-1,3-diene-2, 3-dicarboxylate which lowered the enzyme specific activity by 50% when 2 mM of this compound was incubated with methylaspartase for up to 6 minutes.

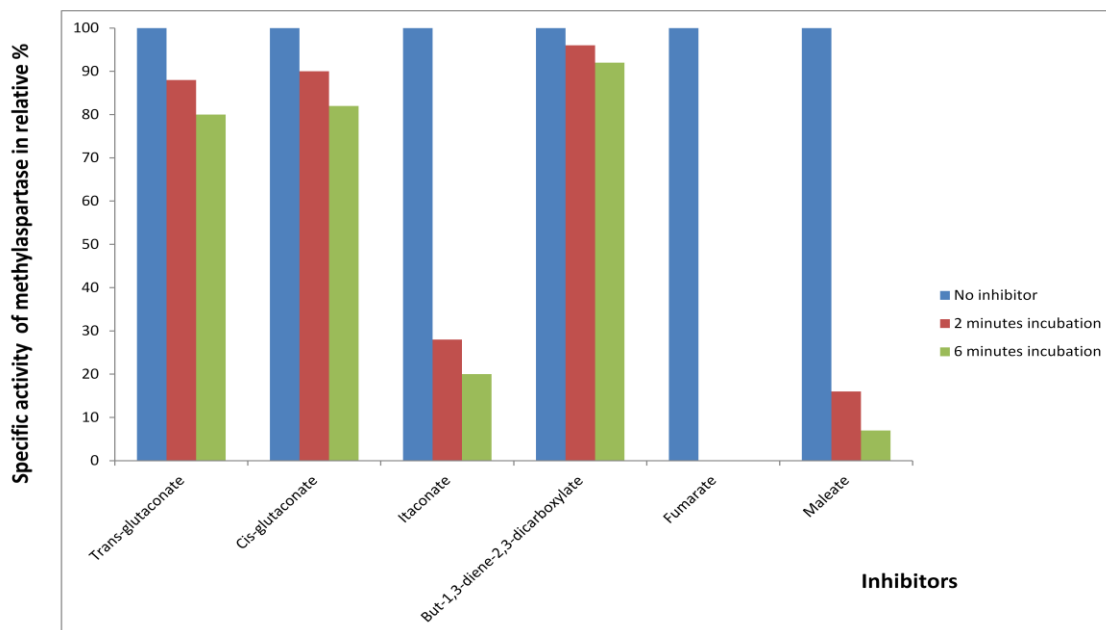


Figure 54: Methylaspartase specific activities in relative percentage of the activity of non-inhibited methylaspartase (blue bars) measured from the incubations of 1 mM of the proposed inhibitors of glutamate mutase with methylaspartase for 2 minutes (red bars) and 6 minutes (light green bars)

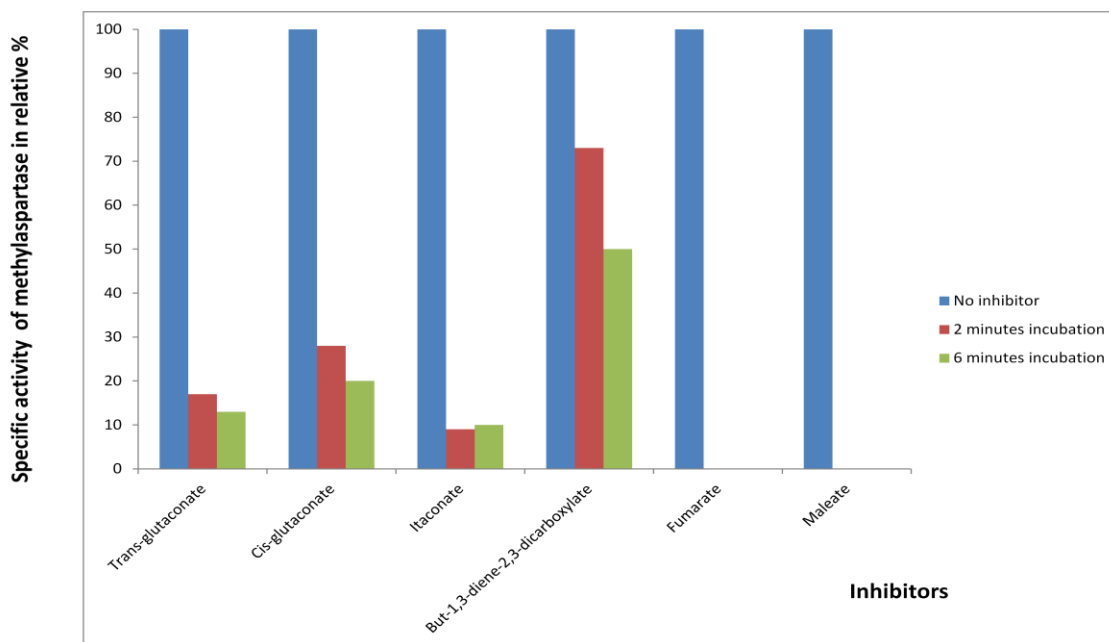


Figure 55: Methylaspartase specific activities in relative percentage of the non-inhibited methylaspartase (blue bars) measured from the incubations of 2 mM of the proposed inhibitors of glutamate mutase with methylaspartase for 2 minutes (red bars) and 6 minutes (light green bars)

### **3.3.2 Evaluations on the interactions of glutamate mutase with its proposed inhibitors by the modified methylaspartase coupled assay**

Since at least 2 mM of each of the proposed inhibitors of glutamate mutase has been demonstrated to inhibit methylaspartase significantly, the filtration of the holo-glutamate mutase incubated with each inhibitor by Sephadex G 25 achieved the removal of both excess inhibitor and coenzyme before the auxiliary enzyme and (*S*)-glutamate were added in the assay (2.2.7.4). In the separate aerobic incubations of holo-glutamate mutase with fumarate, maleate and mesaconate, each up to 3 mM, which were followed by filtrations to remove excess inhibitors and cofactor demonstrated the complete inactivation of the holoenzyme within five minutes. Glutamate mutase activity was almost fully recovered from those assays in which itaconate, buta-1,3-diene-2,3-dicarboxylate, *cis* or *trans*-glutaconates, 3 mM each, were aerobically incubated with the holoenzyme for 6 minutes before the excess inhibitors and cofactor were removed.

Assay description Additions to holo-glutamate mutase	Activity	
	(U/ml)	% activity
none	33	100
<i>trans</i> -glutaconic acid	23	70
<i>cis</i> -glutaconic acid	27	82
buta-1,3-diene-2,3-dicarboxylic acid	33	100
itaconic acid	27	82
fumaric acid	0	0
maleic acid	0	0
mesaconic acid	0	0

Table 8: Activities of glutamate mutase after 6 minutes incubations of the holoenzyme with equimolar concentrations of the proposed inhibitors of glutamate mutase. The incubated mixtures with inhibitor concentrations equivalent to that of the holoenzyme were prepared by Sephadex G25 filtration of excess inhibitor which were added to 3 mM.

UV/visible scanning after up to 1 hour of the anaerobic incubation of 10 mM fumarate with holo-glutamate mutase reconstituted from 68  $\mu$ M GlmS, 19  $\mu$ M GlmE with excess amount of coenzyme B<sub>12</sub> gave the cob(III)alamin spectra (figure 56). The formation of mesaconate could not be detected upon the addition of an auxiliary enzyme; methylaspartase and (*S*)-glutamate to the holoenzyme incubated with fumarate. The reported UV/visible scanning as well as the addition of methylaspartase and (*S*)-glutamate prior to measurement of mesaconate formation was done after centrifugation of excess coenzyme B<sub>12</sub> and fumarate from the incubation mixture. Notably was the formation of mesaconate upon the addition of the methylaspartase and (*S*)-glutamate in the control experiment in which the holoenzyme reconstituted in similar conditions was not incubated with fumarate.

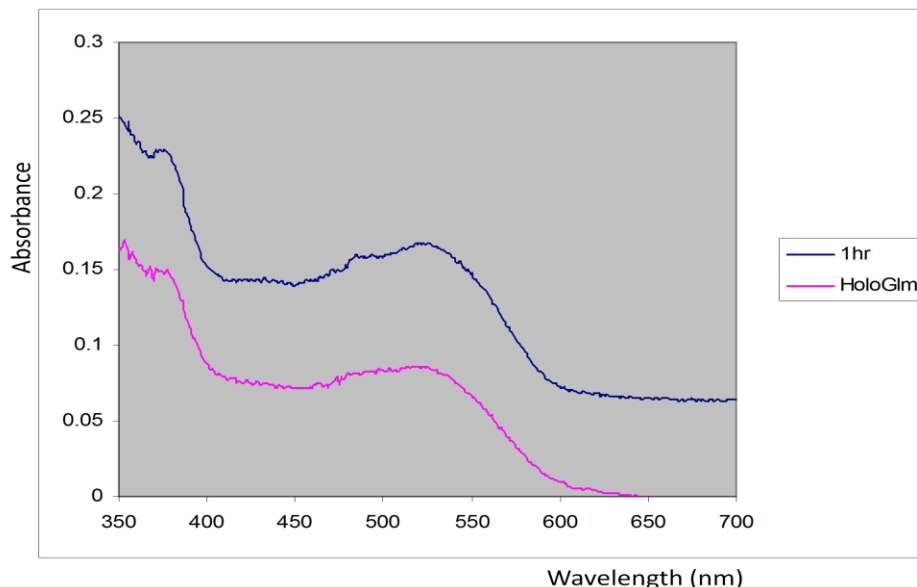


Figure 56: Uv/visible spectra of holo-glutamate mutase reconstituted from GlnS (0.68  $\mu$ M), GlnE (0.05  $\mu$ M) and equimolar amount of coenzyme B<sub>12</sub> (red) and the anaerobic incubation of holo-glutamate reconstituted from GlnS (68  $\mu$ M), GlnE (19  $\mu$ M) and equimolar amount of coenzyme B<sub>12</sub> with fumarate (10 mM) for 1 hour (dark blue).

### 3.3.3 Development of a novel assay for glutamate mutase catalyzed conversion of (2S, 3S)-3-methylaspartate to (S)-glutamate

During the mechanism based inactivation studies on glutamate mutase for this thesis, a novel assay for the glutamate mutase catalyzed conversion of (2S, 3S)-3-methylaspartate to (S) glutamate was developed in order to allow kinetic characterizations on the interactions of glutamate mutase with its inhibitors. The developed assay was also applied in measuring the kinetic constants of (2S, 3S)-3-methylaspartate in the reaction of glutamate mutase. Together with the kinetic constants of (S)-glutamate which were measured by the methylaspartase coupled assay, the equilibrium constant of the partial purified glutamate mutase was calculated by Briggs-Haldane equation. This new assay employs two auxiliary reactions which are coupled to the coenzyme B<sub>12</sub> dependent conversion of (2S, 3S)-3-methylaspartate to (S) –glutamate. The pyridoxal-5'-phosphate dependent glutamic pyruvic transaminase catalysed respective conversions of pyruvate and (S)-glutamate produced by glutamate mutase to alanine and 2-oxoglutarate. The 2-oxoglutarate produced from the transamination is further coupled to the

NADH dependent reduction by 2-hydroxyglutarate dehydrogenase to 2-hydroxyglutarate. Since the two auxiliary enzymes have high specific activity and are added in excess, the NADH depletion during the 2-hydroxyglutarate dehydrogenase catalyzed reduction allow the determination of the rate for conversion of (2*S*, 3*S*)-3-methylaspartate to (*S*)-glutamate by glutamate mutase at 340 nm.

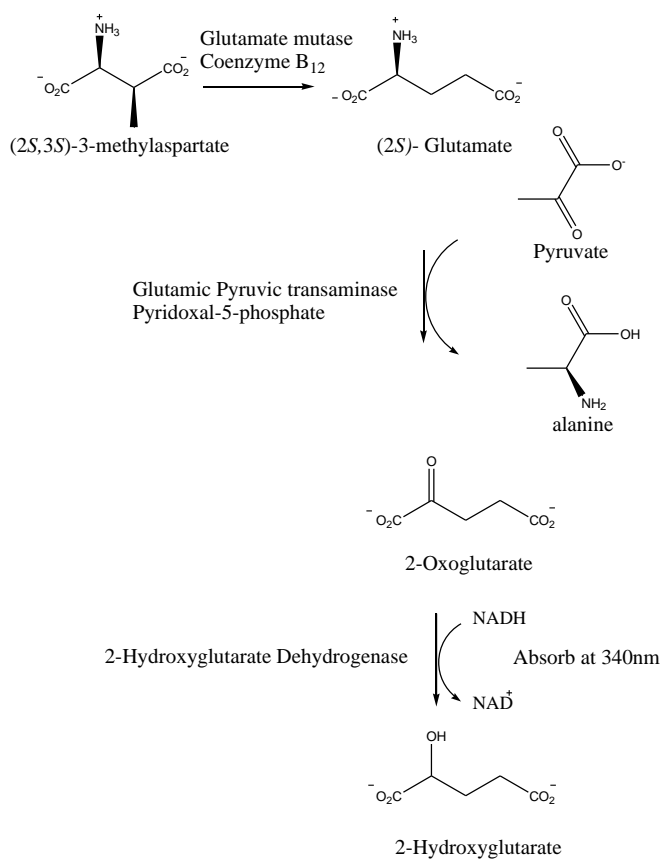


Figure 57: Enzymatic transformations for assaying the glutamate mutase catalyzed conversion of (2*S*, 3*S*)-3-methylaspartate to (*S*) glutamate.

The decreasing NADH absorption with time was demonstrated at 340 nm ( $\epsilon_{340} = 6.3 \text{ mM}^{-1} \text{ cm}^{-1}$ ) upon addition of 300 mM (2*S*, 3*S*)-3-methylaspartate to the mixture of holo-glutamate mutase reconstituted from  $10 \mu\text{g ml}^{-1}$  GlmS,  $5.2 \mu\text{g ml}^{-1}$  GlmE and 0.025 mM coenzyme B<sub>12</sub>, 20 mM pyruvate,  $40 \mu\text{g ml}^{-1}$  glutamic-pyruvic transaminase ( $81 \text{ U mg}^{-1}$ ), 0.02 mM pyridoxal-5'-

phosphate, 20  $\mu\text{g ml}^{-1}$  2-hydroxyglutarate dehydrogenase (1 kU  $\text{mg}^{-1}$ ) and 0.2 mM NADH in 30 mM Tris- HCl pH 8.3 and 0.05 mM mercaptoethanol.

(2*S*, 3*S*)-3-Methylaspartate = (*S*)-Glutamate

(*S*)-Glutamate + Pyruvate = 2-Oxoglutarate + L-Alanine

2-Oxoglutarate + NADH +  $\text{H}^+$   $\rightarrow$  (*R*)-2-Hydroxyglutarate +  $\text{NAD}^+$

Sum: (2*S*, 3*S*)-3-Methylaspartate + Pyruvate + NADH +  $\text{H}^+$   $\rightarrow$  L-Alanine + (*R*)-2-Hydroxyglutarate +  $\text{NAD}^+$

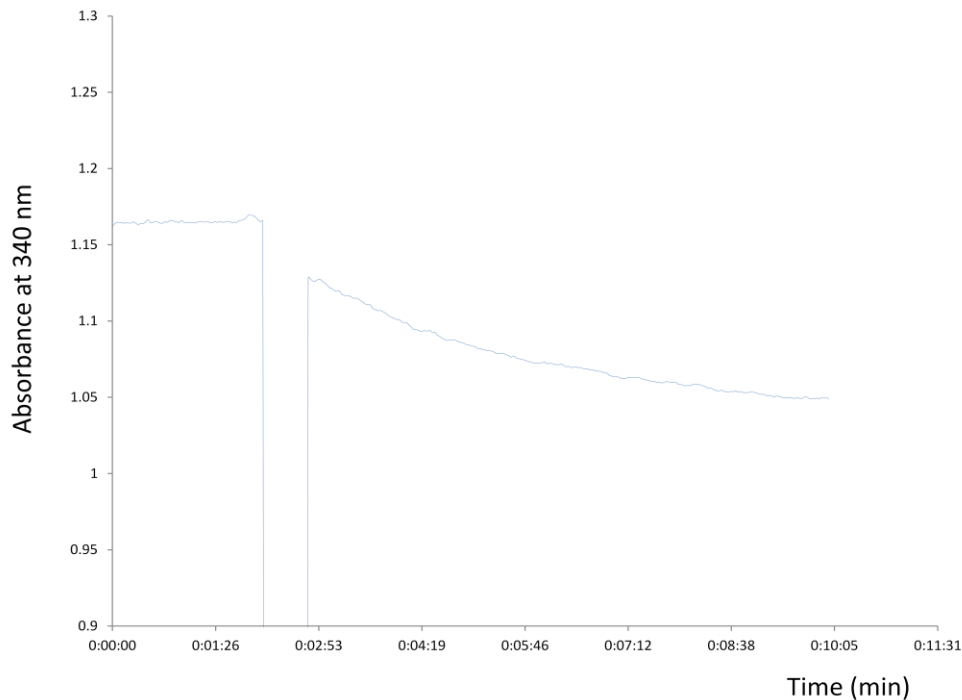


Figure 58: Activity of glutamate mutase catalyzed conversion of (2*S*, 3*S*)-3-methylaspartate to (*S*) glutamate measured as the rate of NADH depletion by the new glutamic-pyruvic transaminase and 2-hydroxyglutarate dehydrogenase coupled assay. The NADH absorption started to decrease with time from 02:43 minutes when (2*S*, 3*S*)-3-methylaspartate was added to the mixture of holo-glutamate mutase, pyruvate, holo-glutamic-pyruvic transaminase and holo-2-hydroxyglutarate dehydrogenase as described in the main text with concentrations.



### 3.3.4. Determination of the kinetic constants of (2*S*, 3*S*)-3-methylaspartate in the reaction of glutamate mutase

The developed glutamic-pyruvic transaminase and 2-hydroxyglutarate dehydrogenase coupled assay was used to determine the kinetic constants of (2*S*, 3*S*)- 3-methylaspartate in the reaction of glutamate mutase. Measurement of activities in due to the glutamate mutase reverse reaction by the new assay with the variations of (2*S*, 3*S*) 3-methylaspartate concentration from 5 to 300 mM (section 2.2.7.5) lead to the determination of the kinetic constants of (2*S*, 3*S*) 3-methylaspartate;  $V_{\max} = 0.6 \pm 0.6 \text{ U (mg GImE)}^{-1}$  and  $K_m = 7.00 \pm 0.07 \text{ mM}$  in the reaction of the partial purified glutamate mutase by the Michaelis –Menten method. The partial purified glutamate mutase  $k_{\text{cat}} = 0.54 \text{ s}^{-1}$  and  $k_{\text{cat}}K_m^{-1} = 77 \text{ s}^{-1}\text{M}^{-1}$  were also calculated from the kinetic parameters determined by the Michaelis-Menten method.

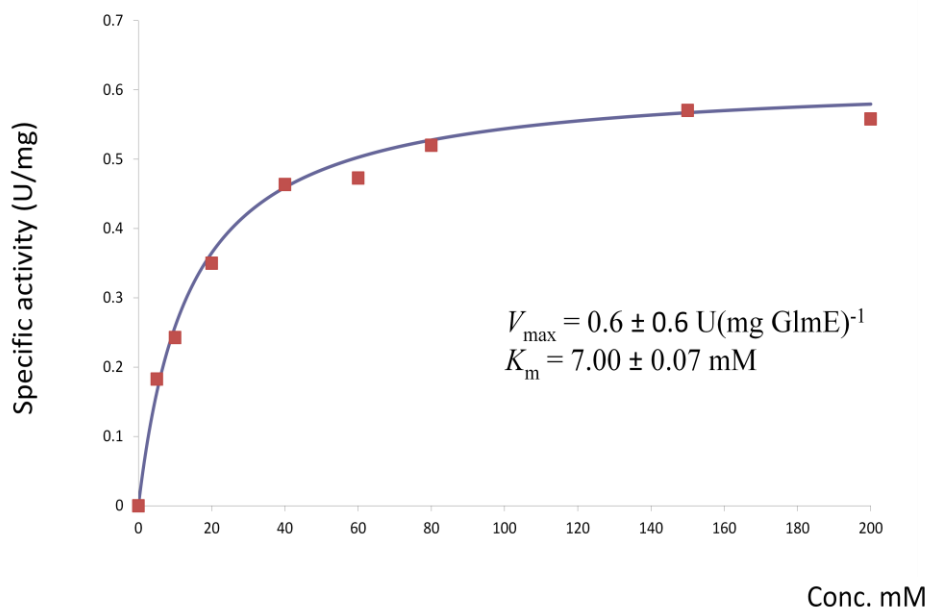


Figure 59; Michaelis-Menten plot for the determination of the kinetic constants of (2*S*, 3*S*)-3-methylaspartate during its conversion to (*S*)-glutamate by the partial purified glutamate mutase reconstituted with 14 folds excess of component S

### 3.3.5 Summary of the kinetic constants for the reaction catalyzed by the partial purified glutamate mutase and determination of the reaction equilibrium constant by Briggs-Haldane equation

	Apparent $K_m$ ( $\mu\text{M}$ )			$k_{\text{cat}}$ ( $\text{s}^{-1}$ )			$k_{\text{cat}}K_m^{-1} \times 10^6$ ( $\text{s}^{-1}\text{M}^{-1}$ )		
	14:1	7:1	2:1	14:1	7:1	2:1	14:1	7:1	2:1
GlmS: GlmE	14:1	7:1	2:1	14:1	7:1	2:1	14:1	7:1	2:1
( <i>S</i> )-glutamate	$(2.25 \times 10^3) \pm 0.03$	NM	NM	$2.85 \pm 0.5$	NM	NM	$1.3 \times 10^{-9}$	NM	NM
(2 <i>S</i> , 3 <i>S</i> )-3-methylaspartate	$(7 \times 10^3) \pm 0.07$	NM	NM	$0.54 \pm 0.6$	NM	NM	$77 \times 10^{-6}$	NM	NM
Coenzyme B <sub>12</sub>	$0.52 \pm 0.06$	$0.7 \pm 0.05$	$1.12 \pm 0.04$	$1.24 \pm 0.36$	$0.90 \pm 0.4$	$1.24 \pm 0.36$	2.38	1.29	1.10

Table 9: Kinetic constants for the reaction of glutamate mutase reconstituted from the partial purified enzyme components S and E. Constants of (*S*)-glutamate and coenzyme B<sub>12</sub> were measured by the standard methylaspartase coupled assay while those of (2*S*, 3*S*)-3-methylaspartate were measured by the new developed glutamic pyruvic transaminase and 2-hydroxylglutarate dehydrogenase coupled assay for the reverse reaction of glutamate mutase. NM means not measured.

The kinetic constants of (2*S*, 3*S*)-3-methylaspartate in the reverse reaction of glutamate mutase together with the available constants of (*S*)-glutamate in the enzyme forward reaction allowed the determination of the reaction equilibrium constant;  $K_{\text{eq}} = 16$  by Briggs-Haldane equation (Literature  $K_{\text{eq}} = 12$ ).<sup>181</sup>

$$K_{\text{eq}} = [k_{\text{cat}}/K_m ((S)\text{-glutamate})] / [k_{\text{cat}}/K_m ((2S, 3S)\text{-3-methylaspartate})] = 16$$

This calculated equilibrium constant  $K_{\text{eq}} = 16$  as well as that from literature implies the formation of (*S*)-glutamate is favored during the reversible rearrangement by glutamate mutase.

### 3.3.6 Evaluations on the interactions of glutamate mutase with its proposed inhibitors by the glutamic-pyruvic transaminase and 2-hydroxylglutarate dehydrogenase coupled assay

Interactions of proposed inhibitors of glutamate mutase with the auxiliary enzymes; glutamic pyruvic transaminase and 2-hydroxylglutarate dehydrogenase were evaluated by measuring the activity of the glutamic-pyruvic transaminase after the incubations of auxiliary enzymes with inhibitors and compared to the specific activity of the transaminase which was measured without inhibitors (2.2.7.6). The activity of glutamic-pyruvic transaminase was fully recovered from the interactions of auxiliary enzymes (glutamic pyruvic transaminase and 2-hydroxylglutarate dehydrogenase) with up to 20 mM of *cis*-glutaconate, *trans*-glutaconate, itaconate, fumarate, maleate and mesaconate in separate incubations for 5 to 10 minutes.

Activity in due to glutamate mutase conversion of (2*S*, 3*S*)-3-methylaspartate to (*S*)-glutamate was measured by coupling the reaction of glutamate mutase with the auxiliary glutamic pyruvic transaminase and 2-hydroxylglutarate dehydrogenase in the presence of *trans*-glutaconate and itaconate. These inhibitors were allowed to interact with glutamate mutase for at least 5 minutes in separate incubations and the measured activities were compared to glutamate mutase activity measured without inhibitor (2.2.7.7). Both *trans*-glutaconate and itaconate demonstrated the potential to inhibit glutamate mutase (figure 60).

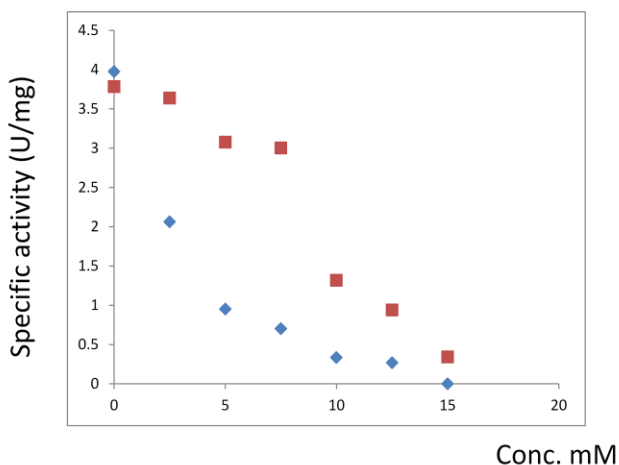


Figure 60: Inhibitions of glutamate mutase catalyzed conversion of (2*S*, 3*S*)-3-methylaspartate to (*S*)-glutamate by itaconate (blue) and *trans*-glutaconate (red)

Itaconate exhibited more potent inhibition by reducing the activity of glutamate mutase to 50 % following the incubation of holo-glutamate mutase with 2.5 mM of itaconate and complete inactivation from the incubation of holoenzyme with 15 mM of itaconate. *Trans*-glutaconate required about 8 mM to lower the glutamate mutase activity by 50%. Glutamate mutase was almost completely inactivated (activity reduced to less than 10%) in due to its incubation with 15 mM of *trans*-glutaconate.

### 3.3.7 The reaction of glutamate mutase with 2-fluoroglutaric acid

Since the activity of methylaspartase was completely recovered from its incubation with up to 6 mM of 2-fluoroglutarate (2.2.7.3), the standard methylaspartase coupled assay was used to evaluate the interaction of 2-fluoroglutarate with glutamate mutase. The formation of mesaconate was not detected when 2-fluoroglutarate (10 mM) was added to the mixture of methylaspartase ( $72 \mu\text{g ml}^{-1}$ ) and holo-glutamate mutase reconstituted from GlnS ( $10 \mu\text{g ml}^{-1}$ ), GlnE ( $5.2 \mu\text{g ml}^{-1}$ ) and coenzyme B<sub>12</sub> (0.05 mM) in Tris-HCl pH 8.3 (30 mM) and mercaptoethanol (1 mM) (2.2.8.0). However, the activity of glutamate mutase measured by the standard methylaspartase assay was reduced to 45 % by incubation of holo-glutamate mutase with 2-fluoroglutarate (10 mM) for 5 minutes (2.2.8.0). Glutamate mutase was completely inactivated by incubation with 2-fluoroglutarate (40 mM) for 5 minutes (2.2.8.0). The proton coupling <sup>19</sup>F NMR spectrum for the reaction mixture of holo-glutamate mutase and 2-fluoroglutarate showed further splinting of peaks in comparison to the proton coupling <sup>19</sup>F NMR spectrum of 2-fluoroglutaric acid. This <sup>19</sup>F NMR analysed mixture was taken from the experiment in which GlnS (6.8  $\mu\text{M}$ ), GlnE (0.5  $\mu\text{M}$ ) and coenzyme B<sub>12</sub> (250  $\mu\text{M}$ ) were aerobically incubated in darkness with 2-fluoroglutarate (10 mM) at room temperature for overnight (2.2.7.9). However, the proton decoupling <sup>19</sup>F NMR spectrum of the same reaction mixture gave a single peak. Further analysis of the reaction mixture by LC-MS revealed two peaks of compounds with masses 149 which appear after 1.67 to 1.86 and 3.55 to 4.51 minutes retention times during the separation by C-18 column (figure 61). Other organic compounds included in the analyzed mixture were Tris, coenzyme B<sub>12</sub> and 2-mercaptoethanol.

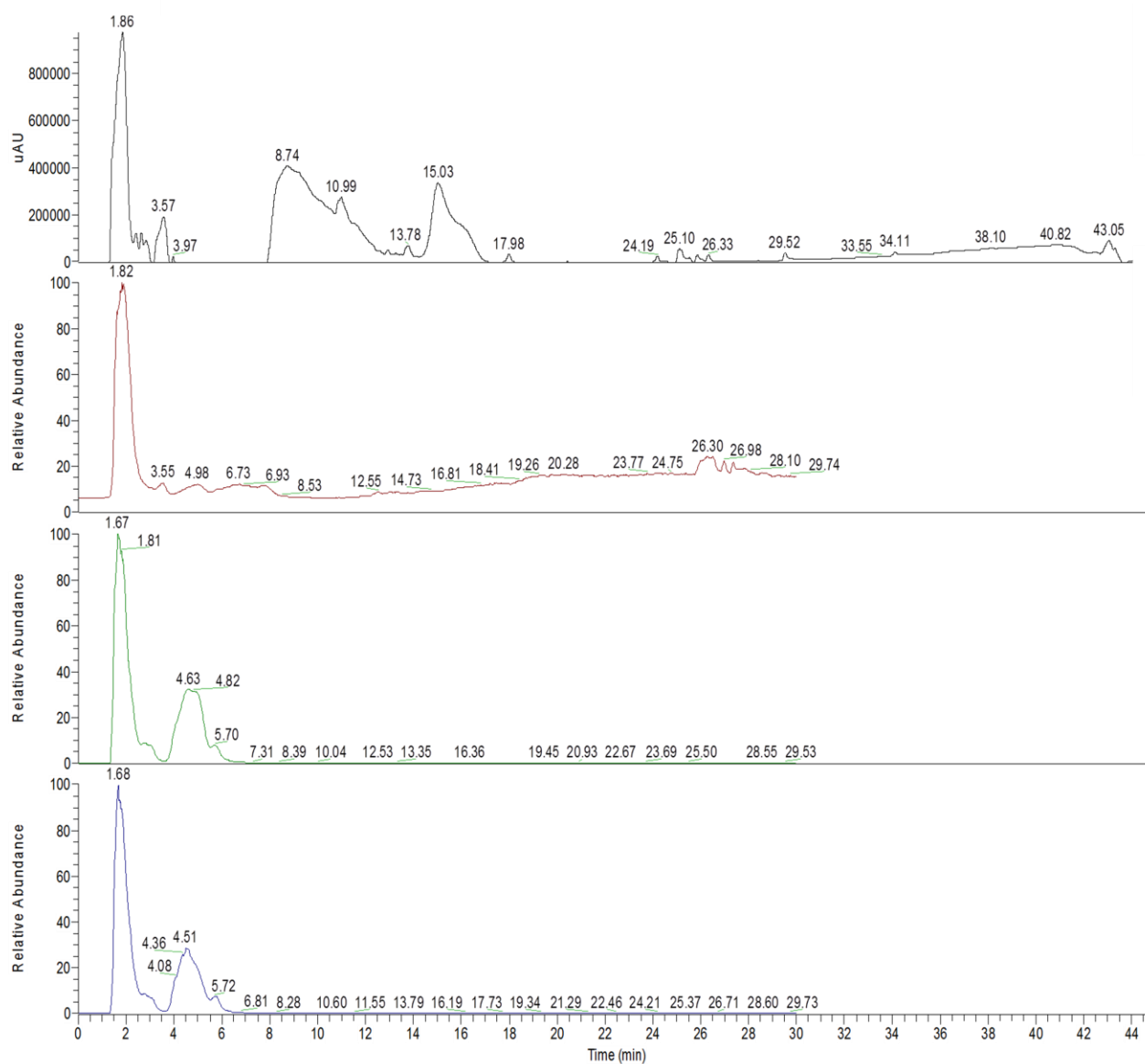
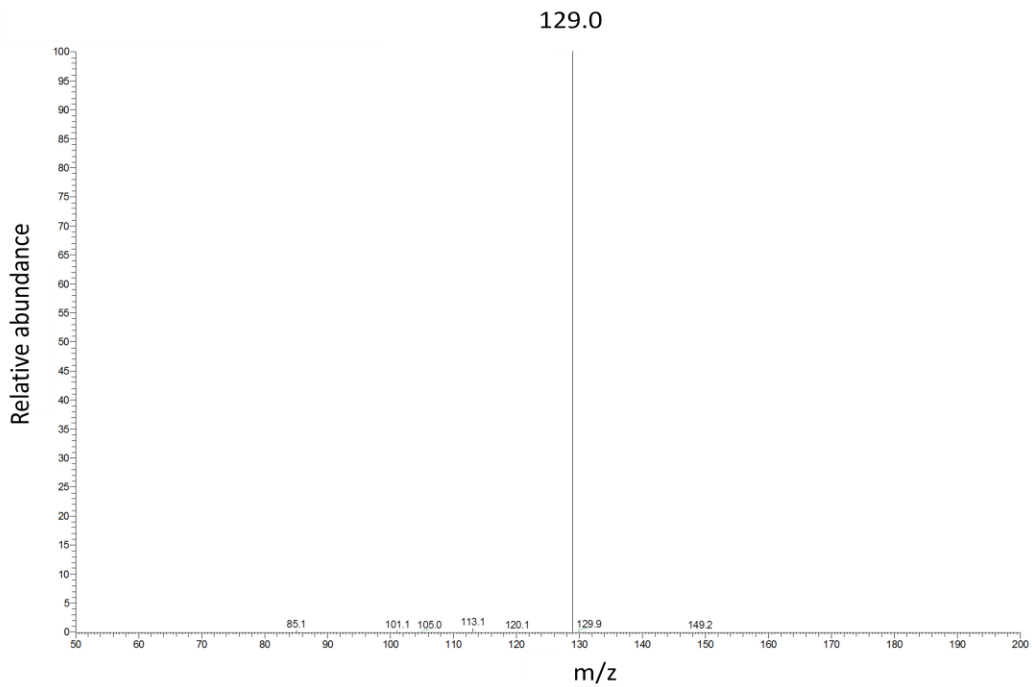
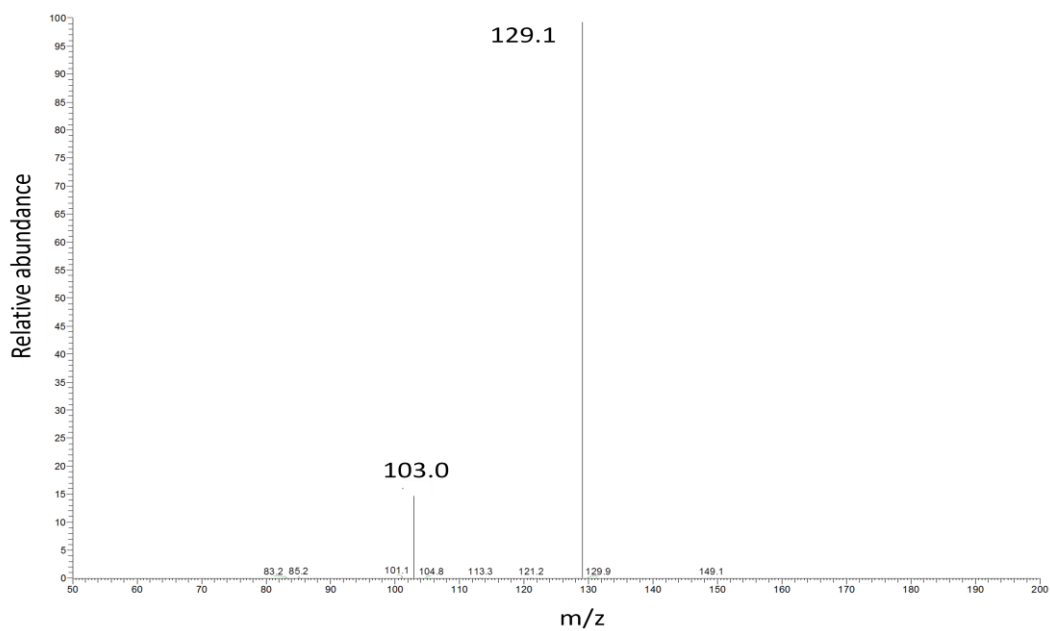


Figure 61: Separation of compounds in the reaction mixture of 2-fluoroglutarate and glutamate mutase by C-18 liquid chromatography. Two fluorinated compounds with 149 masses and retention times between 1.67 and 1.86 minutes as well as 3.55 and 4.51 minutes were separated. Other components of the mixture which was obtained after centricon removal of proteins GImS and GImE are coenzyme B<sub>12</sub>, Tris and mercaptoethanol.

Mass spectrum of the compound with retention time 1.68 minutes matches with that of 2-fluoroglutaric acid while the peak with retention time 4.51 minutes gave mass spectrum with fragments which correspond with 2-fluoro-3-methylaspartate.



(A)



(B)

Figure 62: Mass spectra of the compounds with retention times 1.68 minutes (A) and 4.51 minutes (B) in the liquid chromatography which was obtained from the C-18 separation

### 3.4 Kinetic probing of the glutamate mutase reaction by the structural derivatives of coenzyme B<sub>12</sub> cofactors

#### 3.4.1 Investigations into the role of the 5, 6 -dimethylbenzimidazole D-ribonucleotide tail of coenzyme B<sub>12</sub> in the “base off, his on” catalysis by glutamate mutase

Binding of coenzyme B<sub>12</sub> to apo-glutamate mutase accomplishes the reconstitution of holoenzyme system for the reversible inter-conversions between (S)-glutamate and (2S, 3S)-3-methylaspartate. The described “base off, his on” binding of the coenzyme B<sub>12</sub> to protein is achieved by replacing the free cofactor  $\alpha$ -ligand coordination to cobalt by imidazole base of the histidine residue from the protein cobalamin binding His-Asp-Ser triad. This cobalamin binding motif is conserved in mutases and therefore enables their assembling with coenzyme B<sub>12</sub> by the “base off, his on” mode. The glutamate mutase cobalamin binding motif; the His16-Asp-Ser triad is located in the component S of the apo-enzyme. Crystal structures of glutamate mutase have disclosed the location of the cofactor displaced  $\alpha$ -coordinate (the 5, 6 -dimethylbenzimidazole D-ribonucleotide tail) which has been revealed to end up deposited in the hydrophobic patch of the enzyme component S after the “base off, his on” binding of coenzyme B<sub>12</sub>. Besides the binding of cofactor, the catalytic significance from the replacement of this ligand by protein histidine especially its contribution to enzymatic turnovers after being displaced is still uncovered in most mutases including the glutamate mutase. The conspicuous catalytic role by this ligand with which it has been linked with the mechanism by which the Co-C bond is homolytically cleaved has been mainly due to the mechanochemical *trans*-ligand effect that apply only in ‘base on, his off’ eliminases in which the catalysis progress with cofactor intact 5, 6 -dimethylbenzimidazole. *“A significant body of evidence suggests that the bulky lower 5, 6-dimethylbenzimidazole axial ligand, is important in catalysis either by sterically destabilizing the ground state, or by electronically stabilizing the transition state for Co-C bond homolysis”* Kenneth L. Brown, Department of Chemistry and Biochemistry, Ohio State University. Although the similar *trans*-ligand role in Co-C bond homolysis has been ascribed to the axial histidine ligands in mutases “base off, his on” catalysis, a coenzyme B<sub>12</sub> analog; AdoCbi-GDP has been demonstrated to bind methylmalonyl -CoA mutase in the “his off” mode and accomplished the rearrangement reaction with significant high  $k_{cat}$  without the axial histidine

ligand.<sup>182</sup> However, in contrast to the catalysis by the methylmalonyl –CoA mutase, AdoCbi-GDP as well as the AdoCbi bind glutamate mutase by “his on” and reconstitute the holoenzyme which catalyze the rearrangement of (*S*)-glutamate to (2*S*, 3*S*)-3-methylaspartate in 10<sup>4</sup>- folds reduced  $k_{\text{cat}}K_m^{-1}$  in comparison to coenzyme B<sub>12</sub>.<sup>183</sup> Besides the revealed usual enzyme catalysis in the presence of the axial *trans*-histidine coordinate by these results which support further endeavors for uncovering the role of the axial  $\alpha$ -ligand towards trillion folds labilization of the  $\beta$  Co-C coordinate, also notably from these results has been the dependence of glutamate mutase catalytic turnover on the displaced 5, 6-dimethylbenzimidazole D-ribonucleotide tail.

Studies approach by the structure activity relationship toward defining the role of the coenzyme B<sub>12</sub> 5, 6 -dimethylbenzimidazole D-ribonucleotide tail in the reaction of glutamate mutase were carried out during the period of this thesis by using an adenosylpeptide B<sub>12</sub> (**31**) derivative of coenzyme B<sub>12</sub> (**4**) as an artificial cofactor for glutamate mutase. The derivative cofactor (**31**) has a neutral peptidomimetic unit of two glycines which connect the dimethylbenzimidazole to ethanol propanamide side group of the corrin ring instead of ribose and the negatively charged phosphodiester linker in coenzyme B<sub>12</sub> (**4**). This modification on the coenzyme B<sub>12</sub>  $\alpha$ -ligand was postulated to modulate the cobalamin base on/base off equilibrium and subsequently affect the enzymatic catalysis in both “base off, his on” mutases and “base on, his off” eliminases.<sup>184</sup> This thesis presents the results obtained from the measurements of the kinetics of glutamate mutase reconstituted with the artificial cofactor (**31**) as well as provides mechanistic insights related to the catalytic role of the displaced bulk ribonucleotide tail in the reaction of glutamate mutase from comparison with the kinetics of the coenzyme B<sub>12</sub> (**4**) dependent reaction.



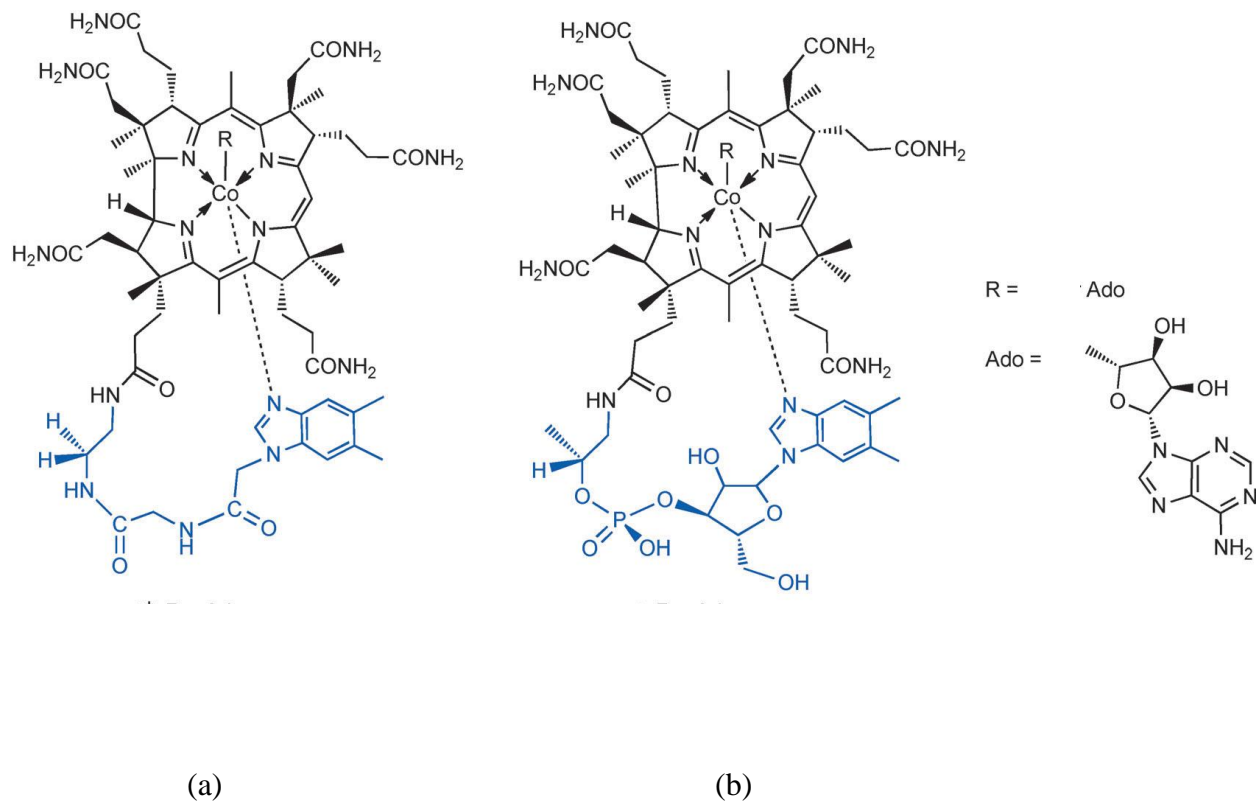


Figure 63: Structures of (a) an artificial adenosylpeptide B<sub>12</sub> cofactor (**31**) and (b) coenzyme B<sub>12</sub> (**4**) with their  $\alpha$ -ligand shown in blue. Note the coenzyme B<sub>12</sub> (**4**)  $\alpha$ -ligand ribose phosphodiester moiety is replaced by peptidomimetic unit of two glycines in the adenosylpeptide B<sub>12</sub> (**31**).

#### 3.4.1.1 Reconstitution of hologlutamate mutase with an adenosylpeptide B<sub>12</sub> (**31**) as a cofactor

The UV/visible spectrum of an artificial adenosylpeptide B<sub>12</sub> (**31**) differs from that of ‘base on’ coenzyme B<sub>12</sub> only between 400 and 450 nm by a continuous steep slope of increasing absorption with increasing wavelength as compared to coenzyme B<sub>12</sub> absorptions in this region. The spectrum of coenzyme B<sub>12</sub> has a characteristic absorption which forms a plateau peak between 410 and 445 nm. Since the maximum absorption of ribose is within this region, the absorption difference has been attributed to the ribose unit of coenzyme B<sub>12</sub>  $\alpha$ -ligand which is missing in the adenosylpeptide B<sub>12</sub> (**31**).

Between 350 and 400 nm as well as from 450 to 600 nm the spectrum of an adenosylpeptide B<sub>12</sub> (**31**) closely resembles that of coenzyme B<sub>12</sub> with an absorption at 490 nm and maximum absorption at 520 nm (figure 64). Similar to the reconstitution of holo-glutamate mutase from its apoenzyme components and coenzyme B<sub>12</sub>, the UV/visible spectrum of the reconstituted holoenzyme from the assembling of components S and E with an adenosylpeptide B<sub>12</sub> (**31**) closely follow that of an adenosylpeptide B<sub>12</sub> (**31**) (figure 64).

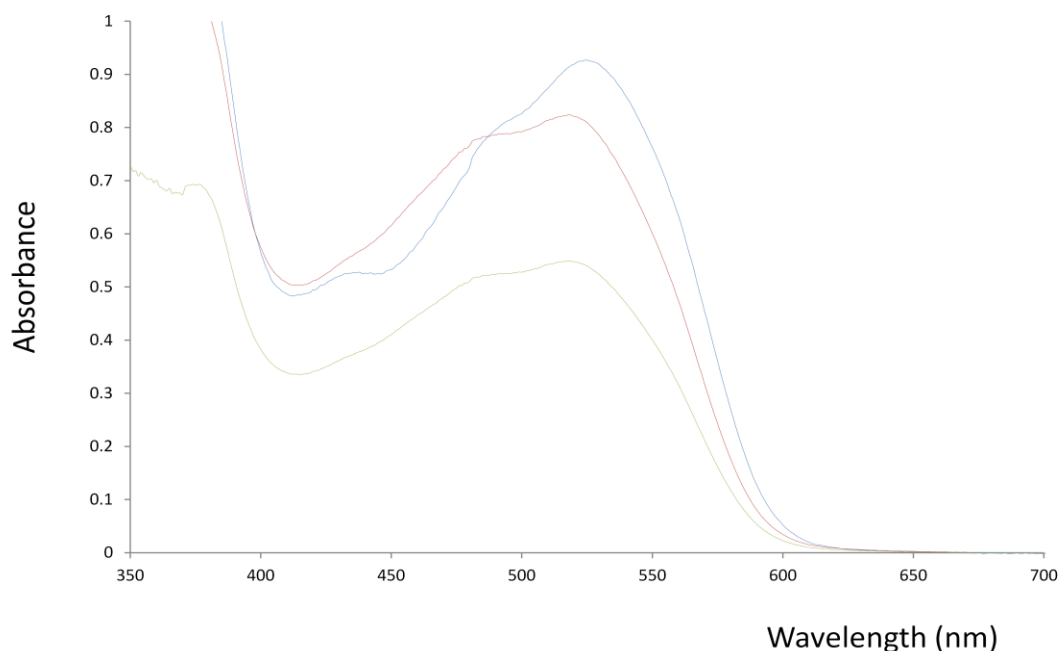


Figure 64: UV/visible spectra of 0.13 mM “base on” coenzyme B<sub>12</sub> (blue), 0.1 mM adenosylpeptide B<sub>12</sub> (**31**) (red) and holo-glutamate mutase reconstituted with 0.43 μM component S, 0.03 μM component E and equivalent molar concentration of an adenosylpeptide B<sub>12</sub> (**31**) (grey).

An activity due to the conversion of (*S*)-glutamate to (2*S*, 3*S*)-3-methylaspartate by glutamate mutase was demonstrated by the standard methylaspartase coupled assay when the enzyme was reconstituted with adenosylpeptide B<sub>12</sub> (**31**). However, to attain the rate of mesaconate formation equivalent to that achieved by holoenzyme reconstituted with coenzyme B<sub>12</sub>, 10 times more amount of apoenzyme components have been required to reconstitute the holoenzyme with an adenosylpeptide B<sub>12</sub> (**31**).

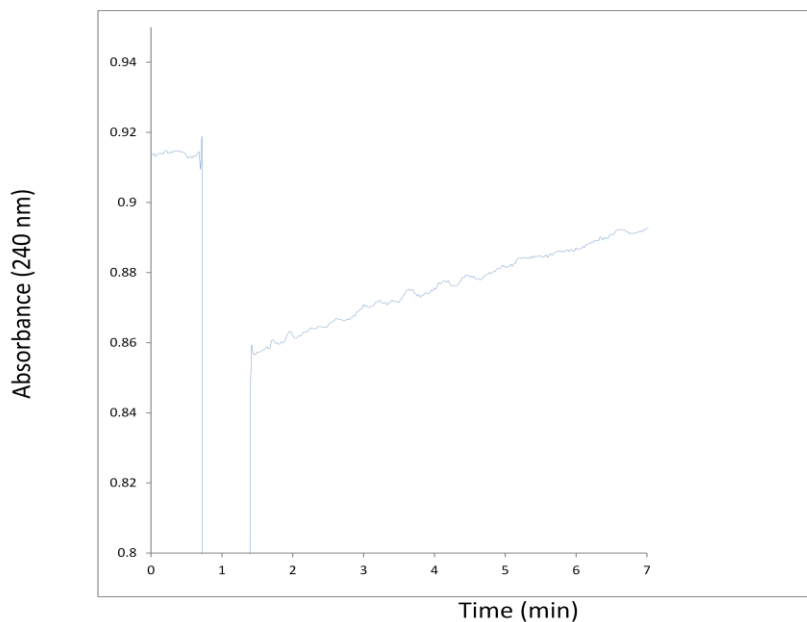


Figure 65: Activity of holo-glutamate mutase reconstituted from 6.8  $\mu\text{M}$  S, 0.5  $\mu\text{M}$  E and excess adenosylpeptide B<sub>12</sub> (**31**) measured as the rate of mesaconate formation by the standard methylaspartase coupled assay. The 0.14 U (mg GlmE)<sup>-1</sup> specific activity of glutamate mutase was determined from this activity in due to the reconstitution of holoenzyme with an adenosylpeptide B<sub>12</sub> (**31**) as a cofactor.

### 3.4.1.2 Kinetic constants of an adenosylpeptide B<sub>12</sub> (**31**) in the reaction of glutamate mutase

Kinetic constants of an adenosylpeptide B<sub>12</sub> (**31**) in the reaction of glutamate mutase were determined by the Michaelis-Menten method from the reconstitution of the holoenzyme in 14 and 2-fold excess of component S with an adenosylpeptide B<sub>12</sub> as the cofactor. The kinetic constants  $V_{\text{max}} = 0.13 \pm 0.01$  U (mg GlmE)<sup>-1</sup> ( $k_{\text{cat}} = 0.12 \pm 0.01$  s<sup>-1</sup>) were obtained along with  $K_m$  values for the adenosylpeptide B<sub>12</sub>:  $0.35 \pm 0.05$   $\mu\text{M}$  and  $1.07 \pm 0.04$   $\mu\text{M}$  to the apo-glutamate mutase from the respective reconstitutions in 14 and 2 fold excess of component S. Almost equal  $K_m$  but 10-times higher  $V_{\text{max}}$  values were found with the native coenzyme B<sub>12</sub> (**4**) (see table 10).

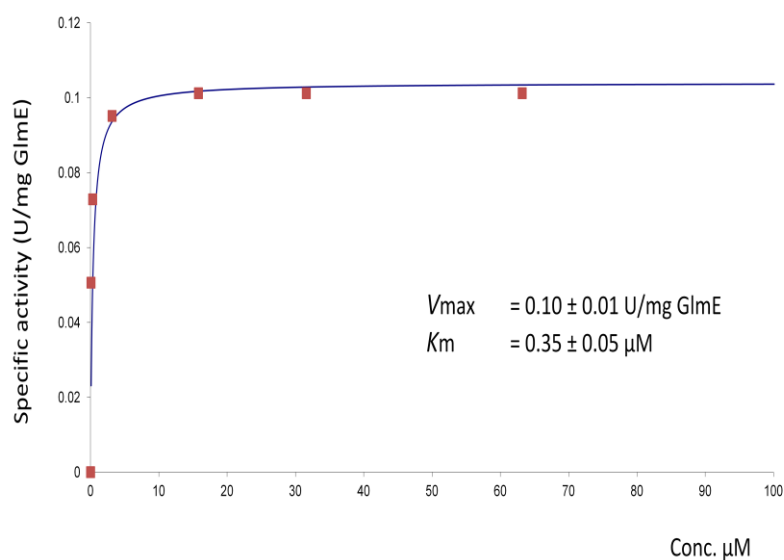


Figure 66: Michaelis-Menten plot for the determination of the kinetic constants of an adenosylpeptide B<sub>12</sub> (**31**) in the conversion of (*S*)-glutamate to (*2S*, *3S*)-3-methylaspartate by glutamate mutase reconstituted with 14 excess folds of component S

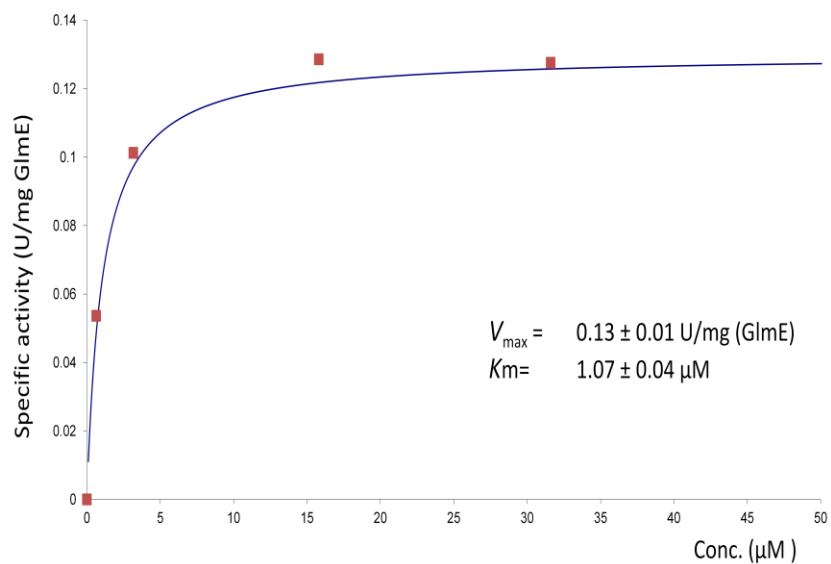


Figure 67: Michaelis-Menten plot for the determination of the kinetic constants of an adenosylpeptide B<sub>12</sub> (**31**) in the conversion of (*S*)-glutamate to (*2S*, *3S*)-3-methylaspartate by glutamate mutase reconstituted with 2-fold excess of component S

	$K_m$ ( $\mu\text{M}$ )		$V_{max}$ (U/mg GlmE)		$k_{cat}$ ( $\text{s}^{-1}$ )		$k_{cat}/K_m$ ( $\text{s}^{-1}\text{M}^{-1}$ )	
	14	2	14	2	14	2	14	2
GlmS:GlmE	14	2	14	2	14	2	14	2
Coenzyme B <sub>12</sub> ( <b>4</b> )	0.52±0.06	1.12±0.04	1.39±0.40	1.39±0.40	1.24±0.36	1.24±0.36	2.38 × 10 <sup>6</sup>	1.10 × 10 <sup>6</sup>
Adenosylpeptide B <sub>12</sub> ( <b>31</b> )	0.35±0.05	1.07±0.04	0.10±0.01	0.13±0.01	0.09±0.01	0.12±0.01	2.57 × 10 <sup>5</sup>	1.12 × 10 <sup>5</sup>

Table 10: Kinetic constants of an adenosylpeptide B<sub>12</sub> (**31**) and coenzyme B<sub>12</sub> (**4**) in the forward reaction of glutamate mutase measured from reconstitutions of enzyme in 14 and 2 excess folds of component S.

### 3.4.1.3 B<sub>12</sub> dependent bacteria growth on three carbon substrates

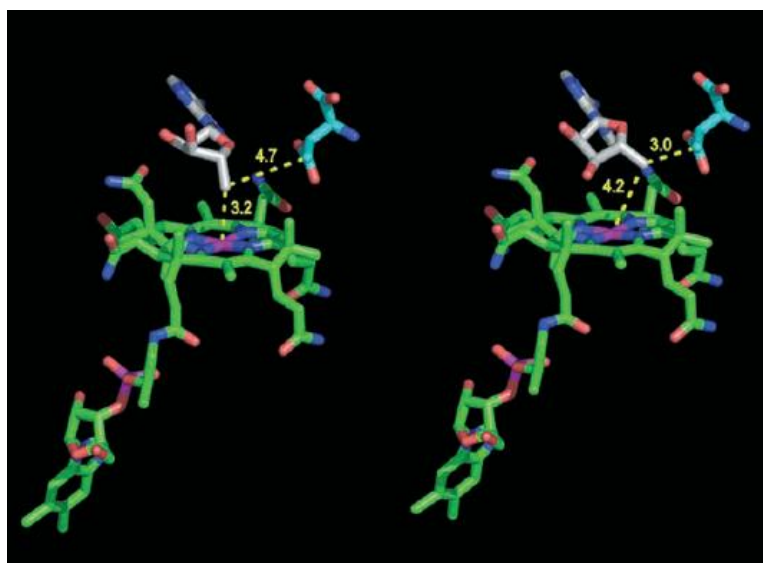
Demonstration on the in vivo bioactivity of an adenosylpeptide B<sub>12</sub> (**31**) requires the B<sub>12</sub> dependent growth of bacteria. This type of growth is possible via the aerobic oxidation of propionate to pyruvate which exploits coenzyme B<sub>12</sub> for the intermediate rearrangement of (*R*)-methylmalonyl -CoA to succinyl -CoA by methylmalonyl -CoA mutase. The assimilation of propionate or (*R*)-methylmalonyl-CoA by this pathway is accomplished by the B<sub>12</sub> dependent reaction which allows these substrates to enter the central carbon metabolism at the succinyl -CoA level. The annotation of methylmalonyl-CoA mutase and adenosyltransferase encoding genes in the genome of *E. coli* MG1655 lead to the design of an experiment which the strain was cultivated on minimum medium with propionate or (*R*) –methylmalonyl -CoA as the only carbon sources. The experimental set up (2.2.1.4) provided five sets of media which differ in carbon sources as well as the supplementation with B<sub>12</sub> to accommodate the control experiments. In the first and second set the minimum media were supplemented with propionate and propionate + cyanocobalamin, respectively, while third and fourth sets were designed similarly with (*R*)-methylmalonate as a carbon source. The fifth set contained glucose was a control experiment.

Neither the propionate nor (*R*)-methylmalonate as well as their supplementation with cyanocobalamin supported the growth of *E. coli* MG1655. The control experiment demonstrated the growth on glucose.

### **3.4.2 Probing the formation of the primary organic radical; 5'-deoxyadenosyl and the participation of cob(II)alamin in the stabilization of substrate activation during the glutamate mutase reaction**

The paramagnetic species cob(II)alamin formed along with the 5'-deoxyadenosyl radical from the homolytic cleavage of the coenzyme B<sub>12</sub> Co-C bond was once thought of being marginal toward the rearrangement mechanisms of the coenzyme B<sub>12</sub> dependent enzymes. The curiosity on the involvement of cob(II)alamin in rearrangements arise from its close proximity to the intermediate species in rearrangements during the catalysis by enzymes of the mutase class. In contrast to the catalysis by coenzyme B<sub>12</sub> dependent enzymes of the eliminase class in which the cob(II)alamin locates at a distance of 10 Å from intermediates of rearrangements for which it has been considered insensitive to rearrangements, in mutases cob(II)alamin remains within 7 Å from the intermediates of rearrangements.<sup>149</sup> Besides the location, another evidence to convict the cob(II)alamin from non-participation in the eliminases catalyzed rearrangements is the fact that other eliminases, which do not use coenzyme B<sub>12</sub> to generate the primary organic radical are known. These enzymes e.g class I and III RNR's use other radical generators like diiron(III)-tyrosine metalocofactor and SAM to initiate the chain of radical reactions which accomplish similar rearrangements without cob(II)alamin.<sup>157</sup> Since in mutase catalyses there is no other known radical generator than coenzyme B<sub>12</sub>, the cob(II)alamin which locates close to the intermediates species of reactions has been postulated to contribute in the mechanisms of rearrangements by mutases. The terms “spectator” to implies just watching the rearrangement at a distance without being involved and “conductor” for explaining the cob(II)alamin participation by interacting with intermediates species formed during the rearrangements were introduced to describe the two cob(II)alamin scenarios in respective catalysis by eliminases and mutases. In the glutamate mutase catalyzed reaction cob(II)alamin remains about 3 Å from the 5'-deoxyadenosyl radical and further 4 Å from the intermediates of rearrangement which predicts the stabilizations of these intermediates by interactions with cob(II)alamin.<sup>149</sup> The EPR studies for the identification of intermediate radical species during the reaction of glutamate mutase

demonstrated the interaction of the 4-glutamyl radical with cob(II)alamin which supports the proposed cob(II)alamin conductor role in the glutamate mutase reaction.<sup>105</sup> Crystal structures of holo-glutamate mutase revealed the two different orientations of the coenzyme B<sub>12</sub> β-ligand during the catalysis by this enzyme (Figure 68). While in the orientation (A) the 2' -OH and 3' -OH groups of the ribose extends away from corrin ring, the orientation (B) which permits the abstraction of hydrogen from the substrate by the 5' deoxyadenosyl radical brings the 3'OH close to corrin. The crystal structure shows the hydrogen bonding distance between 3'OH and C<sub>19</sub>-H from the corrin ring in the orientation (B) which suggests the facilitation of the ribose re-orientation that aid the homolysis of the Co-C bond and stabilization of substrate activation step by 3'OH hydrogen bonding interaction with the C<sub>19</sub>-H.



(A)

(B)

Figure 68; Crystal structures of coenzyme B<sub>12</sub> in action after the homolytic cleavage of Co-C bond. (a) Ribose O3' points away from the corrin ring and (b) an orientation that brings the ribose O3' at the hydrogen bonding distance to C<sub>19</sub>-H from corrin.<sup>149</sup> (Note in these structures the protein is omitted)

Gas phase calculations by the functional density theory (FDT) reported critical interactions between the C<sub>19</sub>H and ribose 3'OH which contribute to stabilization amounting to 30 kJmol<sup>-1</sup>.<sup>185</sup> These calculations further suggested the polarization of C<sub>19</sub>-H bond after the homolytic cleavage of the cofactor Co-C bond which facilitate the interaction. The same computational studies also

reported sizable stabilization ( $5 \text{ kJmol}^{-1}$ ) in due to 2'OH interactions. Studies on the glutamate mutase reaction conducted for this thesis used the three derivatives of coenzyme B<sub>12</sub> (**4**): 2',5'-dideoxyadenosylcobalamin (**32**), 3',5'-dideoxyadenosylcobalamin (**33**) and peptidoadenosylcobalamin (**34**) as cofactors in order to demonstrate the influence of 2'OH and 3'OH towards the formation of the 5'-deoxyadenosyl radical and the participation of cob(II)alamin in the formation and stabilization of 5'-deoxyadenosyl radical. The latter cobalamin consists of a peptide mimic unit that contains the same number of atoms between Co(III) and the adenosine base instead of ribose unit on the  $\beta$ -ligand. With these cofactor derivatives the interactions of the enzyme-coenzyme complex with either O2' or O3' of ribose or with both oxygen during the reaction were not possible. This thesis reports on the impairments of the enzyme kinetics resulted from the replacement of coenzyme B<sub>12</sub> by **32**, **33**, and **34** as well as providing structure related mechanistic implications derived from the impairments.

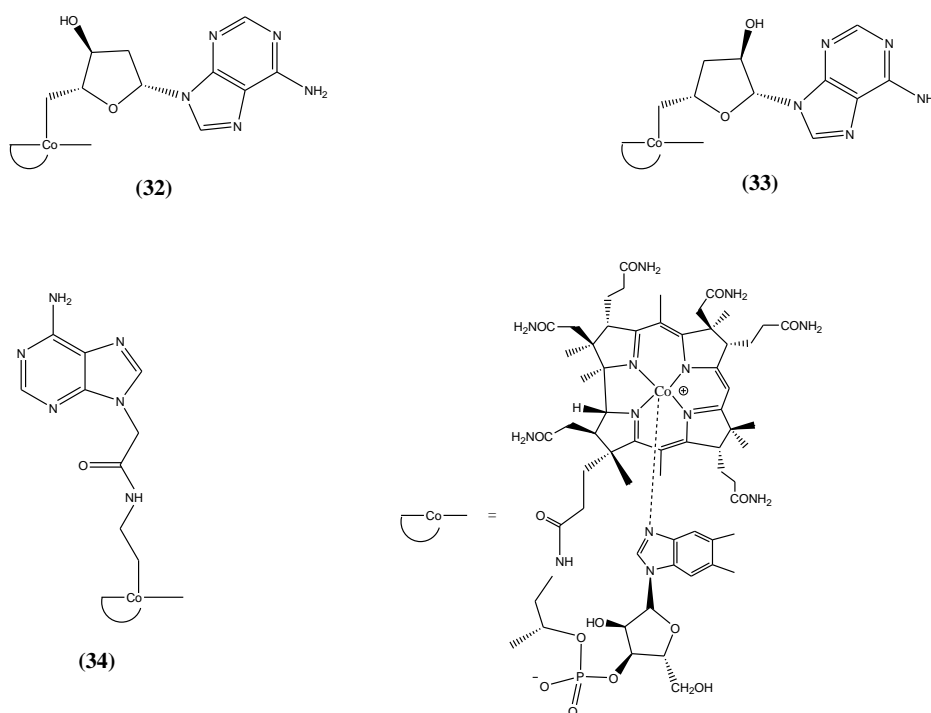


Figure 69: Structures of the  $\beta$ -ligand modified coenzyme B<sub>12</sub> derivatives used in probing the cob(II)alamin participations in the formation of the 5'-deoxyadenosyl radical and its stabilization during the substrate activation by hydrogen abstraction in the reaction of glutamate mutase. 2',5'-dideoxyadenosylcobalamin (**32**), 3',5'-dideoxyadenosylcobalamin (**33**) and peptidoadenosylcobalamin (**34**)



### 3.4.2.1 Assembling of apoglutamate mutase with $\beta$ -ligand modified coenzyme $B_{12}$ derivatives

The UV-visible spectra of used  $\beta$ -ligand modified derivatives of coenzyme  $B_{12}$  (**4**); 2',5'-dideoxyadenosylcobalamin (**32**), 3',5'-dideoxyadenosylcobalamin (**33**) and peptidoadenylcobalamin (**34**) as well as that of coenzyme  $B_{12}$  (**4**) were similar from 350 to 700 nm. All the derivatives exhibited absorption peak at 430 nm as well as the maximum absorption at 520 nm with a 490 nm shoulder like the coenzyme  $B_{12}$  (figure 70). The absorptions similarities between 300 and 700 nm shown by these cobalamins were expected since they differ only on  $\beta$ -ligand that has been modified to structures which absorbs below 300 nm like an adenosine moiety in the coenzyme  $B_{12}$ . The UV-visible spectra of holo-glutamate mutase reconstituted with these derivatives as cofactors also closely follow their corresponding “base on” spectra like in the reconstitution of the holoenzyme with coenzyme  $B_{12}$  (figure 70).

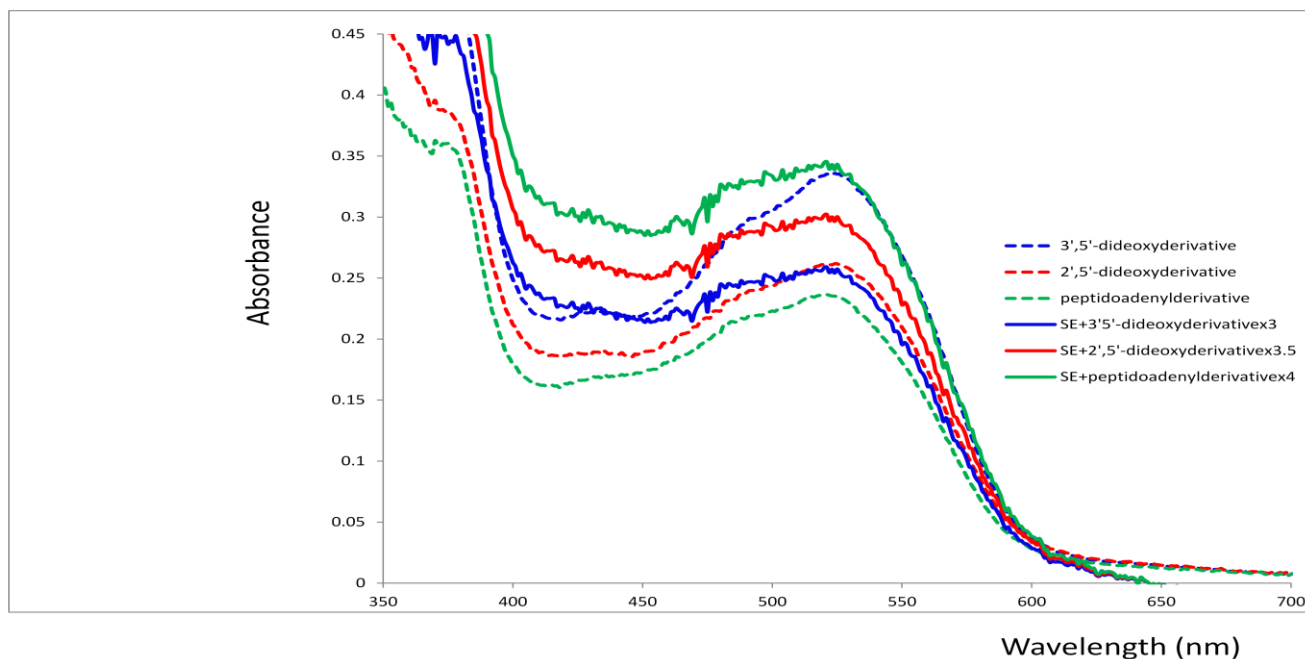


Figure 70: UV-visible spectra of 0.063 mM 2',5'-dideoxyadenosylcobalamin (**32**) (dashed red), 0.07 mM 3',5'-dideoxyadenosylcobalamin (**33**) (dashed blue), 0.063 mM peptidoadenylcobalamin (**34**) (dashed green) and holo-glutamate mutase reconstituted from 0.68  $\mu$ M S, 0.05  $\mu$ M E and equivalent amounts of 2',5'-dideoxyadenosylcobalamin (**32**) (red), 3',5'-dideoxyadenosylcobalamin (**33**) (blue) and peptidoadenylcobalamin (**34**) (green) as cofactors. Note the holoenzyme reconstituted with 3',5'-dideoxyadenosylcobalamin (**33**) is 3 times magnified while those from 2',5'-dideoxyadenosylcobalamin (**32**) and peptidoadenyl derivatives were 3.5 and 4 times magnified respectively.

The glutamate mutase activity due to the conversion of (*S*)-glutamate to (2*S*, 3*S*)-3-methylaspartate was detected from the reconstitution of holoenzyme with 3',5'-dideoxyadenosylcobalamin (**33**) as a cofactor (figure 71). However, 10 times more holoenzyme reconstituted with 3', 5'-dideoxyadenosylcobalamin(**33**) was needed to attain the conversion rate equivalent to that achieved by holoenzyme reconstituted with coenzyme B<sub>12</sub> (**4**).

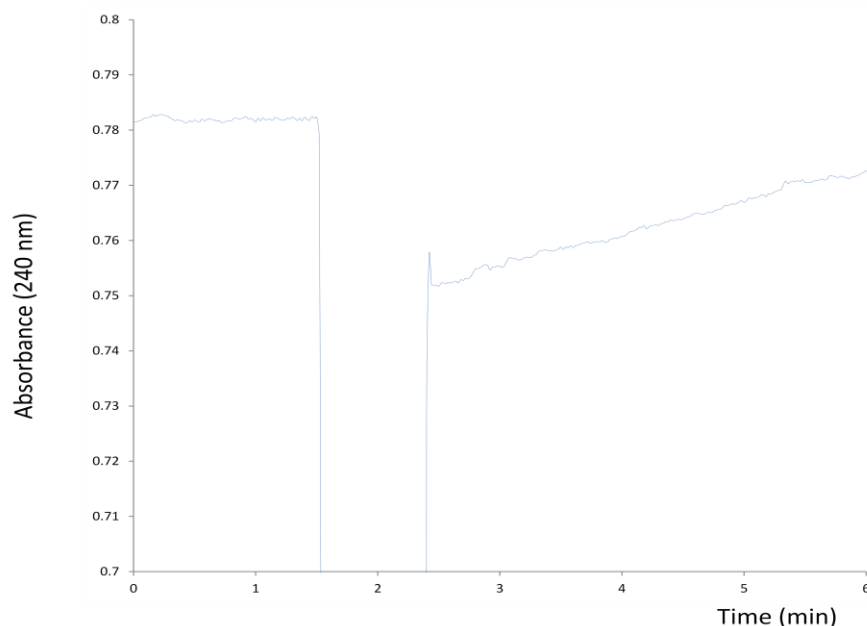


Figure 71: Measurement of glutamate mutase activity as the rate of mesaconate formation by the methylaspartase coupled assay. The measured rate of mesaconate formation from the assay in which the holoenzyme was reconstituted by 6.8  $\mu\text{M}$  S, 0.5  $\mu\text{M}$  E and 35  $\mu\text{M}$  3',5'-dideoxyadenosylcobalamin (**33**) was used to determine the enzyme specific activity,  $0.11 \text{ U (mg GlmE)}^{-1}$  which is 15 times less compared to specific activity determined from the coenzyme B<sub>12</sub> (**4**) dependent reaction

The reconstitution of holoenzyme with 2',5'-dideoxyadenosylcobalamin (**32**), and peptidoadenosylcobalamin (**34**) as cofactors could not accomplish the enzymatic conversion of (*S*)-glutamate to (2*S*,3*S*)-3-methylaspartate. Addition of coenzyme B<sub>12</sub> to these complexes did not restore activity.

### 3.4.2.2 Determination of kinetic constants of 3', 5'-dideoxyadenosycobalamin (33) in the reaction of glutamate mutase

Kinetic constants of 3', 5'-dideoxyadenosycobalamin (33) in the glutamate mutase catalyzed conversion of (*S*)-glutamate to (2*S*, 3*S*)-3-methylaspartate were determined by the Michaelis-Menten method from the reconstitution of holoenzyme in 14 folds excess of component S. Measurements of initial rate of mesaconate formation were recorded from various concentrations of 3',5'-dideoxyadenosycobalamin (33) used to reconstitute the holoenzyme (section 2.2.7.8) and subsequently applied to plot the Michael-Menten curve. The enzyme  $V_{\max} = 0.10 \text{ U (mg GImE)}^{-1}$  ( $K_{\text{cat}} = 0.089 \pm 0.01 \text{ s}^{-1}$ ) were obtained from the plotted Michaelis –Menten curve along with the  $K_m = 0.56 \pm 0.02 \text{ }\mu\text{M}$  of 3',5'-dideoxyadenosycobalamin(33) for glutamate mutase. The  $k_{\text{cat}}K_m^{-1} = 1.59 \times 10^5 \text{ s}^{-1}\text{M}^{-1}$  of the 3',5'-dideoxyadenosycobalamin (33) dependent glutamate mutase reaction was also calculated from these kinetic constants.

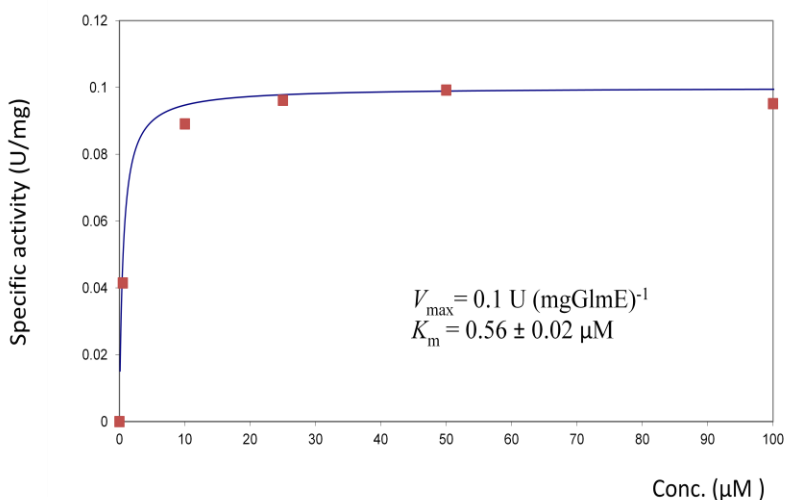


Figure 72: Michaelis-Menten plot for the determination of the kinetic constants of 3', 5'-dideoxyadenosycobalamin (33) in the conversion of (*S*)-glutamate to (2*S*, 3*S*)-3-methylaspartate by glutamate mutase reconstituted with 14 folds excess of component S

The measured  $K_m$  values of 3', 5'-dideoxyadenosylcobalamin (33) and coenzyme B<sub>12</sub> (4) in the reaction of glutamate mutase reconstituted by 14 folds excess of component S were equal. However, the  $k_{\text{cat}}$  as well as  $k_{\text{cat}} K_m^{-1}$  in the coenzyme B<sub>12</sub> (4) dependent reaction were about 15

fold higher than those measured from the reconstitution of the holoenzyme with 3', 5'-dideoxyadenosylcobalamin (**33**) as cofactor.

	Coenzyme B <sub>12</sub> ( <b>4</b> )	3',5'-Dideoxyadenosylcobalamin ( <b>33</b> )
$K_m$	$0.52 \pm 0.06 \mu\text{M}$	$0.56 \pm 0.02 \mu\text{M}$
$k_{\text{cat}}$	$1.24 \pm 0.36 \text{ s}^{-1}$	$0.089 \pm 0.01 \text{ s}^{-1}$
$k_{\text{cat}} K_m^{-1}$	$2.38 \times 10^6 \text{ s}^{-1} \text{ M}^{-1}$	$1.59 \times 10^5 \text{ s}^{-1} \text{ M}^{-1}$

Table 11: Summary of the kinetic constants of coenzyme B<sub>12</sub> (**4**) and 3', 5' –dideoxyadenosylcobalamin (**33**) in the reaction of glutamate mutase reconstituted with 14 folds excess of component S.

The  $k_{\text{cat}}$  for coenzyme B<sub>12</sub> (**4**) dependent reaction and that obtained from the kinetics of 3', 5' dideoxyadenosylcobalamin (**33**) were used to determine the energy difference between the coenzyme B<sub>12</sub> (**4**) and 3', 5' dideoxyadenosylcobalamin (**33**) co-catalyzed reactions of glutamate mutase at their assayed condition (37 °C).

$$\Delta E = E_{(4)} - E_{(33)} = -RT \ln [k_{\text{cat}(4)}] / [k_{\text{cat}(33)}] = 7 \text{ kJmol}^{-1}$$

This calculated 7 kJmol<sup>-1</sup> energy difference between the coenzyme B<sub>12</sub> (**4**) dependent reaction and that which 3', 5' -dideoxyadenosylcobalamin (**33**) was used as cofactor is the extent of facilitation towards Co-C bond homolysis and stabilization of the hydrogen abstraction by 5'-deoxyadenosyl radical contributed from the interaction of 3'OH with cob(II)alamin.<sup>186</sup>

### 3.5 Investigations into the role of MutL chaperone in glutamate mutase catalysis

After about 100,000 turnovers glutamate mutase becomes inactive due to loss of the 5'-deoxyadenosyl radical leaving cob(II)alamin tightly bound to the protein. This happens not only in vitro but also in vivo as shown by isolation of component E, component S and inactive cob(II)alamin containing holo-glutamate mutase from *Clostridium cochlearium*.<sup>168</sup> The presence of cob(II)alamin in the cell, which is formed as an intermediate in the pathway for cobalamin biosynthesis, is also another possibility to form an inactive complex with component E and S. The mechanism for removal of cob(II)alamin bound to the enzyme has been studied in methylmalonyl-CoA mutase as well as diol dehydratase. The methylmalonyl -CoA mutase associated MeaB chaperone protein, which is not required for the functional production of the enzyme, has been demonstrated to play a central role in preventing the binding of cob(II)alamin to the mutase as well as the removal of cob(II)alamin by exchange with coenzyme B<sub>12</sub> when bound to the mutase in an ATP dependent mechanisms.<sup>138</sup> A similar role of the protein known as reactivase has been established in diol dehydratase.<sup>139</sup> Between the genes encoding for glutamate mutase components E and S in *C. cochlearium*, an open reading frame coding for a putative chaperon GmL (50.21 kDa) has been detected (figure 73). Similar to MeaB of methylmalonyl -CoA mutase and reactivase of diol dehydratase, the deduced GmL sequence has a conserved ATP binding motif and is not required for the functional production of glutamate mutase. The protein has therefore been speculated to help to reactivate inactive glutamate mutase by exchange of cob(II)alamin with coenzyme B<sub>12</sub> as well as preventing the binding of cob(II)alamin to glutamate mutase. An investigation on the role of GmL requires the recombinant production of this protein in *E. coli*. Thus in this thesis the cloning of *mutL* gene from *C. tetanomorphum* is reported, from which the MutL chaperone can be over-produced in *E.coli* and used in the proposed experiments toward establishing its in vivo role in provision of active enzyme.

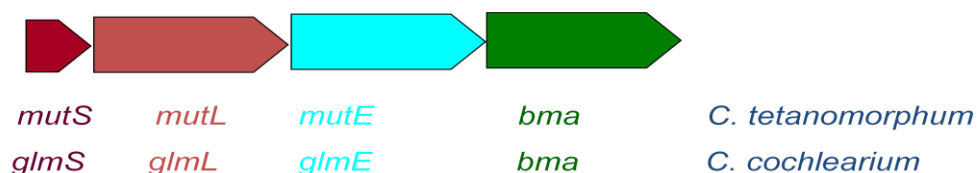


Figure 73: Genes encoding glutamate mutase components S, L and E in *C. cochlearium* and *C. tetanomorphum*. *bma* encodes the subsequent enzyme; the methylaspartase in the (S)-glutamate fermentation pathway.

### 3.5.1 Cloning of *Clostridium tetanomorphum mutL* gene in pASG-IBA3 and pASG-IBA5 expression vectors

The *mutL* gene consists of 1386 base pairs of which 484 (35%) are G-C and 902 (65%) are A-T. The gene is expressed as a sequence of 462 amino acids which forms the 50.21 kDa MutL protein. The PCR multiplied *mutL* gene with terminal *Lgul* restriction sites, which were included via the used primers, was successfully incorporated into the pre-entry IBA-20 vector by *Lgul* restriction and T4 ligation reactions. The constructed pre-entry vector with a *mutL* insert was transformed into *E. coli* DH5 $\alpha$  which grew on agar and later in broth culture from where it was purified. Cloning of *mutL* into pre-entry IBA-20 vector was confirmed by both sequencing (figure 74) as well as analysis by a DNA agarose gel which gave respective 1.8 and 1.4 kbp bands for IBA-20 and *mutL* after being digested by *Esp3I*. Constructions of the expression vectors pASG-IBA 3 and pASG-IBA 5 with *mutL* inserts were accomplished in the respective in frame *Esp3I* restrictions and T4 ligation reactions. The vectors were transformed in *E. coli* DH5 $\alpha$  and clones of *mutL* in pASG-IBA 3 and pASG-IBA 5 were purified and confirmed by DNA agarose gel which when digested by *Hind III* and *Xba I* gives the vector band (2.8 kbp) as well as other three bands with sizes between 400 and 800 kbp. These three bands arise from the digestion of *mutL* by *HindIII*. Analysis of the *mutL* sequence by a restriction map confirmed the restriction sites of *HindIII* at 148, 657 and 977 of the *mutL* sequence. Further confirmation of the successful cloning of *mutL* into pASG-IBA 3 and pASG-IBA 5 was obtained by the recombinant production of the MutL protein (3.5.2).

1 GTGGATGCTT ATTTACTTTT AGATTTTGGT AGCACCTATA CAAACTTAC  
 51 TGCAGTAGAT ATAGAAAATG AAGGGATATT AGCTACAGCA AAAGATATAA  
 101 CAACTATAGA AAGCGATATA ATGGTAGGGT TTAACAAAGC CTACGAAAAG  
 151 CTTACTGAAC AGTTAGAAGG AAAAGAAGTG AATTTTGTTA AAAAGTTAGC  
 201 ATGTTTCATCT GCAGCAGGTG GACTAAAGAT GATAGCCATC GGTCTTGATC  
 251 CAGAACTTAC AGCAGAAGCT GCAAAGAGAG CTGCTCTTGG AGCAGGAGCT  
 301 AGGGTACTAA ATGTATATAG TTACGATTG ACTAATAAAG AAGTTGAAGA  
 351 AATAAAAAAT TCTAACTTGG ACATAACTT TTAGCAGGT GGTACAGATG  
 401 GTGGAAATAA AGAATGTATG ATTCATAATG CAAAATGCT AGCTGAGCAT  
 451 GGAGTTAAAC TTCCAATAGT TGTAGCAGGA AATAAAGTAG TTAGTGATGA  
 501 AGTATCAGAA ATATTTGATA AAGCAGGTAT ATTTTATAGA GTTACTGAAA  
 551 ATGTAATGCC CAAGTTAAAT ACATTAATG TAGAACCTGC AAGAGAAGAA  
 601 ATAAGACAAA TATTTATGAA AAAAATTGTA GAAGCAAAAG GAATGTCAAA  
 651 TGCTGAAAGC TTTATTAATG GAATACTTAT GCCTACTCCA GCAGCAGTTT  
 701 TAAAGGCAGC TAGAGTATTA GCAGAAGGAA CCGATAAAGA AGATGGTATT  
 751 GGCGATTTAA TAGTAGTAGA TATTGGTGGT GCTACTACAG ATGTACTCTC  
 801 ACTTGACAGT GGCGAGCCAT CTAAGCCAGG AGTTACATTA AGAGGGCTTG  
 851 AAGAACCTTT TGCAAAAAGA ACTGTTGAAG GCGACCTAGG AATGAGATAT  
 901 TCTGCCATTT CCTTATGGGA GGCATCAGGA ACAAGAAAAC TTCAAAAATA  
 951 TCTATGTGAT AATACTGTAG ATGTAGAAGC TTGTTGTAAT TATAGAGCTG  
 1001 AACATATAAA AATGGTACCC GAGACAGAAG AAGAAATTA GTTTGATGAA  
 1051 GCTATGGCTA AGGTTGCAAC TGATATGGCT ATGGAAAGAC ATGTAGGAGT  
 1101 TATAGAAAGT ATGTATACTC CTATGGGAGT CATATATAGT CAGATAGGTA  
 1151 AAGACTTGTT AAACGTAAAG TGTGTAATAG GAACTGGAGG AGTACTAGTT  
 1201 CATAGTAAGA ATCCAGGTGA AATACTAAAA GCAGGGTCAT TTGATATGGC  
 1251 CGATGCTACT CATTGAAAC CACAGCATCC AGAATATTAT ATAGATAAAA  
 1301 CATATATATT ATCTGCAATG GGGCTTCTAG CAGAAGATCT TCCAGATAAA  
 1351 GCAGTTAGAA TAATGAAAAA GTATTTGGTT AAA**GTGGGT** GA

Figure 74; Sequence of the *mutL* insert in the pre-entry IBA-20 vector. The 1<sup>st</sup> codon (**GTG**) which is translated to methionine and the last (**GTT**) which encodes valine are shown in red. The triplet **GGG** between **GTT** and stop codon (**TGA**) is derived from primers used in the PCR, where it formed the restriction site for *Lgul*.

### 3.5.2 Expression of *mutL* in *E.coli*

The LC-MS analysis of the SDS-PAGE bands of the 50 kDa proteins from the cell free extracts of *E. coli* Rosetta, which were transformed with pASG-IBA3 and pASG-IBA5 vectors with *mutL* insert and respective induced by IPTG and AHT revealed the expression of *mutL* in both constructs. These expressions are in the meantime pending for Streptag or Histag purification of MutL. Experiments for this thesis have already demonstrated the formation of an inactive glutamate mutase complex by incubation of GlnS and E with hydroxycobalamin (**2**). Since no enzymatic activity could be obtained upon addition of coenzyme B<sub>12</sub> (**4**) and (*S*)-glutamate to this complex, pending experiments are the inclusion of GlnL and ATP or GTP into the incubation mixture.



## 4. Discussion

### 4.1 Reconstitution of holo-glutamate mutase from protein components S and E with cofactors

The kinetic investigations on the reaction of glutamate mutase reported in this thesis have described the two active coenzyme B<sub>12</sub> (4) derived cofactors, 3', 5'-dideoxyadenosylcobalamin (33) and adenosylpeptide B<sub>12</sub> (31). While the former differs from coenzyme B<sub>12</sub> (4) only by the absence of the 3'OH- group of the β-ligand ribose, the latter consists of two glycine units in place of the phosphodiester bond and ribose in the coenzyme B<sub>12</sub> α-ligand. Despite the described structure modifications, these coenzyme B<sub>12</sub> derivatives were able to assemble with glutamate mutase components S and E to form a heterotetrameric holoenzyme that accomplishes the reversible conversion of (S)-glutamate to (2S, 3S)-3-methylaspartate, although their co-catalysis were with significant reductions in the reaction rates as compared to coenzyme B<sub>12</sub> (4). The reported measurements of the kinetic constants for these cofactor derivatives as well as for coenzyme B<sub>12</sub> (4) in the reaction of glutamate mutase reconstituted with 14, 7 and 2-fold excess of component S, have demonstrated similar  $K_m$  values for these cofactors compared to the coenzyme B<sub>12</sub> (4). Detailed discussions of these results in the context of structural roles for cofactor binding to the apoenzyme during the glutamate mutase catalysis are given later in this chapter. A significant mechanistic insight related to the reconstitution of holo-glutamate mutase drawn from the trend of  $K_m$  values of these derivatives and those of coenzyme B<sub>12</sub> (4) is the dependence of the cofactor affinities to the apo-enzyme on the concentration of component S. The measured  $K_m$  values for coenzyme B<sub>12</sub> (4),  $0.52 \pm 0.06 \mu\text{M}$ ,  $0.7 \pm 0.05 \mu\text{M}$  and  $1.12 \pm 0.04 \mu\text{M}$  at 14, 7, and 2-folds excess of component S, respectively, as well as for the adenosylpeptide B<sub>12</sub> (31),  $0.35 \pm 0.05 \mu\text{M}$  and  $1.07 \pm 0.04 \mu\text{M}$  at respective 14 and 2-fold excess of component S, have demonstrated an increase of the cofactor's  $K_m$  with decreasing concentration of protein S. These data suggest that the affinities of coenzyme B<sub>12</sub> (4) as well as those of the two derived cofactors to apo-glutamate mutase decrease with decreasing amounts of component S during reconstitution of the holoenzyme. Since the cofactor is bound by component S of glutamate mutase and the reconstituted heterotetrameric holo-glutamate mutase complex E<sub>2</sub>S<sub>2</sub> is postulated to be composed of two cofactors, which form two active sites each at the interface of component S and E, these results have led to an insight into the order of assembling. It is logical to put

forward an argument that component S is able to bind coenzyme B<sub>12</sub> (4) as well as the other two cofactor derivatives before it joins with component E resulting in an increase of the cofactor affinity to the enzyme with increasing concentration of component S. There is no doubt with the other order of assembling, which brings components S and E together before the cofactor is bound, since other laboratories use the fused component S and E apoenzyme system to reconstitute the holoenzyme with coenzyme B<sub>12</sub> (4). This is likely to be the case in vivo, where a native chaperone, which is not necessary for functional expression of the enzyme, is also a part of the enzyme. The  $K_m$  value of  $5.5 \pm 0.7 \mu\text{M}$  for coenzyme B<sub>12</sub> (4)<sup>187</sup> obtained from the kinetic measurements with fused SE apoenzyme is almost five times larger than  $1.12 \pm 0.04 \mu\text{M}$ , which was obtained from reconstitution of the holoenzyme with a 2-fold excess of component S. These  $K_m$  values show that the reconstitution of the holoenzyme from the protein components S and E with coenzyme B<sub>12</sub> (4) increases the apparent affinity of the cofactor five times in comparison with reconstitution by assembling of fused SE with coenzyme B<sub>12</sub> (4). Raising the amount of component S further by 7 and 14-fold excess has demonstrated that increasing cofactor affinity to glutamate mutase is due to reconstitutions from separated components S and E. These kinetic results suggest that component S is able to bind its cofactor before it joins with component E with higher affinity than it does after its partnership with E.

## 4.2 Mechanism based inactivations of glutamate mutase

### 4.2.1 Evaluations on the interactions of glutamate mutase with its proposed inhibitors by the coupled assay with methylaspartase

Since at least 2 mM of each of the following inhibitors; *cis*-glutaconate, *trans*-glutaconate, itaconate, buta-1,3-diene-2,3-dicarboxylate, fumarate and maleate were demonstrated to inactivate methylaspartase to less than 50% of its activity, an application of the standard methylaspartase coupled method for assaying the interactions of these inhibitors with glutamate mutase was not appropriate. An assay for evaluating the interactions of glutamate mutase with these inhibitors requires an auxiliary enzyme which is not inactivated by an inhibitor in much higher concentrations than the  $K_m$  value of its natural substrate in the reaction that it catalyzes. Therefore an alternate assay without auxiliary enzyme was established. Hologlutamate mutase was incubated with the potential inhibitor for a certain time followed by the removal of the

excess inhibitor by gel filtration. The residual activity was assayed with methylaspartase. This modified assay, however, only works with irreversible inhibitors, i.e. inactivators. The non inactivations of glutamate mutase by itaconate, buta-1, 3-diene-2, 3-dicarboxylate, *cis*-glutaconate and *trans*-glutaconate reported in this work indicated that these compounds either did not affect glutamate mutase at all or were reversible competitive, noncompetitive or uncompetitive inhibitors. In contrast the related coenzyme B<sub>12</sub>-dependent 2-methyleneglutarate mutase exhibited inactivation by buta-1,3-diene-2,3-dicarboxylate and *cis*-glutaconate as indicated by the formation of cob(II)alamin.<sup>106</sup> The observed potentials of fumarate, maleate and mesaconate to inactivate holo-glutamate mutase was surprising. However, these results are contrast to the in vivo situation where mesaconate is present as intermediate in the pathway for glutamate fermentation, although several cases in which a substrate or cofactor of an intermediate metabolic step inhibits another enzyme of the same metabolic pathway are known. Rescuing enzyme inhibitions by intermediates of the same or other metabolic pathways are mostly achieved kinetically by those intermediates having high affinities to enzymes which they are taken as substrates through which their effect on other enzymes becomes minimal. Although the  $K_m$  values for mesaconate in the respective reactions of mesaconase and mesaconate hydratase are known, the inquiry on how the inactivation of glutamate mutase by mesaconate is prevented in vivo cannot be addressed since its effect on glutamate mutase has not been well established. Also important to be considered has been the results obtained from further characterization on the interaction of fumarate with glutamate mutase, which could not establish the formation of cob(II)alamin by UV/visible spectroscopy as hypothesized in the mechanism based inactivations of glutamate mutase. This observation suggests the binding of fumarate on the enzyme active site does not trigger the homolysis of the cofactor Co-C bond.

However, since the modified standard methylaspartase assay cannot characterize the interactions of these inhibitors with glutamate mutase kinetically, their effects on glutamate mutase has remained unclear pending the development of an appropriate assay with an auxiliary enzyme system which is not affected by these inhibitors.

#### 4.2.2 Evaluations on the interactions of glutamate mutase with its inhibitors by a coupled assay with glutamic-pyruvic transaminase and 2-hydroxyglutarate dehydrogenase

Coupling the glutamate mutase catalyzed reverse conversion of (2*S*, 3*S*)-3-methylaspartate to (*S*)-glutamate with glutamic-pyruvic transaminase and 2-hydroxyglutarate dehydrogenase catalyzed reactions achieves the conversion of (*S*)-glutamate to 2-hydroxyglutarate via 2-oxoglutarate (figure 57). These transformations are accomplished in the new developed assay by the two auxiliary conversions; the pyridoxal-5-phosphate dependent glutamic-pyruvic transaminase conversion of (*S*)-glutamate produced from the glutamate mutase reaction to 2-oxoglutarate and NADH dependent 2-hydroxyglutarate dehydrogenase catalyzed reduction of 2-oxoglutarate to 2-hydroxyglutarate. Pyruvate, the co-substrate of transamination, is included in the assay mixture to be converted to alanine along with the formation of 2-oxoglutarate. Decreasing absorptions of the assay mixture at 340 nm with time due to depletion of NADH during the dehydrogenase catalyzed reduction permits the measurement of the rate of the glutamate mutase reaction. The high specific activities of glutamic-pyruvic transaminase (81 U mg<sup>-1</sup>) and 2-hydroxyglutarate dehydrogenase (1 kU mg<sup>-1</sup>) enabled the inclusion of relative small amounts of these auxiliary enzymes in the optimized assay with efficient conversions to 2-hydroxyglutarate, and hence reliable determination of the kinetics of the glutamate mutase reverse reaction. Furthermore, the inability of *cis*-glutaconate, *trans*-glutaconate, itaconate, maleate, fumarate and mesaconate to inhibit glutamic-pyruvic transaminase and 2-hydroxyglutarate dehydrogenase as demonstrated with up to 20 mM of each inhibitor has qualified this assay for application toward determinations of the kinetics for glutamate mutase interactions with these inhibitors. Evaluations on the interactions of holo-glutamate mutase with itaconate and *trans*-glutaconate by this assay revealed the potentials of the two inhibitors to inactivate glutamate mutase (figure 60). These preliminary results demonstrated the reduction of glutamate mutase activity to 50% by 2.5 mM itaconate whereas 8 mM *trans*-glutaconate was required to reduce glutamate mutase activity to 50% and therefore suggesting that itaconate is more potent inhibitor than *trans*-glutaconate. Further experiments for this project will explore potentials for inactivating glutamate mutase by other designed inhibitors (table 7) as well as kinetic characterizations on their interactions with glutamate mutase. This study has therefore demonstrated the reliability of the optimized glutamic-pyruvic transaminase and 2-

hydroxyglutarate dehydrogenase coupled assay for the reverse reaction of glutamate mutase in evaluating the interactions of glutamate mutase with these inhibitors including their kinetic characterizations.

Also evaluated in this study was fitting of these inhibitors to mimic the 4-glutamyl and (2*S*, 3*S*)-3-methyleneaspartate radicals at the active site of glutamate mutase. Preliminary fitting of *cis*-glutaconate indicated an orientation that brings *cis*-glutaconate COO<sup>-1</sup> (1) into interaction with arginines 66 and 149 whereas COO<sup>-1</sup> (5) interacts with arginine 100, as being the only possibility for *cis*-glutaconate to bind to the enzyme active site. Because the rotation between C2-C3 of *cis*-glutaconate is restricted by the double bond, the skeletal structure of *cis*-glutaconate cannot fit into the arginine claw in an alternative orientation. Critical in relation to the orientation, with which *cis*-glutaconate skeletal structure fits in the arginine claw, has been the C2-C3  $\pi$  electrons which locates close to carboxylate of the active site glutamate 171 residue, and hence leads to C2-C3  $\pi$  electrons repulsions with the carboxylate. A similar phenomenon is predicted in the binding of (*Z*, *S*)-aminoglutaconate. These model fittings predict reduced affinity of *cis*-glutaconate and (*Z*, *S*)-aminoglutaconate to glutamate mutase and thus suggesting the use of glutamate 171 mutant enzyme in order to improve the binding of these inhibitors. However, since this project is focusing on spectroscopic characterizations of radical adducts of 5'-deoxyadenosyl radical with these inhibitors (figure 52), the use of mutant enzyme will be useful only in case of poor inhibitions of wild type glutamate mutase by *cis*-glutaconate and (*Z*, *S*)-aminoglutaconate or any other inhibitors with which significant  $\pi$  electrons repulsion with active site carboxylate will occur.

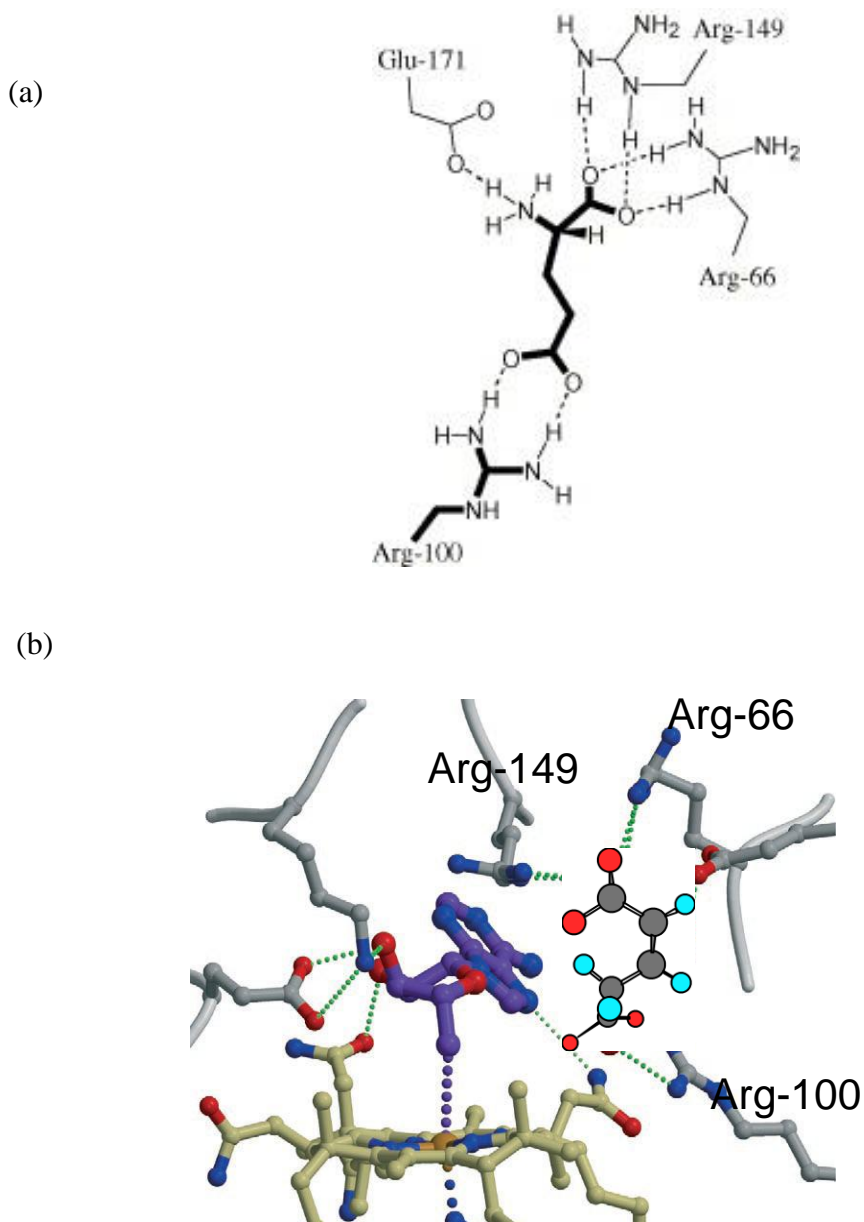


Figure 75; Binding of molecules to the active site of glutamate mutase (a) binding of (*S*)-glutamate by interactions of its carboxylates with the active site arginines (arginine claw). The  $\text{COO}^{-1}$  (1) of (*S*)-glutamate interacts by hydrogen bonding with arg-66 and arg-149 and  $\text{COO}^{-1}$  (5) with arg-100, (b) Preliminary model fitting of *cis*-glutaconate on the arginine claw by the orientation which brings  $\text{COO}^{-1}$  (1) of *cis*-glutaconate in interactions with arg-66 and arg-149, whereas  $\text{COO}^{-1}$  (5) interacts with arg-100. The  $\pi$  electrons from *cis*-glutaconate C2-C3 locate close to  $\text{COO}^{-}$  of glutamate 171.

### 4.2.3 The reaction of glutamate mutase with 2-fluoroglutarate

Since methylaspartase is not inactivated by 2-fluoroglutarate, the interaction of glutamate mutase with 2-fluoroglutarate was investigated by using the standard methylaspartase coupled assay. The demonstrated reduced activity in conversion of (*S*)-glutamate to (2*S*, 3*S*)-3-methylaspartate by glutamate mutase resulting from the incubation of glutamate mutase with 2-fluoroglutarate suggested the binding of 2-fluoroglutarate on the glutamate mutase active site which inhibit the binding of (*S*)-glutamate. On the other hand,  $^{19}\text{F}$  NMR analysis of the protein free mixture obtained from Centricon filtration after the overnight incubation of holo-glutamate mutase with 2-fluoroglutarate reveals spectral changes in comparison to the  $^{19}\text{F}$  NMR of 2-fluoroglutarate which suggested another fluoro compound had been formed during the incubation. This result was further supported by LC-MS analysis of the same preparation which was analyzed by  $^{19}\text{F}$  NMR. The LC-MS chromatograph showed two separated fluorinated compounds, each with a mass of 150 and thus suggesting the rearrangement of 2-fluoroglutarate to 2-fluoro-3-methylaspartate by holo-glutamate mutase. However, when 2-fluoroglutarate was used as the substrate of glutamate mutase in the standard methylaspartase coupled assay, the formation of mesaconate could not be demonstrated. Together, these results suggest that 2-fluoroglutarate is both an inhibitor and substrate of glutamate mutase, by which is rearranged to 2-fluoro-3-methylaspartate that cannot be deaminated to mesaconate by methylaspartase. (figure 76)

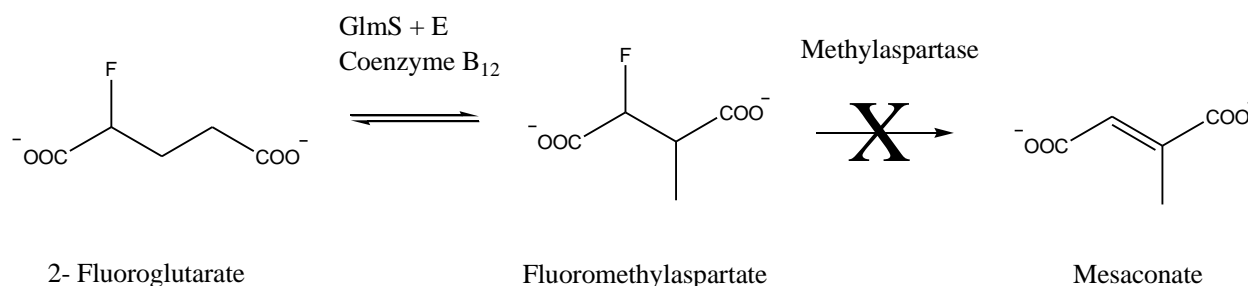


Figure 76: Respective reactions of glutamate mutase and methylaspartase with 2-fluoroglutarate and 2-fluoro-3-methylaspartate as postulated from the results of experiments in which 2-fluoroglutarate was incubated with holo-glutamate mutase and that which it was used as the substrate of glutamate mutase and assayed by the standard methylaspartase coupled assay.

Also proposed for further characterization of fluoromethylaspartate formed from the reaction of glutamate mutase with 2-fluoroglutarate is the extraction of the two fluorinated compounds by an organic solvent to allow their identification by  $^1\text{H}$  and  $^{13}\text{C}$  NMR. The extraction of fluorinated compounds by organic solvent is relevant for excluding coenzyme  $\text{B}_{12}$ , which is in the mixture after protein was removed. In this experimental design the presence of fluoromethylaspartate will be demonstrated by the methyl peak in both  $^1\text{H}$  and  $^{13}\text{C}$  NMR which is not found in 2-fluoroglutarate.

This study has also suggested a rearrangement by fragmentation of the 2-fluoroglutaryl radical (**35**) which is derived from 2-fluoroglutarate, into fluoroacetate radical (**36**) and acrylate (**24**) which recombine to the product related radical, fluoromethylaspartate radical (**38**) (figure 77), like the proposed rearrangement of (*S*)-glutamate to (2*S*, 3*S*)-3-methylaspartate (figure 25).

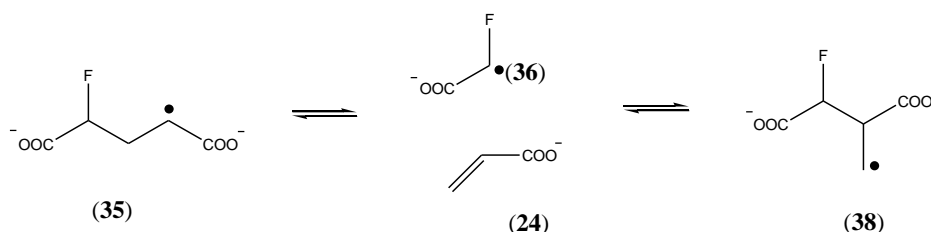


Figure 77: Proposed mechanism for the reaction of 2-fluoroglutarate with holo-glutamate mutase. The substrate derived 2-fluoroglutaryl radical (**35**) fragments into fluoroacetate radical (**36**) and acrylate (**24**) which recombine to form the fluoromethylaspartate radical (**38**).

The above proposed mechanism for the reaction of holo-glutamate mutase with 2-fluoroglutarate predicts the formation of a highly stable fluoroacetate radical (**36**) due to radical stabilization by fluorine. This phenomenon suggests an easy EPR characterization of this intermediate mimic of the glycine radical (**30**) in the reaction of glutamate mutase with (*S*)-glutamate. The ability of 2-fluoroglutarate to bind at the glutamate mutase active site and react like (*S*)-glutamate together with the usefulness of the high electronegative property of fluorine in stabilizing radicals have lead to the suggestion of the application of the fluoro-compounds (**39**) and (**40**) in demonstrating the formation of the fluoromethyleneaspartate radical which mimics the (2*S*, 3*S*)-3-methyleneaspartate radical in the reaction of glutamate mutase.



Similar chemistry is predicted in the reaction of holo-glutamate mutase with 2-chloroglutarate.

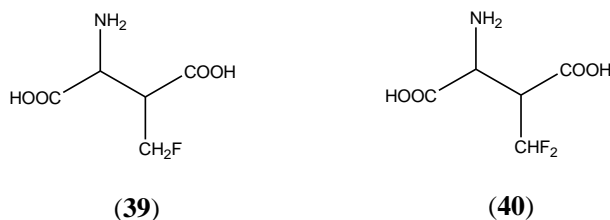


Figure 78: Structures of proposed fluorinated methylaspartic acids probes for demonstrating the formation of (2*S*, 3*S*) 3- methylaspartate related radical in the reaction of glutamate mutase.

### 4.3 Kinetic probing of glutamate mutase reaction by coenzyme B<sub>12</sub> derived cofactors

#### 4.3.1 Investigations on the role of the 5, 6-dimethylbenzimidazole ribonucleotide tail of coenzyme B<sub>12</sub> in the reaction of glutamate mutase

The ability of an adenosylpeptide B<sub>12</sub> (**31**) to act as a cofactor indicates successful assembling of apo-glutamate mutase with the artificial cofactor (**31**) to reconstitute the functioning holoenzyme system. Strong evidence of the potential for this artificial cofactor to bind to glutamate mutase like coenzyme B<sub>12</sub> (**4**) is from the comparison of its kinetic constants in the reaction of glutamate mutase with those of coenzyme B<sub>12</sub> (**4**). The reported similarities in the  $K_m$  values of coenzyme B<sub>12</sub> (**4**) and the artificial cofactor (**31**) in the glutamate mutase reaction from the reconstitution of holoenzyme in 14 as well as 2-fold excess of component S during these studies have implied equal affinities of these cofactors for the apo-glutamate mutase. These kinetic results provisionally suggest that the coenzyme B<sub>12</sub>  $\alpha$ -ligand especially the ribose and phosphodiester units are not involved in the mechanism of cofactor binding to apo-glutamate mutase, since their modification has not affected the binding of the cofactor to the protein. However, the established adenosylpeptide B<sub>12</sub> (**31**) equilibrium shifts towards the base-off state by the spectrophotometric pH titrations of the artificial cofactor predicted impairment on the binding of the modified cofactor to both mutases as well as the eliminases partner proteins.<sup>184</sup>

The shift of the cobalamin base-on/base-off equilibrium towards the base-off state due to coenzyme B<sub>12</sub> (**4**) structure modification to adenosylpeptide B<sub>12</sub> (**31**) was further supported by the observed dissociation of 5,6-dimethylbenzimidazole from the Co<sup>3+</sup> center in an UV/visible experiment.<sup>184</sup> In contrast to the equilibrium based prediction on the binding to enzyme, the results reported in this thesis demonstrated that the binding of an adenosylpeptide B<sub>12</sub> (**31**) to glutamate mutase is insensitive to the cofactor base-on/base-off equilibrium.

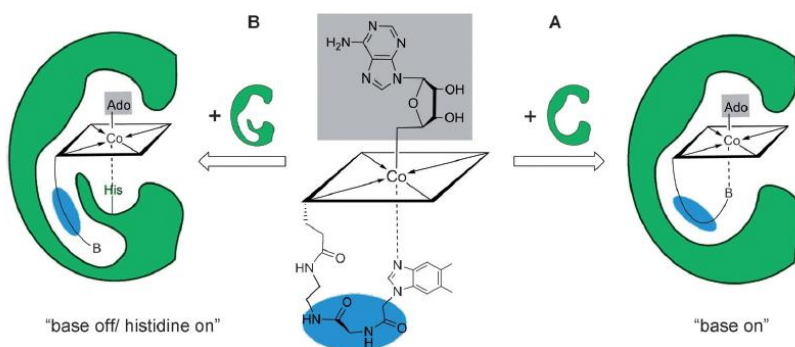


Figure 79: Schematic model for loading of an artificial adenosylpeptide B<sub>12</sub> (**31**) in proteins of the coenzyme B<sub>12</sub> dependent enzymes. A) ‘base-on, his-off’ and B) ‘base-off, his-on’ binding of the artificial cofactor.

However, the limitation of results reported in this thesis with relation to the context of the discussed affinity of an adenosylpeptide B<sub>12</sub> (**31**) to glutamate mutase has been the absence of experimental evidence for the mode by which an adenosylpeptide B<sub>12</sub> (**31**) binds apo-glutamate mutase. The UV/visible wavescan which demonstrated the cob(III)alamin spectrum of holo-glutamate mutase reconstituted with an adenosylpeptide B<sub>12</sub> (**31**) is not sufficient to conclude the artificial cofactor binds apo-enzyme by “base-off, his-on” since the possibility for ‘his-off’ binding with retained cofactor  $\alpha$ -ligand coordinate as in eliminases or  $\alpha$ -coordination to -OH cannot be perceptibly excluded. The unexpected ‘his-off’ binding of the  $\alpha$ -ligand modified base-off AdoCbi-GDP analogue of coenzyme B<sub>12</sub> (**4**) has been demonstrated in methylmalonyl-CoA mutase with which the analogue accomplished the co-enzymatic catalytic role with  $k_{\text{cat}}$  comparable to coenzyme B<sub>12</sub> (**4**).<sup>182</sup>

The demonstrated decrease of reaction rate from the reconstitution of holo-glutamate mutase with an adenosylpeptide B<sub>12</sub> (**31**) implies the 5, 6-dimethylbenzimidazole ribonucleotide tail is important in enhancing the rate of the reaction during the glutamate mutase catalytic cycle. This 10 folds decrease of  $k_{\text{cat}}$  as well as the  $k_{\text{cat}}K_m^{-1}$  is predicted to be caused by the alteration on the extent of conformational changes imposed by the peptidomimetic structure while deposited in protein pocket in comparison to coenzyme B<sub>12</sub> (**4**) ribonucleotide structure (figure 80). These conformation changes are part of whole conformational changes by protein and cofactor which are initiated by substrate binding and being direct linked with the coenzyme Co-C bond homolysis. Assistance of the Co-C bond homolytic cleavage by protein as well as the cofactor conformational changes was estimated to about 10<sup>11</sup> in the mechanism which has remained uncovered.<sup>65,66</sup> The demonstrated reduction of glutamate mutase  $k_{\text{cat}}K_m^{-1}$  resulted from the structure modification to an adenosylpeptide B<sub>12</sub> (**31**) implies significant contribution by the histidine replaced tail towards glutamate mutase efficient catalytic turnover.

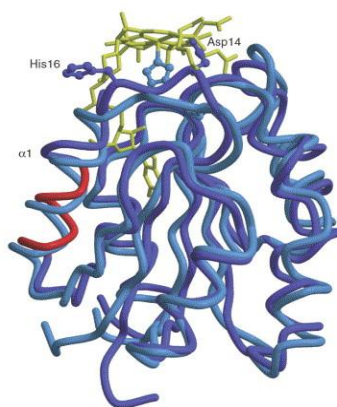


Figure 80: The superposition of glutamate mutase components S ( $\sigma$ -subunits) solution structures. Magenta is in the absence of the cofactor, whereas in cyan the ‘base off, his on’ bound coenzyme B<sub>12</sub> is shown with the histidine 16 displaced 5, 6-dimethylbenzimidazole ribonucleotide tail buried in protein pocket.<sup>146</sup>

### 4.3.2 Probing the stabilization of hydrogen abstraction from the substrate by 5'-deoxyadenosyl radical in the reaction of glutamate mutase

The mechanistic usefulness of the  $\beta$ -ligand modified derivatives of coenzyme B<sub>12</sub>, 2', 5'-dideoxyadenosylcobalamin (32), 3',5'-dideoxyadenosylcobalamin (33) and peptidoadenosylcobalamin (34), as cofactors for the glutamate mutase reaction is their ability to reconstitute the holoenzyme system without the enzyme-coenzyme complex interactions by either 2'-OH or 3'-OH of the ribose or both OH groups. Since the crystal structures of holo-glutamate mutase led to proposals of the requirements of the ribose 2'-OH and 3'-OH interactions with the active site Glu 330 and cob(II)alamin for the sp<sup>2</sup> radical carbon of the 5'-deoxyadenosyl radical to reach its target hydrogen on the substrate by pseudorotation, the use of these derivatives have been important in revealing the mechanism by which the highly reactive 5'-deoxyadenosyl radical is guided to the substrate including the cob(II)alamin participation in the stabilization of this radical during the substrate activation by hydrogen abstraction.

In contrast to the gas-phase calculations by density functional theory (DFT) which reported strong interactions between C<sub>19</sub>-H of the corrin backbone and the ribose 3'-OH ( $\Delta G \approx -30 \text{ kJmol}^{-1}$ ) from which without this interaction the reaction of glutamate mutase was considered impossible,<sup>185</sup> the reconstitution of holoenzyme with 3',5'-dideoxyadenosylcobalamin (33) as a cofactor accomplished the rearrangement of (*S*)-glutamate to (2*S*, 3*S*)-3-methylaspartate without 3'-OH. The measured 15-fold reduced rate of the glutamate mutase reaction from the reconstitution of holoenzyme with 3',5'-dideoxyadenosylcobalamin (33) as compared with coenzyme B<sub>12</sub> (4) indicated that the 3'-OH is a useful functional group for rate enhancement in the reaction of glutamate mutase. Besides the demonstrated reduction in reaction rate, the difference in kinetics; the  $k_{\text{cat}}$  as well as the  $k_{\text{cat}}K_m^{-1}$  between the reaction catalyzed by enzyme reconstituted with 3', 5'-dideoxyadenosylcobalamin (33) and that depends on coenzyme B<sub>12</sub> (4) has been converted to ( $\Delta G \approx -7 \text{ kJmol}^{-1}$ ). This energy difference is the contribution by the interactions of the 3'-OH of the ribose toward facilitating the abstraction of hydrogen on the substrate by 5'-deoxyadenosyl radical.<sup>186</sup> This effect has been specifically attributed to the weak hydrogen bonding between the 3'-OH with either the C<sub>19</sub>-H from the corrin or the active site Glu 330.

Further experimental contradiction to the gas-phase calculations by DFT which reported sizable stabilization of the substrate activation step by 2'-OH interactions ( $\Delta G \approx -5 \text{ kJmol}^{-1}$ )<sup>185</sup> is the deletion of 2'-OH demonstrated by 2',5'-dideoxyadenosylcobalamin (**32**) which resulted in complete loss of glutamate mutase activity. This loss has also been demonstrated with the reconstitution of the holoenzyme with peptidoadenosylcobalamin (**34**), which forms the holoenzyme without both 2'-OH and 3'-OH. These results have suggested the requirement of critical interactions by 2'-OH to accomplish the abstraction of hydrogen from the substrate by the 5'-deoxyadenosyl radical. The crystal structures of the holoenzyme show the conformational changes of the ribose moiety of the coenzyme B<sub>12</sub>  $\beta$ -ligand after homolytic cleavage of the Co-C bond which brings the ribose 3'OH close to the corrin's C<sub>19</sub>-H and thereby takes the sp<sup>2</sup> radical carbon of the 5'-deoxyadenosyl radical to the substrate which is located at 6.6 Å from Co(II) (figure 68). These conformational changes correspond with the pseudorotation of the ribose moiety from the C2'-*endo* to the C3'-*endo* in a fixed C-N torsion angle which links the adenine.<sup>188</sup> The strong hydrogen bonding interactions between the 2'-OH and Glu 330 before the homolytic cleavage of the Co-C bond as well as after the bond cleavage as revealed by the crystal structures has been suggested to act as a hinge during the pseudorotation. The complete loss of the glutamate mutase activity caused by the deletion of 2'-OH conforms to these crystal structure based explanations. Furthermore, the suggestion of the assistance on the homolytic cleavage of the Co-C bond by 3'-OH interactions with C<sub>19</sub>-H from the DFT calculations have been supported by the deletion of 3'-OH which demonstrated the 15-fold reduction in the reaction rate that was translated to a weak interaction ( $\Delta G \approx -7 \text{ kJmol}^{-1}$ ) with 3'-OH. The pseudorotation of the ribose is believed to be caused by conformational changes which are induced by binding of the substrate to the holoenzyme. Results obtained from the use of the  $\beta$ -ligand modified derivatives of coenzyme B<sub>12</sub> predict the inability to cleave the Co-C bond due to the deletion of the hinge (2'-OH). Since the pseudorotation stretch the Co-C bond, the less stretching on the bond resulted from the pseudorotation which is not assisted by the 3'-OH weak interaction with C<sub>19</sub>-H due to the deletion of 3'-OH caused the 15 fold reduction in the reaction rate. The inability to cleave the Co-C bond due to the deletion of 2'-OH can be further tested by anaerobic UV/visible scanning for detection of cob(II)alamin upon the addition of the substrate to holoenzyme reconstituted with 2',5'-dideoxyadenosylcobalamin (**32**).

These results from the use of  $\beta$ -ligand modified derivatives of coenzyme B<sub>12</sub> (**4**) have thus suggested that the highly reactive 5'-deoxyadenosyl radical is anchored to the protein and the cob(II)alamin by hydrogen bonding interactions of its ribose OH groups and guided along to the substrate which is located 6.6 Å away from Co(II). The hydrogen bonds are notable in preventing the primary radical from any side reactions on its way to the substrate. The association of the corrin interactions with ribose 3'-OH demonstrates the speculated cob(II)alamin conductor role in the reactions catalyzed by mutases as proposed by Buckel et al.<sup>149</sup> The illustrated hydrogen bonding controlled mechanism for 5'-deoxyadenosyl radical conformational changes which accomplish the substrate activation by hydrogen abstraction in the reaction of glutamate mutase is an example of negative catalysis.<sup>188</sup> This concept of negative catalysis elaborates on the enzymatic stabilisation of highly reactive radical species from their formation to the site where they react by which they are prevented from causing side reactions.<sup>189</sup>

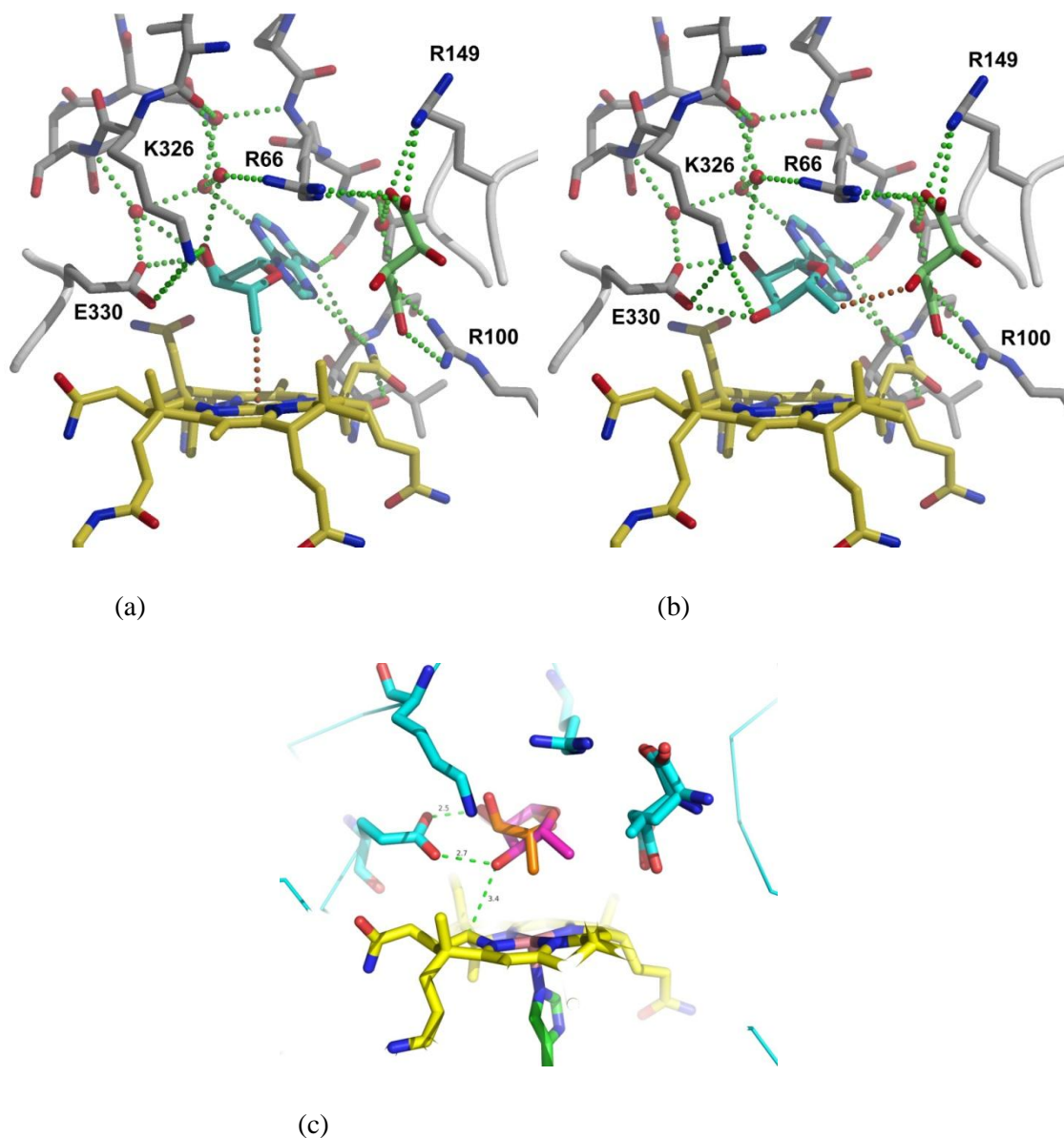


Figure 81. Crystal structures of holo-glutamate mutase active site with bound tartrate (an analogue of (2*S*, 3*S*)-3-methylaspartate) after the homolytic cleavage of the Co-C-bond. (a) Before and (b) after pseudorotation, which brings the  $sp^2$  radical carbon of the 5'-deoxyadenosyl radical close to tartrate fixed by arginines (red dotted lines). Note, the ribose pseudorotation from the C2'-endo to the C3'-endo brings the O3' into hydrogen bonding distance to both C<sub>19</sub>-H and E330. O2' locates within hydrogen bonding distance with E330 before and after pseudorotation. (c) two overlapping ribose conformations (before and after pseudorotation) in one plane showing intact 2.5 Å hydrogen bonding interaction between 2'-OH and Glu 330 (hinge), as well as the non-interacting 3'-OH before pseudorotation which locates at respective 2.7 Å and 3.4 Å distances from Glu 330 and C<sub>19</sub>-H after the pseudorotation. Adapted from reference 146.

The mutual importance of 2'-OH and 3'-OH respective interactions towards the formation of the 5'-deoxyadenosyl radical as well as their role in guiding this primary radical to the substrate as concluded from the studies reported in this thesis is consistent with the results from the new computational studies.<sup>190</sup> Although the calculations for these new computational studies were with methylmalonyl-CoA mutase, their results lead to the conclusion that the formation of 5'-deoxyadenosyl radical is due to the ribose pseudorotation which is aided by 2'-OH and 3'-OH respective interactions as well as the potential of 2'-OH and 3'-OH interactions in guiding the radical to the substrate. The established weak interactions by 3'-OH has also been supported by other studies which investigated the dependence of the  $pK_a$  value of C<sub>19</sub>-H on the cobalt redox state in which the exchange of C<sub>19</sub>-H with deuterium from D<sub>2</sub>O was analyzed by NMR. Since the DFT calculations claimed the polarization of the C<sub>19</sub>-H bond after the homolytic cleavage of the Co-C bond, which was hypothesized to promote the C<sub>19</sub>-H critical interactions with the ribose 3'-OH by hydrogen bonding, the acidity of the C<sub>19</sub>-H was consequently evaluated in cob(I)alamin, cob(II)alamin as well as cob(III)alamin. These studies demonstrated the inability of C<sub>19</sub>-H in cob(I)alamin, cob(II)alamin as well as in cob(III)alamin to exchange with deuterium from D<sub>2</sub>O in pH ranging from 3 to 10.8 and therefore implied weak hydrogen bonding in case of any C<sub>19</sub>-H interactions as established from the use of the 3',5'-dideoxyderivative (**33**).<sup>186</sup>

Other experimental explorations for determination of the extent of C<sub>19</sub>-H and 3'-OH interactions were provided by studies which used the diastereoisomers; (*R*)- and (*S*)-2,3-dihydroxypropylcobalamin as models for coenzyme B<sub>12</sub>. Both the NOE and HMBC based 1D as well as the results from the 2D NMR spectroscopic studies for these model compounds were not able to reveal spatial interactions of C<sub>19</sub>-H with  $\beta$ -ligands of *R*2 and *S*2. These results were compromised by description on the inability to demonstrate the interactions by NMR spectroscopy in due to the course of C<sub>19</sub>-H weak interactions as established by other studies designs. Furthermore, the crystal structures of the model compounds revealed C<sub>19</sub>-H O distances of 3.214 and 3.281 for respective *R* and *S*-isomers which suggested weak hydrogen bonding interactions. The dissociation energies for these crystal structures predicted hydrogen bonds were estimated to  $< 6 \text{ kJmol}^{-1}$ .<sup>186</sup>



Also mechanistically significant in relation to the studies which used modified  $\beta$ -ligand coenzyme B<sub>12</sub> derivatives has been the same  $K_m$  values of 3',5'-dideoxyadenosylcobalamin (**33**) and coenzyme B<sub>12</sub> (**4**) for apo-glutamate mutase. These values have suggested coenzyme B<sub>12</sub> (**4**) and 3', 5'-dideoxyadenosylcobalamin (**33**) equal affinities to glutamate mutase protein. The demonstrated inhibition of glutamate mutase by 2',5'-dideoxyadenosylcobalamin (**32**), peptidoadenylcobalamin (**34**) as well as the peptidoindolecobalamin further implies the strength of binding to glutamate mutase exhibited by these  $\beta$ -ligand modified cobalamin derivatives is comparable to coenzyme B<sub>12</sub>. Hydroxocobalamin has also inhibitory properties to glutamate mutase similar to these  $\beta$ -ligand modified derivatives. Mechanistic implication related to the cofactor structure derived from these results has been the suggestion that the ribose moiety of the 5'-deoxyadenosyl ligand does not have a role in "base-off, his-on" binding of cofactor to apo-glutamate mutase.

## 5. References

1. Combe, J.S., (1824), History of a case of anaemia, *Trans. Med. Chir. Soc. Edinb.* **1**, 194-203
2. Graner, J.L., (1985), Addison, pernicious anemia and adrenal insufficiency, *Can. Med. Assoc. J.* **133**, 855-857, 880
3. Addison, A., (1855), On the Constitutional and Local Effects of Disease of the Supra-renal Capsules, In Ellis, H., (2009), *BMJ* ,**339**, b4183
4. Biermer, A., (1872), Über eine Form von progressiver perniciöser Anämie, *Correspondenz-Blatt Schw. Ärzte.*, **2**, 15-17
5. Chanarin, I., (2000), Historical review, a history of pernicious anaemia, *British Journal of Haematology*, **111**: 407 – 415
6. Hurst, A.F., Bell, J.R., (1922), The pathogenesis of subacute combined degeneration of the spinal cord, with special reference to its connections with Addison's (pernicious) anaemia, achlorhydria and intestinal infection. *Brain*, **45**, 266 – 281
7. Cahn, A., Mering, J., (1886), Die Säuren des gesunden und kranken Magens, *Deutsches Arch Klin Med*, **39**, 233-53
8. Sinclair, L., (2007), Recognising, treating and understanding pernicious anaemia. *JLL Bulletin*: Commentaries on the history of treatment evaluation ([www.jameslindlibrary.org](http://www.jameslindlibrary.org))
9. Pepper, W., (1875), Progressive pernicious anaemia or anhaematosi, *Am. J. M. Sc.*, **70**, 313-347
10. Whipple, G. H., Robscheit, F. S., Hooper, C. W., (1920), Blood regeneration following simple anemia. IV. Influence of meat, liver and various extractives, alone or combined with standard diets, *American Journal of Physiology*, **53**, 236-262
11. Minot, G.R., Murphy, W.P., (1926), Treatment of pernicious anemia by a special diet, *JAMA*, **87**, 470- 476
12. Okuda, K., (1999), Discovery of vitamin B<sub>12</sub> in the liver and its absorption factor in the stomach: A historical review, *Journal of Gastroenterology and Hepatology* , **14**, 301–308
13. Rickes, E., Brink, N.G., Koniuszy, F.R., Wood, T.R., Folkers, K., (1948), Crystalline Vitamin B<sub>12</sub>, *Science*,**107**, 396-397

14. Smith, E.L., (1948), Purification of Anti-pernicious Anæmia Factors from Liver, *Nature*, **161**, 638-639
15. Brink, C., Hodgkin, D.C., Lindsey, J., Pickworth, J., Robertson, J.H., White, J.G., (1954), Structure of Vitamin B<sub>12</sub>: X-ray Crystallographic Evidence on the Structure of Vitamin B<sub>12</sub>, *Nature*, **174**, 1169-1171
16. Hodgkin, D.C., (1964), The X-ray Analysis of Complicated Molecules, Nobel Lecture, [www.nobelprize.org/nobel\\_prizes/chemistry/laureates/1964/hodgkin-lecture.html](http://www.nobelprize.org/nobel_prizes/chemistry/laureates/1964/hodgkin-lecture.html)
17. Golding, B.T., (1979), Vitamin B<sub>12</sub>, In Barton., D.H.R., Ollis, W.D., Comprehensive Organic Chemistry, In Haslam, E., (eds), Biological Compounds, p. 549-584, Oxford, Pergamon
18. Banerjee, R.V., Matthews, R.G., (1990), Cobalamin-dependent methionine synthase, *FASEB J.*, **4**, 1450-1459
19. Gruber, K., Kratky, C., (2001), Cobalamin-dependent methionine synthase, Messerschmidt, A., Huber, R., Poulos, T., Wieghardt, K., (eds), Handbook of metalloproteins, John Wiley & Sons, Ltd, Chichester
20. Stabler, S.P., (1999), B<sub>12</sub> and Nutrition, In Banerjee, R.,(ed), Chemistry and Biochemistry of B<sub>12</sub>, p. 343-365, John Wiley & Sons, Inc, New York
21. Petrus, A.K., Fairchild, T.J. and Doyle, R.P., (2009), Traveling the Vitamin B<sub>12</sub> Pathway: Oral Delivery of Protein and Peptide Drugs, *Angew. Chem. Int. Ed.*, **48**: 1022–1028
22. Alpers, D.H., Russell-Jones, G.J., (1999), Intrinsic factor, haptocorrin, and their receptors, In Banerjee, R., (ed), Chemistry and Biochemistry of B<sub>12</sub>, p. 411-440 John Wiley & Sons, Inc., New York
23. Rosenblat, D.S., Fenton, W.A., (1999), Inborn errors of cobalamin metabolism, In Banerjee, R.,(ed), Chemistry and Biochemistry of B<sub>12</sub>, p. 367-384, John Wiley & Sons, Inc., New York
24. Rothenberg, S.P., Quadros, E.V., Regec, A., (1999), Transcobalamin II, In Banerjee, R.,(ed), Chemistry and Biochemistry of B<sub>12</sub>, p. 441-474, John Wiley & Sons, Inc., New York
25. Wuerges, J., Garau, G., Geremia, S., Fedosov, S.N., Petersen, T.E., Randaccio, L., (2006), Structural basis for mammalian vitamin B<sub>12</sub> transport by transcobalamin, *PNAS*, **103**, 4386 – 4391

26. Allen, R.H., Seetharam, B., Podell, E., Alpers, D.H., (1978), Effect of Proteolytic Enzymes on the Binding of Cobalamin to R Protein and Intrinsic Factor: In vitro evidence that a failure to partially degrade protein is responsible for cobalamin malabsorption in pancreatic insufficiency, *J Clin Invest.*, **61**,47–54
27. Ralph Gräsbeck, R., (1984), Biochemistry and clinical chemistry of vitamin B<sub>12</sub> transport and the related diseases, *Clin. Biochem.*, **17**, 99-107
28. Moestrup, S.K., Verroust, P.J., (1999), Mammalian receptors of vitamin B<sub>12</sub>-binding proteins, In Banerjee, R., (ed), Chemistry and Biochemistry of B<sub>12</sub>, pg. 475-488, John Wiley & Sons, Inc, New York
29. Hogenkamp, H.P.C., Collins, D.A., Grissom, C.B., West, F.G., (1999), Diagnostic and therapeutic analogues of cobalamin, In Banerjee, R., (ed), Chemistry and Biochemistry of B<sub>12</sub>, p. 385-410, John Wiley & Sons, Inc., New York
30. Russell-Jones, G.J., Westwood, S.W., Habberfields, A.D, (1995), Vitamin B<sub>12</sub> Mediated Oral Delivery Systems for Granulocyte-Colony Stimulating Factor and Erythropoietin, *Bioconjugate Chem.*, **6**, 459-465
31. Habberfield, A., Jensen-Pippo, K., Ralph, L., Westwood, S.W., Russell-Jones, G. J., (1996), Vitamin B<sub>12</sub>-mediated uptake of erythropoietin and granulocyte colony stimulating factor in vitro and in vivo, *Int. J. Pharm.*, **145**, 1-8
32. Russell-Jones, G., Westwood, S., Farnworth, P., Findlay, J., Burger, H., (1995), Synthesis of LHRH Antagonists Suitable for Oral Administration via the Vitamin B<sub>12</sub> Uptake System, *Bioconjugate Chem.*, **6**, 34-42
33. Petrus, A.K., Vortherms, A.R., Fairchild, T.J., Doyle, R.P., (2007), Vitamin B<sub>12</sub> as a carrier for the oral delivery of insulin, *ChemMedChem.*, **2**, 1717-1721
34. Mukherjee, R., Donnay, E.G., Radomski, M.A., Miller, C., Redfern, D.A., Gericke, A., Damronc, D.S., Brasch, N.E., (2008), Vanadium–vitamin B<sub>12</sub> bioconjugates as potential therapeutics for treating diabetes, *Chem. Commun.*, 3783–3785
35. Collins, D.A., Hogenkamp, H.P., Gebhard, M.W., (1999), Tumor imaging via indium 111-labeled DTPA-adenosylcobalamin, *Mayo Clin Proc.*, **74**, 687-691
36. Collins, D.A., Hogenkamp, H.P., O'Connor, M.K., Naylor, S., Benson, L.M., Hardyman, T.J., Thorson, L.M., (2000), Biodistribution of radiolabeled adenosylcobalamin in patients diagnosed with various malignancies, *Mayo Clin Proc.*, **75**, 568-580

37. Collins, D.A., Hogenkamp, H.P.C., (1997), Transcobalamin II Receptor Imaging via Radiolabeled Diethylene-Triaminepentaacetate Cobalamin Analogs, *J. Nucl. Med.*, **(38)**, 717-723
38. Viola-Villegas, N., Rabideau, A.E., Bartholoma, M., Zubieta, J., Doyle, R.P., (2009), Targeting the Cubilin Receptor through the Vitamin B<sub>12</sub> Uptake Pathway: Cytotoxicity and Mechanistic Insight through Fluorescent Re(I) Delivery, *J. Med. Chem.*, **52**, 5253–5261
39. Banerjee, R., Ragsdale, S.W., (2003), The many faces of vitamin B<sub>12</sub>: catalysis by cobalamin –dependent enzymes, *Annu. Rev. Biochem.*, **72**, 209-247
40. Wohlfarth, G., Diekert, G., (1999), Reductive Dehalogenases, In Banerjee, R., (ed), *Chemistry and Biochemistry of B<sub>12</sub>*, p. 871-893, John Wiley & Sons, Inc., New York
41. Glod, G., Angst, W., Holliger, C., Schwarzenbach, R.P., (1997), Corrinoid-Mediated Reduction of Tetrachloroethene, Trichloroethene, and Trichlorofluoroethene in Homogeneous Aqueous Solution: Reaction Kinetics and Reaction Mechanisms, *Environ. Sci. Technol.*, **31**, 253-260
42. Gantzer, C.J., Wackett, L.P., (1991), Reductive dechlorination catalyzed by bacterial transition-metal coenzymes, *Environ. Sci. Technol.*, **25**, 715-722
43. Miller E, Wohlfarth G, Diekert G., (1996), Studies on tetrachloroethene respiration in *Dehalospirillum multivorans*, *Arch Microbiol.*, **166**, 379-387
44. Miller E, Wohlfarth G, Diekert G., (1997), Comparative studies on tetrachloroethene reductive dechlorination mediated by *Desulfitobacterium* sp. strain PCE-S, *Arch Microbiol.*, **168**, 513-519
45. Gribble, G.W., (1994), The natural production of chlorinated compounds, In *Environ. Sci. Technol.*, **28**, 310A–319A
46. Banerjee, R., (1997), The Yin-Yang of cobalamin biochemistry, *Chemistry & Biology*, **4**, 175-186
47. Frasca, V., Banerjee, R. V., Dunham, W. R., Sands, R. H., Matthews, R. G., (1988), Cobalamin-dependent methionine synthase from *Escherichia coli* B: electron paramagnetic resonance spectra of the inactive form and the active methylated form of the enzyme, *Biochemistry*, **27**, 8458–8465

48. Chen, Z., Crippen, K., Gulati, S., Banerjee, R., (1994), Purification and kinetic mechanism of a mammalian methionine synthase from pig liver, *J. Biol. Chem.*, **269**, 27193–27197
49. Jarrett, J. T., Hoover, D. M., Ludwig, M. L., Matthews, R. G., (1998), The mechanism of adenosylmethionine-dependent activation of methionine synthase: a rapid kinetic analysis of intermediates in reductive methylation of cob(II)alamin enzyme, *Biochemistry*, **37**, 12649–12658
50. Banerjee, R. V., Harder, S. R., Ragsdale, S. W., Matthews, R. G., (1990), Mechanism of reductive activation of cobalamin-dependent methionine synthase: an electron paramagnetic resonance spectroelectrochemical study, *Biochemistry*, **29**, 1129–1135
51. Taylor, R. T., Hanna, M. L., (1970), *Escherichia coli* B 5-methyltetrahydrofolate-homocysteine cobalamin methyltransferase: catalysis by a reconstituted methyl-14C-cobalamin holoenzyme and the function of S-adenosyl-l-methionine, *Arch. Biochem. Biophys.*, **137**, 453–459
52. Banerjee, R. V., Frasca, V., Ballou, D. P., Matthews, R. G., (1990), Participation of cob(I)alamin in the reaction catalyzed by methionine synthase from *Escherichia coli*: a steady-state and rapid reaction kinetic analysis, *Biochemistry*, **29**, 11101–11109
53. Jarrett, J. T., Amaratunga, M., Drennan, C. L., Scholten, J. D., Sands, R. H., Ludwig, M. L., Matthews, R. G., (1996), Mutations in the B<sub>12</sub>-binding region of methionine synthase: how the protein controls methylcobalamin reactivity, *Biochemistry*, **35**, 2464–2475
54. Ludwig, M. L., Matthews, R. G., (1997), Structure-based perspectives on B<sub>12</sub>-dependent enzymes. *Annu. Rev. Biochem.* **66**, 269–313
55. Goulding, C. W., Postigo, D., Matthews, R. G., (1997), Cobalamin-dependent methionine synthase is a modular protein with distinct regions for binding homocysteine, methyltetrahydrofolate, cobalamin, and adenosylmethionine, *Biochemistry*, **36**, 8082–8091
56. Wolthers, K.R., Scrutton, N.S., (2007), Protein interactions in the human methionine synthase-methionine synthase reductase complex and implications for the mechanism of enzyme reactivation, *Biochemistry*, **46**, 6696–6709
57. Banerjee, R.V., Johnston, N.L., Sobeski, J.K., Datta, P., Matthews, R.G., (1989), Cloning and sequence analysis of the *Escherichia coli metH* gene encoding cobalamin-dependent methionine synthase and isolation of a tryptic fragment containing the cobalamin-binding domain, *J. Biol. Chem.*, **264**, 13888–13895

58. Drummond, J. T., Huang, S., Blumenthal, R. M., Matthews, R. G., (1993), Assignment of enzymatic function to specific protein regions of cobalamin-dependent methionine synthase from *Escherichia coli*, *Biochemistry*, **32**, 9290–9295
59. González, J. C., Peariso, K., Penner-Hahn, J. E., Matthews, R. G., (1996), Cobalamin-independent methionine synthase from *Escherichia coli*: a zinc metalloenzyme, *Biochemistry*, **35**, 12228–12234
60. Taylor, R. T., Weissbach, H., (1968), *Escherichia coli* B N5-methyltetrahydrofolate-homocysteine vitamin-B<sub>12</sub> transmethylase: formation and photolability of a methylcobalamin enzyme, *Arch. Biochem. Biophys.*, **123**, 109–126
61. Zhao, S., Roberts, D. L., Ragsdale, S. W., (1995), Mechanistic studies of the methyltransferase from *Clostridium thermoaceticum*: origin of the pH dependence of the methyl group transfer from methyltetrahydrofolate to the corrinoid/iron-sulfur protein, *Biochemistry*, **34**, 15075–15083
62. Drennan, C. L., Matthews, R. G., Ludwig, M. L., (1994), Cobalamin-dependent methionine synthase: the structure of a methylcobalamin-binding fragment and implications for other B<sub>12</sub>-dependent enzymes, *Curr. Opin. Struct. Biol.*, **4**, 919–929
63. Poppe, L., Stupperich, E., Hull, W. E., Buckel, T. and Rétey, J. (1997), A Base-Off Analogue of Coenzyme-B<sub>12</sub> with a Modified Nucleotide Loop. *Eur. J. Biochem.*, **250**, 303–307
64. Finke, R. G., Martin, B. D., (1990), Coenzyme AdoB<sub>12</sub> vs AdoB<sub>12</sub>-homolytic Co-C cleavage following electron transfer: a rate enhancement greater than or equal to 10<sup>12</sup>, *J. Inorg. Biochem.* **40**, 19–22
65. Padmakumar, R., Banerjee, R., (1997), Evidence that cobalt-carbon bond homolysis is coupled to hydrogen atom abstraction from substrate in methylmalonyl-CoA mutase, *Biochemistry*, **36**, 3713–3718
66. Krouwer, J. S., Holmquist, B., Kipnes, R. S., Babior, B. M., (1980), The mechanisms of action of ethanolamine ammonia-lyase, an adenosylcobalamin-dependent enzyme. Evidence that carbon-cobalt bond cleavage is driven in part by conformational alterations of the corrin ring, *Biochim. Biophys. Acta*, **612**, 153–159
67. Golding, B.T., Buckel, W., (1997), 'Corrin-dependent Reactions', In Sinnott, M.L., (ed), '*Comprehensive Biological Catalysis*', Academic Press, London, Ch 33, 239-259

68. Marsh, E.N.G., Drennan, C.L., (2001), Adenosylcobalamin-dependent isomerases: new insights into structure and mechanism, *Curr. Opin Chem Biol*, **5**, 499-505
69. Mellman, I. S., Youngdahl-Turner, P., Willard, H. F., Rosenberg, L. E., (1977), Intracellular binding of radioactive hydroxocobalamin to cobalamin-dependent apoenzymes in rat liver, *Proc. Natl. Acad. Sci. U.S.A.*, **74**, 916–920
70. Schneider, K., Peyraud, R., Kiefer, P., Christen, P., Delmotte, N., Massou, S., Portais, J.C., Vorholt, J.A., (2012), The ethylmalonyl-CoA pathway is used in place of the glyoxylate cycle by *Methylobacterium extorquens* AM1 during growth on acetate, *J. Biol. Chem.* **287**, 757–766.
71. Filatova, L. V., Berg, I. A., Krasil'nikova, E. N., Ivanovskii, R. N., (2005), The mechanism of acetate assimilation in purple nonsulfur bacteria lacking the glyoxylate pathway: enzymes of the citramalate cycle in *Rhodobacter sphaeroides*, *Mikrobiologiia*, **74**, 319–328
72. Jarling, R., Sadeghi, M., Drozdowska, M., Lahme, S., Buckel, W., Rabus, R., Widdel, F., Golding, B. T., Wilkes, H., (2012), Stereochemical Investigations Reveal the Mechanism of the Bacterial Activation of *n*-Alkanes without Oxygen, *Angew. Chem. Int. Ed.*, **51**, 1334–1338
73. Malouf R., Grimley E. J., Areosa S. A. (2003), Folic acid with or without vitamin B<sub>12</sub> for cognition and dementia, *Cochrane Database of Systematic Reviews*, Issue 4. Art. No.: CD004514. DOI: 10.1002/14651858.CD004514
74. Buck, N. E., Wood, L. R. Hamilton, N. J., Bennett, M. J., Peters, H. L., (2012), Treatment of a methylmalonyl-CoA mutase stopcodon mutation, *Biochem. Biophys. Res. Commun.*, **427**, 753–757
75. Decker, K., Jungermann, K., Thauer, R. K., (1970), Energy production in anaerobic organisms, *Angew. Chem. Int. Ed. Engl.*, **9**, 138–158
76. Wadham, J. L., Arndt, S., Tulaczyk, S., Stibal, M., Tranter, M., Telling, J., Lis, G.P., Lawson, E., Ridgwell, A., Dubnick, A., Sharp, M.J., Anesio, A.M., Butler, C.E., (2012), Potential methane reservoirs beneath Antarctica, *Nature*, **488**, 633–637
77. Schippers, A., Neretin, Lev N., Kallmeyer, J., Ferdelman, T. G., Cragg, B. A., Parkes, R. J., Jørgensen, Bo B., (2005), Prokaryotic cells of the deep sub-seafloor biosphere identified as living bacteria, *Nature*, **433**, 861–864



78. Barker, H.A., (1961), Fermentations of nitrogeneous organic compounds, In Gansalus, G., (ed), *The bacteria, Academic Press*, New York, 151-207
79. Barker, H.A., (1981), Amino acid degradation by anaerobic bacteria, *Annu. Rev. Biochem.*, **50**, 23-40
80. Buckel, W., (1999), Anaerobic energy metabolism, In Lengeler, J., Drews, G., Schlegel, H., (eds) *biology of prokaryotes*, Wiley-Blackwell, New Jersey, 278-326
81. Loesche, W.J., Gibbons, R.J., (1968), Amino acid fermentation by *Fusobacterium nucleatum*, *Archives of Oral Biology*, **13**, 191-201
82. Muyzer, G., Stams, A. J. M., (2008), The ecology and biotechnology of sulphate-reducing bacteria, *Nature Rev. Micro.*, **74**, 319–328
83. Cabello, P., Dolores Rolda, M., Moreno-Vivia, C., (2004), Nitrate reduction and the nitrogen cycle in archaea, *Microbiology*, **150**, 3527–3546
84. Thauer, R. K., Jungermann, K., Decker, K., (1977), Energy conservation in chemotrophic anaerobic bacteria, *Bacteriol Rev*, **41**, 100–180
85. Barker, H. A., Kahn, J. M., Hedrick, L., (1982), Pathway of lysine degradation in *Fusobacterium nucleatum*, *J. Bacteriol.*, **152**, 201–207
86. Buckel, W., (2001), Unusual enzymes involved in five pathways of glutamate fermentation, *Appl. Microbiol. Biotechnol.*, **57**, 263–273
87. Barker, H. A., (1978), Explorations of bacterial metabolism, *Annu. Rev. Biochem.*, **47**, 1–33
88. Buckel, W., Miller, S. L., (1987), Equilibrium constants of several reactions involved in the fermentation of glutamate, *Eur. J. Biochem.*, **164**, 565–569
89. Buckel, W., Thauer, R. K., (2012), Energy conservation via electron bifurcating ferredoxin reduction and proton/Na(+) translocating ferredoxin oxidation, *Biochimica et biophysica acta*, **164**, 565–569
90. Lancaster, C. R., Kröger, A., Auer, M., Michel, H., (1999), Structure of fumarate reductase from *Wolinella succinogenes* at 2.2 Å resolution, *Nature*, **402**, 377–385

91. Baker, J. J., Jeng, I., Barker, H. A., (1972), Purification and properties of L-erythro-3,5-diaminohexanoate dehydrogenase from a lysine-fermenting Clostridium, *J. Biol. Chem.*, **247**, 7724–7734
92. Jeng, I., Barker, H. A., (1974), Purification and properties of l-3-aminobutyryl coenzyme A deaminase from a lysine-fermenting Clostridium, *J. Biol. Chem.*, **249**, 6578–6584
93. Alhapel, A., Darley, D. J., Wagener, N., Eckel, E., Elsner, N., Pierik, A. J., (2006), Molecular and functional analysis of nicotinate catabolism in *Eubacterium barkeri*, *Proc. Natl. Acad. Sci. U.S.A.*, **103**, 12341–12346
94. Reitz, S., Alhapel, A., Essen, L., Pierik, A. J. (2008), Structural and kinetic properties of a beta-hydroxyacid dehydrogenase involved in nicotinate fermentation, *J. Mol. Biol.*, **382**, 802–811
95. Lau, S. K. P., Woo, P. C. Y., Woo, G. K. S., Fung, A. M. Y., Ngan, A. H. Y., Song, Y., Liu, C., Summanen, P., Finegold, S.M., Yuen, K., (2006), Bacteraemia caused by *Anaerotruncus colihominis* and emended description of the species, *J. Clin. Pathol.*, **59**, 748–752
96. Lawson, P. A., Song, Y., Liu, C., Molitoris, D. R., Vaisanen, M., Collins, M. D., Finegold, S. M., (2004), *Anaerotruncus colihominis* gen. nov., sp. nov., from human faeces, In *Int. J. Syst. Evol. Microbiol.*, **54**, 413–417
97. Widdel, F., Musat, F., in Handbook of Hydrocarbon and Lipid Microbiology (Ed.: Timmis, K.N.), Springer, Berlin, 2010, p. 981.
98. Heider, J., (2007), Adding handles to unhandy substrates: anaerobic hydrocarbon activation mechanisms, *Curr. Opin. Chem. Biol.*, **11**, 188–194
99. Erb, T. J., Berg, I. A., Brecht, V., Müller, M., Fuchs, G., Alber, B. E., (2007), Synthesis of C5-dicarboxylic acids from C2-units involving crotonyl-CoA carboxylase/reductase: the ethylmalonyl-CoA pathway, *Proc. Natl. Acad. Sci. U.S.A.*, **104**, 10631–10636
100. Erb, T. J., Rétey, J., Fuchs, G., Alber, B. E. (2008), Ethylmalonyl-CoA mutase from *Rhodobacter sphaeroides* defines a new subclade of coenzyme B<sub>12</sub>-dependent acyl-CoA mutases, *J. Biol. Chem.* **283**, 32283–32293
101. Kornberg, H. L., Krebs, H. A., (1957), Synthesis of cell constituents from C2-units by a modified tricarboxylic acid cycle, *Nature*, **179**, 988–991

102. Lorenz, M. C., Fink, G. R., (2002), Life and death in a macrophage: role of the glyoxylate cycle in virulence, *Eukaryotic Cell*, **1**, 657–662
103. Alber, B. E., Spanheimer, R., Ebenau-Jehle, C. and Fuchs, G., (2006), Study of an alternate glyoxylate cycle for acetate assimilation by *Rhodobacter sphaeroides*, *Molecular Microbiology*, **61**, 297–309
104. Zarzycki, J., Schlichting, A., Strychalsky, N., Müller, M., Alber, B. E., Fuchs, G., (2008), Mesoconyl-coenzyme A hydratase, a new enzyme of two central carbon metabolic pathways in bacteria, *J. Bacteriol.*, **190**, 1366–1374
105. Bothe, H., Darley, D. J., Albracht, S. P., Gerfen, G. J., Golding, B. T., Buckel, W., (1998), Identification of the 4-glutamyl radical as an intermediate in the carbon skeleton rearrangement catalyzed by coenzyme B<sub>12</sub>-dependent glutamate mutase from *Clostridium cochlearium*, *Biochemistry*, **37**, 4105–4113
106. Buckel, W., Pierik, A. J., Plett, S., Alhapel, A., Suarez, D., Tu, S.-M., Golding, B. T. (2006), Mechanism-Based Inactivation of Coenzyme B<sub>12</sub>-Dependent 2-Methyleneglutarate Mutase by (Z)-Glutaconate and Buta-1,3-diene-2,3-dicarboxylate, *Eur. J. Inorg. Chem.*, **2006**, 3622–3626
107. Pierik, A. J., Graf, T., Pemberton, L., Golding, B. T., Rétey, J., (2008), But-3-ene-1,2-diol: A Mechanism-Based Active Site Inhibitor for Coenzyme B<sub>12</sub>-Dependent Glycerol Dehydratase. *ChemBioChem*, **9**, 2268–2275
108. Beatrix, B., Zelder, O., Linder, D., Buckel, W. (1994), Cloning, sequencing and expression of the gene encoding the coenzyme B<sub>12</sub>-dependent 2-methyleneglutarate mutase from *Clostridium barkeri* in *Escherichia coli*. *Eur. J. Biochem.*, **221**, 101–109
109. Zelder, O., (1994), Die Coenzym B<sub>12</sub>-abhängige Glutamat-Mutase aus *Clostridium cochlearium*: Klonierung und Überexpression der Gene, Quartärstruktur und EPR-spektroskopische Untersuchungen, *Dr. rer. nat. Dissertation*, Philipps University Marburg
110. Zelder, O., Beatrix, B., Buckel, W., (1994), Cloning, sequencing and expression in *Escherichia coli* of the gene encoding component S of the coenzyme B<sub>12</sub>-dependent glutamate mutase from *Clostridium cochlearium*, *FEMS Microbiol. Lett.*, **118**, 15–21
111. Faust, L. P., Babior, B. M., (1992), Overexpression, purification, and some properties of the AdoCbl-dependent ethanolamine ammonia-lyase from *Salmonella typhimurium*, *Arch. Biochem. Biophys.*, **294**, 50–54

112. Kung, H. F., Cederbaum, S., Tsai, L., Stadtman, T. C., (1970), Nicotinic acid metabolism. V. A cobamide coenzyme-dependent conversion of alpha-methyleneglutaric acid to dimethylmaleic acid, *Proc. Natl. Acad. Sci. U.S.A.*, **65**, 978–984
113. Velarde, M., Macieira, S., Hilberg, M., Bröker, G., Tu, S-M, Golding, B. T., Pierik, A.J., Buckel, W., Messerschmidt, A., (2009), Crystal structure and putative mechanism of 3-methylitaconate-delta-isomerase from *Eubacterium barkeri*, *J. Mol. Biol.*, **391**, 609–620
114. Pierik, A. J., Ciceri, D., Lopez, R. F., Kroll, F., Bröker, G., Beatrix, B., Buckel, W., Golding, B.T., (2005), Searching for intermediates in the carbon skeleton rearrangement of 2-methyleneglutarate to (*R*)-3-methylitaconate catalyzed by coenzyme B<sub>12</sub>-dependent 2-methyleneglutarate mutase from *Eubacterium barkeri*, *Biochemistry*, **44**, 10541–10551
115. Poppe, L., Bothe, H., Bröker, G., Buckel, W., Stupperich, E., Rétey, J., (2000), Elucidation of the coenzyme binding mode of further B<sub>12</sub>-dependent enzymes using a base-off analogue of coenzyme B<sub>12</sub>, *Journal of Molecular Catalysis B: Enzymatic*, **10**, 345-350
116. Hartrampf, G., Buckel, W. (1986), On the steric course of the adenosylcobalamin-dependent 2-methyleneglutarate mutase reaction in *Clostridium barkeri*. *Eur. J. Biochem.*, **156**, 301–304
117. Buckel, W., Golding, B.T., (1996), Glutamate and 2-Methyleneglutarate Mutase; From Microbial Curiosities to Paradigms for Coenzyme B<sub>12</sub>-dependent Enzymes, *Chem. Soc. Rev.*, **1996**, 329-337
118. Smith, D. M., Golding, B. T., Radom, L., (1999), On the Mechanism of Action of Vitamin B<sub>12</sub>. Theoretical Studies of the 2-Methyleneglutarate Mutase Catalyzed Rearrangement, *J. Am. Chem. Soc.*, **121**, 1037–1044
119. Eggerer, H., Overath, P., Lynen, F., Stadtman, E. R., (1960), On the mechanism of the cobamide coenzyme dependent isomirization of methylmalonyl -CoA to succinyl -CoA, *J. Am. Chem. Soc.*, **82**, 2643–2644.
120. Jansen, R., Kalousek, F., Fenton, W. A., Rosenberg, L. E., Ledley, F. D., (1989), Cloning of full-length methylmalonyl-CoA mutase from a cDNA library using the polymerase chain reaction, *Genomics*, **4**, 198–205

121. Marsh, E.N., McKie, N., Davis, N.K., Leadlay, P.F.,(1989), Cloning and structural characterization of the genes coding for adenosylcobalamin-dependent methylmalonyl-CoA mutase from *Propionibacterium shermanii*, *Biochem. J.*, **260**, 345-352
122. Willard, H. F., Rosenberg, L. E., (1980), Inherited methylmalonyl -CoA mutase apoenzyme deficiency in human fibroblasts: evidence for allelic heterogeneity, genetic compounds, and codominant expression, *J. Clin. Invest.*, **65**, 690–698
123. Fenton, W.A., Rosenberg, L.E., (1995), In Scriver, C.R., Beaudet, A.L., Sly, W.S., Valle, D., (eds), *The metabolic molecular basis of inherited disease*, McGraw-Hill, New York, pg. 3111-3128
124. Willard, H. F., Rosenberg, L. E., (1977), Inherited deficiencies of human methylmalonyl -CoA mutase activity: reduced affinity of mutant apoenzyme for adenosylcobalamin, *Biochem. Biophys. Res. Commun.*, **78**, 927–934
125. Gruber, K., Kratky, C., (2001), Methylmalonyl CoA mutase, Messerschmidt, A., Huber, R., Poulos, T., Wiegardt, K., (eds), *Handbook of Metalloproteins*, John Wiley & Sons, Ltd, Chichester
126. Allen, S.H., Kellermeyer, R.W., Stjernholm, R.L., Wood, H.G., (1964), Purification and properties of enzymes involved in the propionic acid fermentation, *J Bacteriol.*, **87**, 171-87
127. Birch, A., Leiser, A., Robinson, J. A., (1993), Cloning, sequencing, and expression of the gene encoding methylmalonyl-coenzyme A mutase from *Streptomyces cinnamonensis*, *J. Bacteriol.*, **175**, 3511–3519
128. Banerjee, R., Chowdhury, S., (1999), Methylmalonyl-CoA mutase, In Banerjee, R. (ed), *Chemistry and Biochemistry of B<sub>12</sub>*
129. Canata, J. J., Focesi, A., Mazumder, R., Warner, R. C., Ochoa, S., (1965), Metabolism of propionic acid in animal tissues. XII. Properties of mammalian methylmalonyl coenzyme A mutase, *J. Biol. Chem.*, **240**, 3249–3257
130. Kellermeyer, R. W., Allen, S. H., Stjernholm, R., Wood, H. G., (1964), Methylmalonyl isomerase.IV. Purification and properties of the enzyme from propionibacteria, *J. Biol. Chem.*, **239**, 2562–2569

131. Mancia, F., Keep, N. H., Nakagawa, A., Leadlay, P. F., McSweeney, S., Rasmussen, B., Bösecke, P., Diat, O., Evans, P.R., (1996), How coenzyme B<sub>12</sub> radicals are generated: the crystal structure of methylmalonyl-coenzyme A mutase at 2 Å resolution, *Structure*, **4**, 339–350
132. Mancia, F., Evans, P. R., (1998), Conformational changes on substrate binding to methylmalonyl CoA mutase and new insights into the free radical mechanism, *Structure*, **6**, 711–720
133. Zhao, Y., Abend, A., Kunz, M., Such, P. and Rétey, J. (1994), Electron Paramagnetic Resonance Studies of the Methylmalonyl-CoA Mutase Reaction, *European Journal of Biochemistry*, **225**, 891–896
134. Wölfle, K., Michenfelder, M., König, A., Hull, W. E., Rétey, J., (1986), On the mechanism of action of methylmalonyl-CoA mutase. Change of the steric course on isotope substitution, *Eur. J. Biochem.*, **156**, 545–554
135. Wollowitz, S., Halpern, J., (1988), 1,2-Migrations in free radicals related to coenzyme B<sub>12</sub>-dependent rearrangements, *J. Am. Chem. Soc.*, **110**, 3112–3120
136. Halpern, J., (1985), Mechanisms of coenzyme B<sub>12</sub>-dependent rearrangements, *Science*, **227**, 869–875
137. Vlasie, M., Chowdhury, S., and Banerjee, R., (2002), Importance of the Histidine Ligand to Coenzyme B<sub>12</sub> in the Reaction Catalyzed by Methylmalonyl-CoA Mutase, *J. Biol. Chem*, **277**, 18523- 18527
138. Padovani, D., Banerjee, R., (2009), A G-protein editor gates coenzyme B<sub>12</sub> loading and is corrupted in methylmalonic aciduria, *PNAS*, **106**, 21567-21572
139. Mori, K., Hosokawa, Y., Yoshinaga, T. and Toraya, T. (2010), Diol dehydratase-reactivating factor is a reactivase – evidence for multiple turnovers and subunit swapping with diol dehydratase, *FEBS Journal*, **277**, 4931–4943
140. Barker, H. A., Weissbach, H., Smyth, R. D., (1958), A Coenzyme Containing Pseudovitamin B(12), *Proc. Natl. Acad. Sci. U.S.A.*, **44**, 1093–1097
141. Patwardhan, A., Marsh, E. N. G., (2007), Changes in the free energy profile of glutamate mutase imparted by the mutation of an active site arginine residue to lysine, *Arch. Biochem., Biophys.*, **461**, 194–199

142. Huhta, M. S., Chen, H. P., Hemann, C., Hille, C. R., Marsh, E. N., (2001), Protein-coenzyme interactions in adenosylcobalamin-dependent glutamate mutase, *Biochem. J.*, **355**, 131–137
143. Huhta, M. S., Ciceri, D., Golding, B. T., Marsh, E. N. G., (2002), A novel reaction between adenosylcobalamin and 2-methyleneglutarate catalyzed by glutamate mutase, *Biochemistry*, **41**, 3200–3206
144. Cheng, M-C., Marsh, E. N. G. (2005), Isotope effects for deuterium transfer between substrate and coenzyme in adenosylcobalamin-dependent glutamate mutase, *Biochemistry*, **44**, 2686–2691
145. Reitzer, R., Gruber, K., Jogl, G., Wagner, U. G., Bothe, H., Buckel, W., Kratky, C., (1999), Glutamate mutase from *Clostridium cochlearium*: the structure of a coenzyme B<sub>12</sub>-dependent enzyme provides new mechanistic insights, *Structure*, **7**, 891–902
146. Gruber, K., Kratky, C., (2002), Coenzyme B(12) dependent glutamate mutase, *Curr. Opin. Chem. Biol.*, **6**, 598–603
147. Chih, H-W, Roymoulik, I., Huhta, M. S., Madhavapeddi, P., Marsh, E. N. G. (2002), Adenosylcobalamin-dependent glutamate mutase: pre-steady-state kinetic methods for investigating reaction mechanism, *Meth. Enzymol.*, **354**, 380–399
148. Yoon, M., Patwardhan, A., Qiao, C., Mansoorabadi, S. O., Menefee, A. L., Reed, G. H., Marsh, E. N. G., (2006), Reaction of adenosylcobalamin-dependent glutamate mutase with 2-thiolglutarate, *Biochemistry*, **45**, 11650–11657
149. Buckel, W., Kratky, C., Golding, B. T., (2006), Stabilisation of Methylene Radicals by Cob(II)alamin in Coenzyme B<sub>12</sub> Dependent Mutases, *Chem. Eur. J.*, **12**, 352–362
150. Bradbeer, C., (1965), The clostridial fermentations of choline and ethanolamine. 1. Preparation and properties of cell-free extracts, *J. Biol. Chem.*, **240**, 4669–4674
151. Bandarin V., Reed, G.H.,(1999), Ethanolamine ammonia-lyase, In Banerjee, R., (ed), *Chemistry and Biochemistry of B12*, p. 811- 833, John Wiley & Sons, Inc., New York

152. Bender, G., Poyner, R. R., Reed, G. H., (2008), Identification of the substrate radical intermediate derived from ethanolamine during catalysis by ethanolamine ammonia-lyase, *Biochemistry*, **47**, 11360–11366
153. Roof, D. M., Roth, J. R., (1988), Ethanolamine utilization in *Salmonella typhimurium*, *J. Bacteriol.*, **170**, 3855–3863
154. Hollaway, M. R., Johnson, A. W., Lappert, M. F., Wallis, O. C., (1980), The number of functional active sites per molecule of the adenosylcobalamin-dependent enzyme, ethanolamine ammonia-lyase, as determined by a kinetic method, *Eur. J. Biochem.*, **111**, 177–188
155. Wetmore, S. D., Smith, D. M., Bennett, J. T., Radom, L., (2002), Understanding the mechanism of action of B<sub>12</sub>-dependent ethanolamine ammonia-lyase: synergistic interactions at play, *J. Am. Chem. Soc.*, **124**, 14054–14065
156. Frey, P.A., (1990), Importance of organic radicals in enzymic cleavage of unactivated carbon-hydrogen bonds, *Chem. Rev.*, **90**, 1343–1357
157. Stubbe, J., Riggs-Gelasco, P., (1998), Harnessing free radicals: formation and function of the tyrosyl radical in ribonucleotide reductase, *Trends Biochem. Sci.*, **23**, 438–443
158. Zhang, Y., Stubbe, J., (2011), *Bacillus subtilis* class Ib ribonucleotide reductase is a dimanganese(III)-tyrosyl radical enzyme, *Biochemistry*, **50**, 5615–5623
159. Cox, N., Ogata, H., Stolle, P., Reijerse, E., Auling, G., Lubitz, W., (2010), A tyrosyl-dimanganese coupled spin system is the native metalloradical cofactor of the R2F subunit of the ribonucleotide reductase of *Corynebacterium ammoniagenes*, *J. Am. Chem. Soc.*, **132**, 11197–11213
160. Persson, A. L., Eriksson, M., Katterle, B., Pötsch, S., Sahlin, M., Sjöberg, B. M., (1997), A new mechanism-based radical intermediate in a mutant R1 protein affecting the catalytically essential Glu441 in *Escherichia coli* ribonucleotide reductase, *J. Biol. Chem.*, **272**, 31533–31541
161. Aberg, A., Hahne, S., Karlsson, M., Larsson, A., Ormö, M., Ahgren, A., Sjöberg, B. M., (1989), Evidence for two different classes of redox-active cysteines in ribonucleotide reductase of *Escherichia coli*, *J. Biol. Chem.*, **264**, 12249–12252



162. Booker, S., Stubbe, J., (1993), Cloning, sequencing, and expression of the adenosylcobalamin-dependent ribonucleotide reductase from *Lactobacillus leichmannii*, *Proc. Natl. Acad. Sci. U.S.A.*, **90**, 8352–8356
163. Herrmann, G., (2008), Enzymes of two clostridial amino-acid fermentation pathways, *Dr. rer. nat. Dissertation*, Philipps University Marburg
164. Jayamani, E., (2008), A unique way of energy conservation in glutamate fermenting clostridia, *Dr. rer. nat. Dissertation*, Philipps University Marburg
165. Textor, S., (1998), Propionat-Stoffwechsel in *Escherichia coli*: Nachweis des Methylcitrat-Zyklus in Bakterien, *Dr. rer. nat. Dissertation*, Philipps University Marburg
166. Djurdjevic, I., (2010), Production of glutaconic acid in recombinant *Escherichia coli*, *Dr. rer. nat. Dissertation*, Philipps University Marburg
167. Bradford, M.M., (1976), A rapid and sensitive method for the quantitation of microgram quantities of protein utilizing the principle of protein-dye binding, *Anal Biochem.*, **72**, 248- 254
168. Leutbecher, U., (1992), Studien zum Mechanismus der Coenzyme B<sub>12</sub>-abhängigen Glutamat-Mutase aus *Clostridium cochlearium*, *Dr. rer. nat. Dissertation*, Philipps University Marburg
169. Bothe, H., (1998), Untersuchungen zum Reaktionsmechanismus der Coenzym B<sub>12</sub>-abhängigen Glutamat-Mutase aus *Clostridium cochlearium*, *Dr. rer. nat. Dissertation*, Philipps University Marburg
170. Tu, S-M. (2009), *PhD thesis*, Newcastle University
171. Rappe, C., (1988), *Cis- $\alpha,\beta$ -unsaturated acids: Isocrotonic acid*, *Organic synthesis*, **Coll. Vol.6**, 711
172. Ciceri, D., (2000), Mechanistic Investigation into Coenzyme B<sub>12</sub> Enzymes, *PhD thesis*, Newcastle University
173. Edwards, C.H., (1996), Investigations into the mechanism of action of the adenosylcobalamin dependent enzymes 2-methyleneglutarate mutase and glutamate mutase, *PhD thesis*, Newcastle university
174. Zagalak, B., Pawelkiewicz, J., (1965), Synthesis and Properties of Co-Adenine Nucleoside Analogue of Coenzyme B<sub>12</sub>, *Acta Biochimica Polonica.*, **XII(3)**, 219-228

175. Brown, K. L., Cheng, S., Zou, X., Li, J., Chen, G., Valente, E. J., Zubkowski, J.D., Marques, H.M., (1998), Structural and enzymatic studies of a new analogue of coenzyme B<sub>12</sub> with an alpha-adenosyl upper axial ligand, *Biochemistry*, **37**, 9704–9715
176. Jacobsen, D. W., Holland, R. J., Montejano, Y., Huennekens, F. M., (1979), Cryptofluorescent analogs of cobalamin coenzymes: synthesis and characterization, *J. Inorg. Biochem.*, **10**, 53–65
177. Jensen, M. P., Halpern, J., (1999), Dealkylation of Coenzyme B<sub>12</sub> and Related Organocobalamins: Ligand Structural Effects on Rates and Mechanisms of Hydrolysis, *J. Am. Chem. Soc.*, **121**, 2181–2192
178. Gschösser, S., Hannak, R. B., Konrat, R., Gruber, K., Mikl, C., Kratky, C., Kräutler, B., (2004), Homocoenzyme B<sub>12</sub> and bishomocoenzyme B<sub>12</sub>: covalent structural mimics for homolyzed, enzyme-bound coenzyme B<sub>12</sub>, *Chemistry*, **11**, 81–93
179. Barker, H. A., Smyth, R. D., Wilson, R. M., Weissbach, H., (1959), The purification and properties of beta-methylaspartase, *J. Biol. Chem.*, **234**, 320–328
180. Barker, H. A., Rooze, V., Suzuki, F., Iodice, A. A., (1964), The Glutamate Mutase System. Assays and Properties, *J. Biol. Chem.*, **239**, 3260–3266
181. Kratky, C., Gruber, K., (2001), Glutamate Mutase, In Messerschmidt, A., Huber, R., Wiegardt, K., (eds), *Handbook of Metalloproteins*, John Wiley & Sons, Ltd, Chichester
182. Chowdhury, S., Thomas, M. G., Escalante-Semerena, J. C., Banerjee, R., (2001), The coenzyme B<sub>12</sub> analog 5'-deoxyadenosylcobinamide-GDP supports catalysis by methylmalonyl-CoA mutase in the absence of trans-ligand coordination, *J. Biol. Chem.*, **276**, 1015–1019
183. Chen, H-P., Hsu, H-J., Hsu, F-C., Lai, C-C, Hsu, C-H., Hsu, C-H., (2008), Interactions between coenzyme B<sub>12</sub> analogs and adenosylcobalamin-dependent glutamate mutase from *Clostridium tetanomorphum*, *FEBS J.*, **275**, 5960–5968
184. Zhou, K., Oetterli, R. M., Brandl, H., Lyatuu, F. E., Buckel, W., Zelder, F., (2012), Chemistry and bioactivity of an artificial adenosylpeptide B(12) cofactor, *Chembiochem*, **13**, 2052–2055
185. Durbeej, B., Sandala, G. M., Bucher, D., Smith, D. M., Radom, L. (2009), On the Importance of Ribose Orientation in the Substrate Activation of the Coenzyme B<sub>12</sub>-Dependent Mutases. *Chem. Eur. J.*, **15**, 8578–8585

186. Friedrich, P., Baisch, U., Harrington, R. W., Lyatuu, F., Zhou, K., Zelder, F., McFarlane, W., Buckel, W., Golding, B. T., (2012), Experimental Study of Hydrogen Bonding Potentially Stabilizing the 5'-Deoxyadenosyl Radical from Coenzyme B<sub>12</sub>., *Chem. Eur. J.*, **18**, 16114–16122
187. Xia, L., Ballou, D. P., Marsh, E. N. G., (2004), Role of Arg100 in the active site of adenosylcobalamin-dependent glutamate mutase, *Biochemistry*, **43**, 3238–3245
188. Buckel, W., Friedrich, P., Golding, B. T., (2012), Hydrogen Bonds Guide the Short-Lived 5'-Deoxyadenosyl Radical to the Place of Action, *Angew. Chem. Int. Ed.*, **51**, 9974–9976
189. Rétey, J., (1990), Enzymic Reaction Selectivity by Negative Catalysis or How Do Enzymes Deal with Highly Reactive Intermediates?, *Angew. Chem. Int. Ed. Engl.*, **29**, 355–361
190. Bucher, D., Sandala, G. M., Durbeej, B., Radom, L., Smith, D. M., (2012), The elusive 5'-deoxyadenosyl radical in coenzyme-B<sub>12</sub>-mediated reactions, *J. Am. Chem. Soc.*, **134**, 1591–1599

## Acknowledgements

I would like to thank my supervisor, Prof. Dr. Wolfgang Buckel for the opportunity to carry the work for my doctorate in his laboratory as well as his guidance and support during the four years of the studies for this thesis. I would also like to thank Prof. Dr. Bernard Golding for co-supervising this work and his support during my stay in his laboratory in Newcastle University.

I gratefully acknowledge Prof. Dr. Johann Heider and Prof. Dr. Hans-Ulrich Mösch for their advices via the Student Advisory Committee of the International Max Planck Research School (IMPRS) during the entire period of these studies. I also wish to express my acknowledgement to the IMPRS for the structured training program in modern microbiology and assistance during the period of the studies for this thesis.

I am gratified to the collaboration with Dr. Felix Zelder, University of Zürich, who provided the derivatives of coenzyme B<sub>12</sub> used in studies reported in this thesis. Particular thanks are also due to Dr. Peter Friedrich, Dr. Anutthaman Parthasarathy, Dr. Ashraf Alhapel and Dr. Shang-min Tu for teaching me laboratory techniques in enzymology, molecular biology and organic chemistry during the studies for this thesis. I extend my thankful appreciations to Mr. Jörg Kahnt (Max Planck Institute, Marburg) and Jan Bamberger (Fachbereich Chemie, Universität Marburg) for assistance with LC-MS measurements.

I also give many thanks to my peer students and workers in the laboratories of Prof. Wolfgang Buckel, Prof. Johann Heider in Marburg and Prof. Bernard Golding in Newcastle, as well as the IMPRS in Marburg for their support during my studies.

I am indebted to Deutscher Akademischer Austausch Dienst (DAAD) for the scholarship I received to study in Marburg as well as the Max Planck Institute and the LOEWE-Zentrum für Synthetische Mikrobiologie in Marburg for extended scholarships to enable the completion of this thesis.

Finally I give many thanks to my family, relatives and friends in Tanzania and Germany for courage and moral support during the time of the studies for this thesis.

## Curriculum vitae

### Personal data

Name: Fredrick Edwin Lyatuu

Address: Geschwister-Scholl-Str. 11B, Zimmer 13  
35039 Marburg

Date of Birth: 09-09-1974

Place of Birth: Tabora, Tanzania

Nationality: Tanzanian

### Education and Employment

1993-1995      Advanced Certificate of Secondary Education (ACSE),  
Ilboru Secondary School, Arusha, Tanzania  
Principal subjects; Physics, Chemistry and Biology  
Subsidiary subjects: Basic Applied Mathematics and General Studies

1996-1999:      BSc. (Hons) in Chemistry and Microbiology  
University of Dar Es Salaam, Tanzania

1999-2003:      Assistant Scientist  
Tropical Pesticides Research Institute  
P. O. Box 3024, Arusha, Tanzania

2003-2004:      M.Sc. in Drug Chemistry  
Newcastle University, UK

2004-2006: Science and Engineering Graduate Scheme (SEGS) Participant, UK.  
Occasionally working in the laboratory of Prof. Dr. Bernard Golding,  
School of Chemistry, Newcastle University

2006- 2007: Scientist  
Tropical Pesticides Research Institute  
P. O. Box 3024 Arusha, Tanzania

2008- Todate: Ph D Student,  
Laboratory for Microbial Biochemistry  
Philipps University, Marburg  
Karl-von-Frisch-Str. 8  
35032 Marburg

Associate Member  
International Max Planck Research School (IMPRS) in Environmental,  
Cellular and Molecular Microbiology.  
Max Planck Institute for Terrestrial Microbiology  
Karl-von-Frisch-Str. 10  
35043 Marburg

## Erklärung

Hiermit versichere ich, dass ich meine Dissertation mit dem Titel

Investigations into the mechanism of the coenzyme B<sub>12</sub> dependent reaction catalyzed by  
glutamate mutase from *Clostridium cochlearium*

selbständig, ohne unerlaubte Hilfe angefertigt und mich dabei keiner anderen als  
der von mir ausdrücklich bezeichneten Quellen und Hilfen bedient habe.

Die vorliegende Dissertation wurde in der jetzigen oder einer ähnlichen  
Form noch bei keiner anderen deutschen Hochschule eingereicht und hat  
noch keinen sonstigen Prüfungszwecken gedient.

---

(Ort, Datum)

---

(Unterschrift)